A COMBINED FINITE ELEMENT–TRANSFER MATRIX METHOD FOR PLATED STRUCTURES

(有限要素・伝達マトリックス法による板構造の解析)

MITAO OHGA

JANUARY 1989

ACKNOWLEDGEMENTS

The author would like to express his deepest gratitude to Professor Yuhshi Fukumoto of Osaka University for his constant encouragement and invaluable advice in compilation of the manuscript.

A special acknowledgement of gratitude goes to Professor Yukio Ueda and Professor Hiroshi Kitagawa of Osaka University for their valuable suggestions in compiling the dissertation. He is also indebted to Professor Sadaji Ohkubo of Ehime University for his understanding and support in the course of this studies.

The author wishes to thank Associate Professor Tunemi Shigematsu of Tokuyama Technical College and Associate Professor Takashi Hara of Toyohashi University of Technology for their very helpful advice during the course of this work.

The author is thankful to Mr. Masahito Tai, Mr. Syohji Kataoka, Mr. Motoji Murata and so on, for their help.

This is a good opportunity for the author to extend his appreciation to his parents, Mr. Miyao Ohga and Mrs. Sachiko Ohga, and his wife, Mrs. Mikiko Ohga, for their infinite affection and complete devotion to helping him.

CONTENTS

Chapter 1 INTRODUCTION

1-1 STATEMENT OF THE PROBLEM

In static and dynamic analysis of structures, the finite element method is the most widely used and powerful tool. However, the disadvantage of this method is that, in the case of complex and large structures, it is necessary to use a large number of nodes, resulting in very large matrices which require large computers for their management and regulation. Furthermore, in the dynamic analysis of the structures subjected to random excitations by a direct integration method, these disadvantages of the finite element method become more serious, because in these methods the sequence of calculations must be repeated many times, i.e. small time steps must be used to obtain response of the structure accurately.

On the other hand, the transfer matrix method of structural analysis is also applied to many structural problems. Since, in the transfer matrix method, analysis is performed by the subsequent multiplication of transfer and point matrices, the order of final matrix is as same as those of transfer and point matrices. Hence this method has an advantage over the finite element method in the number of degrees of freedom of the structure to be considered and, consequently, the computer memory requirement.

Although the transfer matrix method is naturally a solution procedure for one-dimensional problems, this method is applied to two-dimensional problems by introducing Fourier series into the governing equations of problems. It's successful application to two-dimensional problems is, however, restricted to simple structures with particular boundary conditions; otherwise considerable complications arise in the derivation of transfer matrix. In order to avoid the limitations in the derivation of transfer matrix, Dokainish proposed a combined use of finite element and transfer matrix method (FETM), in which transfer matrix was derived from the stiffness matrix used in the finite element method.

In this paper, the FETM method is applied to linear and nonlinear static and dynamic problems of plated structures, and the accuracy and efficiency of this procedure are also studied. Furthermore, a combined use of boundary element and transfer matrix (BETM), in which transfer matrix is derived from the system of equations obtained by the procedure based on the boundary element method, is proposed for two-dimensional and plate bending problems.

1-2 REVIEW OF PREVIOUS RESEARCH

In this section, previous studies of analytical methods of plated structures are mainly reviewed.

Since Turner(1) presented the concept of the finite element method(FEM) in 1956, numerous studies for development of this method have been made by many researchers, and these were summarized in many text books(2-11). On the other hand, many investigations of the boundary element method(BEM) in engineering problems have been also made since the early 1960′s, and these are summarized in Ref.(12-24). Some of them are mentioned in subsequently related chapters.

In 1968, Cheung(25,26) suggested the finite strip method (FSM) which was a formulation of combining the finite element method and Fourier series technique for a plated structure. Powell and Ogden(27) also reported the same procedure in 1969.

Since then this method was extended to various types problems of plate structures. Cheung applied this method to folded plate structures in 1969(28), and free vibration problems in 1971(31). In 1971, Yoshida(29) presented a buckling analysis of plated structures by FSM, and Yoshida and Oka(30) described the bending analysis of plate structures with stiffeners in 1972. A summary of studies mentioned above is described in Ref.(32). In 1978, Pardoen and Marienthal (33) presented FSM for a structure in polar coordinate system. The extension of FSM to sandwich plate structures was explored by Chan and Cheung in 1972(34), and by Ibrahim and Monforton in 1979(35).

In 1974, inelastic buckling strength analysis of stiffened plates by FSM was reported separately by Usami(36) and by Hasegawa, Ota and Nishino(37). Komatsu and Ushio(38) also studied the application of this method to inelastic buckling problems in 1978, and Yoshida and Maegawa(39) applied this method to a orthogonally stiffened plate in 1979.

Ueda, Matsuishi, Yamauchi and Tanaka(40) presented inelastic large deformation analysis by FSM in 1974. Maeda, Hayashi and Mori(41) investigated finite displacement analysis by FSM, in which stiffness matrix was derived analytically to reduce the computational effort in 1981.

In 1983, Yamamoto, Hotta, Obata and Sakimoto(42) proposed to reduce the size of the system matrices by using the two types of element, i.e. the plate element and the beam element. Okamura and Ishikawa(43) analyzed the multi-span plate structures by the stiffness matrix method combined with a relaxation technique. In this approach, the displacement functions in series form and the point-matching method are adopted to derive the stiffness matrix of large-size rectangular plate panels in 1984.

Combined use of finite difference and transfer matrix method was investigated by some researchers(44,45,46). In this method a partial differential equation for the structure is reduced to an ordinary differential equation by adopting finite difference technique. In 1975, a combined use of finite strip and finite difference was presented by Sundararajan and Reddy(47) for plate vibration problems. This procedure was also applied to skew orthotropic plate vibration (48) and buckling problems (49)

Transfer matrix was first applied to plate structures by Schnell in 1956(50). In this approach, partial differential equations of plate is reduced to an ordinary differential equation by adopting continuous functions which satisfying the boundary conditions in one direction and transfer matrix is evaluated by numerical integration. Since then, a number of studies for development of this method were investigated by many researchers (51-58). In 1971, Wurmest(52) applied transfer matrix method to the plate with shear deformation. In 1972, Dobovisek(56) also applied this method to shell structures. Shigematsu, Hara and the author (57) investigated the buckling analysis of thin walled members by transfer matrix method in 1984. In 1963, Leckie(59) applied TMM to vibration problems of plates, in which a plate was replaced by an equivalent network of beams.

In 1972, Dokainish(60) used the combined finite element - transfer matrix (FETM) method in the study of the dynamics of tapered or rectangular plate. McDaniel and Eversole(61) have proposed a similar approach in treating a stiffened plate structures along with some numerical values that warrant consideration in 1977. In 1979, Chiatti and Sestieri(62) introduced isoparametric shell elements, taking into consideration elements with nodes situated not only on corners but also on the midpoints of edges in dealing with complex structures. In 1980, Sankar and Hoa (63) offered an approach, in which an extended transfer matrix relating the state vectors which consist of state variables (displacements and forces) and their derivatives with respect to frequency was used. Mucino and Paveric(64), as a further generalization of the FETM method, have proposed a method in which structures are modeled by means of substructures connected in a chain-like manner. For each of these substructures, a transfer matrix was derived.

In 1983, Shigematsu, Hara and the author (65) described the application of the FETM method to bending and buckling problems of plates, and presented various techniques for treating the more complicated structures, especially those with the intermediate conditions are presented. In 1984, this procedures was applied to the elastic-plastic large displacement problems(66). In 1986, the extension of this method to the elastic-plastic large displacement analysis of thin-walled members was presented by Hara and the author (68). The substructuring procedure was adopted in order to treat complex structures, such as I-section and box-section plate girders with vertical stiffeners and web perforations. The application of this procedure to the transient response of structures under various random excitations was described by Shigematsu and the author in 1986(69). This procedure was extended to nonlinear dynamic problems of plate structures by Shigematsu and the author in 1988(70).

In 1974, Tomlin and Butterfield (71) proposed the procedure, in which the body was subdivided into some regions and for each of them system equations were derived, and they applied this procedure to piecewise homogeneous anisotropic foundation engineering problems. This work was extended to three dimensional problem by Banerjee in 1976(72) and Lachat and Watson in 1977(73), whose main incentive for subdividing the body into distinct regions was to reduce the bandwidth of the resultant system of algebraic equations.

Combined use of finite element and boundary element has been investigated by many researchers (74-76). In 1983, Komatsu, Nagai and Nishimaki(77) presented a combined use of boundary element and block element method for thin-walled box girders.

In 1977, Banarjee and Butterfield(78) proposed the combined use of boundary element and transfer matrix method, in which the transfer matrix was derived from the boundary element equations for a geomechanical problem. Recently, this method was applied to a two-dimensional problem (79) by Shigematsu, Hara and the author, and a plate bending problems (80) by Shigematsu and the author.

1-3 OBJECTIVES AND SCOPE

The aim of this dissertation is to propose the structural analysis methods based on the combined use of finite element and transfer matrix method(FETM), and boundary element and transfer matrix method(BETM) for plated structure problems.

In Chapter 2, a combined finite element - transfer matrix is applied to linear structural problems. Transfer matrix is derived from linear system matrix used in the ordinary finite element method. Various techniques for treating the more complicated structures such as those with the intermediate elastic and rigid columns, and stiffeners are proposed. Numerical examples for plate bending and buckling problems are presented and the results obtained by the FETM method are compared with those by the finite element method and other methods.

A combined finite element - transfer matrix method is extended to elastic-plastic problems with large displacements. In the calculation program developed in this chapter, the same procedures as those used in the finite element method based on load increment, are applied except for the estimation of approximate displacements for each specified incremental load. The Prandtl-Reuss′ law obeying the von Mises yield criterion is assumed, and a set of moving coordinate systems is used to take geometric nonlinearity into consideration. The results obtained by the FETM method are compared with those by other methods.

Chapter 4 proposes the linear and nonlinear analysis methods of thin-walled members by a combined finite element - transfer matrix method. Transfer matrix is derived from the tangent stiffness matrix for thin-walled member. To deal with complex structures such as box-section and I-section plate girders with stiffeners and web perforations, the transfer matrix for the substructure, into which thin-walled member is divided, is introduced. The results obtained by the FETM method for thin-walled members are compared with those by other methods.

In Chapter 5, a linear transient analysis method of the structures under random excitations by a combined finite element - transfer matrix method is proposed. Transfer matrix relating the state vector on the left and right boundaries of a strip at a certain time is derived from the system of equations of motion for a strip. An approximation is introduced in the equations of motion for the case of in-plane excitations in order to reduce computational efforts, and the technique of exchanging the state vectors is proposed to avoid the propagation of round-off errors occurred in recursive multiplications of the transfer and point matrices. Numerical examples of the plates under out-of-plane and in-plane excitations are presented and the results obtained by the FETM method are compared with those by the finite element method.

A linear transient analysis method based on a combined use of finite element and transfer matrix methods described in previous chapter is extended to nonlinear dynamic problems of plates under random excitations in Chapter 6. Equilibrium iteration based on the pseudo-force method is employed to improve the solution accuracy and to avoid the development of numerical instabilities. Numerical examples of the plates under various excitations are presented for inelastic problems and large deformation problems, and the results obtained by the FETM method are compared with those by the finite element method.

In Chapter 7, a structural analysis method based on a combined use of boundary element - transfer matrix method for two-dimensional and plate bending problems is investigated. A transfer matrix is derived from the system of equations derived by the procedure based on the boundary element method. The technique of exchanging the state vectors is proposed to avoid the propagation of round-off errors occurred in recursive multiplications of the transfer matrix, and rotation matrix is employed for axisymmetric structures to reduce computational efforts. Furthermore, the technique for the structure with intermediate supports is proposed. Numerical examples of two-dimensional and plate bending problems are presented and the results obtained by the BETM method are compared with those by the other methods.

Finally, Chapter 8 consists of a summary of this dissertation, conclusions for each chapter.

REFERENCES

1. Turner, M.J., Clough, R.W., Martin, H.C. and Topp, L.J., "Stiffness and Deflection Analysis of Complex Structures," J. Aero. Sci., Vol.23, No.9, September 1956, pp.805-823.
2. Zienkiewicz, O.C., "The Finite Element Method in Engineering Science," McGraw-Hill, 1971.
3. Gallagher, R.H., "Finite Element Analysis, Fundamentals," Prentice-Hall, 1973.
4. Nath, B., "Fundamentals of Finite Elements for Engineers," The Athlone Press of the University of London, London, England, 1974.
5. Heubner, K.H., "The Finite Element Method for Engineers," John Wiley & Sons, 1975.
6. Desai, G.S. and Abel, J.A., "Introduction to the Finite Element Method," von Nostrand Co., 1972.
7. Segerlind, L.J., "Applied Finite Element Analysis," Jhon Wiley & Sons, 1976.
8. Bathe, K. and Wilson E.L., "Numerical Method in Finite Element Analysis," Prentice-Hall, 1976.
9. Hinton, H. and Owen, D.R.J., "Finite Element Programming," Academic Press,1977.
10. Zienkiewicz, O.C., "The Finite Element Method," Third Edition, John Wiley & Sons, 1978.
11. Owen, D.R.J. and Hilton E., "Finite Elements in Plasticity, Theory and Practice," Pineridge Press Limited, 1980.
12. Brebbia, C.A., "The Boundary Element Method for Engineers," Pentech Press, London, 1978.
13. Brebbia, C.A. and Walker, S., "Boundary Element Techniques in Engineering," Newness-Butterworths, London, 1980.
14. Brebbia, C.A., Telles, J.C.F. and Wrobel, L.C., "Boundary Element Techniques, Theory and Applications in Engineering," Springer-Verlag, 1984.
15. Banerjee, P.K. and Butterfield, R., "Developments in Boundary Element Methods-1," Applied Science Publishers, London, 1979.
16. Banerjee, P.K. and Shaw, R.P., "Developments in Boundary Element Methods-2," Applied Science Publishers, London, 1982.
17. Brebbia, C.A., "Recent Advances in Boundary Element Methods," Pentech Press, London, 1978.
18. Brebbia, C.A., "New Developments in Boundary Element Methods," CML Publications, Southampton, 1980.
19. Brebbia, C.A., "Boundary Element Methods," Springer-Verlag, 1981.

20. Brebbia, C.A., "Boundary Element Methods in Engineering," Springer-Verlag, 1982.
21. Brebbia, C.A., Futagami, T. and Tanaka, M., "Boundary Elements," Springer-Verlag, 1983.
22. Brebbia, C.A.,"Boundary Elements-VI," Springer-Verlag, 1984.
23. Brebbia, C.A. and Maier, G., "Boundary Elements VII," Springer-Verlag, 1985.
24. Tanaka, M. and Brebbia C.A., "Boundary Elements VIII," Springer-Verlag, 1986.
25. Cheung, Y.K., "Finite Strip Method in the Analysis of Elastic Plates with Two Opposite Simply Supported Ends," Proc. I.C.E., Vol.40, May, 1968, pp.1-7.
26. Cheung, Y.K., "Finite Strip Method Analysis of Elastic Slabs," J. ASCE, Vol.94, No.EM6, December, 1968, pp.1365-1378.
27. Powell, G.H. and Ogden, D.W., "Analysis of Orthotropic Plate Bridge Decks," J. ASCE, Vol.95, No.ST5, May, 1969, pp.909-922.
28. Cheung, Y.K., "Folded Plate Structures by Finite Strip Method," J. ASCE, Vol.95, No.ST12, December, 1969, pp.2963-2979.
29. Yoshida, K., "Buckling Analysis of Plate Structures by Strip Elements," J. SNAJ, Vol.130, 1971, pp.161-171 (in Japanese).
30. Yoshida, K. and Oka, N., "Bending Analysis of Plate Structures by Strip Elements," J. SNAJ, Vol.132, 1972, pp.289-298 (in Japanese).
31. Cheung, Y.K., "Flexural Vibrations of Rectangular and Other Polygonal Plates," J. ASCE, Vol.97, No.EM2, April, 1971, pp.391-411.
32. Cheung, Y.K., "Finite Strip Method in Structural Analysis," Pergamon Press, Oxford, England, 1976.
33. Pardoen, G.C. and Marienthal, M.J., "Finite Strip Method in Polar Coordinates," J. ASCE, Vol.104, No.EM3, June, 1978, pp.587-604.
34. Chan, H.C. and Cheung, Y.K.,"Static and Dynamic Analysis of Multi-Layered Sandwich Plates," Int. J. Mech. Sci., Pergamon Press, Vol.14, 1972, pp.399-406.
35. Ibrahim, M.I. and Monforton, G.R., "Finite Strip Laminated Sandwich Roof Analysis," J. ASCE, Vol.105, No.ST5, May, 1979, pp.905-919.
36. Usami, T., "Elastic and Inelastic Buckling Strength of Stiffened Plates in Compression," Proc. of JSCE, No.228, August, 1974, pp.13-28 (in Japanese).
37. Hasegawa, A., Ota, K. and Nishino, F., "Some Considerations on Buckling Strength of Stiffened Plates," Proc. of JSCE,

No.232, December, 1974, pp.1-15 (in Japanese).
38. Komatsu S. and Ushio, M., "On Elasto-Plastic Buckling Strength of Stiffened Plates under Compression and Their Rational Design Method," Proc. of JSCE, No.278, October, 1978, pp.39-52 (in Japanese).
39. Yoshida, H. and Maegawa K., "Analysis of Buckling Strength of Plates with Longitudinal and Transverse Stiffeners," Proc. of JSCE, No.282, February, 1979, pp.15-29 (in Japanese).
40. Ueda, Y., Matsuishi, M., Yamauchi, Y. and Tanaka, M., "Non-Linear Analysis of Plates Using the Finite Strip Method," J. of the Kansai Society of Naval Architects, Japan, No.154, September,1974, pp.83-92 (in Japanese).
41. Maeda, Y., Hayashi, M. and Mori, K., "Finite Displacement Analysis of Thin Plates by Finite Strip Method," Proc. of JSCE, No.316, December, 1981, pp.23-36.
42. Yamamoto, T., Hotta, M., Obata, K. and Sakimoto, T., "Analysis of Thin-Walled Structures by Combined Use of Plate and Beam Elements," Preprint of Annual Meeting of JSCE, October, 1983, pp.155-156 (in Japanese).
43. Okamura, H. and Ishikawa, K., "Analysis of Multi-Span Plate Structures by a Small Computer," Proc. of JSCE, No.344/I-1, April 1984, pp.313-322 (in Japanese).
44. Paue, E., "Zur Berechnung von Platten mit unstetigen Belastungen und Randmomenten," Wissenschaftliche Zeitschrift der Hochschule für Architektur und Bauwesen Weimar, Vol.17, Heft 5, 1970, pp.509-515.
45. Pirna, G.D., "Berechnung von Platten mit dem Übertragungsverfahren," Maschinenbautechnik, Vol.26, Heft 2, 1977, pp.72-74.
46. Migita, Y. and Enda, Y., "Analysis of Free Flexural Vibration of Rectangular Plates by the Finite Difference Transfer Matrix Method," Proc. of JSCE, No.392/I-9, April, 1988, pp.239-247 (in Japanese).
47. Sundararajan, C. and Reddy, D.V., "Finite Strip-Difference Calculus Technique for Plate Vibration Problems," International Journal of Solids & Structures, Vol.11, April, 1975, pp.425-435.
48. Thangam Babu, P.V. and Reddy, D.V., "Finite Strip - Difference Calculus Technique of Skew Orthotropic Plate Vibration," Proc. Int. Conf. on Finite Element Methods in Engineering, Adelaide, Sydney, Australia, 1976.
49. Thangam Babu, P.V. and Reddy, D.V., "Finite Strip - Difference Calculus Technique for Skew Orthotropic Plate Buckling," Proc. sixth Canadian Congress of Applied Mechanics (CANCAM), Vancouver, B.C., May-June, 1977.

50. Schnell, W., "Zur Berechnung der Beulwerte von längs- oder querversteiften rechteckigen Platten unter Drucklast," ZAMM 36, Jan./Febr., 1956, pp.36-51.
51. Klöppel, K. und Schiedel, E., "Beulwert der dreiseitig gelenkig gelagerten, am freien Rand versteiften Pechteckplatte mit beliebig verteilter Randspannung," Der Stahlbau, Vol.37, Dezember, 1968, pp.372-379.
52. Wurmnest, W., "Untersuchung der Stabilität einseitig gedrückter, isotroper, schubelastischer Pechteckplatten mit Hilfe von Übertragungsmatrizen," Der Stahlbau, Vol.40, Juni, 1971, pp.178-186.
53. Uhrig, R., "Elastostatik und Elastokinetik in Matrizenschreibweise: Das Verfahren der Übertragungsmatrizen," Springer-Verlag, 1973.
54. Misawa, T., Shigematsu, T., Ohga, M. and Hara, T., "Buckling Analysis of Shear-Elastic Plate with Stiffener," Proc. of JSCE, June, 1980, pp.1-8 (in Japanese).
55. Shigematsu, T., Hara, T. and Ohga, M., "Untersuchung der Stabilität einseitig gedrückter, längsausgesteifter, orthotroper Rechteckplatten mit Schubverformung," Der Stahlbau, Juni,1982, pp.171-176.
56. Dobovisek, B., "Berechnung prismatischer Schalen," Der Bauingenieur, Vol.47, November, 1972, pp.393-400.
57. Shigematsu, T., Ohga, M. and Hara, T., "Buckling Analysis of Thin Walled Opened and Closed Sectional Members with Shear Deformation," Proc. of JSAE, No.342, August, 1984, pp.39-45.
58. Ohga, M., Shigematsu, T. and Shugiyama, T., "Buckling Analysis of Cylindrical Shells with Stiffeners by Transfer Matrix Method," Memoirs of the Faculty of Engineering, Ehime University, Vol.10, No.4, February, 1985, pp.169-177 (in Japanese).
59. Leckie, F.A., "The Application of Transfer Matrices to Plate Vibrations," Ingenieur-Archiv, Vol.XXXII, 1963, pp.100-111.
60. Dokainish, M.A., "A New Approach for Plate Vibrations: Combination of Transfer Matrix and Finite-Element Technique," Trans. ASME, Vol.94, No.2, 1972, pp.526-530.
61. McDaniel, T.J. and Eversole, K.B., "A Combined Finite Element-Transfer Matrix Structural Analysis Method," Journal of Sound & Vibration, Great Britain, Vol.51, No.2, 1977, pp.157-169.
62. Chiatti, G. and Sestieri,A, "Analysis of Static and Dynamic Structural Problems by a Combined Finite Element - Transfer Matrix Method," Journal of Sound & Vibration, Vol.67, No.1, 1979, pp.35-42.

63. Sankar, S. and Hoa, S.V., "An Extended Transfer Matrix - Finite Element Method for Free Vibration of Plates," Journal of Sound & Vibration, Vol.70, No.2, 1980, pp.205-211.
64. Mucino, V.H. and Pavelic, V., "An Exact Condensation Procedure for Chain-Like Structures Using a Finite Element - Transfer Matrix Approach," Trans. ASME, J. Mech. Des., No.80-C2/DET-123, 1980, pp.1-9.
65. Ohga, M., Shigematsu, T. and Hara, T., "Structural Analysis by a Combined Finite Element - Transfer Matrix Method," Computers & Structures, Pergamon Press, Vol.17, No.3, 1983, pp.321-326.
66. Ohga, M., Shigematsu, T. and Hara, T., "A Combined Finite Element - Transfer Matrix Method," J. ASCE Vol.110, No.EM9, September, 1984, pp.1335-1349.
67. Degen, E.E., Shephard, M.S. and Loewy, R.G., "Combined Finite Element - Transfer Matrix Method Based on a Mixed Formulation," Computers & Structures, Vol.20, No.1-3, 1985, pp.173-180.
68. Ohga, M. and Hara, T., "Analysis of Thin-Walled Members by Finite Element - Transfer Matrix Method," Proc. of JSCE, No.368/I-5, April, 1986, pp.95-102.
69. Ohga, M. and Shigematsu, T., "Transient Analysis of Plates by a Combined Finite Element - Transfer Matrix Method," Computers & Structures, Vol.26, No.4, 1987, pp.543-549.
70. Ohga, M. and Shigematsu, T., "Large Deformation Dynamic Analysis of Plates," J. ASCE, Vol.114, No.EM4, April, 1988, pp.624-637.
71. Tomlin, G.R. and Butterfield, R., "Elastic Analysis of Zoned Orthotropic Continua," J. ASCE, Vol.100, No.EM3, June, 1974, pp.511-529.
72. Banerjee, P.K., "Integral Equation Methods for Analysis of Piece-Wise Non-Homogeneous Three-Dimensional Elastic Solids of Arbitrary Shape," Int. J. Mech. Sci., Vol.18, 1976, pp.293-303.
73. Lachat, J.C. and Watson, J.O., " Progress in the Use of Boundary Integral Equations, Illustrated by Examples," Comput. Meth. Appl. Mech. Engng, Vol.10, 1977, pp.273-289.
74. Zienkiewicz, O.C., Kelly, D.W. and Bettes, P., "The Coupling of the Finite Element Method and Boundary Solution Procedures," Int. J. Num. Meth. Eng., Vol.11, 1977, pp.355-375.
75. Kelly, D.W., Mustoe, G.G.W. and Zienkiewicz, O.C., "Coupling Boundary Element Methods with Other Numerical Methods", Developments in Boundary Element Methods-1, Appl. Science Publishers, 1979, pp.65-95.

76. Margulles, M., "Exact Treatment of the Exterior Problem in the Combined FEM-BEM," New Developments in Boundary Element Methods, CML Publications, Southmpton/U.K., 1980, pp.43-63.
77. Komatsu, S., Nagai, M. and Nishimaki, T., "Three-Dimensional Analysis of Thin-Walled Box Girders by Analytical Combination of Boundary Element Method and Block Element Method," Proc. of JSCE, No.334, June, 1983, pp.13-24 (in Japanese).
78. Banerjee, P.K. and Butterfield, R., "Boundary Element Methods in Geomechanics," In Finite Elements in Geomechanics. Wiley, New York, 1977.
79. Ohga, M., Shigematsu, T. and Hara, T., "Structural Analysis by a Combined Boundary Element - Transfer Matrix Method," Computers & Structures, Vol.24, No.3, 1986, pp.385-389.
80. Ohga, M. and Shigematsu, T., "Bending Analysis of Plates with Variable Thickness by Boundary Element - Transfer Matrix Method," Computers & Structures, Vol.28, No.5, 1988, pp.635-640.

Chapter 2 STRUCTURAL ANALYSIS BY A COMBINED FINITE ELEMENT-TRANSFER MATRIX METHOD

2-1 INTRODUCTION

The finite element method is the most widely used and powerful tool for structural analysis. However, the disadvantage of this method is that, in the case of a complex structure, it is necessary to use a large number of nodes, resulting in very large matrices which require large computers for their management and regulation. In order to reduce the size of the matrices in the ordinary finite element method, some techniques have been proposed (condensation, substructuring method) (7).

One numerical technique for reducing matrix size in the ordinary finite element method is the use of finite strips (FSM) suggested by Cheung (1). Another is the transfer matrix technique (TMM). Leckie(5) applied this method to plate vibration problems. At that time, the problems were formulated by using the Hrennikoff model. The above techniques (FSM, TMM) can be successfully applied only for simple structures with particular boundary conditions; otherwise considerable complications arise in the formulation of problems.

Dokainish(3) used the combined finite element - transfer matrix (FETM) method in the study of the dynamics of tapered or rectangular plate. Since the size of stiffness and mass matrix, in his method, was equal to the number of degrees of one strip, the frequency determinant for a clamped-clamped plate considered by Dokainish was 18x18 by the FETM method compared to a 108x108 matrix eigenvalue problem obtained using the standard finite element method with the same number of nodes.

McDaniel and Eversole(6) have proposed a similar approach in treating a stiffened plate structures along with some numerical values that warrant consideration.

In dealing with complex structures, Chiatti and Sestieri(2) introduced isoparametric shell elements, taking into consideration elements with nodes situated not only on corners but also on the midpoints of edges.

Sankar and Hoa(15) offered an approach, in which an extended transfer matrix relating the state vectors which consist of state variables (displacements and forces) and their derivatives with respect to frequency was used. In this method, a Newton-Raphson iterative technique is used to determine natural frequencies.

Mucino and Pavelic(9), as a further generalization of the FETM method, have proposed a method in which structures are modeled by means of substructures connected in a chain-like manner. For each of these substructures, a transfer matrix was derived.

Application of the FETM method is generally found in literature concerned with vibration problems of structure. This paper shows a successful application of the FETM method to other structural fields, especially to bending and buckling problems. Also, various techniques for treating the more complicated structures, especially those with the intermediate conditions are presented.

Some numerical examples of bending and buckling problems are proposed and their results are compared with those obtained by the ordinary finite element method and others.

2-2 FINITE ELEMENT-TRANSFER MATRIX METHOD

Fig.2-1 shows a plate divided into m strips and each of which subdivided into finite elements. The vertical sides dividing or bordering the strips are called sections, while the horizontal boundaries are the edges. Thus **BE** is the left section of strip i+1 and the right sections of i. There are a total of 2n nodes on strip i with n nodes on the left section **AD** and n nodes on the right section **BE**.

To derive the transfer matrix relating the left and right state variables (displacements and forces) of the strip i, it is required first to determine the stiffness matrix $\mathbf{K}_i$ of strip i: we obtain

$$\mathbf{K}_i \ \boldsymbol{\delta}_i = \mathbf{F}_i \qquad \cdots\cdots\cdots\cdots (2\text{-}1)$$

where $\mathbf{K}_i$ is the stiffness matrix of strip i, $\boldsymbol{\delta}_i$, $\mathbf{F}_i$ are the displacements and forces of strip i, respectively.

Eq.(2-1) holds well for bending problems, but in buckling problems, the matrix $\mathbf{K}_i$ in Eq.(2-1) becomes:

$$\mathbf{K}_i = \mathbf{K}_{b\,i} - \mathbf{P}\ \mathbf{K}_{m\,i} \qquad \cdots\cdots\cdots\cdots (2\text{-}2)$$

where $\mathbf{K}_{b\,i}$ and $\mathbf{K}_{m\,i}$ are the bending stiffness matrix and the modified stiffness matrix of strip i, respectively; **P** is the in-plane load.

Matrix $\mathbf{K}_i$ is partitioned into four submatrices. Eq.(2-1) then becomes:

$$\begin{bmatrix} \mathbf{K}_{\ell\ell} & \mathbf{K}_{\ell r} \\ \mathbf{K}_{r\ell} & \mathbf{K}_{rr} \end{bmatrix}_i \begin{Bmatrix} \boldsymbol{\delta}_\ell \\ \boldsymbol{\delta}_r \end{Bmatrix}_i = \begin{Bmatrix} \mathbf{F}_\ell \\ \mathbf{F}_r \end{Bmatrix}_i \qquad \cdots\cdots\cdots\cdots (2\text{-}3)$$

where $\boldsymbol{\delta}_\ell$, $\boldsymbol{\delta}_r$, $\mathbf{F}_\ell$ and $\mathbf{F}_r$ are the left and right displacements and forces of strip i, respectively. By expanding Eq.(2-3) and solving for $\boldsymbol{\delta}_{r\,i}$ and $\mathbf{F}_{r\,i}$ in terms of $\boldsymbol{\delta}_{\ell\,i}$ and $\mathbf{F}_{\ell\,i}$ the following equations can be obtained;

$$\delta_{ri} = -K_{\ell r}^{-1} K_{\ell\ell} \delta_{\ell i} + K_{\ell r}^{-1} F_{\ell i} \qquad \cdots\cdots\cdots\cdots (2\text{-}4a)$$

and

$$F_{ri} = K_{r\ell} - K_{rr} K_{\ell r}^{-1} K_{\ell\ell} \delta_{\ell i} + K_{rr} K_{\ell r}^{-1} F_{\ell i} \qquad \cdots\cdots\cdots\cdots (2\text{-}4b)$$

which, when arranged in matrix form, become:

$$\begin{Bmatrix} \delta_r \\ F_r \\ 1 \end{Bmatrix}_i = \begin{bmatrix} -K_{\ell r}^{-1} K_{\ell\ell} & K_{\ell r}^{-1} & 0 \\ K_{r\ell} - K_{rr} K_{\ell r}^{-1} K_{\ell\ell} & K_{rr} K_{\ell r}^{-1} & 0 \\ 0 & 0 & 1 \end{bmatrix}_i \begin{Bmatrix} \delta_\ell \\ F_\ell \\ 1 \end{Bmatrix}_i \qquad \cdots\cdots\cdots (2\text{-}5)$$

On simplifying the notation, we obtain:

$$\begin{Bmatrix} \delta_r \\ F_r \\ 1 \end{Bmatrix}_i = \begin{bmatrix} T_{11} & T_{12} & 0 \\ T_{21} & T_{22} & 0 \\ 0 & 0 & 1 \end{bmatrix}_i \begin{Bmatrix} \delta_\ell \\ F_\ell \\ 1 \end{Bmatrix}_i \qquad \cdots\cdots\cdots\cdots (2\text{-}6)$$

or

$$z_{ri} = T_i z_{\ell i} \qquad \cdots\cdots\cdots\cdots (2\text{-}7)$$

Eq.(2-7) can be recognized as the transfer matrix relating the state vectors z_r and z_ℓ which consist of the displacements and forces.

After continuous multiplications of the transfer matrix T, we obtain the relation between the state vectors at two ends of the structure:

$$z_m = U z_0 \qquad \cdots\cdots\cdots\cdots (2\text{-}8)$$

where $U = T_m T_{m-1} \cdots T_1$.

In bending problems, on considering the left and right boundary conditions of the structure, simultaneous equations are obtained from Eq.(2-8). The number of these equations is as same as that of the unknown state variables in z_0. Thus, we can evaluate the unknown elements in $\mathbf{z}_0$ by solving these equations (13).

On the other hand, in buckling problems, it is essential that the determinant of a portion $\bar{\mathbf{U}}$ of the matrix U be zero:

$$\det |\bar{\mathbf{U}}| = 0 \qquad \cdots\cdots\cdots\cdots (2\text{-}9)$$

Now, the matrix $\bar{\mathbf{U}}$ is obtained from the matrix U by deleting the columns corresponding to zero elements of $\mathbf{z}_0$ and the rows corresponding to the nonzero elements of $\mathbf{z}_m$.

2-3 TECHNIQUES FOR INTERMEDIATE CONDITIONS

1) Point Matrix for Elastic Columns

Point matrix for treating structure with elastic columns at the intermediate section, as shown in Fig.2-2, is obtained by taking the elastic support restoring forces into consideration.

Consider, for example, elastic columns attached to nodes ℓ and m of section i (Fig.2-2). The relations of the shearing forces at the left and right of the section i are then,

$$Q_{i1}{}^R = Q_{i1}{}^L, \quad Q_{i2}{}^R = Q_{i2}{}^L, \ldots, \quad Q_{i\ell}{}^R = Q_{i\ell}{}^L + k_\ell w_{i\ell}, \ldots,$$
$$Q_{im}{}^R = Q_{im}{}^L + k_m w_{im}, \ldots, \quad Q_{ij}{}^R = Q_{ij}{}^L$$
$$\cdots\cdots\cdots\cdots (2\text{-}10)$$

where k_ℓ and k_m are the elastic column stiffness; superscripts L and R indicate the left and right sides of the section. Since other elements of the state vector are continuous throughout section i, the following identity exists:

$$\mathbf{w}_i{}^R = \mathbf{w}_i{}^L, \quad \boldsymbol{\theta}_{xi}{}^R = \boldsymbol{\theta}_{xi}{}^L, \quad \boldsymbol{\theta}_{yi}{}^R = \boldsymbol{\theta}_{yi}{}^L,$$
$$\mathbf{M}_{xi}{}^R = \mathbf{M}_{xi}{}^L, \quad \mathbf{M}_{yi}{}^R = \mathbf{M}_{yi}{}^L \qquad \cdots\cdots\cdots\cdots (2\text{-}11)$$

In matrix notation, Eqs.(2-10) and (2-11) become:

$$
\begin{Bmatrix} w_1 \\ w_2 \\ \cdot \\ w_\ell \\ \cdot \\ w_m \\ \cdot \\ w_j \\ \theta_x \\ \theta_y \\ Q_1 \\ Q_2 \\ \cdot \\ Q_\ell \\ \cdot \\ Q_m \\ \cdot \\ Q_j \\ M_x \\ M_y \end{Bmatrix}_i^R
=
\left[\begin{array}{cccccccc|cc|cccccccccc}
1 \\
& 1 \\
&& \cdot \\
&&& 1 \\
&&&& \cdot \\
&&&&& 1 \\
&&&&&& \cdot \\
&&&&&&& 1 \\ \hline
&&&&&&&& I \\
&&&&&&&&& I \\ \hline
0 &&&&&&&&&& 1 \\
& 0 &&&&&&&&&& 1 \\
&& \cdot &&&&&&&&&& \cdot \\
&&& k_\ell &&&&&&&&&& 1 \\
&&&& \cdot &&&&&&&&&& \cdot \\
&&&&& k_m &&&&&&&&&& 1 \\
&&&&&& \cdot &&&&&&&&&& \cdot \\
&&&&&&& 0 &&&&&&&&&& 1 \\ \hline
&&&&&&&&&&&&&&&&&& I \\
&&&&&&&&&&&&&&&&&&& I
\end{array}\right]
\begin{Bmatrix} w_1 \\ w_2 \\ \cdot \\ w_\ell \\ \cdot \\ w_m \\ \cdot \\ w_j \\ \theta_x \\ \theta_y \\ Q_1 \\ Q_2 \\ \cdot \\ Q_\ell \\ \cdot \\ Q_m \\ \cdot \\ Q_j \\ M_x \\ M_y \end{Bmatrix}_i^L
\qquad \cdots\cdots (2\text{-}12)
$$

or

$$
\mathbf{z}_i^R = \mathbf{P}_k \ \mathbf{z}_i^L \qquad \cdots\cdots (2\text{-}13)
$$

2) Point Matrix for Ribs

In the orthogonally stiffened plate, as shown in Fig.2-3(a), the plate is divided into strips containing x-rib (shown in Fig.2-3(b)) and lines containing y-rib (shown in Fig.2-3(c)). Therefore, x-rib is included in the transfer matrix described previously but y-rib must be considered in the point matrix.

Considering the continuous condition of displacements and equilibrium condition of forces at the y-rib line, we obtain the following expression:

$$\mathbf{w}^R = \mathbf{w}^L, \qquad \boldsymbol{\theta}_x{}^R = \boldsymbol{\theta}_x{}^L, \qquad \boldsymbol{\theta}_y{}^R = \boldsymbol{\theta}_y{}^L$$
$$\mathbf{Q}^R = \mathbf{Q}^L + \mathbf{Q}^*, \quad \mathbf{M}_x{}^R = \mathbf{M}_x{}^L + \mathbf{M}_x{}^*, \quad \mathbf{M}_y{}^R = \mathbf{M}_y{}^L + \mathbf{M}_y{}^* \qquad \cdots(2\text{-}14)$$

where L and R indicate the left and right sides of y-rib line, $\mathbf{Q}^*$, $\mathbf{M}_x{}^*$ and $\mathbf{M}_y{}^*$ are nodal forces on the y-rib.

Introducing the stiffness matrix for y-rib line, the nodal forces on the y-rib in Eq.(2-14) are related to the nodal displacements as follows:

$$\{\mathbf{Q}^* \ \mathbf{M}_x{}^* \ \mathbf{M}_y{}^*\}^T = \mathbf{K}^* \ \{\mathbf{w} \ \boldsymbol{\theta}_x \ \boldsymbol{\theta}_y\}^T \qquad \cdots\cdots\cdots\cdots(2\text{-}15)$$

where $\mathbf{K}^*$ is the stiffness matrix for y-rib line. Substituting Eq.(2-15) into Eq.(2-14) and eliminating the nodal forces, $\mathbf{Q}^*$, $\mathbf{M}_x{}^*$, $\mathbf{M}_y{}^*$, the state vector at the left and right sides of y-rib line are related as follows:

$$\begin{Bmatrix} \mathbf{w} \\ \boldsymbol{\theta}_x \\ \boldsymbol{\theta}_y \\ \mathbf{Q} \\ \mathbf{M}_x \\ \mathbf{M}_y \end{Bmatrix}^R = \left[\begin{array}{c|c} \mathbf{I} & \mathbf{0} \\ \hline \mathbf{K}^* & \mathbf{I} \end{array} \right] \begin{Bmatrix} \mathbf{w} \\ \boldsymbol{\theta}_x \\ \boldsymbol{\theta}_y \\ \mathbf{Q} \\ \mathbf{M}_x \\ \mathbf{M}_y \end{Bmatrix}^L \qquad \cdots\cdots\cdots\cdots(2\text{-}16)$$

or

$$\mathbf{z}^R = \mathbf{P}_r \ \mathbf{z}^L \qquad \cdots\cdots\cdots\cdots(2\text{-}17)$$

Consequently the matrix $\mathbf{P}_r$ is referred to as the point matrix for the y-rib line. Eq.(2-13) relates the left state vectors of the section which has some elastic columns, to the right state vectors. Consequently the matrix $\mathbf{P}_k$ is referred to as the point matrix for the elastic column.

3) Intermediate Rigid Conditions

Point matrix for elastic columns break down when elastic columns become infinitely stiff. In this case, since the deflections at the intermediate rigid columns are zero, the initial unknowns corresponding to the constrained displacements can be eliminated and introduced new unknowns.

For example, consider the structure, shown in Fig.2-4, which has rigid columns at nodes ℓ and m of section i, with its left boundary simply supported. The equation relating the left state vector of the section i, $\mathbf{z}_i{}^L$, to the initial unknowns, $\mathbf{z}_0$, is

$$\mathbf{z}_i{}^L = \mathrm{U}_i \ \mathbf{z}_0 \qquad \cdots\cdots\cdots\cdots (2\text{-}18)$$

From the left boundary condition $\mathbf{w}_0 = \boldsymbol{\theta}_{x0} = \mathbf{M}_{y0} = 0$, the elementary form of Eq.(2-18) is

$$\{\mathbf{w}^L \quad \boldsymbol{\theta}_x{}^L \quad \boldsymbol{\theta}_y{}^L \quad \mathbf{Q}^L \quad \mathbf{M}_x{}^L \quad \mathbf{M}_y{}^L\}_i{}^T = \mathrm{U}_i \ \{\boldsymbol{\theta}_y \quad \mathbf{Q} \quad \mathbf{M}_x\}_0{}^T \qquad \cdots\cdot (2\text{-}19)$$

Setting $w_{i\ell} = w_{im} = 0$ from the rigid conditions at the node ℓ and m, we obtain the following two equations:

$$\mathrm{U}_{\ell i} \ \{\boldsymbol{\theta}_y \quad \mathbf{Q} \quad \mathbf{M}_x\}_0{}^T = w_{i\ell} = 0$$
$$\mathrm{U}_{m i} \ \{\boldsymbol{\theta}_y \quad \mathbf{Q} \quad \mathbf{M}_x\}_0{}^T = w_{im} = 0 \qquad \cdots\cdots\cdots\cdots (2\text{-}20)$$

where $\mathrm{U}_{\ell i}$ and U_{mi} are the ℓ-th, m-th row of the matrix U_i, respectively, $w_{i\ell}$ and w_{im} are the deflection at nodes ℓ and m of section i. Solving Eq.(2-20) for $Q_{o\ell}$ and Q_{om}, we eliminate these two shearing forces from the initial state vector $\mathbf{z}_o$.

Because of the reactions at the rigid columns, the shearing forces at these points are discontinuous. Introducing the new unknown $V_{i\ell}$ and V_{im} instead of $Q_{o\ell}$ and Q_{om} just above eliminated the right state vectors of section i are expressed as,

$$\{\mathbf{w}^R \quad \theta_x{}^R \quad \theta_y{}^R \quad \mathbf{Q}^R \quad \mathbf{M}_x{}^R \quad \mathbf{M}_y{}^R\}_i{}^T = U_i{}'\{\theta_y \quad \mathbf{Q}' \quad \mathbf{M}_x\}_0{}^T \quad \cdots(2\text{-}21)$$

where

$$\mathbf{Q}_o{}' = \{Q_{o1},\ Q_{o2}, \ldots,\ V_{i1}, \ldots,\ V_{im}, \ldots,\ Q_{on}\}^T.$$

By the above technique, the transfer procedure can be performed throughout a section having intermediate rigid columns.

The structure which has the intermediate simple support as shown in Fig.2-5 can be treated as previously described. In this case, the deflections and rotations about the x-axis are constrained at the intermediate simple support. By eliminating the initial shear forces and moments about the x-axis, which correspond to the constrained displacements, from the initial state vector $\mathbf{z}_0$, the new unknown discontinuous shears and moments can be introduced to the state vector $\mathbf{z}$.

2-4 NUMERICAL EXAMPLES

1) Bending Analysis of a Plate Structure

In order to investigate the accuracy and efficiency of the proposed method in bending problems of plate structures, the simply supported rectangular plates subjected to the uniform load and the concentrated load at the center of the plate are analysed. A quarter of the plate is divided into 1x1, 2x2, 3x3,····· and 10x10 elements as shown in Fig.2-6.

The rectangular element with three degrees of freedom per one node, shown in Fig.2-7, is used in examples of this chapter; the deflection w is assumed to have the form,

$$w = a_1 + a_2\bar{x} + a_3\bar{y} + a_4\bar{x}^2 + a_5\overline{xy} + a_6\bar{y}^2 + a_7\bar{x}^3 + a_8\bar{x}^2\bar{y} + a_9\overline{xy}^2 + a_{10}\bar{y}_3 + a_{11}\bar{x}_3\bar{y} + a_{12}\overline{xy}_3 \quad \cdots\cdots\cdots\cdots(2\text{-}22)$$

where $\bar{x}=x/a$, $\bar{y}=y/b$ and $a_1,\ldots,a_{12}$ are unknown coefficients.

Fig.2-8 shows the convergence condition of the deflection at the center of the plate. Although the results for the uniform load converge little faster than those for the concentrated load, the results for both loads in 6x6 mesh pattern converge within 1 %. In Fig.2-8 the solutions obtained by the finite element method are also shown. In the finite element method the same element and mesh patterns as those used in the FETM method are employed. Good agreement exists between the results obtained by both methods.

Fig.2-9 shows a comparison of the matrix sizes (sizes of the resultant system) required in the finite element and the FETM methods. It is assumed here that in the finite element method the banded matrix is used. The matrix sizes in both methods increase as the number of elements increases. Increasing rate of the matrix size in the FETM method is, however, smaller than that in the finite element method, because the matrix size in the FETM method is dependent on the number of degrees of freedom for one strip in contrast with the finite element method which depends on that for the entire structure.

The matrix size in the finite element method is given by {(the number of total nodes) × (degrees of freedom)} × (the band width). The matrix to be considered in the finite element method is, therefore, $48\times18=864$ for 3-3 mesh pattern and $363\times39=14157$ for 10-10 mesh pattern. Thus the matrix size for latter mesh pattern is 16.4 times larger than that for the former pattern. On the other hand, the matrix size in the FETM method is given by $\{(\text{the number of nodes on a section}) \times (\text{degrees of freedom}) \times 2\}^2$. The matrix to be considered in the FETM method is, therefore, $24\times24=576$ for 3-3 mesh pattern (3 strips mesh pattern) and $66\times66=4356$ for 10-10 pattern (10 strips pattern). The matrix size for latter mesh pattern is, therefore, only 7.6 times larger than that for the former pattern.

A uniformly loaded and simply supported rectangular plate with rib, shown in Fig.2-10(a), is analysed. In this example, a half of the plate is divided into 10 strips and each strip into 5 elements as shown in Fig.2-10(a).

The point matrix for the rib, P_r, is in this example used in considering the rib. The transformation procedure is performed by multiplications of not only the transfer matrix, T, but also the point matrix, P_r:

$$z_{10} = T_{10}\ T_9 \cdots T_7\ T_6\ P_{r5}\ T_5\ T_4\ \cdots\ T_2\ T_1\ z_0 \qquad \cdots\cdots\cdot(2\text{-}23)$$

In Fig.2-10(a), the deflections along the symmetric line obtained by the FETM method are compared with those by the finite element method, in which the same element as that used in the FETM method is employed. It can be seen that the results obtained by both methods are in complete agreement with each other.

The matrix to be considered in the finite element method is, if the banded matrix is used, 198x24, compared to 36x36 for the FETM method.

The deflections for $E_r I_r = \infty$ are also shown in Fig.2-10(a). In this case, the transformation procedure can be performed in a simple schematic manner by using the technique for intermediate simple support described in this chapter. The results by the FETM method agree well with those by the finite element method. In Fig.2-10(b), the deflections along the symmetric line for the case of partial load are shown and similar results to previous example are obtained.

A partially loaded and all edges clamped rectangular slab stiffened orthogonally, shown in Fig.2-11(a), is analysed. In this example, the slab is divided into 18 strips and each strip into 6 rectangular finite elements, as shown in Fig.2-11(a).

As described in Section 2-3, although x-rib is included in the transfer matrix, y-rib must be considered in point matrix for the rib. The transformation procedure for this strips mesh pattern:

$$\mathbf{z}_{18} = \mathbf{T}_{18}\ \mathbf{T}_{17}\cdots\mathbf{T}_{13}\ \mathbf{P}_{r12}\ \mathbf{T}_{12}\cdots\ \mathbf{T}_{7}\ \mathbf{P}_{r6}\ \mathbf{T}_{6}\cdots\mathbf{T}_{2}\ \mathbf{T}_{1}\ \mathbf{z}_{0} \qquad \cdots\cdots\cdots\cdots\cdots (2\text{-}24)$$

In Fig.2-11(b), the deflections along the symmetric line obtained by the FETM method are compared with those by the finite element method, in which the same element as that used in the FETM method is employed. It can be seen that the results obtained by both methods are in complete agreement with each other. The matrix to be considered in the finite element method is, if the banded matrix is used, 399x27 for 18 strips mesh pattern, compared 42x42 for the FETM method.

The deflections for $E_r I_r = \infty$ are also shown in Fig.2-11(b). In this case, the transformation procedure can be performed in a simple schematic manner by using the technique for intermediate simple support. The deflections by the FETM method agree well with those by the finite element method.

To illustrate the efficiency of the technique for an intermediate rigid column and the point matrix for an elastic one, a bridge deck with four intermediate columns acted upon by partially distributed loads, shown in Fig.2-12(a), is analysed. It is divided into 16 strips and each strip into 8 elements, as shown in Fig.2-12(b).

In Fig.2-12(b), the deflections in the case of intermediate rigid columns by the FETM method are compared with those by the finite element method. It can be seen that these results agree well with each other. In this example, the matrix size in the finite element method is 459x33 for banded matrix, while in the

FETM method the order of the matrix is only 54x54.

The deflections for the intermediate elastic columns are shown together in Fig.2-12(b). In this case, the transformation procedure was performed by introducing the point matrix for the elastic column P_k :

$$z_8 = T_8 \ T_7 \ P_{k6} \ T_6 \cdots P_{k2} \ T_2 \ T_1 \ z_0 \qquad \cdots\cdots\cdots\cdots(2\text{-}25)$$

2) Buckling Analysis of a Plate Structure

The same element and degree of freedom in bending problems are, also, used in buckling problems.

A uniformly compressed rectangular plate supported simply along two opposite sides perpendicular to the direction of compression and having two other free sides is analysed. A plate is, in this example, divided into 6 strips and each strip into 6 finite elements.

In Fig.2-13, the buckling coefficients obtained by the FETM method are compared with those by the finite element method and Euler buckling theory (16). In the finite element method the same mesh pattern as in the FETM method is used. Close agreement exists between the results of the FETM and finite element methods and these are agree well with the Euler buckling coefficients.

A simply supported rectangular plate under uniform compression is analysed. The plate is divided into 4, 6, 8, 10 and 12 strips along the direction of compression and each strip into 4 elements, as shown in Fig.2-14(b).

The buckling coefficients obtained by the FETM method and the finite element method are indicated in Fig.2-14(a). The accuracy of these results decreases as the ratio of the plate, a/b, increases, i.e., the number of half-waves of the buckling mode in the direction of compression increases. The accuracy of the results, however, improves as the number of strips, i.e., the number of elements in the direction of compression increases as shown in Fig.2-14(a). It becomes clear that, in the buckling analysis of the long plate, a plate should be divided into many elements in the direction of compression in the finite element method, and many strips in the FETM method. Since the matrix size in the FETM method is dependent on the number of degrees of freedom for only one strip as mentioned previously, the matrix size for every mesh pattern employed in this example is same, 30×30. While in the finite element method, if banded matrix is used, it is 75×21 for 4-4 mesh pattern (4 strips mesh pattern) and 195×21 for 4-12 mesh pattern (12 strips mesh pattern). The matrix size in the finite element method is, therefore, 1.75 and 4.55 times larger than that in the FETM method, respectively.

In Fig.2-15 the buckling coefficients of an all edges clamped rectangular plate under uniform compressions obtained by the FETM method are compared with the exact solutions and those obtained by the finite element method. Similar results as in the previous examples are observed.

Biaxially compressed plate with two adjacent clamped edges and two other simply supported edges as shown in Fig.2-16 is analysed. The transfer matrix for the strip subjected to biaxial compressions is, in this example, employed. The plate is, here, divided into 6 strips and each strip into 6 finite elements. In Fig.2-16 the results obtained by the FETM method are compared with those by Iwato and Ban(4) for the ratios of the load β = P_y/P_x = 0., 0.5, 1.0 and 1.5. Although the results of the FETM method are little smaller than other results, good agreement exists between both results.

As the next buckling problem example, a simply supported rectangular plate with a longitudinal stiffener(x-rib) under uniform compression as shown in Fig.2-17 is analysed. The plate is divided into 6 and 10 strips, and each strip into 6 elements in both mesh patterns. The transfer matrix is, in this example, derived from the stiffness matrices for the strip and x-rib. The ratio of the cross section area between the plate and stiffener is $\delta = A_r/bt = 0.1$ and the ratio of the rigidity is $\gamma = E_r I_r/D = 5$ and 10, where A_r, E_r and I_r = cross section area, modulus of elasticity and moment of inertia of the rib, respectively, b, t and D = width, thickness and flexural rigidity of the plate, respectively.

In Fig.2-17 the buckling coefficients obtained by the FETM method are compared with those obtained by the finite element method, and cross agreement exists between both results.

The buckling coefficients for simply supported plate with intermediate support are given simultaneously in Fig.2-17, to provide the upper limit of the buckling coefficient for this case.

A uniformly compressed rectangular plate clamped along two opposite sides perpendicular to the direction of compression and having reinforced free edges by stiffeners along the other two sides as shown in Fig.2-18, is analysed. The plate is divided into 6 and 12 strips, and each strip, as in the previous example, into 6 elements. The ratio of rigidity is $\gamma = 0, 1, 3, 5$ and the ratio of area is $\delta = 0.1$.

As shown in Fig.2-18, close agreement in the results by the FETM method and the finite element method is obtained. The buckling coefficients for the plate clamped along two opposite sides perpendicular to the direction of compression and simply supported along the other two sides are given simultaneously in Fig.2-18, to provide the upper limit of the buckling coefficient in this case.

Fig.2-19 shows the buckling coefficients of a simply supported rectangular plate with a transverse stiffener(y-rib) under uniform compression as shown in Fig.2-19, obtained by the FETM method and the finite element method. A plate is divided into 6 and 10 strips and each strip into 6 elements in both mesh patterns. The ratio of rigidity is γ = 5 and the ratio of area is δ = 0.1. The transfer procedure is, in this example, performed by multiplications of the transfer matrix and the point matrix for the stiffener, and is described for 6 strips pattern as follows:

$$\mathbf{z}_6 = \mathbf{T}_6 \ \mathbf{T}_5 \ \mathbf{T}_4 \ \mathbf{P}_{r\,3} \ \mathbf{T}_3 \ \mathbf{T}_2 \ \mathbf{T}_1 \ \mathbf{z}_0 \qquad \cdots\cdots\cdots\cdots (2\text{-}26)$$

Good agreement exists in the results obtained by both methods. In Fig.2-19 the results for simply supported continuous plates are given simultaneously to provide the upper limit of the buckling coefficient for this case.

As the last buckling problem example, a simply supported rectangular plate stiffened orthogonally under a uniform compression is analysed. The same mesh pattern as in the previous example is employed, and the ratio of rigidity is γ = 5, 10 and the ratio of area is δ = 0.1. In Fig.2-20 the buckling coefficients obtained by the FETM method are compared with those by the finite element method and exact solutions (14). Although cross agreement exists between the results by the FETM and finite element methods, the accuracy of these results decreases as the buckling mode increases. But it is seen that the accuracy of the results improve as the number of strips increases.

2-5 CONCLUSIONS

In this chapter, the procedures of the combined finite element - transfer matrix method are applied to the bending and buckling problems of plated structures. Furthermore techniques for treating the complicated structures such as those with intermediate elastic and rigid columns, and with stiffeners are proposed. From the numerical examples presented in this chapter, following conclusions are obtained.

(1) In bending and buckling problems good agreement exists between the FETM solutions and the exact solutions, which demonstrates the accuracy of this method.

(2) Since the size of the transfer matrix in the FETM method is equal to the number of degrees of only one strip, this method has the advantage of reducing the size of matrix to less than that obtained by the ordinary finite element method for long plated structures.

(3) Point matrices for elastic support and rib make possible the application of the FETM method to bending and buckling problems of the plates with intermediate elastic supports and stiffeners.

(4) By using the techniques for intermediate rigid column and simple support, the transformation procedure can be performed in a simple schematic manner.

REFERENCES

1. Cheung, Y.K., "Finite Strip Method in Structural Analysis," Pergamon Press, Oxford, England, 1976.
2. Chiatti, G. and Sestieri, A., "Analysis of Static and Dynamic Structural Problems by a Combined Finite Element-Transfer Matrix Method," J. Sound & Vibration, Vol.67, No.1, 1979, pp.35-42.
3. Dokainish, M.A., "A New Approach for Plate Vibrations: Combination of Transfer Matrix and Finite-Element Technique," Trans. ASME, Vol.94, No.2, 1972, pp.526-530.
4. JAPAN, C.R.C. ed., "Handbook of Structural Stability," Corona, Tokyo, 1971.

5. Leckie, F.A., "The Application of Transfer Matrices to Plate Vibrations," Ingenieur-Archiv, Vol.XXXII, 1963, pp.100-111.
6. McDaniel, T.J. and Eversole, K.B., "A Combined Finite Element-Transfer Matrix Structural Analysis Method," J. Sound & Vibration, Great Britain, Vol.51, No.2, 1977, pp.157-169.
7. McGuire, W. and Gallagher, R.H., "Matrix Structural Analysis," John Wiley & Sons, Inc., New York, N.Y., 1979.
8. Misawa, S., Shigematsu, T., Ohga, M. and Hara, T., "On the Buckling Analysis of Plates by FE-TM Method," Memoirs of the Faculty of Engineering, Ehime University Vol.10, No.1, February 1982, pp.133-142 (in Japanese).
9. Mucino, H.V. and Pavelic, V., "An Exact Condensation Procedure for Chain-Like Structures Using a Finite Element-Transfer Matrix Approach," Trans. ASME, J. Mech. Des., No.80-C2/DET-123, 1980, pp.1-9.
10. Nath, B., "Fundamentals of Finite Elements for Engineers," The Athlone Press of the University of London, London, England, 1974.
11. Ohga, M., Shigematsu, T. and Hara, T., "On the Bending Analysis of Plates by FE-TM Method," Memoirs of the Faculty of Engineering, Ehime University, Vol.10, No.2, February 1983, pp.151-159 (in Japanese).
12. Ohga, M., Shigematsu, H. and Hara, T., "Structural Analysis by a Combined Finite Element-Transfer Matrix Method," Computers & Structures, Vol.17, No.3, 1983, pp.321-326.
13. Pestel, E.C. and Leckie, F.A., "Matrix Method in Elastomechanics," McGraw-Hill Book Co., Inc., New York, N.Y., 1963.
14. Pflüger, A., "Stabilitätsprobleme der Elastostatic," Springer-Verlag, Berlin, 1975.
15. Sankar, S., and Hoa, S.V., "An Extended Transfer Matrix-Finite Element Method for Free Vibration of Plates," J. Sound & Vibration, Vol.70, No.2, 1980, pp.205-211.
16. Timoshenko, S.P. and Gere, J.M., "Theory of Elastic Stability," McGraw-Hill, New York, 1961.
17. Timoshenko, S.P. and Woinowsky-Krieger S., "Theory of Plates and Shells," McGraw-Hill, New York, 1959.

NOTATION

The following symbols are used in this paper:

A_r = cross section area of rib;
a = dimension of finite element or plate;
b = dimension of finite element or plate;
D = flexural rigidity of plate $(Et^3/12(1-\nu^2))$;
E = modulus of elasticity of plate;
E_r = modulus of elasticity of rib;
$\mathbf{F}$ = force vector;
I_r = moment of inertia of rib;
$\mathbf{K}_i$ = stiffness matrix of strip i;
$\mathbf{K}$ = stiffness matrix of rib;
k = buckling coefficient $(Pb^2/\pi^2 D)$;
$\mathbf{P}_k$ = point matrix for elastic column;
$\mathbf{P}_r$ = point matrix for rib;
$\mathbf{T}$ = transfer matrix;
t = thickness of plate;
$\mathbf{z}$ = state vector;
β = ratio of load (P_y/P_x);
γ = ratio of rigidity $(E_r I_r/D)$; and
δ = ratio of area (A_r/bt).

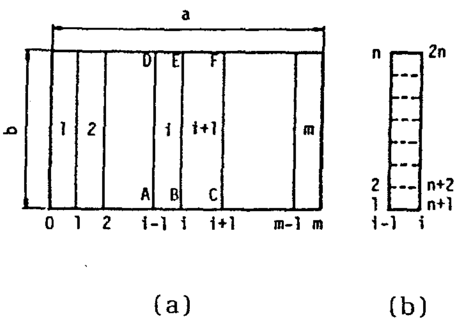

Fig.2-1 Subdivision of Plate into Strips and Finite Elements

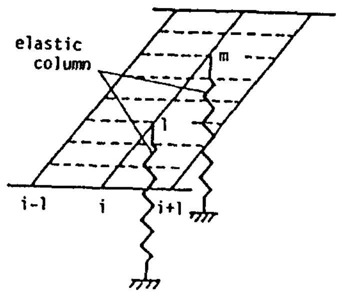

Fig.2-2 Intermediate Elastic Columns

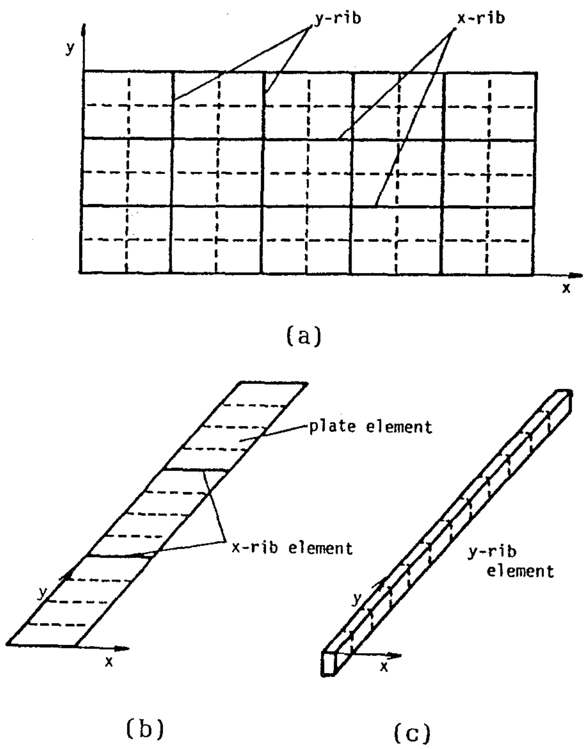

Fig.2-3 Orthogonally Stiffened Plate

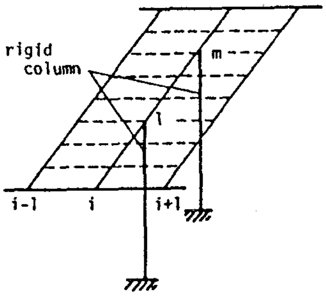

Fig.2-4 Intermediate Rigid Columns

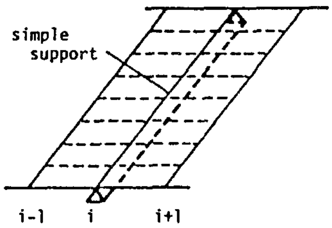

Fig.2-5 Intermediate Simple Support

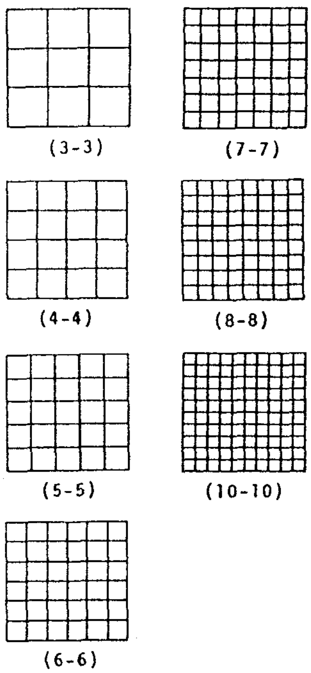

Fig.2-6 Mesh Patterns for Plate Bending Problem

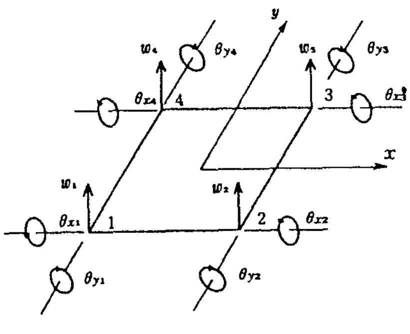

Fig.2-7 Rectangular Element and Degrees of Freedom

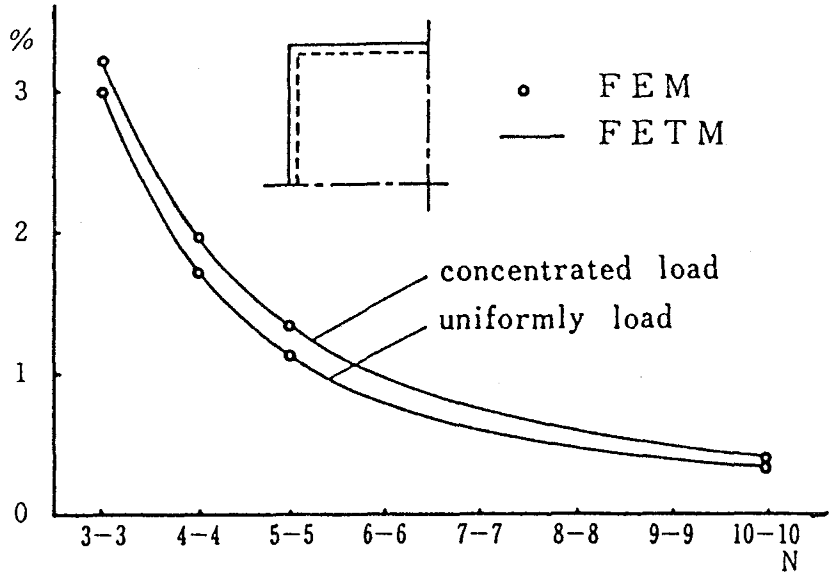

Fig.2-8 Convergence Condition of the Deflections

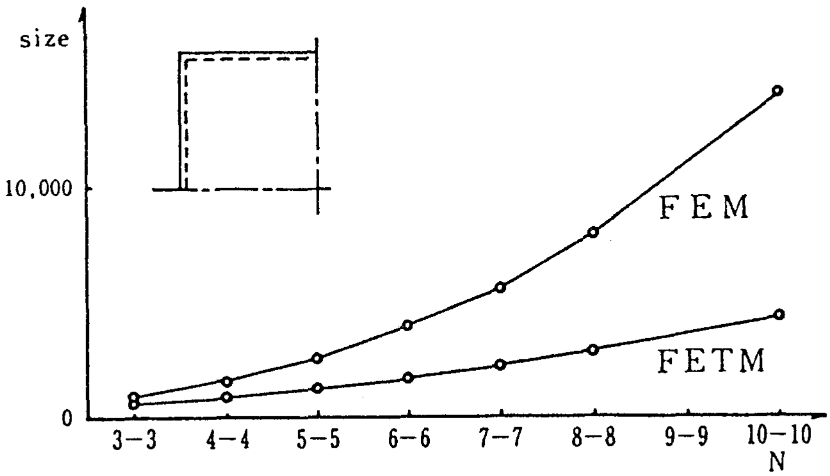

Fig.2-9 Comparison of Matrix Size

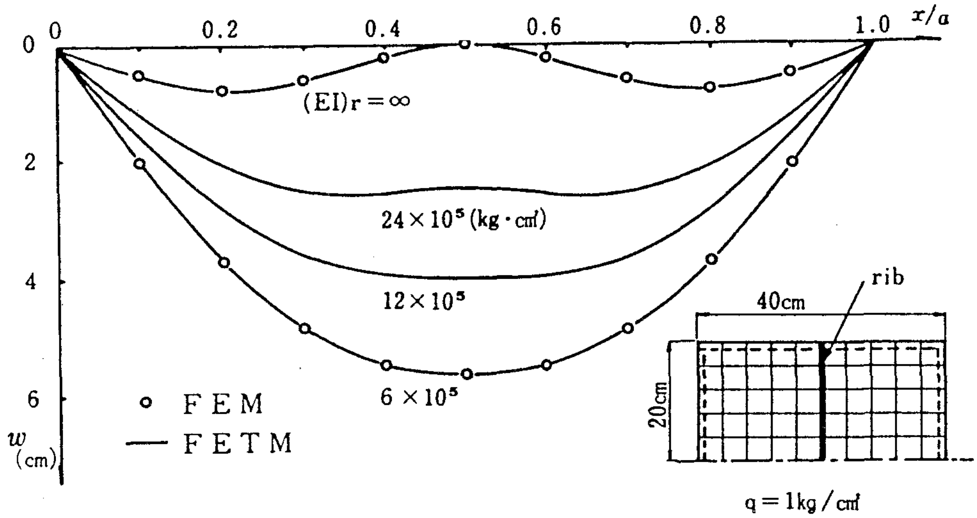

Fig.2-10(a) Deflections along the Symmetric Line of Simply Supported Rectangular Plate with Intermediate Rib (Uniform Load)

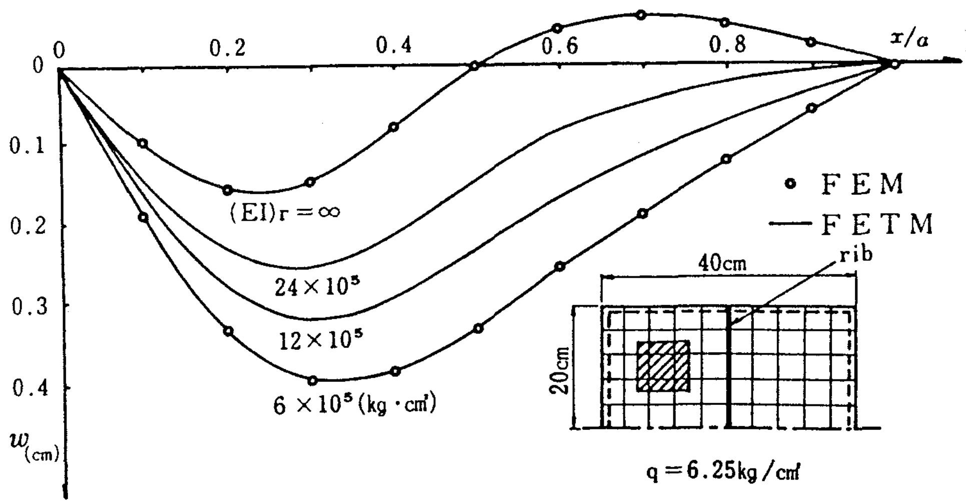

Fig.2-10(b) Deflections along the Symmetric Line of Simply Supported Rectangular Plate with Intermediate Rib (Partial Load)

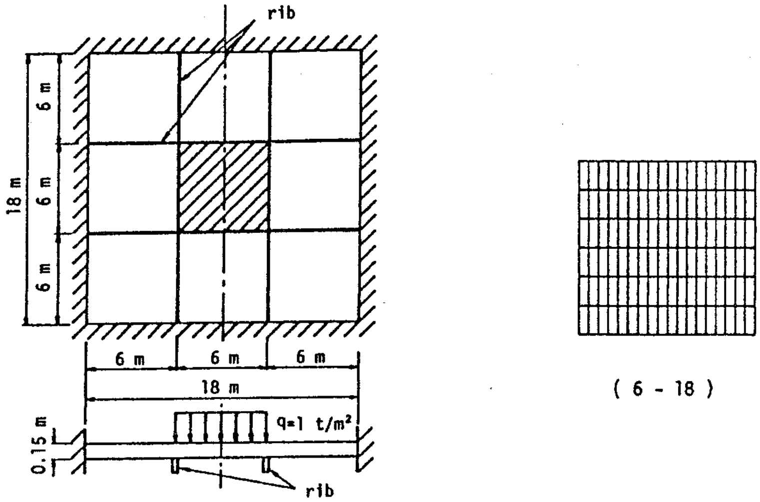

Fig.2-11(a) All Edges Clamped Plate with Intermediate Ribs

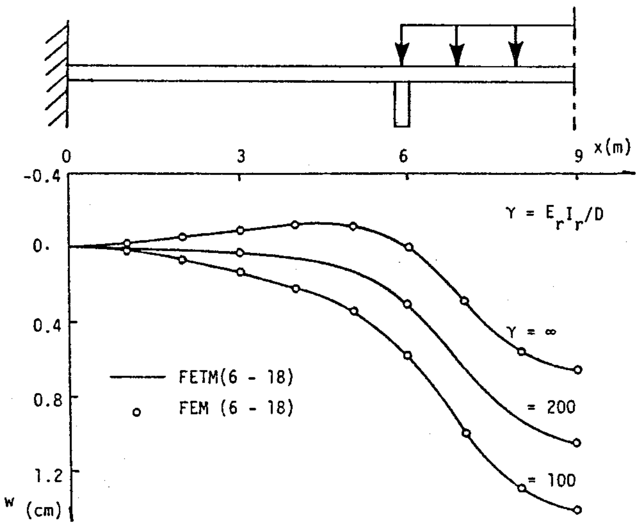

Fig.2-11(b) Deflections along the Symmetric Line

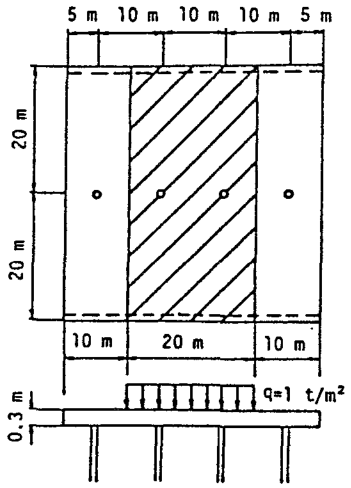

Fig.2-12(a) Simply Supported Bridge Deck with Intermediate Columns

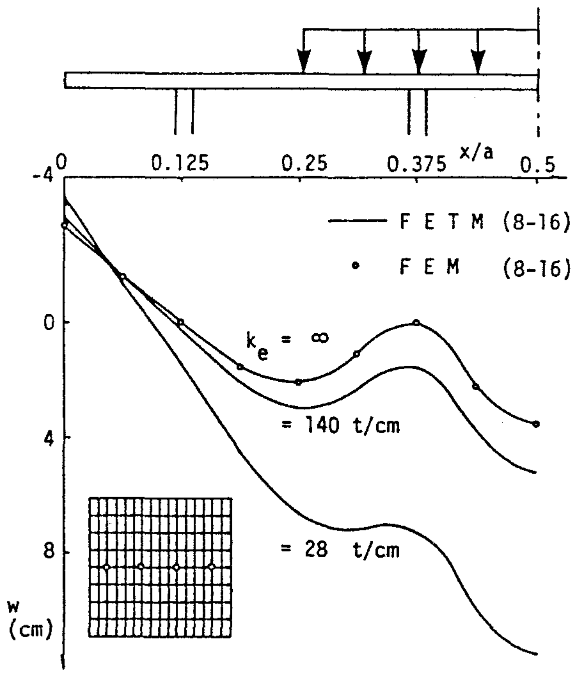

Fig.2-12(b) Deflections at Line of Columns

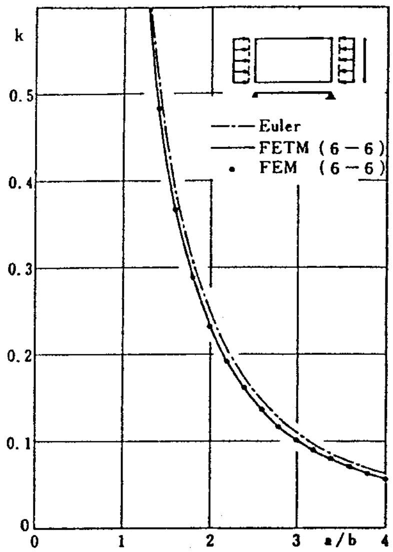

Fig.2-13 Buckling Coefficients of Plate Simply Supported along Two Opposite Sides

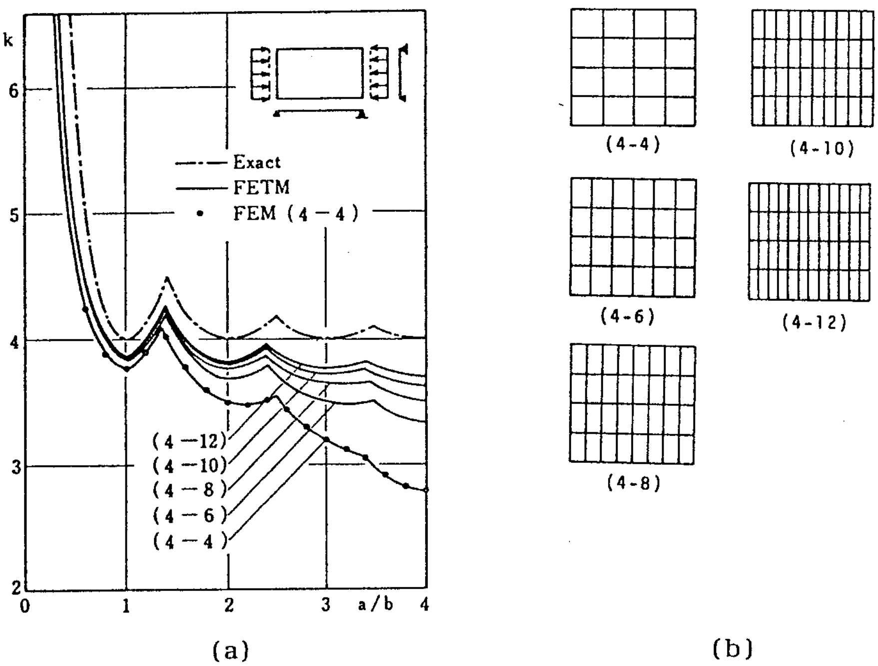

Fig.2-14 Buckling Coefficients of Simply Supported Plate

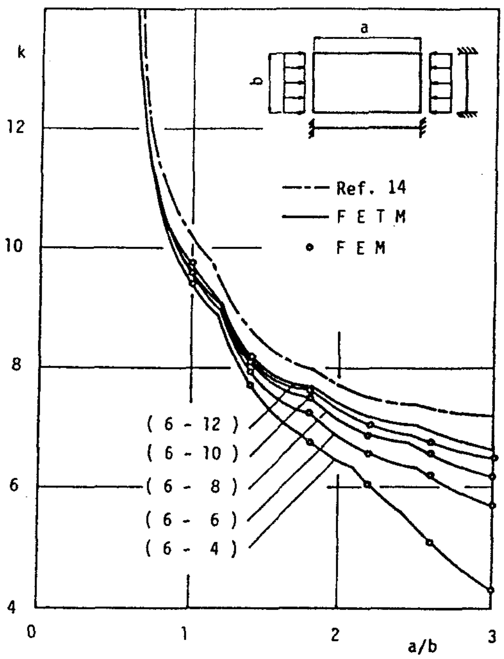

Fig.2-15 Buckling Coefficients of All Edges Clamped Plate

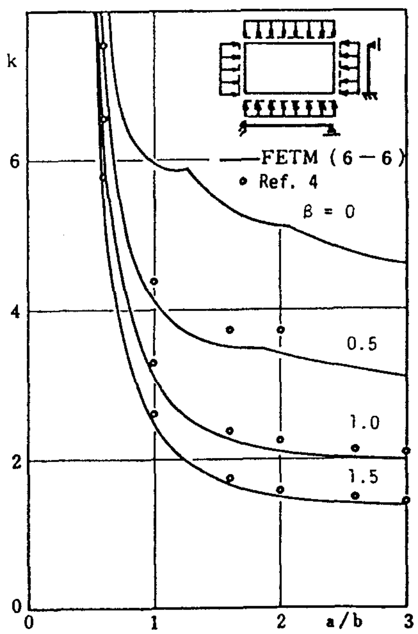

Fig.2-16 Buckling Coefficients of Biaxially Compressed Plate with Two Adjacent Clamped Edges and Two Other Simply Supported Edges

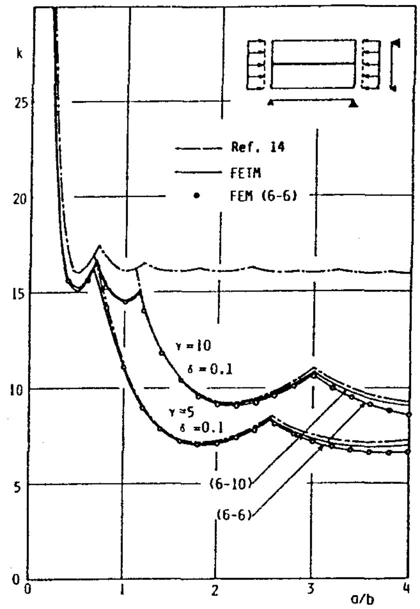

Fig.2-17 Buckling Coefficients of Simply Supported Plate with a Longitudinal Stiffener

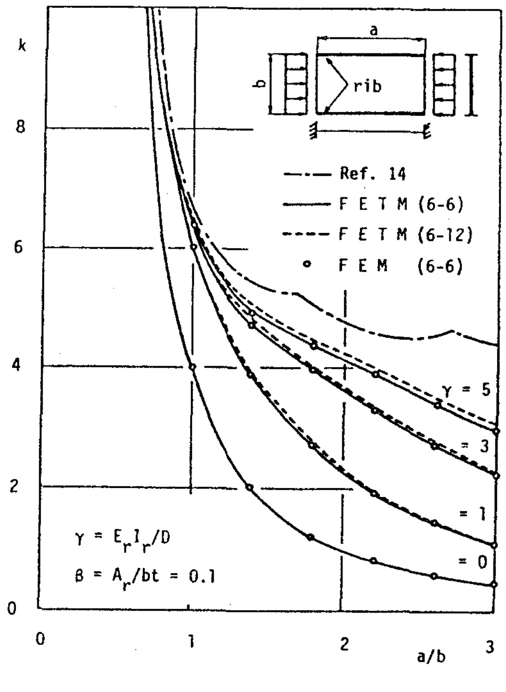

Fig.2-18 Buckling Coefficients of Plate with Two Clamped Edges and Two Other Reinforced Free Edges

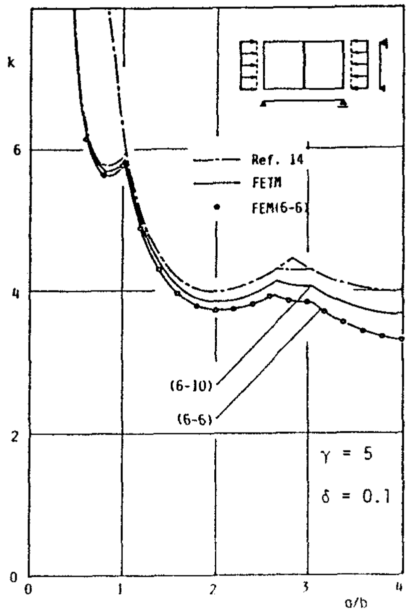

Fig.2-19 Buckling Coefficients of Simply Supported Plate with a Transverse Stiffener

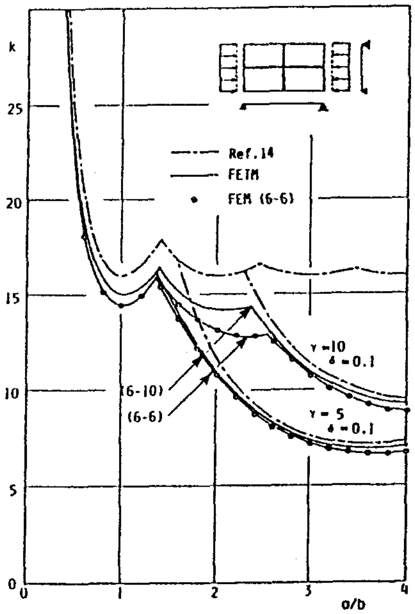

Fig.2-20 Buckling Coefficients of Orthogonally Stiffened Plate

Chapter 3 NONLINEAR ANALYSIS OF PLATES BY A COMBINED FINITE ELEMENT-TRANSFER MATRIX METHOD

3-1 INTRODUCTION

The finite strip method suggested by Cheung (1) and the transfer matrix method which was applied to plate vibration problems for the first time by Leckie (7) have the advantage of reducing the size of the matrix in the ordinary finite element method, but these methods can be successfully applied only for simple structures with particular conditions, otherwise considerable complications arise in the formulation of problems.

The combined finite element - transfer matrix (FETM) method, which has similar advantages to the previous two methods was proposed for the first time by Dokainish (3) and has been successfully applied to various linear problems (2,8,10,13,16). A combined finite strip - difference calculus technique was developed by Sundararajan and Reddy (18) and Thangam and Reddy (19,20). However, there are no studies on the extension of this method to geometric and material nonlinear problems.

The purpose of this chapter is to propose a method of analyzing the elastic-plastic large displacement behavior of structures under various loading conditions by the combined finite element-transfer matrix method. It is well known that in the finite element method the computer storage and time requires for analysis of nonlinear problems are usually more than those involved in linear problems. Thus it is expected that for long structures in which these are significantly more strips than nodes on section, advantages attainable through matrix size reduction in the FETM method will become more evident.

In this chapter the same incremental procedures in the finite element method (5) can be applied, except for the evaluation of incremental displacements for each specified incremental load. The Newton-Raphson method is employed in convergence procedures of each iterative step. It is assumed that the Prandtl-Reuss′ law, and the von Mises yield criterion (21) are valid in this chapter. In order to consider the extent of the yielded portions in the directions of the cross sections, the cross section of the structure is divided into some layers, and geometric nonlinearity is considered by using a set of moving coordinate systems (11).

Some numerical examples of nonlinear problems are proposed and their results are compared with those obtained by the ordinary finite element method and others.

3-2 FINITE ELEMENT-TRANSFER MATRIX METHOD FOR NONLINEAR PROBLEMS

1) Transfer Matrix

The plate, shown in Fig.3-1, is divided into m strips, each of which is subdivided into finite elements. Although any type of element may be used, triangular elements illustrated in Fig.3-1 are used in this chapter. The vertical sides dividing or bordering the strips are called sections.

Assembling the tangent stiffness matrix of the elements for each strip, the incremental equilibrium equations for the nodes on strip i are obtained as follows:

$$\mathbf{K}_i \Delta\boldsymbol{\delta}_i = \Delta\mathbf{F}_i \qquad \cdots\cdots\cdots\cdots (3\text{-}1)$$

in which $\mathbf{K}_i$ = the tangent stiffness matrix of strip i; and $\Delta\boldsymbol{\delta}_i$, $\Delta\mathbf{F}_i$ = the displacement and force increment vectors of strip i, respectively.

The transfer matrix relating the left and right displacements and forces of the strip may be obtained by suitably transforming the strip stiffness matrix into four submatrices; then Eq.(3-1) becomes

$$\begin{bmatrix} \mathbf{K}_{\ell\ell} & \mathbf{K}_{\ell r} \\ \mathbf{K}_{r\ell} & \mathbf{K}_{rr} \end{bmatrix}_i \begin{Bmatrix} \Delta\boldsymbol{\delta}_{\ell} \\ \Delta\boldsymbol{\delta}_{r} \end{Bmatrix}_i = \begin{Bmatrix} \Delta\mathbf{F}_{\ell} \\ \Delta\mathbf{F}_{r} \end{Bmatrix}_i \qquad \cdots\cdots\cdots\cdots (3\text{-}2)$$

in which $\Delta\boldsymbol{\delta}_{\ell i}$, $\Delta\boldsymbol{\delta}_{ri}$, $\Delta\mathbf{F}_{\ell i}$, and $\Delta\mathbf{F}_{ri}$ = the left and right displacement and force increment vectors of strip i, respectively; and $\mathbf{K}_{\ell\ell}$, $\mathbf{K}_{\ell r}$, $\mathbf{K}_{r\ell}$, and $\mathbf{K}_{rr}$ = the submatrices of **K**.

By expanding Eq.3-2 and solving for $\Delta\boldsymbol{\delta}_r$ and $\Delta\mathbf{F}_r$ in terms of $\Delta\boldsymbol{\delta}_\ell$ and $\Delta\mathbf{F}_\ell$ the following equations can be obtained:

$$\begin{Bmatrix} \Delta\boldsymbol{\delta}_r \\ \Delta\mathbf{F}_r \\ 1 \end{Bmatrix}_i = \begin{bmatrix} -\mathbf{K}_{\ell r}^{-1}\mathbf{K}_{\ell\ell} & \mathbf{K}_{\ell r}^{-1} & 0 \\ \mathbf{K}_{r\ell}-\mathbf{K}_{rr}\mathbf{K}_{\ell r}^{-1}\mathbf{K}_{\ell\ell} & \mathbf{K}_{rr}\mathbf{K}_{\ell r}^{-1} & 0 \\ 0 & 0 & 1 \end{bmatrix}_i \begin{Bmatrix} \Delta\boldsymbol{\delta}_\ell \\ \Delta\mathbf{F}_\ell \\ 1 \end{Bmatrix}_i \qquad \cdots\cdots\cdots (3\text{-}3)$$

On simplifying the notation, we obtain

$$\begin{Bmatrix} \Delta\boldsymbol{\delta}_r \\ \Delta\mathbf{F}_r \\ 1 \end{Bmatrix}_i = \begin{bmatrix} \mathbf{T}_{11} & \mathbf{T}_{12} & 0 \\ \mathbf{T}_{21} & \mathbf{T}_{22} & 0 \\ 0 & 0 & 1 \end{bmatrix}_i \begin{Bmatrix} \Delta\boldsymbol{\delta}_\ell \\ \Delta\mathbf{F}_\ell \\ 1 \end{Bmatrix}_i \qquad \cdots\cdots\cdots\cdots (3\text{-}4)$$

or

$$\Delta\mathbf{z}_{ri} = \mathbf{T}_i\,\Delta\mathbf{z}_{\ell i} \qquad \cdots\cdots\cdots\cdots (3\text{-}5)$$

Eq.(3-5) can be recognized as the transfer matrix relating the increment state vectors $\Delta\mathbf{z}_\ell$ and $\Delta\mathbf{z}_r$ which consist of the displacements and forces at a strip.

After continuous multiplications of the transfer matrix **T**, the relation between the increment state vectors at two ends of the structure is obtained (15).

$$\Delta \mathbf{z}_m = \mathbf{U} \, \Delta \mathbf{z}_0 \qquad \cdots\cdots\cdots\cdots (3\text{-}6)$$

On considering the left and right boundary conditions of the structure, simultaneous equations are obtained from Eq.(3-6)

$$\bar{\mathbf{U}} \, \Delta \bar{\mathbf{z}}_0 = \bar{\mathbf{U}}_F \qquad \cdots\cdots\cdots\cdots (3\text{-}7)$$

As the number of these equations is the same as that of the unknown state variables in $\Delta \mathbf{z}_0$, they can be determined from Eq.(3-7). Matrix $\bar{\mathbf{U}}$ of Eq.(3-7) is obtained from matrix $\mathbf{U}$ by deleting the columns corresponding to zero elements of $\Delta \mathbf{z}_0$ and the rows corresponding to the nonzero elements of $\Delta \mathbf{z}_m$; $\bar{\mathbf{U}}_F$ is the force vector of the external loads.

2) Tangent Stiffness Matrix

In the combined finite element - transfer matrix method, a transfer matrix is derived from a stiffness matrix used in the ordinary finite element method. As the derivation of the stiffness matrix is detailed (9,12), brief descriptions which mainly relate to elastic-plastic problems are given here. It is illustrated for the triangular plate element as shown in Fig.3-2 but is general for the other types of elements.

The displacements at any point within a triangular element, Fig.3-2, can be represented as

$$\begin{aligned} \tilde{\boldsymbol{\delta}}_P &= \mathbf{N}_P \, \boldsymbol{\delta}_P \\ \tilde{\boldsymbol{\delta}}_B &= \mathbf{N}_B \, \boldsymbol{\delta}_B \end{aligned} \qquad \cdots\cdots\cdots\cdots (3\text{-}8)$$

in which $\tilde{\boldsymbol{\delta}}_p$ and $\tilde{\boldsymbol{\delta}}_B$ = in-plane and out-of-plane displacement at any point within an element, and $\boldsymbol{\delta}_p$ and $\boldsymbol{\delta}_B$ are nodal displacements defined as follows:

$$\delta_P = \{u_1, v_1, u_2, v_2, u_3, v_3\}^T$$

$$\delta_B = \{w_1, \theta_{x1}, \theta_{y1}, w_2, \theta_{x2}, \theta_{y2}, w_3, \theta_{x3}, \theta_{y3}\}^T \qquad \cdots\cdots\cdots\cdots (3\text{-}9)$$

and $\mathbf{N}_P$, $\mathbf{N}_B$ are matrices of interpolating functions associated with the corresponding nodal displacements.

For the nonlinear problems, a strain increment vector $\Delta\boldsymbol{\varepsilon}$ at any point within an element is defined in terms of displacements as follows:

$$\Delta\varepsilon = \begin{Bmatrix} \Delta\varepsilon_x \\ \Delta\varepsilon_y \\ \Delta\gamma_{xy} \end{Bmatrix} = \begin{Bmatrix} \dfrac{\partial\Delta u}{\partial x} \\ \dfrac{\partial\Delta v}{\partial y} \\ \dfrac{\partial\Delta u}{\partial y}+\dfrac{\partial\Delta v}{\partial x} \end{Bmatrix} + \frac{1}{2}\begin{Bmatrix} \left(\dfrac{\partial\Delta w}{\partial x}\right)^2 \\ \left(\dfrac{\partial\Delta w}{\partial y}\right)^2 \\ \dfrac{2\partial\Delta w}{\partial x}\cdot\dfrac{\partial\Delta w}{\partial y} \end{Bmatrix}$$

$$+ \begin{Bmatrix} \dfrac{\partial w_0}{\partial x}\cdot\dfrac{\partial\Delta w}{\partial x} \\ \dfrac{\partial w_0}{\partial y}\cdot\dfrac{\partial\Delta w}{\partial y} \\ \dfrac{\partial w_0}{\partial x}\cdot\dfrac{\partial\Delta w}{\partial y}+\dfrac{\partial w_0}{\partial y}\cdot\dfrac{\partial\Delta w}{\partial x} \end{Bmatrix} - Z\begin{Bmatrix} \dfrac{\partial^2\Delta w}{\partial x^2} \\ \dfrac{\partial^2\Delta w}{\partial y^2} \\ \dfrac{2\partial^2\Delta w}{\partial x\partial y} \end{Bmatrix} \qquad \cdots\cdots\cdots\cdots (3\text{-}10)$$

$$= \mathbf{B}_P\Delta\delta_P + \mathbf{B}_G\Delta\delta_B + \mathbf{B}_0\Delta\delta_B + \mathbf{B}_B\Delta\delta_B \qquad \cdots\cdots\cdots\cdots (3\text{-}11)$$

$$= \mathbf{B}\Delta\delta \qquad \cdots\cdots\cdots\cdots (3\text{-}12)$$

in which u, v, and w are the displacements in the x, y, and z directions, respectively; $\mathbf{B}_P$, $\mathbf{B}_G$, $\mathbf{B}_0$, and $\mathbf{B}_B$ are matrices obtained by substituting Eq.(3-8) into Eq.(3-10), and $\mathbf{B}$, $\Delta\boldsymbol{\delta}$ are defined by identification of terms in Eqs.(3-11) and (3-12).

Furthermore, a stress increment vector, $\Delta\sigma$, can be represented as follows:

$$\Delta\sigma = \begin{Bmatrix} \Delta\sigma_x \\ \Delta\sigma_y \\ \Delta\gamma_{xy} \end{Bmatrix} = \mathbf{D}\Delta\varepsilon \qquad \cdots\cdots\cdots\cdots (3\text{-}13)$$

in which **D** = the stress-strain matrix. Details of matrix **D** will be described in a later section.

Applying the principle of virtual displacements, and using the expressions of Eqs.3-12 and 3-13, the element tangent stiffness matrix is obtained as follows:

$$\mathbf{k} = \int_V \mathbf{B}^T \mathbf{D}\ \mathbf{B}\ dv \qquad \cdots\cdots\cdots\cdots (3\text{-}14)$$

3-3 STRESS-STRAIN MATRIX

A description of the stress-strain matrices used in the development of the element tangent stiffness matrix and the calculation of stress increments due to an increment of load is presented herein. For the element in the elastic range, the elastic stress-strain matrix obtained from Hooke's law for the isotropic material is used:

$$\mathbf{D}_e = \frac{E}{1-\nu^2}\begin{bmatrix} 1 & \nu & 0 \\ \nu & 1 & 0 \\ 0 & 0 & \frac{(1-\nu)}{2} \end{bmatrix} \qquad \cdots\cdots\cdots\cdots (3\text{-}15)$$

in which E = modulus of elasticity, and ν = Poisson's ratio.

The plastic stress-strain matrix for the element in plastic range is derived by applying the Prandtl-Reuss stress-strain relation following the von Mises yield criterion; it can be written as

$$D_p = D_e - \frac{D_e \left\{\frac{\partial\bar{\sigma}}{\partial\sigma}\right\} \left\{\frac{\partial\bar{\sigma}}{\partial\sigma}\right\}^T D_e}{H' + \left\{\frac{\partial\bar{\sigma}}{\partial\sigma}\right\}^T D_e \left\{\frac{\partial\bar{\sigma}}{\partial\sigma}\right\}} \qquad \cdots\cdots\cdots\cdots (3\text{-}16)$$

in which $\sigma = \{\sigma_x, \sigma_y, \tau_{xy}\}^T$ = the stress vector; $\bar{\sigma} = (\sigma_x{}^2 - \sigma_x\sigma_y + \sigma_y{}^2 + 3\gamma_{xy}{}^2)^{1/2}$ is the equivalent stress; and H′ = the slope of the equivalent stress versus plastic strain curve in uniaxial test. The derivation of D_p is given in Appendix 3-1.

In calculation of equilibrating nodal forces at each iteration step, to reduce the number of iterations required for convergence to the required accuracy, the stress-strain matrix D_{ep} is applied for the element, which is elastic during the preceding cycle of the iteration but becomes plastic during the current cycle. D_{ep} is represented as follows:

$$D_{ep} = rD_e + (1-r)D_p \qquad \cdots\cdots\cdots\cdots (3\text{-}17)$$

in which r = the weight coefficient given in Fig.3-3.

In order to consider the extension of the yield portions in the directions of thickness of the element, it is divided into many layers, Fig.3-4, and linear distribution of the stress and the stress-strain matrix is assumed to improve the efficiency of the calculation. Hence, the stress of the k-th layer is represented by the stress at the upper and lower borders of the strip:

$$\sigma_\zeta = (\sigma_{k+1} - \sigma_k)\frac{\zeta}{t_k} + \frac{1}{2}(\sigma_{k+1} + \sigma_k) \qquad \cdots\cdots\cdots\cdots (3\text{-}18)$$

Similarly, the stress-strain matrix is

$$D_\zeta = (D_{k+1} - D_k)\frac{\zeta}{t_k} + \frac{1}{2}(D_{k+1} + D_k) \qquad \cdots\cdots\cdots\cdots (3\text{-}19)$$

in which t_k = the thickness of the k-th layer, ζ = the distance from the centroid of the k-th layer; and σ_k , $\mathbf{D}_k$ = the stress and stress-strain matrix at the k-th border line. Integrations of the stress σ and the stress-strain matrix **D** requires for development of the stiffness matrix are given in Appendix 3-2.

3-4 PROCEDURE FOR NONLINEAR PROBLEMS

The procedure for geometric and material nonlinear problems by the combined finite element - transfer matrix method will now be described.

<u>1) Transformation of Nodal Displacements</u>

In determining an equilibrium configuration of the structure under a given set of loads, the current local displacements which are related to the displaced local coordinate axes x, y, z, shown in Fig.3-5, are used to determine the local nodal forces. The local displacements are established by the transformation of nodal displacements from the global coordinate system to the local coordinate system.

A typical element before and after deformation is shown in Fig.3-5. Three sets of rectangular cartesian axes: (1) the global coordinate system X, Y, Z; (2) the initial local coordinate system x*, y*, z*; and (3) the displaced local coordinate system x, y, z are defined. The last two of them translate and rotate with the element. A reference element, 1", 2", 3" is established on the displaced local axes having the same shape and size as the original element, 1, 2, 3, and the same relative orientation to the local axes. The displacements 2"-2',3"-3' and the corner rotations with respect to the x and y axes represent the local nodal displacement.

S' designates a point S after deformation and S'' indicates a point S in the reference element. As shown in Fig.3-5, the vector $1S'$ may be described in two ways:

$$\overrightarrow{1S'} = \overrightarrow{1S} + \overrightarrow{SS'} \qquad \cdots\cdots\cdots\cdots (3\text{-}20)$$

or

$$\overrightarrow{1S'} = \overrightarrow{11'} + \overrightarrow{1'S''} + \overrightarrow{S''S'} \qquad \cdots\cdots\cdots\cdots (3\text{-}21)$$

Equating the right hand sides of Eqs.(3-20) and (3-21) and solving for the vector $\overrightarrow{S''S'}$, local displacement vector $\overrightarrow{S''S'}$ is represented as follows:

$$\overrightarrow{S''S'} = \overrightarrow{1S} - \overrightarrow{1'S''} + \overrightarrow{SS'} - \overrightarrow{11'} \qquad \cdots\cdots\cdots\cdots (3\text{-}22)$$

in which the displacement vector $\overrightarrow{SS'}$ and $\overrightarrow{11'}$ are related to the global coordinate system.

Recognizing that the vector $\overrightarrow{1S}$ related to the initial local coordinate system is equal to the vector $\overrightarrow{1'S''}$ related to the global coordinate system, we obtain:

$$\begin{Bmatrix} u \\ v \\ w \end{Bmatrix} = \mathbf{L}_A \begin{Bmatrix} U \\ V \\ W \end{Bmatrix} \qquad \cdots\cdots\cdots\cdots (3\text{-}23)$$

in which

$$\begin{Bmatrix} U \\ V \\ W \end{Bmatrix} = \mathbf{L}_B{}^T \mathbf{r} - \mathbf{L}_A{}^T \mathbf{r} + \begin{Bmatrix} U \\ V \\ W \end{Bmatrix} - \begin{Bmatrix} U_1 \\ V_1 \\ W_1 \end{Bmatrix} \qquad \cdots\cdots\cdots\cdots (3\text{-}24)$$

in which $\mathbf{r}$ = the vector $\overrightarrow{1S}$; $\mathbf{L}_A$, $\mathbf{L}_B$ = the transformation matrices relating the global coordinate system to the displaced local one, and the global system with the initial local one, respectively. U, V, and W are displacements which refer to the global coordinate system and u, v, and w refer to the displaced local one.

The rotations in the local coordinate system may be recovered from the following relationships:

$$\theta_x = \tan\frac{\partial w}{\partial y} \fallingdotseq \frac{\partial w}{\partial y}$$

$$\theta_y = -\tan\frac{\partial w}{\partial x} \fallingdotseq -\frac{\partial w}{\partial x} \qquad \cdots\cdots\cdots\cdots(3\text{-}25)$$

As shown in Fig.3-5, the vector $\boldsymbol{\rho} = \overrightarrow{0S'}$ may be described in two ways:

$$\boldsymbol{\rho} = \overrightarrow{01} + \overrightarrow{1S} + \overrightarrow{SS'} \qquad \cdots\cdots\cdots\cdots(3\text{-}26)$$

or

$$\boldsymbol{\rho} = \overrightarrow{01} + \overrightarrow{11'} + \overrightarrow{1'S''} + \overrightarrow{S''S'} \qquad \cdots\cdots\cdots\cdots(3\text{-}27)$$

Expressing as components related to the global coordinate system (X, Y, Z), Eqs.(3-26) and (3-27) become:

$$\begin{Bmatrix} X \\ Y \\ Z \end{Bmatrix} = \begin{Bmatrix} X_1 \\ Y_1 \\ Z_1 \end{Bmatrix} + L_B{}^T \begin{Bmatrix} x_0 \\ y_0 \\ 0 \end{Bmatrix} + \begin{Bmatrix} U \\ V \\ W \end{Bmatrix} \qquad \cdots\cdots\cdots\cdots(3\text{-}28)$$

or

$$\begin{Bmatrix} X \\ Y \\ Z \end{Bmatrix} = \begin{Bmatrix} X_1 \\ Y_1 \\ Z_1 \end{Bmatrix} + \begin{Bmatrix} U_1 \\ V_1 \\ W_1 \end{Bmatrix} + L_A{}^T \begin{Bmatrix} x_0 \\ y_0 \\ 0 \end{Bmatrix} + L_B{}^T \begin{Bmatrix} u \\ v \\ w \end{Bmatrix} \qquad \cdots\cdots\cdots\cdots(3\text{-}29)$$

Solving the last line of Eq.(3-29) for w, and recognizing from Eq.(3-28) that $W = Z - Z_1$, the following expression can be obtained:

$$w = L_{A31}(X-X_1-U_1) + L_{A32}(Y-Y_1-V_1) + L_{A33}(W-W_1) \qquad \cdots\cdots(3\text{-}30)$$

in which L_{A31}, L_{A32}, and L_{A33} = the components of the rotation matrix L_A, respectively.

By differentiating both sides of Eq.(3-30) by x and y, respectively, the following expressions can be obtained:

$$\frac{\partial w}{\partial x} = \frac{\partial w}{\partial X} \cdot \frac{\partial X}{\partial x} + \frac{\partial w}{\partial Y} \cdot \frac{\partial Y}{\partial x}$$

$$\frac{\partial w}{\partial y} = \frac{\partial w}{\partial X} \cdot \frac{\partial X}{\partial y} + \frac{\partial w}{\partial Y} \cdot \frac{\partial Y}{\partial y} \qquad \cdots\cdots\cdots\cdots (3\text{-}31)$$

in which

$$\frac{\partial w}{\partial X} = L_{A31} + L_{A33}\frac{\partial W}{\partial X}, \quad \frac{\partial w}{\partial Y} = L_{A32} + L_{A33}\frac{\partial W}{\partial Y}$$

Considering that, in the displaced coordinate system (x, y, z), x = x_0+u and y = y_0+v, the following expressions are obtained from Eq.(3-29):

$$X = X_1 + U_1 + L_{A11}x + L_{A21}y + L_{A31}w$$

$$Y = Y_1 + V_1 + L_{A12}x + L_{A22}y + L_{A32}w \qquad \cdots\cdots\cdots\cdots (3\text{-}32)$$

Differentiating both sides of Eq.(3-32) by x and y, respectively, the following expression can be obtained:

$$\frac{\partial X}{\partial x} = L_{A11} + L_{A31}\frac{\partial w}{\partial x}, \quad \frac{\partial X}{\partial y} = L_{A21} + L_{A31}\frac{\partial w}{\partial y}$$

$$\frac{\partial Y}{\partial x} = L_{A12} + L_{A32}\frac{\partial w}{\partial x}, \quad \frac{\partial Y}{\partial y} = L_{A22} + L_{A32}\frac{\partial w}{\partial y} \qquad \cdots\cdots (3\text{-}33)$$

Substituting $\partial X/\partial x$, $\partial X/\partial y$, $\partial Y/\partial x$, and $\partial Y/\partial y$ obtained above into Eq.(3-31) and considering Eq.(3-25), the rotational transformation are finally established as follows:

$$\theta_x = \{(L_{A31} - L_{A33}\theta_Y)L_{A21} + (L_{A32} + L_{A33}\theta_X)L_{A22}\}/\alpha$$

$$\theta_y = -\{(L_{A31} - L_{A33}\theta_Y)L_{A11} + (L_{A32} + L_{A33}\theta_X)L_{A21}\}/\alpha \quad \cdots(3\text{-}34)$$

in which

$$\alpha = 1 - (L_{A31} - L_{A33}\theta_Y)L_{A31} - (L_{A32} + L_{A33}\theta_X)L_{A32}$$

2) Iterative Scheme

The convergence procedures of nonlinear problems by the Newton-Raphson method, used in this paper, are illustrated in Fig.3-6. If the solution M at load P_M is known and incremental loads are applied to the structure, *only approximate displacements in the global coordinate system* $\Delta\boldsymbol{\delta}$, can be estimated by solving the next incremental equations:

$$\Delta\mathbf{z}_m = \mathbf{T}_m\mathbf{T}_{m-1}\cdots\mathbf{T}_1\Delta\mathbf{z}_0 = \mathbf{U}\ \Delta\mathbf{z}_0 \quad \cdots\cdots\cdots\cdots(3\text{-}35)$$

in which $\mathbf{T}_1$, $\mathbf{T}_2\cdots$ are obtained from the tangent stiffness matrix of the strip at the current stage.

Transforming the nodal displacements from the global coordinate system to the displaced local one, local nodal forces which equilibrate the current local displacements are now determined by premultiplying the local displacement by the element stiffness matrix as follows:

$$\Delta\mathbf{f}_M = \mathbf{k}_M\ \Delta\boldsymbol{\delta}_M \quad \cdots\cdots\cdots\cdots(3\text{-}36)$$

in which $\Delta\mathbf{f}_M$ and $\Delta\boldsymbol{\delta}_M$ are the increment of nodal forces and displacements, respectively; and $\mathbf{k}_M$ is the element stiffness matrix, which contains no terms corresponding to the geometric nonlinearity.

The differences between the applied loads and the equilibrating forces are the unbalanced loads that must be reapplied to the structure to estimate the next approximate solution at load P_{M+1}. This procedure is continued until the differences between the equilibrating forces and the applied loads become sufficiently small. The flow diagram of the calculation procedure developed in this chapter is shown in Fig.3-7.

3-5 NUMERICAL EXAMPLES

In order to confirm the accuracy of the procedure developed above numerical results are compared with those obtained by the ordinary finite element method and others.

A square plate under uniform load with all edges clamped is analysed for the first example. Fig.3-8 shows a comparison between the FETM solutions with finite element solutions by 1): Kawai (4), 2): Schmidt (17). In the numerical calculation, a quarter of the plate is divided into 3, 4, and 5 strips, respectively, as shown in Fig.3-8. Only the geometrical non-linearity is considered herein. Although the deflections of the FETM method are a little greater than those of other methods, good agreement exists between these sets of results.

In Fig.3-9, the stresses obtained from the FETM method for 4 strips are compared with those of the finite element method. The agreement is good for membrane stress, but the flexural (tension and compression) stresses of the FETM method are smaller. This is mainly due to the fact that, in the FETM method, the stresses at midpoint of the element in which maximum stresses are caused, are taken.

Fig.3-10 shows the deflections of the same plate as that used in the previous example. The plate is, herein, divided into 2, 4, 6, and 8 layers and geometrical and material nonlinearity are taken into consideration. The yield stress σ_Y is assumed to be 3100kg/cm^2. As shown in Fig.3-10, the effect of the number of the layers on the result is small, hence, in numerical examples proceeded in this chapter the 4-layers are used.

Fig.3-11 shows the center deflections of the in-plane loaded, simply supported rectangular plate with a=b=100cm and t=1cm. The initial deflection of plate bending mode is assumed, and defined as follows:

$$w_0 = \bar{w}_0 \sin\frac{\pi}{a}x \sin\frac{\pi}{b}y \qquad \cdots\cdots\cdots\cdots(3\text{-}37)$$

in which $\bar{w}_0$ = the maximum value of initial deflection and here $\bar{w}_0$ = t/10 is assumed. A quarter of the plate is divided into 2, 3, and 4 strips and $E=2.1\times10^6$ kg/cm^2 are used for calculation. In Fig.3-11, the finite element solutions are also shown, in which the same element and mesh pattern as those used in the FETM method are employed, and both results coincide completely with each other.

The matrix to be considered in the finite element method is, if the banded matrix is used, 125×35 for 4-strips mesh (8×4 elements), compared 50×50 for the FETM method.

Fig.3-12(b) shows the center line configurations of a uniformly loaded bridge deck with four intermediate columns shown in Fig.3-12(a). The half deck is divided into 4 strips and each strip into 16 triangular elements. Geometric and material nonlinearity are taken into consideration and yield stress σ_Y is 3100kg/cm^2. In the transfer procedure, the technique for the intermediate rigid column proposed in chapter 2 is applied to overcome the intermediate column located at 2-nd and 4-th nodal line. In this technique, the initial unknowns corresponding to the constrained displacements should be eliminated and new unknowns introduced.

As shown in Fig.3-12(b), close agreement exists between the results obtained by the FETM method and the finite element method. The effect of geometrical nonlinearity is more substantial compared to that of material nonlinearity, and the deflections obtained by the nonlinear theory are, therefore, smaller than those obtained by the linear one at both load levels, and the first yield in the element occurred at $q_0 = 5$. The matrix to be considered in the finite element method is 225×55, compared to 90×90 for the FETM method.

Fig.3-13(b) shows the centerline configurations of a uniformly loaded plate with an intermediate simple support shown in Fig.3-13(a). Half of the plate is divided into 8 strips and each strip into 6 elements. The transformation procedure at the intermediate simple supported nodal line can be performed in a simple schematic manner by using the technique for the intermediate simple support proposed in chapter 2. As shown in Fig.3-13(b), both the results of the FETM method and the finite element method are in good agreement. As in the previous example, the deflections obtained by the nonlinear theory are smaller than those obtained by the linear one, and the first element yielding occurred at $q_0 = 4$. The matrix to be considered in the finite element method is 180×30 for this mesh pattern, and in the FETM method 40×40.

Table 3-1 shows comparisons of size of matrix and computation time for the FETM method and the finite element method in above examples, where it is assumed that computation time is proportional to Nn^2 (N = size of matrix, n = band width of matrix). It is found from Table 3-1 that in computation time the FETM has less advantage for example 2 (case of strips < intervals), no or little advantage for example 1 (case of strips = intervals) and some advantage for example 3 (case of strips >

intervals), but in size of matrix considerable advantage for all examples.

3-6 CONCLUSIONS

The combined finite element - transfer matrix method for the elastic-plastic problems with large displacement is studied. The transfer matrix is derived from the tangent stiffness matrix used in the finite element method. The Prandtl-Reuss′ law obeying the von Mises yield criterion is assumed, and a set of moving coordinate systems is used to take geometric nonlinearity into consideration.

A computer program based on this theory has been developed. In this program, procedures used in the finite element method based on load increment are employed except for the estimation of approximate displacements for each specified increment load. From the numerical examples presented in this chapter, following conclusions are obtained:

(1) Good agreement exists between the results obtained by the FETM method and the conventional finite element method based on incremental procedures, which demonstrates the accuracy of this method in the elasto-plastic problems with large deformation.

(2) In the nonlinear problems, the FETM method has the advantage of reducing the size of matrix compared to the ordinary finite element method as in the linear problems.

(3) In the plate bending problems, the effect of the number of the layers on the result is small, thus, in numerical examples stated in this chapter, 4-layers pattern is used.

APPENDIX 3-1 DERIVATION OF STRESS-STRAIN MATRIX

The yield condition according to the von Mises criterion may be represented by the yield surface which is given by

$$F(\sigma_{ij}) = \bar{\sigma} = \sigma_Y \qquad \cdots\cdots\cdots\cdots(3\text{-}38)$$

where

$$\bar{\sigma} = (\sigma_x{}^2 + \sigma_x\sigma_y + \sigma_y{}^2 + 3\tau_{xy}{}^2)^{1/2} \qquad \cdots\cdots\cdots\cdots(3\text{-}39)$$

is an equivalent stress and σ_Y is a yield stress confirmed by a uniaxial test. If principal stresses σ_1 and σ_2 are taken with rectangular coordinates, the yielding curve given by Eq.(3-38) can be an ellipse shown with a solid line in Fig.3-14.

For an isotropic material strain-hardening curve is given by

$$F(\sigma_{ij}) = k \qquad \cdots\cdots\cdots\cdots(3\text{-}40)$$

and this curve can be represented by a dotted elliptic curve as shown in Fig.3-14 which is similar to the original yielding curve.

In the plastic flow theory, the incremental plastic-strain vector $d\boldsymbol{\varepsilon}_p$ is assumed to be described as follows:

$$d\boldsymbol{\varepsilon}_p = \frac{\partial F}{\partial \boldsymbol{\sigma}} d\lambda \qquad \cdots\cdots\cdots\cdots(3\text{-}41)$$

where $d\lambda$ is a non-negative scalar, and $\boldsymbol{\sigma} = \sigma_{ij}$.

If a structure is in an elastic-plastic state, the incremental strain vector $d\boldsymbol{\varepsilon}$ at any point may be considered as the sum of an incremental elastic-strain vector $d\boldsymbol{\varepsilon}_e$ and an incremental plastic-strain vector $d\boldsymbol{\varepsilon}_p$ as follows:

$$d\boldsymbol{\varepsilon} = d\boldsymbol{\varepsilon}_e + d\boldsymbol{\varepsilon}_p \qquad \cdots\cdots\cdots\cdots(3\text{-}42)$$

The incremental elastic-strain vector is given for plane stress situation as follows:

$$d\boldsymbol{\varepsilon}_e = \mathbf{D}_e^{-1}\, d\boldsymbol{\sigma} \qquad \cdots\cdots\cdots\cdots(3\text{-}43)$$

where

$$\mathbf{D}_e = \frac{E}{1-\nu^2}\begin{bmatrix} 1 & \nu & 0 \\ \nu & 1 & 0 \\ 0 & 0 & (1-\nu)/2 \end{bmatrix} \qquad \cdots\cdots\cdots\cdots(3\text{-}44)$$

is the elasticity matrix for a plane stress. Substituting Eq.(3-41) and Eq.(3-43) into Eq.(3-42) yields

$$d\boldsymbol{\sigma} = \mathbf{D}_e\,(d\boldsymbol{\varepsilon} - \frac{\partial \mathbf{F}}{\partial \boldsymbol{\sigma}}\, d\lambda) \qquad \cdots\cdots\cdots\cdots(3\text{-}45)$$

When plastic yield is occurring the stresses are on the yield surface given by Eq.(3-38). Differentiating this we can write therefore

$$\{\frac{\partial \mathbf{F}}{\partial \boldsymbol{\sigma}}\}^T\, d\boldsymbol{\sigma} - d\bar{\sigma} = 0 \qquad \cdots\cdots\cdots\cdots(3\text{-}46)$$

The value $\bar{\sigma}$ increases as a function of equivalent plastic strain $\bar{\varepsilon}_p$, and the incremental value $d\bar{\sigma}$ is

$$d\bar{\sigma} = H'\, d\bar{\varepsilon}_p \qquad \cdots\cdots\cdots\cdots(3\text{-}47)$$

where H' is the strain-hardening rate. Now an increment dW_p of the plastic work done during the plastic deformation is expressed as follows:

$$dW_p = \boldsymbol{\sigma}^T \, d\boldsymbol{\varepsilon}_p \qquad \cdots\cdots\cdots\cdots (3\text{-}48)$$

Then, dW_p can be represented by an equivalent stress $\bar{\sigma}$ and an equivalent strain $d\bar{\varepsilon}_p$

$$dW_p = \bar{\sigma} \, d\bar{\varepsilon}_p \qquad \cdots\cdots\cdots\cdots (3\text{-}49)$$

Using Eq.(3-38), (3-48), (3-49) in (3-41),

$$d\lambda = d\bar{\varepsilon}_p \qquad \cdots\cdots\cdots\cdots (3\text{-}50)$$

Thus the increment $d\bar{\sigma}$ can be given by eliminating $d\bar{\varepsilon}_p$ from Eq.(3-47) and Eq.(3-50) as follows:

$$d\bar{\sigma} = H' \, d\lambda \qquad \cdots\cdots\cdots\cdots (3\text{-}51)$$

Substituting Eqs.(3-45) and (3-51) into Eq.(3-46), the following equation for non-negative scalar $d\lambda$ results:

$$d\lambda = \frac{\{\frac{\partial F}{\partial \boldsymbol{\sigma}}\}^T \mathbf{D}_e \, d\boldsymbol{\varepsilon}}{H' + \{\frac{\partial F}{\partial \boldsymbol{\sigma}}\}^T \, \mathbf{D}_e \, \{\frac{\partial F}{\partial \boldsymbol{\sigma}}\}} \qquad \cdots\cdots\cdots\cdots (3\text{-}52)$$

Substituting the above equation into Eq.(3-45) and considering the identity $F = \bar{\sigma}$, the incremental stress vector is then given by

$$d\boldsymbol{\sigma} = \mathbf{D}_p \; d\boldsymbol{\varepsilon} \qquad \cdots\cdots\cdots\cdots (3\text{-}53)$$

where $\mathbf{D}_p = \mathbf{D}_e - \mathbf{D}_p{}^*$ is a plastic stress-strain matrix, and

$$\mathbf{D}_p{}^* = \frac{\mathbf{D}_e \left\{ \dfrac{\partial \bar{\sigma}}{\partial \boldsymbol{\sigma}} \right\} \left\{ \dfrac{\partial \bar{\sigma}}{\partial \boldsymbol{\sigma}} \right\}^T \mathbf{D}_e}{H' + \left\{ \dfrac{\partial \bar{\sigma}}{\partial \boldsymbol{\sigma}} \right\}^T \mathbf{D}_e \left\{ \dfrac{\partial \bar{\sigma}}{\partial \boldsymbol{\sigma}} \right\}} \qquad \cdots\cdots\cdots\cdots (3\text{-}54)$$

The elements of the matrix $\mathbf{D}_p$ are given for plane stress situation in the following form:

$$\mathbf{D}_p = \frac{1}{S} \begin{bmatrix} S_x{}^2 & S_x S_y & S_x S_{xy} \\ S_x S_y & S_y{}^2 & S_y S_{xy} \\ S_x S_{xy} & S_y S_{xy} & S_{xy}{}^2 \end{bmatrix} \qquad \cdots\cdots\cdots\cdots (3\text{-}55)$$

where

$$S_x = \frac{E}{1-\nu^2} \left(\frac{2\sigma_x - \sigma_y}{3} + \nu \frac{2\sigma_y - \sigma_x}{3} \right)$$

$$S_y = \frac{E}{1-\nu^2} \left(\nu \frac{2\sigma_x - \sigma_y}{3} + \frac{2\sigma_y - \sigma_x}{3} \right)$$

$$S_{xy} = \frac{E}{1+\nu} \tau_{xy}$$

$$S = \frac{4}{9} \bar{\sigma}^2 H' + S_x \frac{2\sigma_x - \sigma_y}{3} + S_y \frac{2\sigma_y - \sigma_x}{3} + 2 S_{xy} \tau_{xy}$$

APPENDIX 3-2 INTEGRATION OF STRESS AND STRESS-STRAIN MATRIX

Integration of stress σ and stress-strain matrix **D** are as follows:

$$\int \sigma dz = \sum_{k=1}^{n+1} \frac{1}{2}(t_{k-1}+t_k)\sigma_k$$

$$\int \mathbf{D}dz = \sum_{k=1}^{n+1} \frac{1}{2}(t_{k-1}+t_k)\mathbf{D}_k$$

$$\int z\mathbf{D}dz = \sum_{k=1}^{n+1} \left[\left(\frac{z_{k-1}t_{k-1}}{2} + \frac{t_{k-1}^2}{12} \right) + \left(\frac{z_k t_k}{2} + \frac{t_k^2}{12} \right) \right] \mathbf{D}_k$$

$$\int z^2 \mathbf{D}dz = \sum_{k=1}^{n+1} \left[\frac{t_{k-1}}{2} \left(z_{k-1}^2 + \frac{t_{k-1}^2}{12} + \frac{z_{k-1}t_{k-1}}{3} \right) + \frac{t_k}{2} \left(z_k^2 + \frac{t_k}{12} + \frac{z_k t_k}{3} \right) \right] \mathbf{D}_k \qquad \cdots\cdots\cdots\cdots (3\text{-}56)$$

in which n = the number of layers, and z_k = the distance from the centroid of the structure to the centroid of the k-th layer (Fig.3-4).

REFERENCES

1. Cheung, Y.K., "Finite Strip Method in Structural Analysis," Pergamon Press, Oxford, England 1976.
2. Chiatti, G. and Sestieri, A., "Analysis of Static and Dynamic Structural Problems by a Combined Finite Element - Transfer Matrix Method," J. Sound & Vibration, Vol.67, No.1, 1979, pp.35-42.
3. Dokainish, M.A., "A New Approach for Plate Vibrations: Combination of Transfer Matrix and Finite-Element Technique," Trans. ASME, Vol.94, No.2, 1972, pp.526-530.
4. Kawai, T. and Yoshimura, N., "Analysis of Large Deflection of Plates by the Finite Element Method," International Journal for Numerical Methods in Engineering, Great Britain, Vol.1, No.1, 1969, pp.123-133.

5. Komatsu, S., Kitada, T. and Miyazaki, S., "Elasto-Plastic Analysis of Compressed Plate with Residual Stress and Initial Deflection," Proc. of JSCE, No.244, Dec., 1975, pp.1-14 (in Japanese).
6. Komatsu, S. and Kitada, T., "Refined Finite Element Analysis of Plane Elasto-Plastic Problems," Technology Reports of Osaka University, Vol.25, 1975, pp.415-437.
7. Leckie, F.A., "The Application of Transfer Matrices to Plate Vibrations," Ingenieur-Archiv, Vol.XXXII, 1963, pp.100-111.
8. McDaniel, T.J. and Eversole, K.B., "A Combined Finite Element - Transfer Matrix Structural Analysis Method," J. Sound & Vibration, Great Britain, Vol.51, No.2, 1977, pp.157-169.
9. McGuire, W., and Gallagher, R.H., "Matrix Structural Analysis," John Wiley & Sons, Inc., New York, N.Y., 1979.
10. Mucino, H.V. and Pavelic, V., "An Exact Condensation Procedure for Chain-Like Structures Using a Finite Element-Transfer Matrix Approach," Trans. ASME, J. Mech. Des., No.80-C2/DET-123, 1980, pp.1-9.
11. Murray, D.W. and Wilson, E.L., "Finite-Element Large Deflection Analysis of Plates," J. ASCE, Vol.95, No. EMI, Feb. 1969, pp.143-163.
12. Nath, B., "Fundamentals of Finite Elements for Engineers," The Athlone Press of the University of London, London, England, 1974.
13. Ohga, M., Shigematsu, T. and Hara, T., "Structural Analysis by a Combined Finite Element-Transfer Matrix Method," An International Journal Computers & Structures, Pergamon Press, Vol.17, No.3, 1983, pp.321-326.
14. Ohga, M., Shigematsu, T. and Hara, T., "Structural Analysis by a Combined Finite Element-Transfer Matrix Method," J. ASCE, Vol.110, No.EM9, September 1984, pp.1335-1349.
15. Pestel, E.C. and Leckie, F.A., "Matrix Method in Elastomechanics," McGraw-Hill Book Co., Inc., New York, N.Y., 1963.
16. Sankar, S. and Hoa, S.V., "An Extended Transfer Matrix-Finite Element Method for Free Vibration of Plates," J. Sound & Vibration, Vol.70, No.2, 1980, pp.205-211.
17. Schmidt, B., "Ein Geometrisch und Physikalisch Nichtlineares Finite Element - Verfahren zur Berechnung von Ausgesteiften, Vorverformten Rechteckplatten," Der Stahlbau, Heft 1, Januar, 1979, s.13-21.
18. Sundararajan, C. and Reddy, D.V., "Finite Strip - Difference

Calculus Technique for Plate Vibration Problems," International Journal of Solids and Structures, Vol.11, April, 1975, pp.425-435.
19. Thangam Babu, P.V. and Reddy, D.V., "Finite Strip - Difference Calculus Technique of Skew Orthotropic Plate Vibration," Proc. Int. Conf. on Finite Element Methods in Engineering, Adelaide, Sydney Australia, 1976.
20. Thangam Babu, P.V. and Reddy, D.V., "Finite Strip - Difference Calculus Technique for Skew Orthotropic Plate Buckling," Proc. Sixth Canadian Congress of Applied Mechanics (CANCAM), Vancouver, B.C., May-June, 1977.
21. Yamada, Y., "Matrix Methods of Strength of Materials," Baifukan, 1980 (in Japanese).
22. Yamada, Y., Yoshimura, N. and Sakurai, T., "Plastic Stress-Strain Matrix and its Application for the Solution of Elastic-Plastic Problems by the Finite Element Methods," Int. J. Mech. Sci., Vol.10, 1968, pp.343-354.

NOTATION

The following symbols are used in this paper

a, b = dimensions of plate;
$\mathbf{D}_e$, $\mathbf{D}_p$ = elastic and Plastic stress-strain matrices;
E = modulus of elasticity;
$\mathbf{F}$ = force vector;
$\mathbf{F}_\ell$, $\mathbf{F}_r$ = left and right force vectors of strip;
H' = strain-hardening rate;
$\mathbf{K}$ = strip tangent stiffness matrix;
$\mathbf{k}$ = element tangent stiffness matrix;
$\mathbf{k}_M$ = element tangent stiffness matrix, which contains no terms corresponding to geometric nonlinearity;
$\mathbf{L}$, $\mathbf{L}^*$ = transformation matrices relating the global coordinate system with the displaced local and initial local one;
$\mathbf{T}$ = transfer matrix;
t, t_k = thickness of plate and layer;
U, V, W = displacements related to the global coordinate system;
u, v, w = displacements related to the local coordinate system;
$\mathbf{z}$ = state vector;

$\boldsymbol{\delta}$ = displacement vector;

$\boldsymbol{\delta}_\ell$, $\boldsymbol{\delta}_r$ = left and right displacement vectors of strip;

$\boldsymbol{\varepsilon}$ = strain vector;

θ_x, θ_y = rotations about x and y axis;

ν = Poisson's ratio;

$\boldsymbol{\sigma}$ = stress vector; and

$\bar{\sigma}$ = equivalent stress.

Table 3-1 Comparisons of Matrix Size and Computation Time

Scheme	Example 1 (4 Strips x 4 Intervals)		Example 2 (4 Strips x 8 Intervals)		Example 3 (8 Strips x 3 Intervals)	
	Nn	Nn^2	Nn	Nn^2	Nn	Nn^2
FEM	4375	153125	12375	680625	5400	162000
FETM	2500	125000	8100	729000	1600	64000

N = Size of Matrix; n = Band Width of Matrix

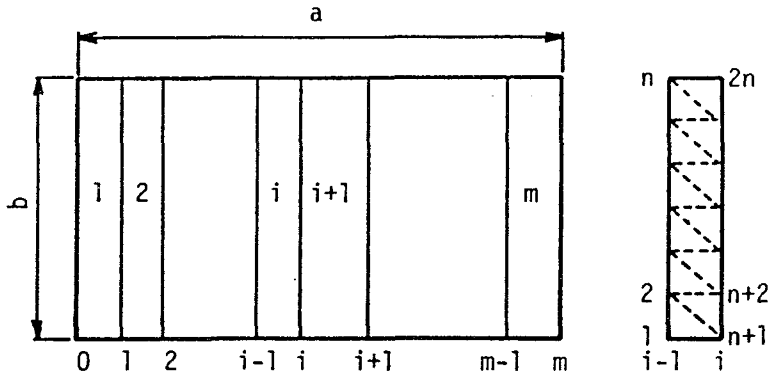

Fig.3-1 Subdivision of Plate into Strips and Finite Elements

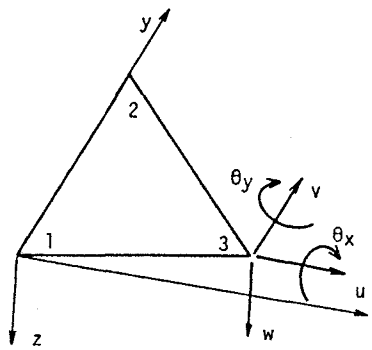

Fig.3-2 Triangular Element and Degrees of Freedom

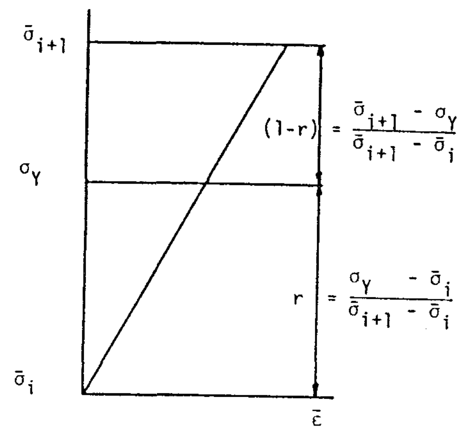

Fig.3-3 Stress-Strain in Element Transforming from Elastic to Plastic State

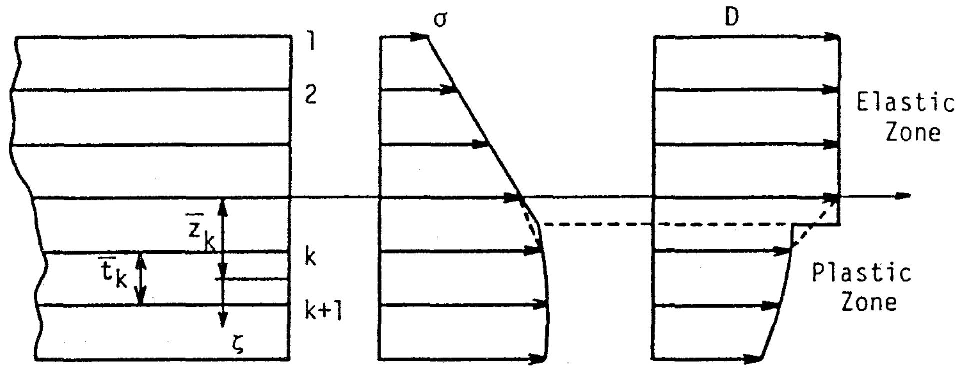

Fig.3-4 Subdivision of Cross Section into Layers

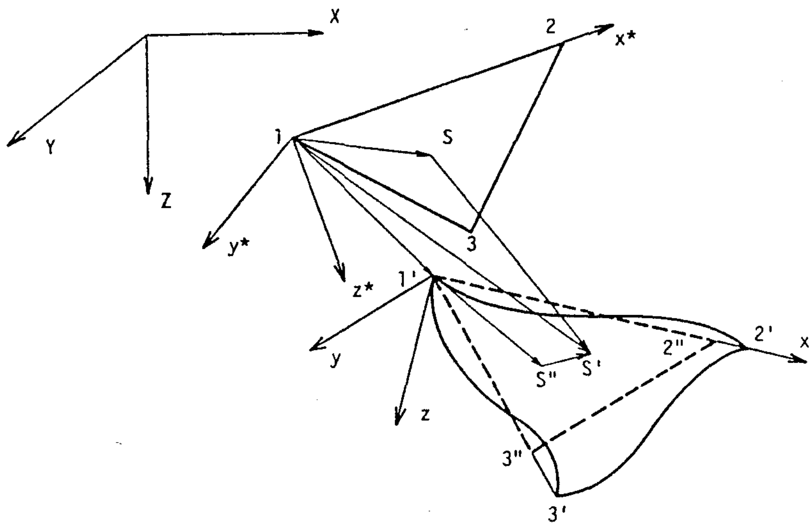

Fig.3-5 Location of Element Before and After Deformation

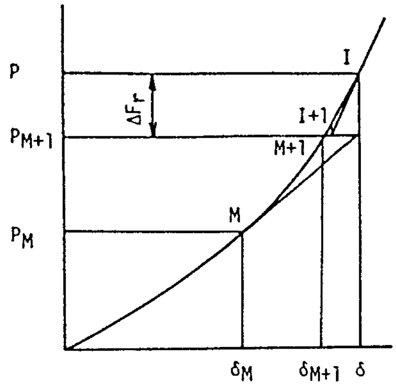

Fig.3-6 Newton-Raphson Iteration Method

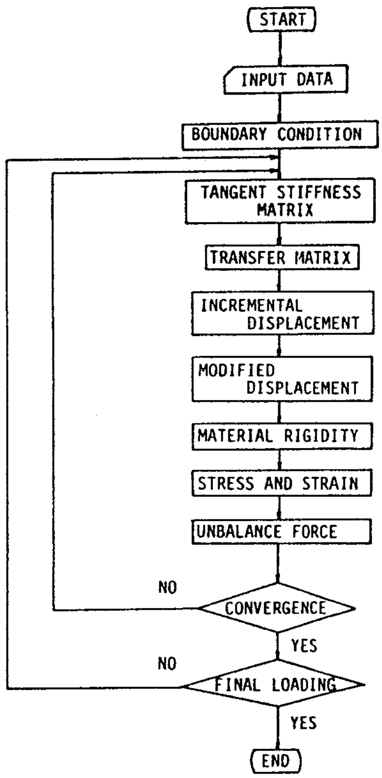

Fig.3-7 Flow-Chart for Computer Program

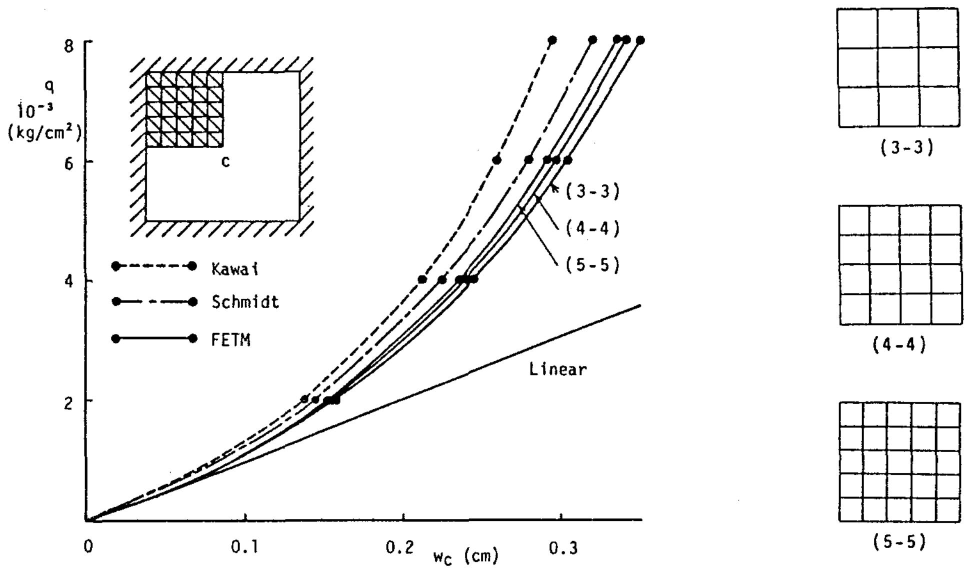

Fig.3-8 Comparison of Deflections for Square Plate with All Edges Clamped

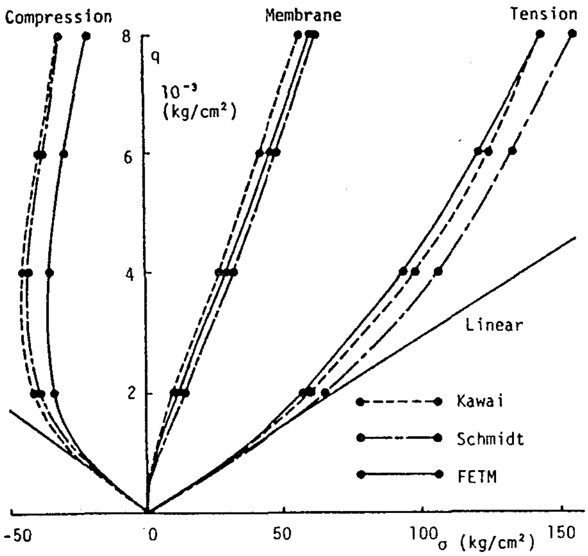

Fig.3-9 Comparison of Stresses for Square Plate with All Edges Clamed

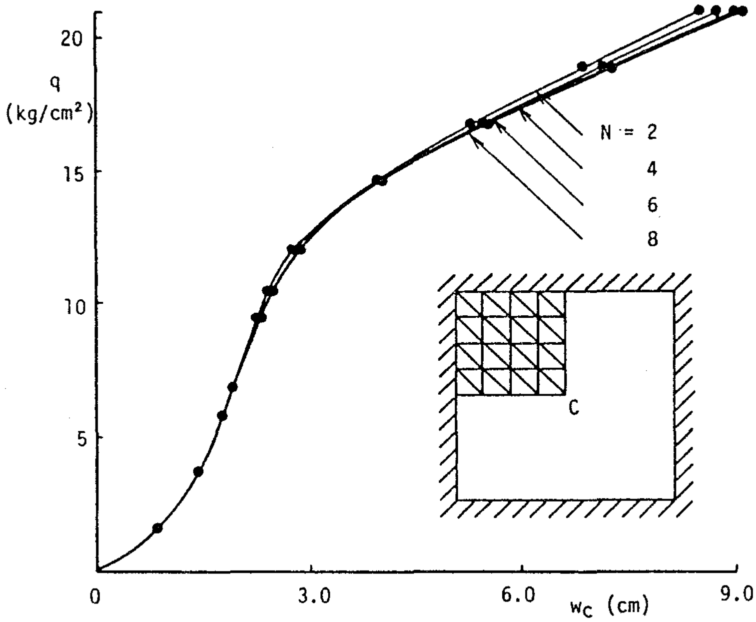

Fig.3-10 Effect of Number of Layers on Deflection

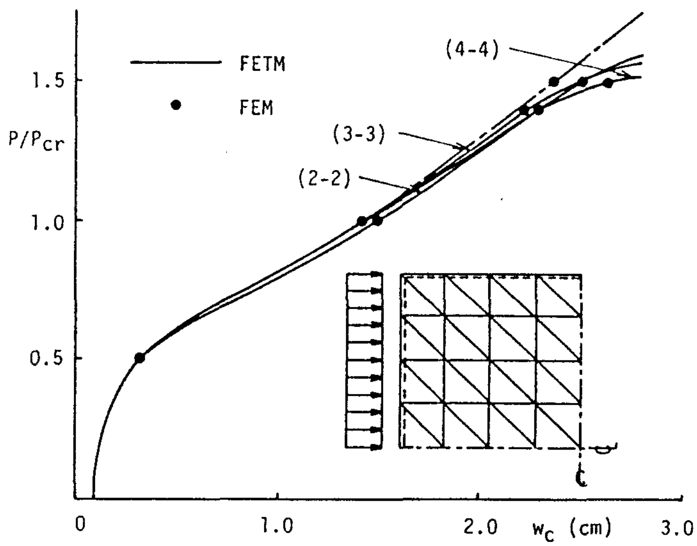

Fig.3-11 Lateral Deflection of Simply Supported Square Plate under In-Plane Load

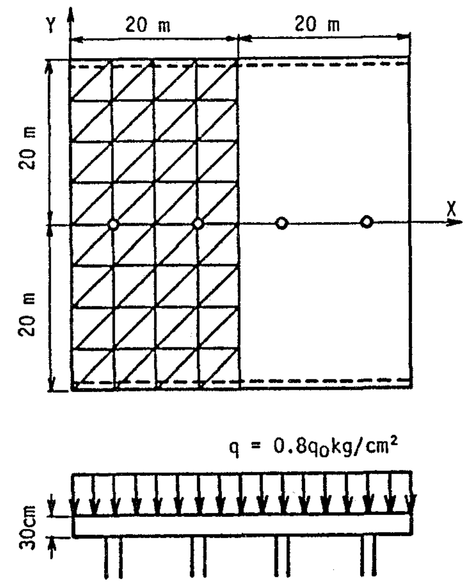

Fig.3-12(a) Simply Supported Bridge Deck with Intermediate Columns

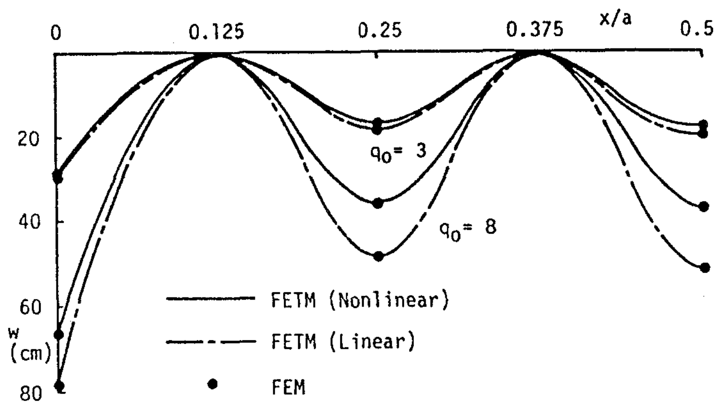

Fig.3-12(b) Deflections at Line of Columns

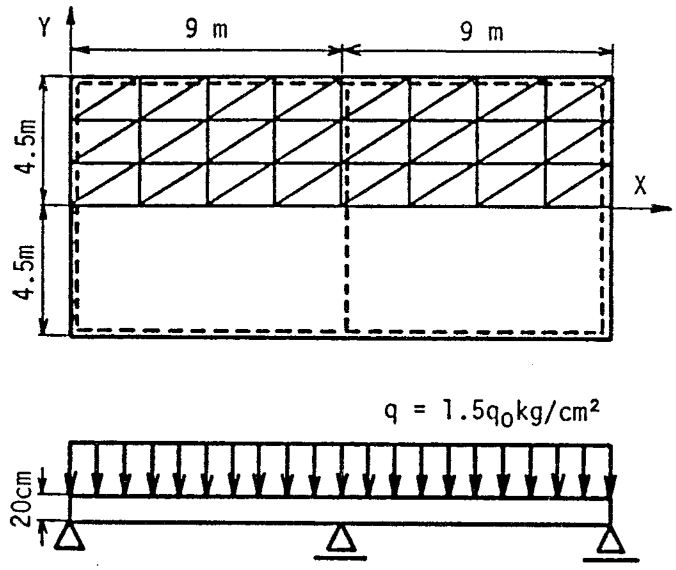

Fig.3-13(a) Simply Supported Rectangular Plate with Intermediate Support

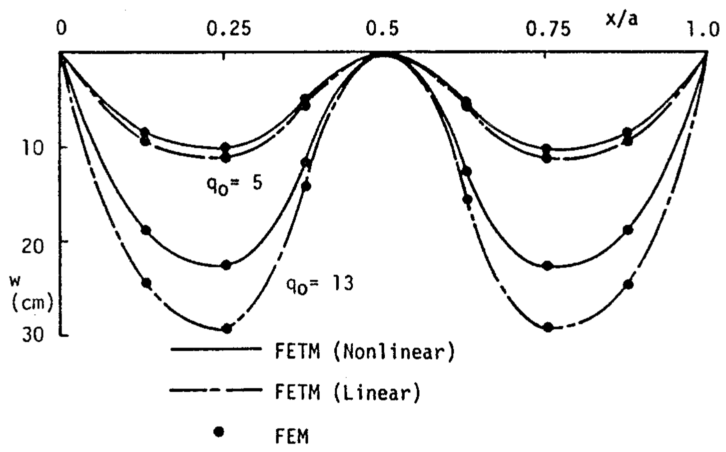

Fig.3-13(b) Deflections along Symmetric Line

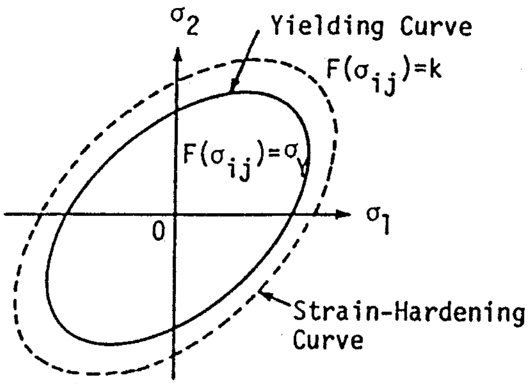

Fig.3-14 Von Mises Yielding Curve

Chapter 4 NONLINEAR ANALYSIS OF THIN-WALLED MEMBERS BY A FINITE ELEMENT-TRANSFER MATRIX METHOD

4-1 INTRODUCTION

Thin-walled members are analyzed by the finite element method, the finite strip method, etc.. Among these methods, the finite strip method suggested by Cheung (1), which is a formulation of combining the finite element method and Fourier series technique, has the advantage of reducing the size of the matrix in the ordinary finite element method. This method can be successfully applied for the only simple thin-walled members with constant cross section and particular boundary conditions; otherwise considerable complication arise in the formulation of problems.

The finite element method is the most widely used and powerful tool for analysis of thin-walled members with complex cross sections (5,13). However, the disadvantage of this method is that, in the case of complex and large structures, it is necessary to use a large number of nodes, resulting is very large matrices which require large computers for their management and regulation. In order to overcome this disadvantage of the finite element method, several technique have been proposed. Sakimoto et al. (12) proposed to reduce the size of the system matrices by using the two types of element, i.e. the plate element and the beam element. The former element was adopted for regions required to be discretized so refined, and the latter for other regions. Okamura and Ishikawa (9) analyzed the multi-span plate structures by the stiffness matrix method combined with a relaxation technique. In this approach, the displacement functions in series form and the point-matching method are adopted to derive the stiffness matrix of large-size rectangular plate panels.

In this chapter the method described in previous chapter is extended to linear and nonlinear problems of thin-walled members under various loading conditions. The substructuring procedure used in the finite element method (5) is, furthermore, adopted in order to treat complex structures, such as I-section and box-section plate girders with vertical stiffeners and web perforations. In the nonlinear analysis, the same incremental procedures in the finite element method can be applied, except for the evaluation of incremental displacements. The Newton-Raphson method (3) is employed in convergence procedures of each iterative step. It is assumed that the Prandtl-Reuss' law, and the von Mises yield criterion (11) are valid in this chapter. In order to consider the extent of the yielded portions in the directions of cross sections, the cross section of the structure is divided into some layers, and geometric nonlinearity is considered by using a set moving coordinate systems.

4-2 FINITE ELEMENT-TRANSFER MATRIX METHOD FOR THIN-WALLED MEMBERS

As the derivations of the tangent stiffness matrix and the transfer matrix for the plate structure and the descriptions related to the procedure for geometrical and material nonlinear problems are described in chapter 3, descriptions which mainly relate to the application of the FETM method to thin-walled members are given here.

1) Transfer Matrix for Thin-Walled Members

The thin-walled member is, in the FETM method, divided into some strips, each of which is subdivided into finite elements as shown in Fig.4-1. Although two types of strip shown in Fig.4-2 may be used, folded strip shown in Fig.4-2(a) are used in this paper, since it is expected that, for long structures, advantages attainable through matrix size reduction in folded strips pattern are greater.

Assembling the stiffness matrix of the elements for each strip, the equilibrium equations for the nodes on strip i are obtained as follows:

$$\mathbf{F}_i = \mathbf{K}_{s\,i}\ \boldsymbol{\delta}_i \qquad \cdots\cdots\cdots\cdots\cdots (4\text{-}1)$$

in which $\mathbf{K}_{s\,i}$ = the stiffness matrix of strip i; and $\boldsymbol{\delta}_i$ and $\mathbf{F}_i$ = the displacement and force vectors of strip i, respectively.

By expanding Eq.(4-1) and solving for the right displacement vector $\boldsymbol{\delta}_r$ and the force vector $\mathbf{F}_r$ in terms of the left displacement vector $\boldsymbol{\delta}_\ell$ and the force vector $\mathbf{F}_\ell$, the transfer matrix relating the left and right displacements and forces of strip can be obtained:

$$\begin{Bmatrix} \boldsymbol{\delta}_r \\ \mathbf{F}_r \\ 1 \end{Bmatrix}_i = \begin{bmatrix} -\mathbf{K}_{\ell r}^{-1}\mathbf{K}_{\ell\ell} & \mathbf{K}_{\ell r}^{-1} & \mathbf{0} \\ \mathbf{K}_{r\ell}-\mathbf{K}_{rr}\mathbf{K}_{\ell r}^{-1}\mathbf{K}_{\ell\ell} & \mathbf{K}_{rr}\mathbf{K}_{\ell r}^{-1} & \mathbf{0} \\ \mathbf{0} & \mathbf{0} & 1 \end{bmatrix}_i \begin{Bmatrix} \boldsymbol{\delta}_\ell \\ \mathbf{F}_\ell \\ 1 \end{Bmatrix}_i \qquad \cdots\cdots\cdots (4\text{-}2)$$

or

$$\mathbf{z}_i = \mathbf{T}_i\ \mathbf{z}_{i-1} \qquad \cdots\cdots\cdots\cdots\cdots (4\text{-}3)$$

in which $\mathbf{K}_{\ell\ell}$, $\mathbf{K}_{\ell r}$, $\mathbf{K}_{r\ell}$, and $\mathbf{K}_{rr}$ = the submatrices of $\mathbf{K}_{s\,i}$; and subscripts ℓ, r indicate the left and right sides of the strip.

2) Transfer Matrix for Substructures

In the case of complex structures such as I-section plate girders with vertical stiffeners and web perforations shown in Figs.4-4(a) and 4-5(a), these members are divided into not only strips shown in Fig.4-3(b) but also substructures in which the vertical stiffeners and web perforations are included as shown in Figs.4-4(b) and 4-5(b). Since in such substructure, adding boundary nodes, inner nodes are exist as shown in Figs.4-4(b) and 4-5(b), the transfer matrix given in Eq.(4-2) can't be applied to a substructure. The transfer matrix for a sub-structure is, therefore, derived herein.

By suitably transforming of the stiffness matrix of the sub-structure, which is obtained by assembling the stiffness matrix of the elements for each substructure, the following equation can be obtained:

$$\begin{Bmatrix} \mathbf{F}_{\ell} \\ \mathbf{F}_{i} \\ \mathbf{F}_{r} \end{Bmatrix}_i = \begin{bmatrix} \mathbf{K}_{\ell\ell} & \mathbf{K}_{\ell i} & \mathbf{K}_{\ell r} \\ \mathbf{K}_{i\ell} & \mathbf{K}_{ii} & \mathbf{K}_{ir} \\ \mathbf{K}_{r\ell} & \mathbf{K}_{ri} & \mathbf{K}_{rr} \end{bmatrix}_i \begin{Bmatrix} \boldsymbol{\delta}_{\ell} \\ \boldsymbol{\delta}_{i} \\ \boldsymbol{\delta}_{r} \end{Bmatrix}_i \qquad \cdots\cdots\cdots\cdots (4\text{-}4)$$

in which, $\boldsymbol{\delta}_i$, and $\mathbf{F}_i$ = the displacement and force vectors at inner nodes (Figs.4-4(b) and 4-5(b)), respectively; and $\mathbf{K}_{\ell\ell}$, $\mathbf{K}_{\ell i}$, $\mathbf{K}_{\ell r}$, $\mathbf{K}_{i\ell}$, $\mathbf{K}_{ii}$, $\mathbf{K}_{ir}$, $\mathbf{K}_{r\ell}$, $\mathbf{K}_{ri}$, and $\mathbf{K}_{rr}$ = the submatrices of the stiffness matrix of the substructure.

Solving the second line of Eq.(4-4) for the $\boldsymbol{\delta}_i$ and sub-stituting in the remaining equations, the following expressions are obtained:

$$\begin{Bmatrix} \mathbf{F}_{\ell} \\ \mathbf{F}_{r} \end{Bmatrix}_i = \begin{bmatrix} \mathbf{K}_{\ell\ell}-\mathbf{K}_{\ell i}\mathbf{K}_{ii}^{-1}\mathbf{K}_{i\ell} & \mathbf{K}_{\ell r}-\mathbf{K}_{\ell i}\mathbf{K}_{ii}^{-1}\mathbf{K}_{ir} \\ \mathbf{K}_{r\ell}-\mathbf{K}_{ri}\mathbf{K}_{ii}^{-1}\mathbf{K}_{i\ell} & \mathbf{K}_{r\ell}-\mathbf{K}_{ri}\mathbf{K}_{ii}^{-1}\mathbf{K}_{ir} \end{bmatrix}_i \begin{Bmatrix} \boldsymbol{\delta}_{\ell} \\ \boldsymbol{\delta}_{r} \end{Bmatrix}_i$$

$$+ \begin{Bmatrix} \mathbf{K}_{\ell i}\mathbf{K}_{ii}^{-1}\mathbf{F}_{i} \\ \mathbf{K}_{ri}\mathbf{K}_{ii}^{-1}\mathbf{F}_{i} \end{Bmatrix}_i \qquad \cdots\cdots\cdots\cdots (4\text{-}5)$$

or simplifying the notation:

$$\begin{Bmatrix} \mathbf{F}_\ell \\ \mathbf{F}_r \end{Bmatrix}_i = \begin{bmatrix} \mathbf{K}_{11} & \mathbf{K}_{12} \\ \mathbf{K}_{21} & \mathbf{K}_{22} \end{bmatrix}_i \begin{Bmatrix} \boldsymbol{\delta}_\ell \\ \boldsymbol{\delta}_r \end{Bmatrix}_i + \begin{Bmatrix} \mathbf{F}_1 \\ \mathbf{F}_2 \end{Bmatrix}_i \qquad \cdots\cdots\cdots\cdots (4\text{-}6)$$

By expanding and rearranging Eq.(4-6), it can be shown after various matrix manipulations that the left and right boundaries can be related by the following expression:

$$\begin{Bmatrix} \boldsymbol{\delta}_r \\ \mathbf{F}_r \end{Bmatrix}_i = \begin{bmatrix} -\mathbf{K}_{12}^{-1}\mathbf{K}_{11} & \mathbf{K}_{12}^{-1} \\ \mathbf{K}_{21}-\mathbf{K}_{22}\mathbf{K}_{12}^{-1}\mathbf{K}_{11} & \mathbf{K}_{22}\mathbf{K}_{12}^{-1} \end{bmatrix}_i \begin{Bmatrix} \boldsymbol{\delta}_\ell \\ \mathbf{F}_\ell \end{Bmatrix}_i$$

$$+ \begin{Bmatrix} -\mathbf{K}_{12}^{-1}\mathbf{F}_2 \\ \mathbf{F}_2-\mathbf{K}_{22}\mathbf{K}_{12}^{-1}\mathbf{F}_1 \end{Bmatrix}_i \qquad \cdots\cdots\cdots\cdots (4\text{-}7)$$

or simplifying the notation:

$$\begin{Bmatrix} \boldsymbol{\delta}_r \\ \mathbf{F}_r \end{Bmatrix}_i = \begin{bmatrix} \mathbf{T}_{11} & \mathbf{T}_{12} \\ \mathbf{T}_{21} & \mathbf{T}_{22} \end{bmatrix}_i \begin{Bmatrix} \boldsymbol{\delta}_\ell \\ \mathbf{F}_\ell \end{Bmatrix}_i + \begin{Bmatrix} \mathbf{T}_{F1} \\ \mathbf{T}_{F2} \end{Bmatrix}_i \qquad \cdots\cdots\cdots\cdots (4\text{-}8)$$

Adding one dummy equation to the system, the following equation can be obtained:

$$\begin{Bmatrix} \boldsymbol{\delta}_r \\ \mathbf{F}_r \\ 1 \end{Bmatrix}_i = \begin{bmatrix} \mathbf{T}_{11} & \mathbf{T}_{12} & \mathbf{T}_{F1} \\ \mathbf{T}_{21} & \mathbf{T}_{22} & \mathbf{T}_{F2} \\ \mathbf{0} & \mathbf{0} & 1 \end{bmatrix}_i \begin{Bmatrix} \boldsymbol{\delta}_\ell \\ \mathbf{F}_\ell \\ 1 \end{Bmatrix}_i \qquad \cdots\cdots\cdots\cdots (4\text{-}9)$$

which is the expanded transfer matrix relating the state vectors of the left and right boundaries of a substructure through the intermediate degrees of freedom. The sizes of the state vector and transfer matrix in Eq.(4-9) are same as those of the state vector and transfer matrix in Eq.(4-3) for the strip shown in Fig.4-3(b). Both transfer matrices can be, therefore, multiplied each other. I-section plate girders shown in Figs.4-4(a) and 4-5(a) can be analyzed by the combined use of the transfer matrix for the strip shown in Fig.4-3(b) and that for the substructures shown in Figs.4-4(b) and 4-5(b).

3) Transformation for Nodal Displacements

In the determining an equilibrium configuration of the structure under a given set of loads, the current local displacements which are related to the displaced local coordinate axes x, y, z, shown in Fig.4-6, are used to determine the local nodal forces. The local displacements are established by the transformation of nodal displacements from the global coordinate system to the local coordinate system. The transformation procedure for displacements U = {u, v, w} employed in this chapter is same as that for plate structures, and is described in Chapter 3. Hence, only descriptions of the transformations of rotations are presented here.

A typical element before and after deformation is shown in Fig.4-6. Four sets of rectangular cartesian axes: (1) the global coordinate system (X, Y, Z); (2) the initial local coordinate system (x^*, y^*, z^*); (3) the displaced local coordinate system (x, y, z); (4) the coordinate system (X^*, Y^*, X^*), which is established by the parallel transformation of the initial local coordinate system, such that the origin of this coordinate system is coincide with that of the global coordinate system are defined. Assuming that **E**, **e***, **e**, and **E*** indicate the unit orthogonal vectors in above four coordinate systems, respectively, the following expressions are obtained:

$$\mathbf{e} = \mathbf{L}_A \mathbf{E}, \quad \mathbf{e}^* = \mathbf{L}_B \mathbf{E}, \quad \mathbf{E}^* = \mathbf{L}_B \mathbf{E} \qquad \cdots\cdots\cdots\cdots (4\text{-}10)$$

in which $\mathbf{L}_A$, and $\mathbf{L}_B$ = the rotation matrices between the global coordinate system and the displaced coordinate system, and the global system and the initial system, respectively.

S′ designates a point S after deformation and S′′ indicates a point S in the reference element (1", 2", 3"), established on the displaced local axes having the same shape and size as the original element (1, 2, 3).

As shown in Fig.4-6, the vector $\rho = \overrightarrow{OS'}$ may be described in two ways:

$$\rho = \overrightarrow{O1} + \overrightarrow{1S} + \overrightarrow{SS'} \qquad \cdots\cdots\cdots\cdots(4\text{-}11)$$

or

$$\rho = \overrightarrow{O1} + \overrightarrow{11'} + \overrightarrow{1'S''} + \overrightarrow{S''S'} \qquad \cdots\cdots\cdots\cdots(4\text{-}12)$$

Expressing as components related to the coordinate system (X^*, Y^*, Z^*), Eqs.(4-11) and (4-12) become:

$$\begin{Bmatrix} X^* \\ Y^* \\ Z^* \end{Bmatrix} = \begin{Bmatrix} X_1^* \\ Y_1^* \\ Z_1^* \end{Bmatrix} + \begin{Bmatrix} x_0 \\ y_0 \\ 0 \end{Bmatrix} + \begin{Bmatrix} U^* \\ V^* \\ W^* \end{Bmatrix} \qquad \cdots\cdots\cdots\cdots(4\text{-}13)$$

$$\begin{Bmatrix} X^* \\ Y^* \\ Z^* \end{Bmatrix} = \begin{Bmatrix} X_1^* \\ Y_1^* \\ Z_1^* \end{Bmatrix} + \begin{Bmatrix} U_1^* \\ V_1^* \\ W_1^* \end{Bmatrix} + L^T \begin{Bmatrix} x_0 \\ y_0 \\ 0 \end{Bmatrix} + L^T \begin{Bmatrix} u \\ v \\ w \end{Bmatrix} \qquad \cdots\cdots\cdots\cdots(4\text{-}14)$$

in which L = the rotation matrix between the initial coordinate system and the displaced coordinate system, i.e. $L = L_A L_B{}^T$.

Solving the last line of Eq.(4-14) for w, and recognizing from Eq.(4-13) that $W^* = Z^* - Z_1{}^*$, the following expression can be obtained:

$$w = L_{31}(X^* - X_1{}^* - U_1{}^*) + L_{32}(Y^* - Y_1{}^* - V_1{}^*) + L_{33}(W^* - W_1{}^*) \qquad \cdots\cdots\cdots\cdots(4\text{-}15)$$

in which L_{31}, L_{32}, and L_{33} = the components of the rotation matrix L, respectively. By differentiating both sides of Eq.(4-

15) by x and y, respectively, the following expressions can be obtained:

$$\frac{\partial w}{\partial x} = \frac{\partial w}{\partial X^*}\cdot\frac{\partial X^*}{\partial x} + \frac{\partial w}{\partial Y^*}\cdot\frac{\partial Y^*}{\partial x}$$

$$\frac{\partial w}{\partial y} = \frac{\partial w}{\partial X^*}\cdot\frac{\partial X^*}{\partial y} + \frac{\partial w}{\partial Y^*}\cdot\frac{\partial Y^*}{\partial y} \qquad \cdots\cdots\cdots\cdots(4\text{-}16)$$

in which

$$\frac{\partial w}{\partial X^*} = L_{31} + L_{33}\frac{\partial W^*}{\partial X^*}, \qquad \frac{\partial w}{\partial Y^*} = L_{32} + L_{33}\frac{\partial W^*}{\partial Y^*}$$

Considering that, in the displaced coordinate system (x, y, z), $x = x_0 + u$ and $y = y_0 + v$, the following expressions are obtained from Eq.(4-14):

$$X^* = X_1^* + U_1^* + L_{11}x + L_{21}y + L_{31}w$$

$$Y^* = Y_1^* + V_1^* + L_{12}x + L_{22}y + L_{32}w \qquad \cdots\cdots\cdots\cdots(4\text{-}17)$$

Differentiating both sides of Eq.(4-17) by x and y, respectively, and substituting $\partial X^*/\partial x$, $\partial X^*/\partial y$, $\partial Y^*/\partial x$, and $\partial Y^*/\partial y$ obtained above into Eq.(4-16), the rotational transformations are finally established as follows:

$$\theta_x = \{(L_{31} - L_{33}\theta_Y^*)L_{21} + (L_{32} + L_{33}\theta_X^*)L_{22}\}/\alpha$$

$$\theta_y = -\{(L_{31} - L_{33}\theta_Y^*)L_{11} + (L_{32} + L_{33}\theta_X^*)L_{21}\}/\alpha \qquad \cdots\cdots\cdots(4\text{-}18)$$

in which

$$\theta_X^* = \partial W^*/\partial Y^*, \qquad \theta_Y^* = -\partial W^*/\partial X^*$$

$$\alpha = 1 - (L_{31} - L_{33}\theta_Y^*)L_{31} - (L_{32} + L_{33}\theta_X^*)L_{32}$$

It is confirmed by the authors that the solutions obtained by the procedure described here are, in the plate structure problems, exactly coincide with those obtained by Komatsu's procedure (3).

4-3 NUMERICAL EXAMPLES

1) Box-Section Plate Girder

To examine the accuracy and efficiency of the FETM method, a box-section plate girder loaded at the midspan shown in Fig.4-7 is analyzed, and the results obtained by the FETM method are compared with those obtained by the finite element method, where the same element and mesh pattern as those used in the FETM method are employed.

In the numerical calculation, a quarter of the entire system is divided into 4, 6, 8, and 10 strips, and each strip into 8 triangular elements for every dividing patterns as shown in Fig.4-7. Neither geometrical nor material nonlinearity is, herein, taken into consideration, and both ends of the box-section plate girder are fixed in this example.

Fig.4-8(a) shows a comparison between the deflections at the point C in Fig.4-7 obtained by the FETM method and those obtained by the finite element method. As shown in Fig.4-8(a), both results coincide within three significant figures with each other. Fig.4-8(b) shows a comparison of computation times of both methods in this example. It can be seen that, in computation time, although the FETM method has less advantage for the small number of strips pattern (4 and 6 strips pattern), this method has much advantage for the large number of strips pattern (8 and 10 strips pattern). Fig.4-8(c) shows a comparison of the matrix sizes required in both methods. The matrix size in the finite element method increases as the number of strips, i.e. the number of total nodes increases, and if the banded matrix is used, it is given by {(the number of total nodes) × (degrees of freedom)} × (the band width). The matrix to be considered in the finite element method for this example is, therefore, 25×6×42 = 6300 for 4-strips pattern, 35×6×42=8820 for 6-strips pattern, 45×6×42 = 11340 for 8-strips pattern, and 55×6×42 = 13860 for 10-strips pattern in this example. On the other side, the matrix size in the FETM method is dependent on the number of degrees of freedom for only one strip in contrast with the finite element method, and it is given by {(the number of nodes on a section) × (degrees of freedom)×2}^{2}. The matrix to be considered in the FETM method is, $(5\times6\times2)^2$=3600 for every dividing pattern.

2) Simply Supported Plate with a Perforation

To illustrate the efficiency of the FETM method based on the substructuring procedure developed in this chapter, the in-plane loaded simply supported plate with a center perforation, as shown in Fig.4-9(a) (a=b=100cm, t=1cm, r=a/10) is analyzed. A quarter of the plate is divided into two types of strip shown in Fig.4-9(b), and in the strip including a perforation, 3 nodes are inner nodes among all the 13 nodes. Geometrical and material nonlinearity are taken into consideration here, and the modulus of elasticity $E=2.1\times10^6$ kg/cm^2, the yield stress σ_y=3100kg/cm^2, and the Poisson's ratio ν = 0.3 are used in numerical calculation. The initial deflection of plate bending mode is assumed, and defined as follows:

$$w = \bar{w}_0 \sin\frac{\pi}{a}x \sin\frac{\pi}{b}y \qquad \cdots\cdots\cdots\cdots(4\text{-}19)$$

in which $\bar{w}_0$ = the maximum value of initial deflection and here $\bar{w}_0$ = t/10 is also assumed. In Fig.4-9(a) the out-of-plane displacements at point C obtained by the FETM method are compared with those by the finite element method. In the finite element method, the same element and mesh pattern as those used in the FETM method are employed, and complete agreement exists in both results.

3) Box-Section Plate Girder with Web Perforations

To illustrate the efficiency of the FETM methods based on the substructuring procedure for the thin-walled member, a box-section plate girder with web perforations loaded at the midspan shown in Fig.4-10(a) is analyzed, and numerical results are compared with those obtained by the finite element method. A quarter of the entire system is divided into 10 strips as shown in Fig.4-10(a). The strip including web perforation (Fig.4-10(c)) is divided into 20 triangular elements. Among all the 18 nodes of this strip, 8 nodes are inner nodes. Geometrical and material nonlinearity are taken into consideration, and the modulus of elasticity $E = 2.1\times10^6$ kg/cm^2, the yield stress σ_Y = 2800kg/cm^2, and the Poisson's ratio ν = 0.3 are used for numerical calculation. Other dimensions are indicated in Fig.4-10(a), and both ends of the box-section plate girder are fixed. The notation q_{0y} indicated in Fig.4-10(a) is the load level corresponding to the yield stress for the box-section plate girder without web perforation.

Fig.4-11(a) shows the comparison between the center deflections of flange at x=0.25L, 0.4L and 0.5L (Points 1, 2 and 3 in Fig.4-11(a)) obtained by the FETM method and those obtained by the finite element method. As shown in Fig.4-11(a), good agreement exists between both results.

Fig.4-11(b) shows the comparison between the out-of-plane displacements of web at points 1 and 2 in Fig.4-11(b) obtained by both methods, and good agreement exists between both results.

4) I-Section Plate Girder with Web Perforations

I-section beam loaded at the midspan with consecutive web perforations, as shown in Fig.4-12(a), is analyzed, and numerical results are compared with those obtained by the finite element method. The half member is divided into five same substructures, and each substructure into 30 triangular elements, as shown in Fig.4-12(b). Among all the 26 nodes of each substructure, 12 nodes are inner nodes. Geometrical and material nonlinearity are taken into consideration, and the modulus of elasticity $E = 2.1\times10^{6}$ kg/cm^2, the yield stress σ_Y=2800kg/cm^2, and the Poisson's ratio ν = 0.3 are used for calculation. Other dimensions are indicated in Fig.4-12(a), and both ends of the I-section plate girder are fixed, as in the previous example. The notation q_{0y} indicated in Fig.4-12(a) is the load level corresponding to the yield stress for the I-section plate girder without web perforation.

Fig.4-13(a) shows the center deflections of the upper and lower flanges at x = 0.1L, 0.3L, and 0.5L. In Fig.4-13(a), the finite element solutions are also shown, and both results coincide with each other. The deflections at x = 0.1L and 0.3L increase almost linearly, and very little difference exists between the deflections of the upper and lower flanges, so that it can't be distinct in Fig.4-13(a). On the other hand, in the deflection of the upper flange at x = 0.5L, the material nonlinearity becomes significant from load level q_0=2.5 and is greater compared with that of the lower flange.

Fig.4-13(b) shows the out-of-plane displacements of midpoint of web at x = 0.1L, 0.2L, 0.3L, 0.4L, and 0.5L. Good agreement exists between the results obtained by the FETM method and the finite element method as the deflections of the flange.

Figs.4-14(a) and 4-14(b) show the axial stresses of the upper and lower flange (A and B in Fig.4-14(a)), and the axial stresses of the web (C and D in Fig.4-14(b)). Both the results of the FETM method and the finite element method are also in good agreement.

The matrix to be considered in the finite element method is, if the banded matrix is used, 726×84 for this example, compared to 84×84 in the FETM method.

5) I-Section Plate Girder with Stiffeners Subjected to Lateral Load

I-section plate girder with stiffeners subjected at the mid-span to lateral line load across the upper flange, shown in Fig.4-15(a), is analyzed. The half member is divided into 4 strips and 2 substructures, and these are into 12 and 36 triangular elements, respectively, as shown in Fig.4-15(b), (c). Among all the 24 nodes of each substructure, 10 nodes are inner nodes. The yield stresses of the member is assumed to be $\sigma_Y = 2800 kg/cm^2$, and other material constants and boundary conditions are same as those in the previous example. The notation q_{0y} indicated in Fig.4-15(a) is the load level corresponding to the yield stress for the I-section plate girder without stiffener.

Fig.4-16(a) shows the center deflections of the upper and lower flanges at x = 0.267L, 0.4L, and 0.5L. In Fig.4-16(a), the finite element solutions are also shown, and both results coincide with each other. Every deflection shows the similar behavior, and the material nonlinearity becomes substantial from the load level of $q_0 = 11$. In the deflections at x = 0.267L and 0.4L, very little difference exists between the deflections of the upper and lower flanges, so that it can't be distinct in Fig.4-16(a).

Fig.4-16(b) shows the out-of-plane displacements of web at point A and B in Fig.4-16(b). Point A is a point of the section with the stiffener, and point B a point of center web. In the displacement at point B, the material nonlinearity becomes substantial from the load level of $q_0=11$. Although the displacement at point A is very little until load level $q_0=3$, it becomes substantial from this load level.

Figs.4-17(a) and 17(b) show the axial stresses of the upper and lower flange (A and B in Fig.4-17(a)), and the axial stresses of the web (C in Fig.4-17(b)). Both the results of the FETM method and the finite element method are also in good agreement.

6) I-Section Plate Girder with Stiffeners under In-Plane Axial Load

For the last example, stiffened I-section plate girder subjected at the edges to in-plane axial load, as shown in Fig.4-18, is analyzed. Numerical calculations are, in this example, proceeding for the following three models. (1) Model I; a model composed of only a sub-panel between the vertical stiffeners, shown in Fig.4-19(a). It is assumed that, in this model, both side boundaries are simply supported, and upper and lower boundaries are fixed. (2) Model II; a model cut out from entire structure by two adjacent vertical stiffeners shown in Fig.4-19(b). In this model, the effects of the flanges on the behaviors of the structure can be, therefore, taken into cosideration, and side boundaries are simply supported as in Model I. (3) Model III; a total system model of the I-section plate girder, shown in Fig.4-19(c). In this model, not only the effects of the flanges but also of the stiffeners can be taken into consideration, and both end boundaries are fixed.

In Models I and II, the initial deflection of plate bending mode defined in Eq.(4-19) is assumed, and maximum value of initial deflection $\bar{w}_0$ = t/5 is used here. On the other hand, in Model III the initial deflection given above is assumed for every sub-panels between the vertical stiffeners, but no initial deflection is assumed for the flange, as shown in Fig.4-20(a). The yield stresses of the web and flanges are assumed to be σ_Y = 2800kg/cm^2 and the yield stress of the vertical stiffener σ_{SY} = 4000kg/cm^2, and other material constants are same as those in the previous example. The half member is, in model Ⅲ, divided into 6 substructures, and each substructure into triangular finite elements as shown in Fig.4-15(b), (c).

Fig.4-21 shows the out-of-plane displacements at the mid-point of web, where the displacement for Model Ⅲ is of the center web. It is shown from Fig.4-21 that until the load level of about P/P_{cr}=2.0 the load-deflection curves for every model show similar tendencies, and the deflection for Model Ⅱ is greatest, and that for Model Ⅲ is next. Since over this load level, in Models I and Ⅱ, the effects of the geometrical nonlinearity on the behaviors of the I-section plate girder become substantial, the increasing rate of the deflections for Models I and Ⅱ become smaller. On the other hand, the deflection for Model Ⅲ increases suddenly in contrast with Models I and Ⅱ, and the ultimate strength for Model Ⅲ is approximately 20% less than that for Model I. In Fig.4-20(b), the mode of deflection of Model Ⅲ at the load level of P/P_{cr} = 2 is shown.

4-4 CONCLUSIONS

The combined finite element - transfer matrix method is extended to the linear and nonlinear problems of thin-walled members, and a computer program based on this theory has been developed. The following conclusions can be drawn from this study:

(1) Good agreement exists between the results obtained by the FETM method and the standard finite element method not only

in the linear problems but also in the nonlinear problems, which demonstrates the accuracy of the proposed method.

(2) From numerical examples presented in this chapter, it is shown that this method can be successfully applied to the long thin-walled members by reducing the size of the matrix and the computation time relative to less than that obtained by the finite element method.

(3) By adopting the transfer matrix for substructures derived in this chapter, complex thin-walled members, such as I-section and box-section plate girders with vertical stiffeners and web perforations, can be treated easily.

(4) Considerable differences exist between the results for the model of entire system and for the model cut out from the structure.

REFERENCES

1. Cheung, Y.K., "Finite Strip Method in Structural Analysis," Pergamon Press, 1976.
2. Dokainish, M.A., "A New Approach for Plate Vibrations: Combination of Transfer Matrix and Finite-Element Technique," Trans. ASME Vol.94, No.2, 1972, pp.526-530.
3. Komatsu, S., Kitada, T. and Miyazaki, S., "Elasto-Plastic Analysis of Compressed Plate with Residual Stress and Initial Deflection," Proc. of JSCE, No.244, Dec., 1975, pp.1-14 (in Japanese).
4. Komatsu, S. and Kitada, T., "Refined Finite Element Analysis of Plane Elasto-Plastic Problems," Technology Reports of Osaka University, Vol.25, 1975, pp.415-437.
5. McGuire, W. and Gallagher, R.H., "Matrix Structural Analysis," John Wiley & Sons, Inc., New York, N.Y., 1979.
6. Ohga, M., Shigematsu, T. and Hara, T., "Structural Analysis by a Combined Finite Element - Transfer Matrix Method," Computers & Structures, Pergamon Press, Vol.17, No.3, 1983, pp.321-326.
7. Ohga, M., Shigematsu, T. and Hara, T., "Structural Analysis

by a Combined Finite Element - Transfer Matrix Method," J. ASCE, Vol.110, No.EM9, September 1984, pp.1335-1349.
8. Ohga, M. and Hara, T., "Analysis of Thin-Walled Member by Finite Element - Transfer Matrix Method," Proc. of JSCE, No.368/I-5, April, 1986, pp.95-102.
9. Okamura, H. and Ishikawa, K., "Analysis of Multi-Span Plate Structures by a Small Computer," Proc. of JSCE, No.344/I-1, April, 1984, pp.313-322 (in Japanese).
10. Yamada, Y., Yoshimura, N. and Sakurai, T., "Plastic Stress-Strain Matrix and Its Application for the Solution of Elastic - Plastic Problems by the Finite Element Methods," Int. J. Mech. Sci., Vol.10, 1968, pp.343-354.
11. Yamada, Y., "Matrix Methods of Strength of Materials," Baifukan, 1980 (in Japanese).
12. Yamamoto, T., Hotta, M., Obata, K. and Sakimoto, T., "Analysis of Thin-Walled Structures by Combined Use of Plate and Beam Elements," 38th Annual Conference of JSCE, pp.155-156, Oct., 1983 (in Japanese).
13. Zienkiewicz, O.C., "The Finite Element Method in Engineering Science," McGraw-Hill, 1971.

NOTATION

The following symbols are used in this paper

$\mathbf{D}_e, \mathbf{D}_p, \mathbf{D}_{ep}$ = elastic, plastic and elastic-plastic stress-strain matrices;
E = modulus of elasticity;
F = force vector;
$\mathbf{F}_\ell, \mathbf{F}_r$ = left and right force vectors of strip;
H = slope of the equivalent stress versus plastic strain curve;
$\mathbf{K}$ = strip tangent stiffness matrix;
$\mathbf{k}$ = element tangent stiffness matrix;
$\mathbf{k}_M$ = element tangent stiffness matrix, which contains no terms corresponding to geometric nonlinearity;
$\mathbf{L}_A, \mathbf{L}_B$ = transformation matrices relating the global coordinate system with the displaced local and initial local one;
$\mathbf{T}$ = transfer matrix;
U, V, W = displacements related to the global coordinate

system;

u,v,w = displacements related to the local coordinate system;

$\mathbf{z}$ = state vector;

$\mathbf{z}_\ell, \mathbf{z}_r$ = left and right state vector of strip;

$\boldsymbol{\delta}$ = displacement vector;

$\boldsymbol{\delta}_\ell, \boldsymbol{\delta}_r$ = left and right displacement vectors of strip;

$\boldsymbol{\varepsilon}$ = strain vector;

θ_x, θ_y = rotations about x and y axis;

ν = Poisson's ratio;

$\boldsymbol{\sigma}$ = stress vector; and

$\bar{\sigma}$ = equivalent stress.

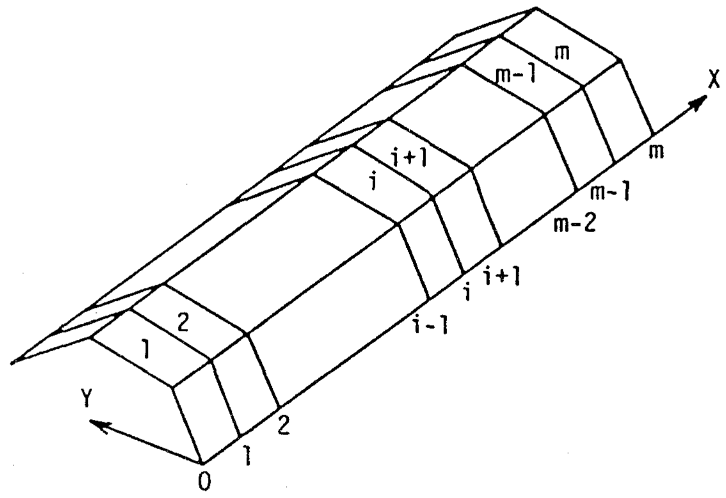

Fig.4-1 Subdivision of Thin-Walled Member

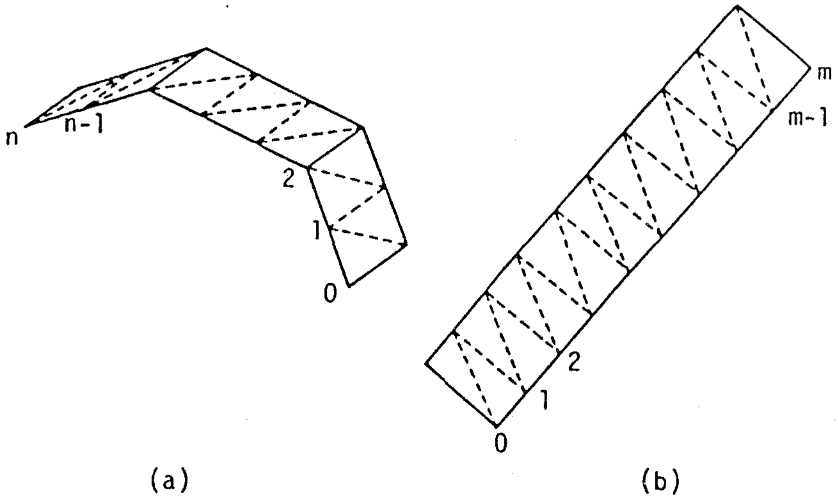

Fig.4-2 Strips for Thin-Walled Member

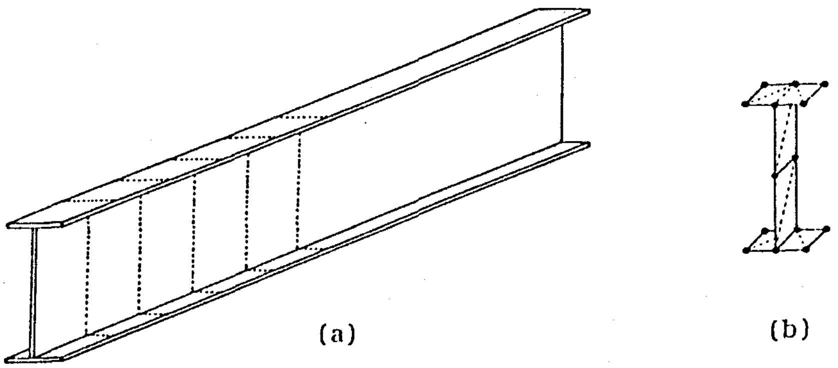

Fig.4-3 I-Section Plate Girder

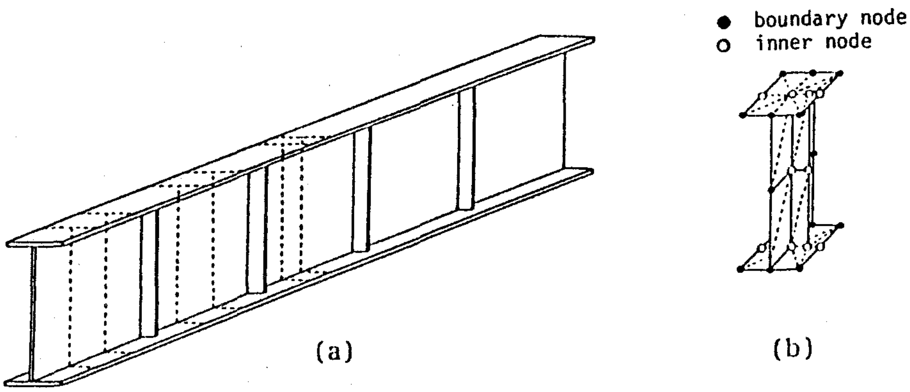

Fig.4-4 I-Section Plate Girder with Vertical Stiffeners

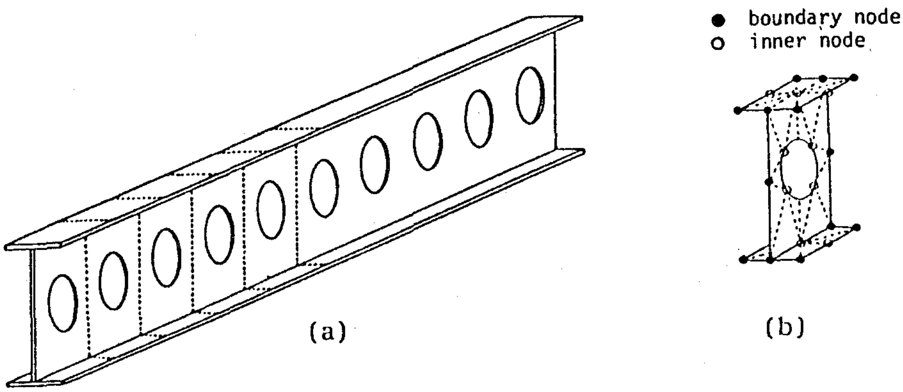

Fig.4-5 I-Section Plate Girder with Web Perforations

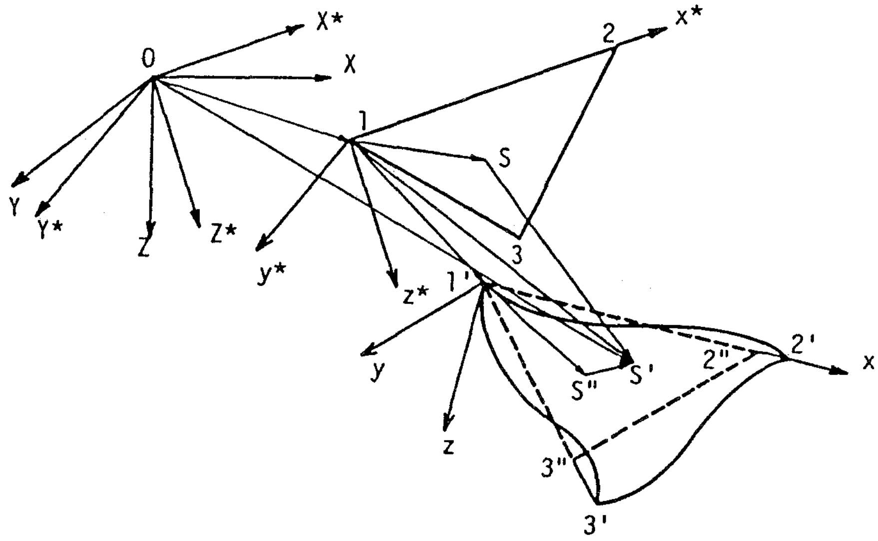

Fig.4-6 Location of Element Before and After Deformation

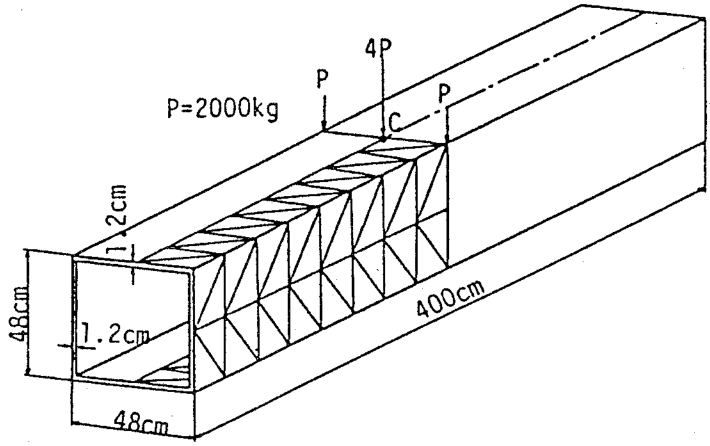

Fig,4-7 Box-Section Plate Girder

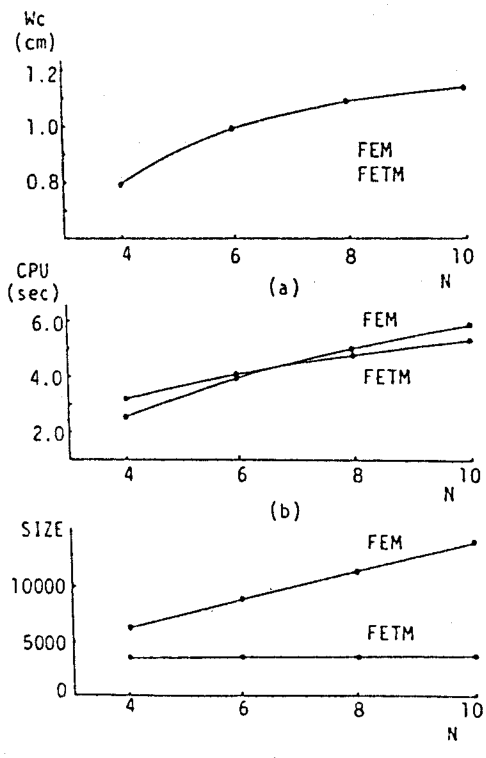

Fig.4-8 Comparison of FETM and FEM

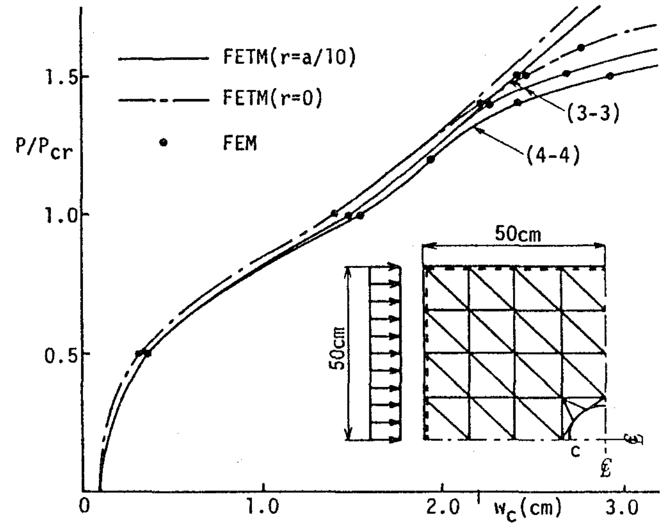

Fig.4-9(a) Displacements of Simply Supported Plate with Center Perforation

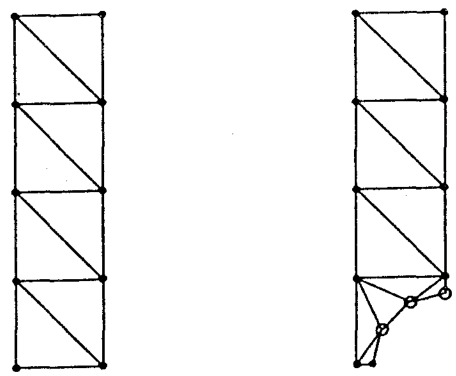

Fig.4-9(b) Strips for Plate with a Center Perforation

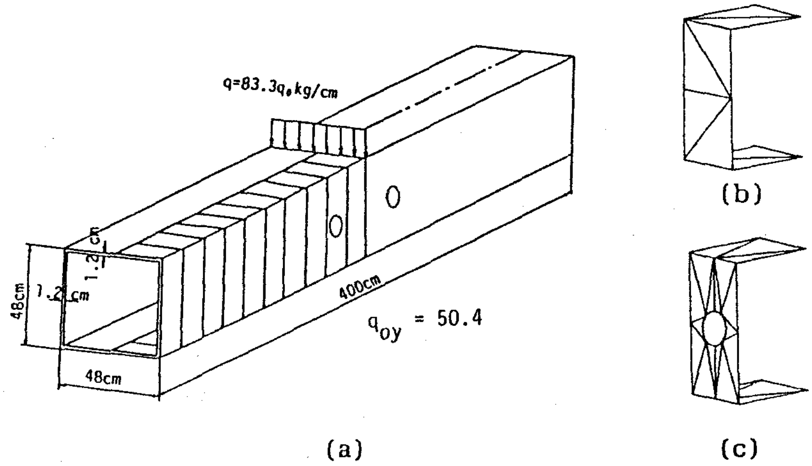

Fig.4-10 Box-Section Plate Girder with Web Perforations

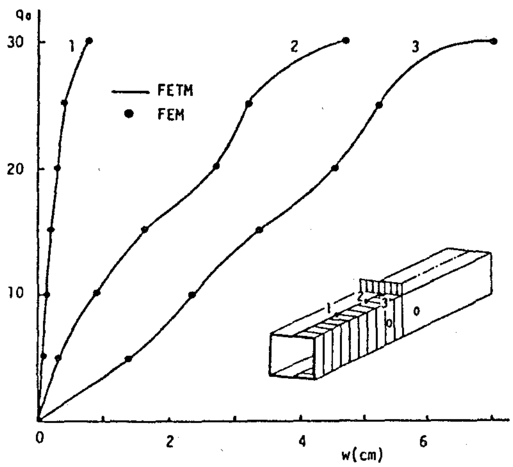

Fig.4-11(a) Deflectons at Upper and Lower Flange

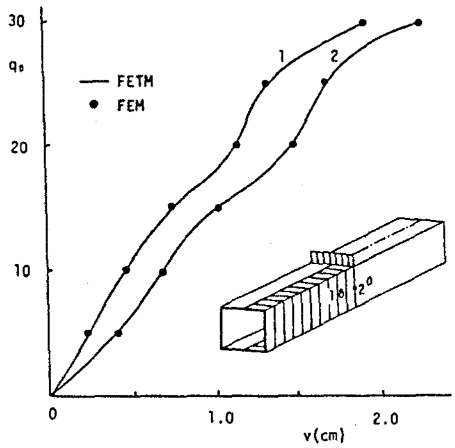

Fig.4-11(b) Out-of-Plane Displacements at Web

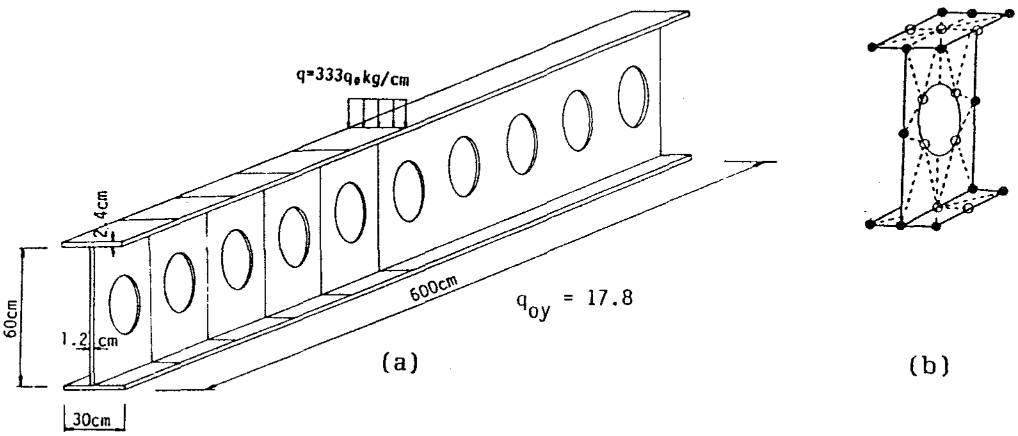

Fig.4-12 I-Section Beam with Web Perforations

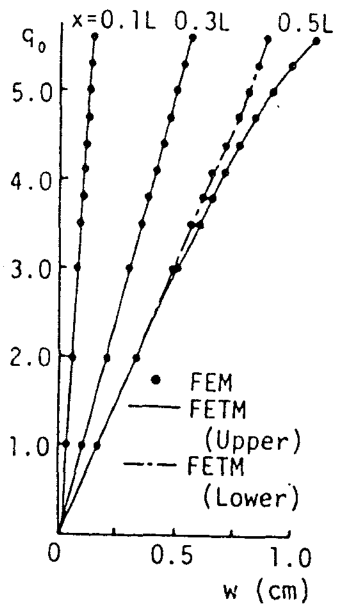

Fig.4-13(a) Deflections at Upper and Lower Flange

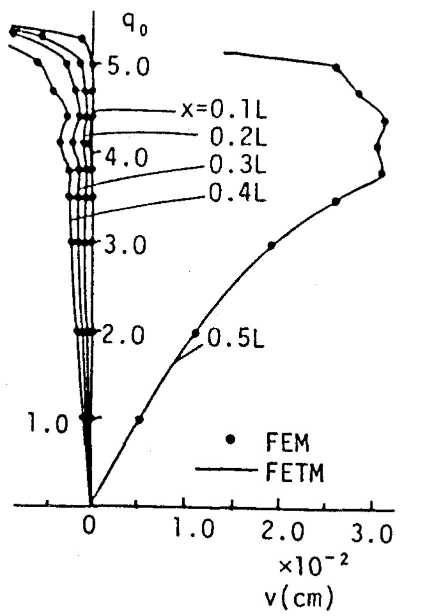

Fig.4-13(b) Out-of-Plane Displacements at Web

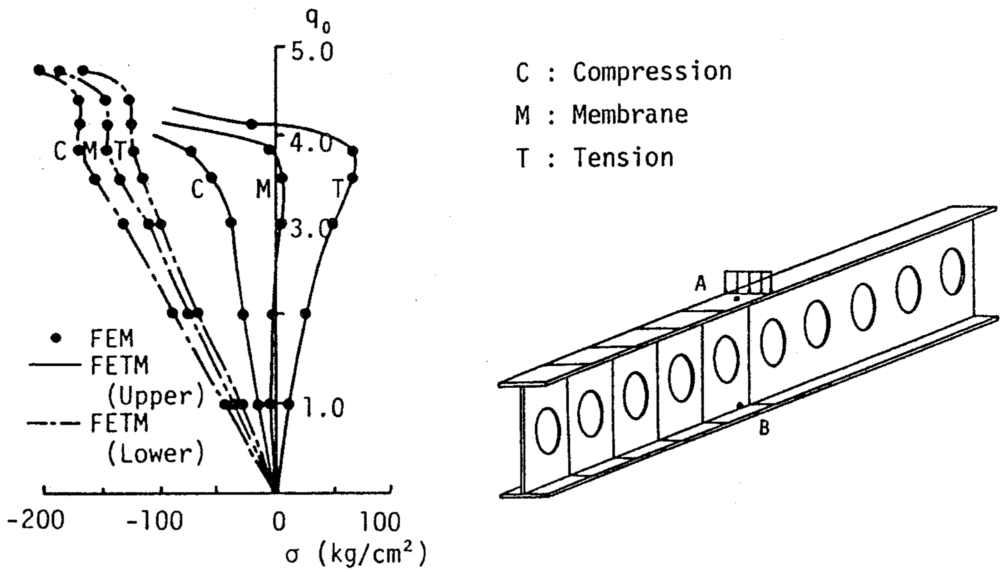

Fig.4-14(a) Stresses at Upper and Lower Flange

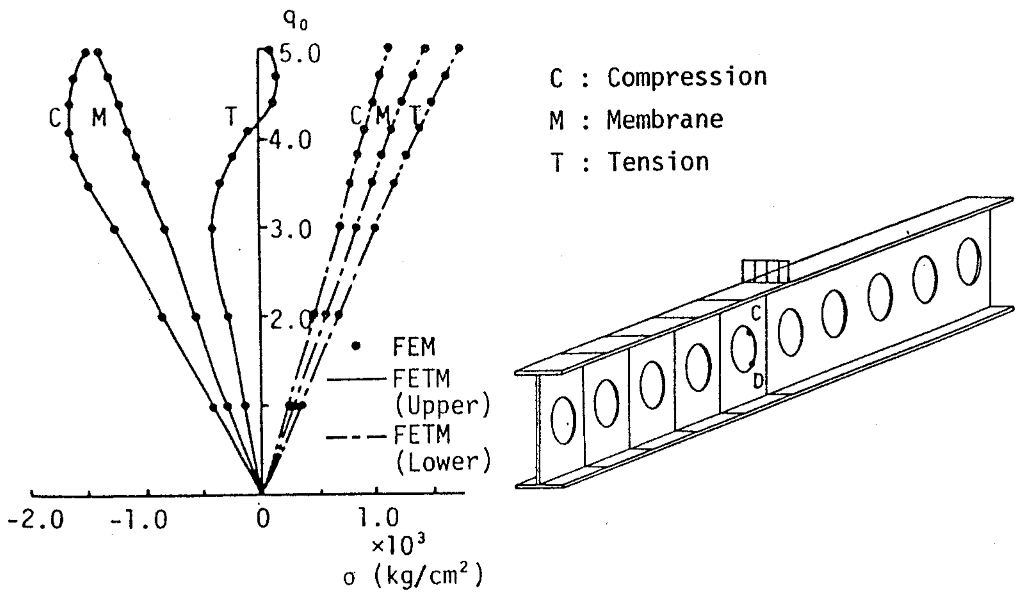

Fig.4-14(b) Stresses at Web

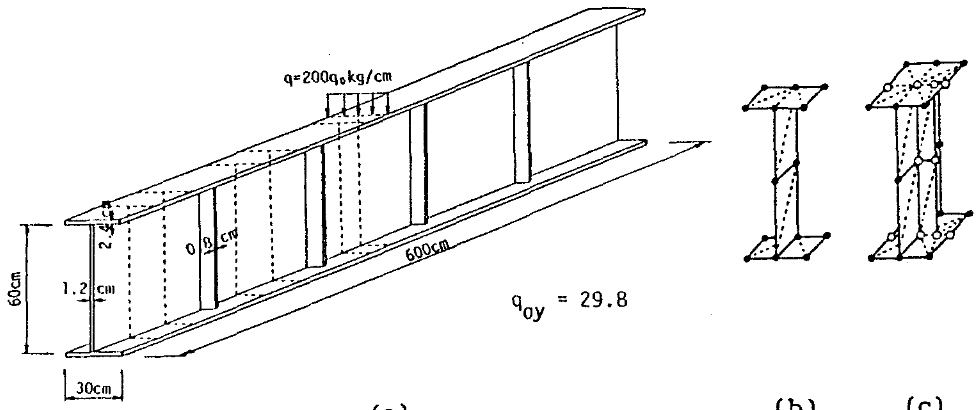

(a) (b) (c)

Fig.4-15 I-Section Plate Girder with Stiffeners

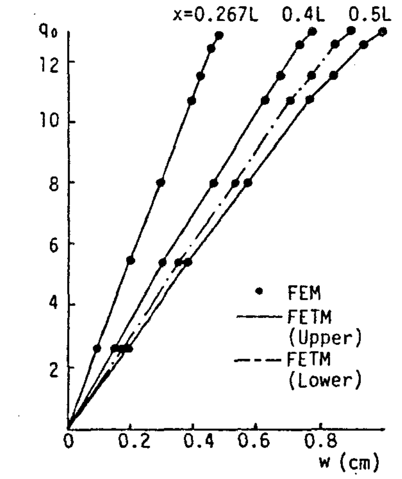

Fig.4-16(a) Deflections at Upper and Lower Flange

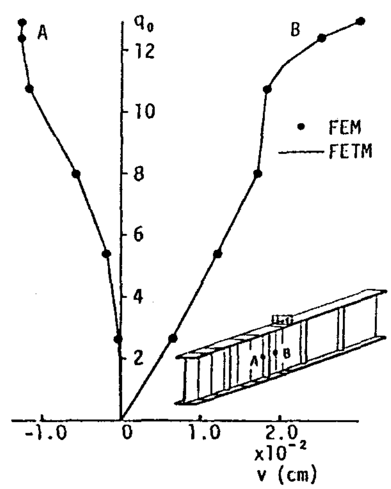

Fig.4-16(b) Out-of-Plane Displacements at Web

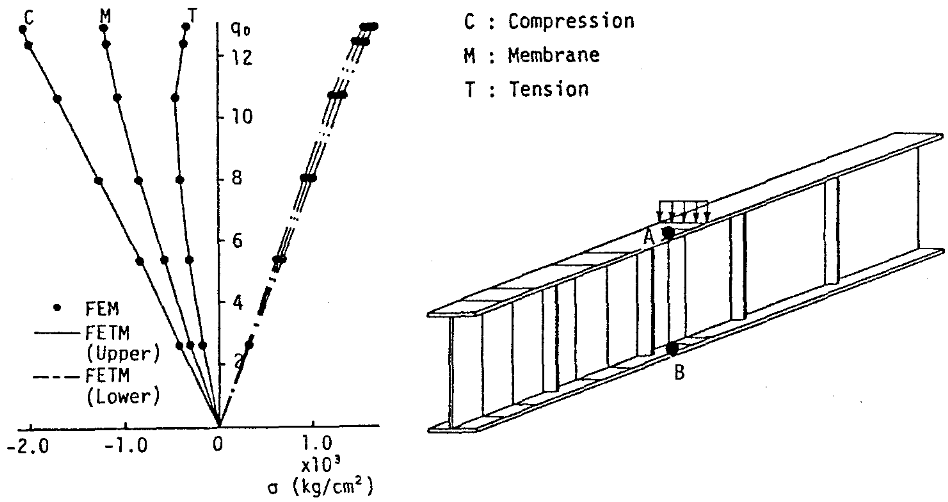

Fig.4-17(a) Stresses at Upper and Lower Flange

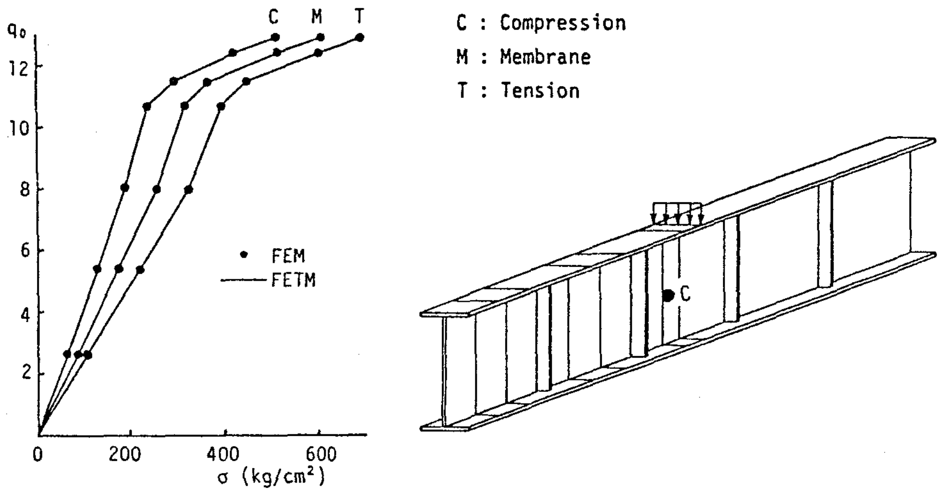

Fig.4-17(b) Stresses at Web

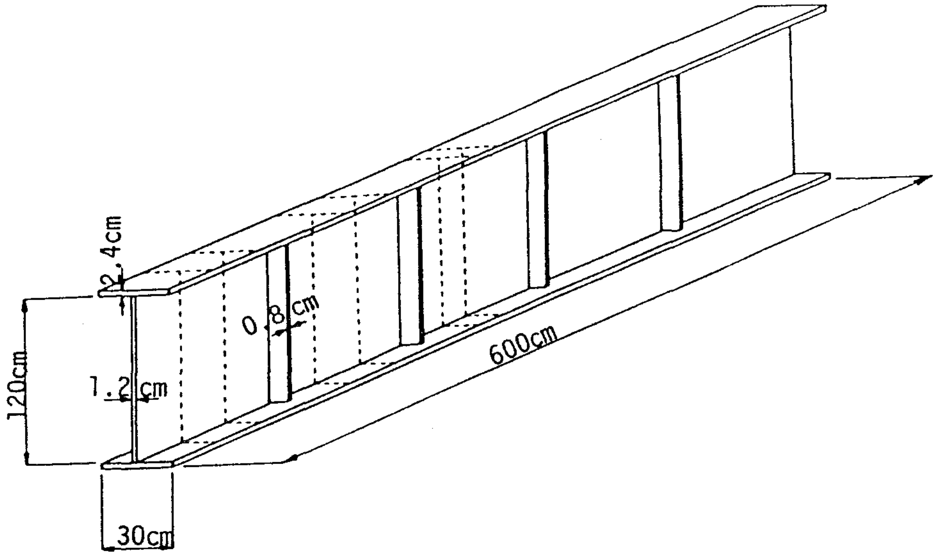

Fig.4-18 I-Section Plate Girder with Stiffeners

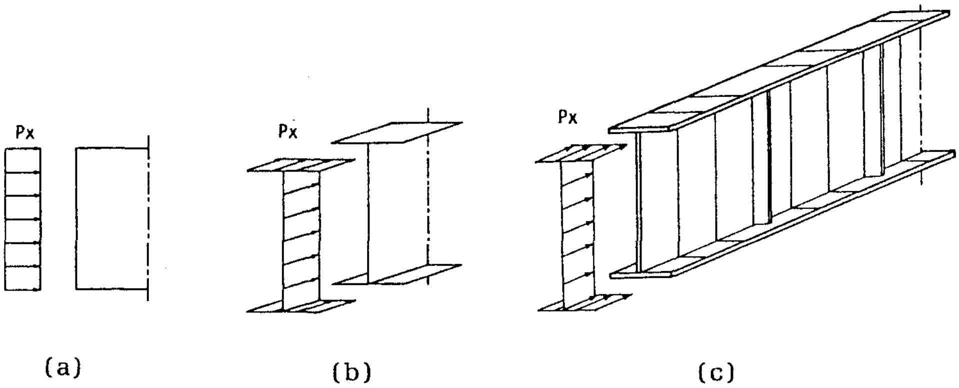

Fig.4-19 Models for Analysis

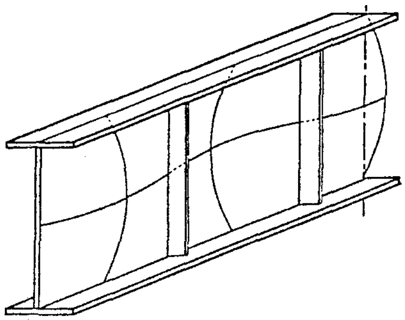

Fig.4-20(a) Mode of Initial Deflection

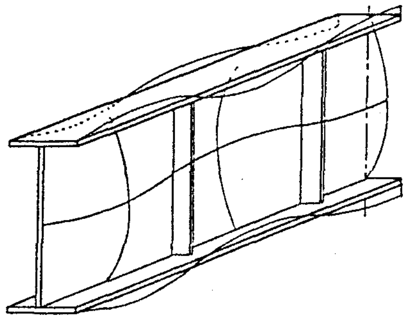

Fig.4-20(b) Mode of Deformation

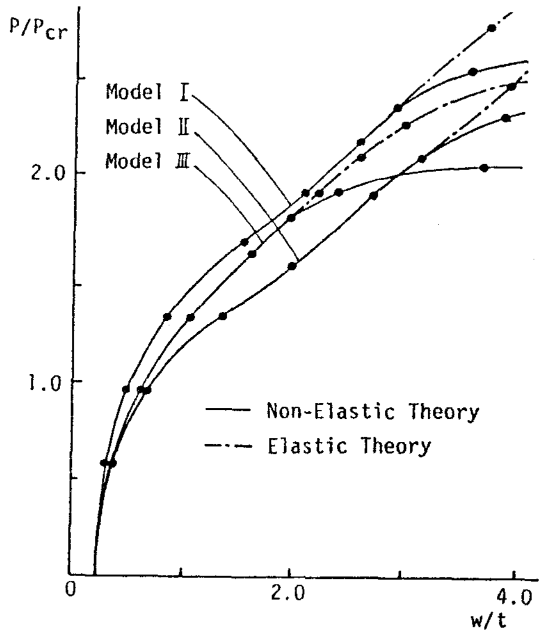

Fig.4-21 Deflections at Midpoint of Center Web

Chapter 5 DYNAMIC ANALYSIS OF PLATES BY A COMBINED FINITE ELEMENT-TRANSFER MATRIX METHOD

5-1 INTRODUCTION

In general, the transient response of complex structures subjected to random excitations can be obtained by the modal superposition or direct integration methods. In the modal superposition method, the eigenvalues and the eigenvectors of the resulting system are first computed. Then the response of the structure is formulated as a linear combination of the mode shapes (8). However, since this method is based on the assumption of linear behaviour, application of this method is restricted to a narrow range (1). In the direct integration method, the system of equations of motion is integrated by a numerical step-by-step procedure such as the Newmark β, Houbolt, Wilson Θ and central difference methods (2, 3, 4, 8, 12, 16). These methods do not require any restrictive assumptions on the damping properties and they are widely employed in linear and nonlinear dynamic problems (19). However, in the case of a complex structure, it is necessary to use a large number of nodes, resulting in a need of very large computers for their management and regulation.

In this chapter a method of analyzing the linear transient response of structures under various random excitations by the combined finite element - transfer matrix method (FETM) is proposed. The combined use of finite element and transfer matrix was proposed by Dokainish for the free vibration problems of plates (7). Since the publication of Dokainish's paper in 1972, several authors have proposed refinements and extensions of this method for static and free vibration problems (5, 6, 9, 11, 13, 14, 18).

This study is an extension of this method to the transient analysis of the plate structures subjected to random out-of-plane and in-plane excitations. The Newmark β method is used for time integration, but other integration methods such as the Houbolt, Wilson θ and central difference methods may be used. Also the technique of exchanging the unknown state vector is introduced to avoid the propagation of round-off errors occurring in recursive multiplications of the transfer and point matrices.

Some numerical examples of the plates subjected out-of-plane and in-plane excitations are proposed and their results are compared with those obtained by other methods.

5-2 DIRECT INTEGRATION METHOD

The governing equation for a plate subjected to out-of-plane excitation at time $t_{s+1} = (s+1)\Delta t$, where s is the number of time steps Δt, is generally given by

$$\mathbf{M}\,\ddot{\mathbf{u}}_{s+1} + \mathbf{C}\,\dot{\mathbf{u}}_{s+1} + \mathbf{K}\,\mathbf{u}_{s+1} = \mathbf{F}_{s+1} \qquad \cdots\cdots\cdots\cdots(5\text{-}1)$$

in which **M**, **C** and **K** are mass, damping, and stiffness matrices; $\mathbf{u}_{s+1}$, $\dot{\mathbf{u}}_{s+1}$, $\ddot{\mathbf{u}}_{s+1}$, and $\mathbf{F}_{s+1}$ are the displacement, velocity, acceleration, and force vectors at time t_{s+1}, respectively.

As described previously, the Newmark β method is used for time integration. In this method we assumed variations for the displacement, $\mathbf{u}$, and velocity, $\dot{\mathbf{u}}$, in the time interval Δt to be such that the values at beginning and end of the time step are related by equations of the form

$$\mathbf{u}_{s+1} = \mathbf{u}_s + \Delta t\,\dot{\mathbf{u}}_s + \left(\frac{1}{2} - \beta\right)\Delta t^2\,\ddot{\mathbf{u}}_s + \beta\,\Delta t^2\,\ddot{\mathbf{u}}_{s+1} \qquad \cdots\cdot(5\text{-}2)$$

$$\dot{\mathbf{u}}_{s+1} = \dot{\mathbf{u}}_s + (1-\gamma)\,\Delta t\,\ddot{\mathbf{u}}_s + \gamma\,\Delta t\,\ddot{\mathbf{u}}_{s+1} \qquad \cdots\cdots(5\text{-}3)$$

where β and γ are parameters that can be determined to obtain integration accuracy and stability. When β = 1/6 and γ = 1/2, this method reduces to the linear acceleration method, and when β = 1/4 and γ = 1/2, to the constant average acceleration method. Solving Eq.(5-2) for $\ddot{\mathbf{u}}_{s+1}$ in terms of $\mathbf{u}_{s+1}$ and then substituting for $\dot{\mathbf{u}}_{s+1}$ in Eq.(5-3), we obtain equations for $\dot{\mathbf{u}}_{s+1}$ and $\ddot{\mathbf{u}}_{s+1}$, each in terms of the unknown displacement $\mathbf{u}_{s+1}$ only:

$$\dot{\mathbf{u}}_{s+1} = \frac{\gamma}{\beta\Delta t}\mathbf{u}_{s+1} + \bar{\mathbf{P}}_s \qquad \cdots\cdots\cdots\cdots\cdots(5\text{-}4)$$

$$\ddot{\mathbf{u}}_{s+1} = \frac{1}{\beta\Delta t^2}\mathbf{u}_{s+1} + \bar{\mathbf{R}}_s \qquad \cdots\cdots\cdots\cdots\cdots(5\text{-}5)$$

where

$$\bar{\mathbf{P}}_s = -\frac{\gamma}{\beta\Delta t}\mathbf{u}_s + \left(1-\frac{\gamma}{\beta}\right)\dot{\mathbf{u}}_s + \left(1-\frac{\gamma}{2\beta}\right)\Delta t\ddot{\mathbf{u}}_s \qquad \cdots\cdots\cdots\cdots\cdots(5\text{-}6)$$

$$\bar{\mathbf{R}}_s = -\frac{1}{\beta\Delta t^2}\mathbf{u}_s - \frac{1}{\beta\Delta t}\dot{\mathbf{u}}_s - \left(\frac{1}{2\beta}-1\right)\ddot{\mathbf{u}}_s \qquad \cdots\cdots\cdots\cdots\cdots(5\text{-}7)$$

The functions $\bar{\mathbf{P}}_s$ and $\bar{\mathbf{R}}_s$ involve variables at previous time only, and hence can be considered as the historical part in the formulation. Substituting Eqs.(5-4) and (5-5) into the governing equations of motion (5-1) at time t_{s+1}, we have:

$$\mathbf{G}\,\mathbf{u}_{s+1} = \mathbf{Q}_{s+1} \qquad \cdots\cdots\cdots\cdots\cdots(5\text{-}8)$$

where **G** is the effective stiffness matrix, **Q** is the generalized external force vector, and these are given as follows:

$$\mathbf{G} = \frac{1}{\beta\Delta t^2}\mathbf{M} + \frac{\gamma}{\beta\Delta t}\mathbf{C} + \mathbf{K} \qquad \cdots\cdots\cdots\cdots\cdots(5\text{-}9)$$

$$\mathbf{Q}_{s+1} = \mathbf{F}_{s+1} - \mathbf{M}\,\bar{\mathbf{R}}_s - \mathbf{C}\,\bar{\mathbf{P}}_s \qquad \cdots\cdots\cdots\cdots(5\text{-}10)$$

Eq.(5-8) is an equation with unknown variables $\mathbf{u}_{s+1}$ only, and hence the dynamic analysis of the plates at each time step (s = 1, 2,···) can be treated as a static problem.

5-3 FINITE ELEMENT-TRANSFER MATRIX METHOD FOR DYNAMIC ANALYSIS

1) Transfer and Point Matrices

To calculate the dynamic response of the given structure using FETM method, it is required to formulate first the transfer matrix which transfers the state variables (displacement and force) from the left section of strip i to the right section in Fig.5-1.

The relation between the state variables of strip i can be described as follows:

$$\mathbf{N}_i = \mathbf{G}_i\,\mathbf{u}_i \qquad \cdots\cdots\cdots\cdots(5\text{-}11)$$

where $\mathbf{G}_i$ is the effective stiffness matrix for strip i, and $\mathbf{N}_i$ and $\mathbf{u}_i$ are force and displacement vectors of strip i, respectively.

Matrix $\mathbf{G}_i$ is partitioned into four submatrices. Eq.(5-11) then becomes:

$$\begin{bmatrix} \mathbf{G}_{\ell\ell} & \mathbf{G}_{\ell r} \\ \mathbf{G}_{r\ell} & \mathbf{G}_{rr} \end{bmatrix} \begin{Bmatrix} \mathbf{u}_\ell \\ \mathbf{u}_r \end{Bmatrix}_i = \begin{Bmatrix} \mathbf{N}_\ell \\ \mathbf{N}_r \end{Bmatrix}_i \qquad \cdots\cdots\cdots\cdots(5\text{-}12)$$

where $\mathbf{u}_\ell$, $\mathbf{u}_r$, $\mathbf{N}_\ell$ and $\mathbf{N}_r$ are the left and right displacements and forces of strip i, respectively. By expanding Eq.(5-12) and solving for $\mathbf{u}_{ri}$ and $\mathbf{N}_{ri}$ in terms of $\mathbf{u}_{\ell i}$ and $\mathbf{N}_{\ell i}$ the following equations can be obtained;

$$\begin{Bmatrix} \mathbf{u}_r \\ \mathbf{N}_r \\ 1 \end{Bmatrix}_i = \begin{bmatrix} \mathbf{T}_{11} & \mathbf{T}_{12} & \mathbf{0} \\ \mathbf{T}_{21} & \mathbf{T}_{22} & \mathbf{0} \\ \mathbf{0} & \mathbf{0} & 1 \end{bmatrix}_i \begin{Bmatrix} \mathbf{u}_\ell \\ \mathbf{N}_\ell \\ 1 \end{Bmatrix}_i \qquad \cdots\cdots\cdots\cdots(5\text{-}13)$$

or

$$\mathbf{z}_{ri} = \mathbf{T}_i \mathbf{z}_{\ell i} \qquad \cdots\cdots\cdots\cdots(5\text{-}14)$$

where

$$\mathbf{T}_{11} = -\mathbf{G}_{\ell r}^{-1}\mathbf{G}_{\ell\ell}, \qquad \mathbf{T}_{12} = \mathbf{G}_{\ell r}^{-1}$$

$$\mathbf{T}_{21} = \mathbf{G}_{r\ell} - \mathbf{G}_{rr}\mathbf{G}_{\ell r}^{-1}\mathbf{G}_{\ell\ell}, \quad \mathbf{T}_{22} = \mathbf{G}_{rr}\mathbf{G}_{\ell r}^{-1}$$

and $\mathbf{G}_{\ell\ell}$, $\mathbf{G}_{\ell r}$, $\mathbf{G}_{r\ell}$ and $\mathbf{G}_{rr}$ are the submatrices of matrix $\mathbf{G}$ in Eq. (5-9); $\mathbf{u}_{\ell i}$, $\mathbf{u}_{ri}$, $\mathbf{N}_{\ell i}$ and $\mathbf{N}_{ri}$ are the left and right displacement and force vectors of strip i at time t_{s+1}, respectively.

It should be noted here that the transfer matrix derived above does not contain a time variable, and so it must be derived only once at the start of the analysis. This results in considerable time reduction and accuracy improvement because the inversion of matrix $\mathbf{G}_{\ell r}$, which is required in the derivation of the transfer matrix, is a source of some numerical errors.

It is required next to derive the point matrix which relates the state vectors just to the left and right of section i. The deflections are continuous across the section, so that

$$\mathbf{u}_i^R = \mathbf{u}_i^L \qquad \cdots\cdots\cdots\cdots(5\text{-}15)$$

where $\mathbf{u}_i^L$ and $\mathbf{u}_i^R$ are the displacement vectors just to the left and right of section i, respectively.

Considering the equilibrium of forces in Fig.5-2, we obtain the following expression:

$$\mathbf{N}_i^R = \bar{\mathbf{Q}}_i + \mathbf{N}_i^L \qquad \cdots\cdots\cdots\cdots (5\text{-}16)$$

where $\mathbf{N}_i^L$ and $\mathbf{N}_i^R$ are the force vectors just to the left and right of section i, respectively, and $\bar{\mathbf{Q}}_i$ is the generalized load vector acting on section i, which is evaluated from the general loading function in Eq.(5-10).

These two relations may be expressed in matrix notation as

$$\begin{Bmatrix} \mathbf{u} \\ \mathbf{N} \end{Bmatrix}_i^R = \begin{bmatrix} \mathbf{I} & \mathbf{0} \\ \mathbf{0} & \mathbf{I} \end{bmatrix}_i \begin{Bmatrix} \mathbf{u} \\ \mathbf{N} \end{Bmatrix}_i^L + \begin{Bmatrix} \mathbf{0} \\ \bar{\mathbf{Q}} \end{Bmatrix}_i \qquad \cdots\cdots\cdots\cdots (5\text{-}17)$$

The two matrix terms on the right-hand side of Eq.(5-17) may be brought together as a single term in the following way:

$$\begin{Bmatrix} \mathbf{u} \\ \mathbf{N} \\ 1 \end{Bmatrix}_i^R = \begin{bmatrix} \mathbf{I} & \mathbf{0} & \mathbf{0} \\ \mathbf{0} & \mathbf{I} & \bar{\mathbf{Q}} \\ \mathbf{0} & \mathbf{0} & 1 \end{bmatrix}_i \begin{Bmatrix} \mathbf{u} \\ \mathbf{N} \\ 1 \end{Bmatrix}_i^L \qquad \cdots\cdots\cdots\cdots (5\text{-}18)$$

or

$$\mathbf{z}_i^R = \mathbf{P}_i \mathbf{z}_i^L \qquad \cdots\cdots\cdots\cdots (5\text{-}19)$$

Once the transfer and point matrices have been formulated for each strip, the state vectors at the section are determined by the same procedures as those used in the standard transfer matrix method (17).

After continuous multiplications of the transfer matrix **T** and the point matrix **P**, we obtain the relation between the state vector at the section i, $\mathbf{z}_i$, and the unknown state vector at left boundary, $\bar{\mathbf{z}}_0$:

$$\mathbf{z}_i = \mathbf{U}_i \bar{\mathbf{z}}_0 \qquad \cdots\cdots\cdots\cdots (5\text{-}20)$$

or

$$\begin{Bmatrix} \mathbf{u} \\ \mathbf{N} \\ 1 \end{Bmatrix}_i = \begin{Bmatrix} \bar{\mathbf{U}} & \mathbf{f} \\ 0 & 1 \end{Bmatrix}_i \begin{Bmatrix} \bar{\mathbf{z}} \\ 1 \end{Bmatrix}_0 \qquad \cdots\cdots\cdots\cdots (5\text{-}21)$$

where $\mathbf{U}_i = \mathbf{P}_i \mathbf{T}_i \mathbf{P}_{i-1} \mathbf{T}_{i-1} \cdots \mathbf{P}_1 \mathbf{T}_1$, and $\mathbf{f}_i$ is the force vector of the generalized load. When the last station m is reached, Eq.(5-21) becomes

$$\begin{Bmatrix} \mathbf{u} \\ \mathbf{N} \\ 1 \end{Bmatrix}_m = \begin{Bmatrix} \bar{\mathbf{U}} & \mathbf{f} \\ 0 & 1 \end{Bmatrix}_m \begin{Bmatrix} \bar{\mathbf{z}} \\ 1 \end{Bmatrix}_0 \qquad \cdots\cdots\cdots\cdots (5\text{-}22)$$

The known state variables at the right-hand boundary are substituted into the above relationship to determine the unknown state variables in $\mathbf{z}_0$. After the initial state vector $\mathbf{z}_0$ is known, the state vectors at the sections can be obtained by recursively applying Eq.(5-20) until all the state vectors are known.

Once the displacement of the whole structure at time t_{s+1} is obtained, the velocities and accelerations at time t_{s+1} are evaluated from Eqs.(5-4) and (5-5), respectively.

2) Improvement for In-Plane Excitation

The formulations described above are concerned with the plate subjected to out-of-plane excitations. In the case of the plate subjected to in-plane excitations, some attention is, however, required. The equation of motion for this case is given by

$$\mathbf{M}\,\ddot{\mathbf{u}}_{s+1} + \mathbf{C}\,\dot{\mathbf{u}}_{s+1} + (\mathbf{K} + \mathbf{F}^*_{s+1}\mathbf{K}_g)\mathbf{u}_{s+1} = 0 \qquad \cdots\cdots\cdots\cdots (5\text{-}23)$$

where $\mathbf{K}_g$ is the geometrical stiffness matrix; $\mathbf{F}^*_{s+1}$ is the in-plane excitation at time t_{s+1}. It is apparent that Eq.(5-23) is a nonlinear expression because $\mathbf{F}^*_{s+1}$ is a time variable.

In the analysis of plates subjected to in-plane excitation, the transfer matrix in Eq.(5-13) must be, therefore, evaluated for every time stage. This results in a considerable increase in computation time. In order to overcome this disadvantage of the proposed method, we rewrite Eq.(5-23) approximately as follows:

$$\mathbf{M}\,\ddot{\mathbf{u}}_{s+1} + \mathbf{C}\,\dot{\mathbf{u}}_{s+1} + \mathbf{K}\,\mathbf{u}_{s+1} = \mathbf{F}_{s+1} \qquad \cdots\cdots\cdots\cdots(5\text{-}24)$$

where $\mathbf{F}_{s+1} = -\mathbf{F}^*_{s+1}\mathbf{K}_g\mathbf{u}_s$ can be considered as a known variable evaluated from the displacement at previous time t_s. Therefore the transfer matrix $\mathbf{T}$ must be evaluated only once as in the case of out-of-plane excitation.

<u>3) Exchange of the State Vectors</u>

It is pointed out that, in the standard transfer matrix method, recursive multiplications of the transfer and point matrices are sources of round-off errors, and this is also true in the proposed method. In order to minimize these errors we introduce the technique described as follows for plates with many elements. Eq.(5-21), which relates the state vector at the section i and the unknown state vector at left boundary, may be written as follows:

$$\begin{Bmatrix} \mathbf{u} \\ \mathbf{N} \\ \mathbf{1} \end{Bmatrix}_i = \begin{bmatrix} \bar{\mathbf{U}}_1 & \mathbf{f}_1 \\ \bar{\mathbf{U}}_2 & \mathbf{f}_2 \\ \mathbf{0} & \mathbf{1} \end{bmatrix}_i \begin{Bmatrix} \bar{\mathbf{z}} \\ \mathbf{1} \end{Bmatrix}_0 \qquad \cdots\cdots\cdots\cdots(5\text{-}25)$$

Solving for $\bar{\mathbf{z}}_0$ in terms of $\mathbf{u}_i$, the following expression can be obtained:

$$\bar{\mathbf{z}}_0 = \bar{\mathbf{U}}_{1\,i}^{-1}\mathbf{u}_i - \bar{\mathbf{U}}_{1\,i}^{-1}\mathbf{f}_{1\,i} \qquad \cdots\cdots\cdots\cdots(5\text{-}26)$$

Substituting in the remaining equation of Eq.(5-25), we obtain:

$$\mathbf{N}_i = \bar{\mathbf{U}}_{2\,i}\bar{\mathbf{U}}_{1\,i}^{-1}\mathbf{u}_i - \bar{\mathbf{U}}_{2\,i}\bar{\mathbf{U}}_{1\,i}^{-1}\mathbf{f}_{1\,i} + \mathbf{f}_{2\,i} \qquad \cdots\cdots\cdots\cdots(5\text{-}27)$$

Eq.(5-27) and the identity $\mathbf{u}_i = \mathbf{u}_i$ yield the alternative expression of Eq.(5-25):

$$\begin{Bmatrix} \mathbf{u} \\ \mathbf{N} \\ 1 \end{Bmatrix}_i = \begin{bmatrix} \mathbf{I} & \mathbf{0} \\ \bar{\mathbf{U}}_2\bar{\mathbf{U}}_1^{-1} & -\bar{\mathbf{U}}_2\bar{\mathbf{U}}_1^{-1}\mathbf{f}_1 + \mathbf{f}_2 \\ \mathbf{0} & 1 \end{bmatrix}_i \begin{Bmatrix} \mathbf{u} \\ 1 \end{Bmatrix}_i \qquad \cdots\cdots\cdots\cdots(5\text{-}28)$$

or

$$\mathbf{z}_i = \mathbf{U}_i{}'\bar{\mathbf{z}}_i \qquad \cdots\cdots\cdots\cdots(5\text{-}29)$$

Hereafter matrix multiplications continue in the usual manner using, however, $\bar{\mathbf{z}}_i$ instead of $\bar{\mathbf{z}}_0$.

5-4 NUMERICAL EXAMPLES

In order to investigate the accuracy as well as the capability of the proposed method, some numerical examples of the plates subjected to out-of-plane and in-plane excitations are presented, and the results obtained by the FETM method are compared with those obtained by the ordinary finite element method. In the numerical examples stated in this chapter, the triangular element with three degrees of freedom per node is used, and the effect of damping is neglected.

1) Transient Analysis of Plates Subjected to Out-of-Plane Excitations

A simply supported square plate subjected to the out-of-plane periodic force at the center ($P(t) = P_1 \sin\omega t$, $P_1 = 1.0$kg, $\omega = 257$rad), shown in Fig.5-3, is analyzed for the first example. In the numerical calculation, a quarter of the plate is divided into 1, 2, 3, 4 and 5 strips, and each of which is subdivided into 2, 4, 6, 8 and 10 triangular elements, respectively. The results obtained by the FETM method coincide completely with those obtained by the finite element method for every mesh pattern. In the finite element method, the same element and mesh pattern as those used in the FETM method are employed. Figs.5-4(a) and 5-4(b) show, for example, comparisons between the dynamic responses of the deflections by both methods for 3 and 5 strips mesh patterns, where time step $\Delta t = 0.00005$ sec is used for 3 strips mesh pattern and $\Delta t = 0.00002$ sec for 5 strips mesh pattern. In the numerical calculation by the FETM method for 5 strips mesh pattern, the technique of exchanging the state vectors presented in this chapter is introduced at the third nodal line to avoid the propagation of round-off errors. In Fig.5-4(b), the results obtained by the FETM method without exchanging the state vectors are also shown to illustrate the efficiency of this technique.

Fig.5-5 shows comparisons of computation time for the FETM method and the finite element method in this example. It is found from Fig.5-5 that although in computation time the FETM has less advantage for a small number of elements patterns, it has much advantage for a number of elements patterns.

Figs.5-6(a) and 5-6(b) show the dynamic responses of an all edges clamped plate subjected to the out-of-plane excitation at the center ($P(t) = P_1 \sin\omega t$, $P_1 = 1.0$kg, $\omega = 257$rad). In the numerical calculation, a quarter of the plate is divided into 3 and 5 strips and each of which is subdivided into 6 and 10 triangular elements, respectively. Time step Δt = 0.00005 sec is used for 3 strips mesh pattern and Δt = 0.00002 sec for 5 strips mesh pattern. As shown in Figs.5-6(a) and 5-6(b), close agreements exist between the results obtained by the FETM method and the finite element method. In the numerical calculation for 5 strips mesh pattern by the FETM method, the technique of exchanging the sate vectors is used as in the previous example.

2) Transient Analysis of Plates Subjected to In-Plane Excitations

To illustrate the efficiency of the FETM method based on the approximate equation(5-24) for in-plane excitations, a simply supported rectangular plate subjected to in-plane excitation ($P(t)=P_0+P_1 \sin\omega t$, P_0=100kg, P_1=1.0kg, ω=257rad), as shown in Fig.5-7, is analyzed. The initial deflection of plate bending mode is assumed, and defined as follows:

$$w_0 = \bar{w}_0 \sin\frac{\pi}{a}x \sin\frac{\pi}{a}y \qquad \cdots\cdots\cdots\cdots(5\text{-}30)$$

in which $\bar{w}_0$ = the maximum value of initial deflection and here $\bar{w}_0$ = h/10 is assumed. A quarter of the plate is, in numerical calculation, divided into 1, 2, 3, 4 and 5 strips, and each of which is subdivided into 2, 4, 6, 8 and 10 triangular elements, respectively.

Fig.5-8(a) shows the dynamic responses of the deflections at points 8, 12 and 16 in Fig.5-7 for 3 strips mesh pattern, where time step Δt = 0.00005 sec is used. In Fig.5-8(a), the result obtained by the finite element method based on Eq.(5-23) is also shown, in which the same mesh pattern and time step as those used in the FETM method are employed. Very little difference exists between the results, so that the plots in Fig.5-8(a) are not distinct. In Fig.5-8(b), the response of the deflections at the center of the plate for 5 strips mesh pattern by the FETM method are compared with those by the finite element method. In the FETM method, the technique of exchanging the state vectors is introduced for this mesh pattern.

Fig.5-9 shows comparisons of computation time for the FETM method and the finite element method in this example, and similar conclusions to those in the case of out-of-plane excitations are obtained. In Fig.5-9, computation time for the FETM method based on Eq.(5-23), in which the transfer matrix in Eq.(5-13) must be derived for every time stage, is also shown to illustrate the efficiency of the proposed approximation.

Figs.5-10(a) and 5-10(b) show the responses of the deflections of a all edges clamped square plate subjected to the in-plane excitation ($P(t) = P_0 + P_1 \sin\omega t$, P_0 = 100kg, P_1 = 100kg, ω = 497rad) for 3 and 5 strips mesh patterns. The same initial deflection as that assumed in the previous example is also assumed in this example. Similar results to those obtained for a simply supported plate subjected to in-plane excitation are obtained.

5-5 CONCLUSIONS

A linear transient analysis method of the structures under random excitations by a combined finite element - transfer matrix method is proposed. Transfer matrix relating the state vector on the left and right boundaries of a strip at a certain time is derived from the system of equations of motion for a strip. An approximation is introduced in the equations of motion for the case of in-plane excitations in order to reduce computational efforts and the technique of exchanging the state vectors is proposed to avoid the propagation of round-off errors occurred in recursive multiplications of the transfer and point matrices. Although the Newmark β method is employed for time integrations, other integration methods such as the Houbolt, Wilson θ and central difference methods may be used. From the numerical examples presented in this chapter, following conclusions are obtained:

(1) For the out-of-plane and in-plane excitations, good agreement exists between the results obtained by the FETM method and the conventional finite element dynamic analysis, which demonstrates the accuracy of linear transient analysis by the FETM method.

(2) In the case of in-plane excitations, the results by the FETM method based on the equations of motion with an approximation described in this chapter agree with those based on the equation without an approximation, and it becomes clear that this approximation of the equations is efficient to reducing computational efforts.

(3) The technique of exchanging the state vectors is very efficient to avoid the propagation of round-off errors occurred in many strips pattern.

From the mentions above, this method can be successfully applied to the transient analyses of the plates subjected to out-of-plane and in-plane excitations by reducing the size of matrix and relative computation time to less than those obtained by the method based on the ordinary finite element procedure.

REFERENCES

1. Adeli, H., Gere, J.M. and Weaver Jr.W., "Algorithms for Nonlinear Structural Dynamics," J. ASCE, Vol.104, No.ST2, Feb., 1978, pp.263-280.
2. Bathe, K.J., Ramm, E. and Wilson, E.L., "Finite Element Formulations for Large Deformation Dynamic Analysis," International Journal for Numerical Methods in Engineering, Vol.9, 1975, pp.353-386.
3. Bathe, K.J. and Ozdemir, H., "Elastic-Plastic Large Deformation Static and Dynamic Analysis," Computers & Structures, Vol.6, 1976, pp.81-92.
4. Brebbia, C.A., Tottenham, H., Warburton, G.B., Wilson, J.M. and Wilson, R.R., "Vibrations of Engineering Structures," Springer, New York, 1985.
5. Chiatti, G. and Sestieri, A., "Analysis of Static and Dynamic Structural Problems by a Combined Finite Element - Transfer Matrix Method," J. Sound & Vibration, Vol.67, No.1, 1979, pp.35-42.
6. Degen, E.E., Shephard, M.S. and Loewy, R.G., "Combined Finite Element - Transfer Matrix Method Based on a Finite Mixed Formulation," Computers & Structures, Vol.20, No.1-3, 1985, pp.173-180.
7. Dokainish, M.A., "A New Approach for Plate Vibrations: Combination of Transfer Matrix and Finite-Element Technique," Trans. ASME Vol.94, No.2, 1972, pp.526-530.
8. Donéa, J., "Advanced Structural Dynamics," Applied Science, London, 1978.
9. McDaniel, T.J. and Eversole, K.B., "A Combined Finite Element - Transfer Matrix Structural Analysis Method," J. Sound & Vibration, Great Britain, Vol.51, No.2, 1977, pp.157-169.
10. McGuire, W. and Gallagher, R.H., "Matrix Structural Analysis," John Wiley, New York, 1979.
11. Mucino, H.V. and Pavelic, V., "An Exact Condensation Procedure for Chain-Like Structures Using a Finite Element - Transfer Matrix Approach," Trans. ASME, J. Mech. Des., No.80-C2/DET-123, 1980, pp.1-9.
12. Newmark, N.M., "A Method of Computation for Structural Dynamics," J. ASCE, Vol.85, No.EM3, 1959, pp.67-94.
13. Ohga, M., Shigematsu, T. and Hara, T., "Structural Analysis by a Combined Finite Element - Transfer Matrix Method," Computers & Structures, Vol.17, No.3, 1983, pp.321-326.
14. Ohga, M., Shigematsu, T. and Hara, T., "Structural Analysis

by a Combined Finite Element-Transfer Matrix Method," J. ASCE, Vol.110, No.EM9, September, 1984, pp.1335-1349.
15. Ohga, M. and Shigematsu, T., "Transient Analysis of Plates by a Combined Finite Element-Transfer Matrix Method," Computers & Structures, Vol.26, No.4, 1987, pp.543-549.
16. Park, K.C., "An Improved Stiffly Stable Method for Direct Integration of Nonlinear Structural Dynamic Equations," Journal of Applied Mechanics, American Society of Mechanical Engineers, Vol.42, 1975, pp.464-470.
17. Pestel, E.C. and Leckie, F.A., "Matrix Method in Elastomechanics," McGraw-Hill, New York, 1963.
18. Sankar, S. and Hoa, S.V., "An Extended Transfer Matrix - Finite Element Method for Free Vibration of Plates," J. Sound & Vibration, Vol.70, No.2, 1980, pp.205-211.
19. Stricklin, J.A. and Haisler, W.E., "Formulations and Solution Procedures for Nonlinear Structural Analysis," Computers & Structures, Vol.7, 1977, pp.125-136.
20. Zienkiewicz, O.C., "The Finite Element Method in Engineering Science," McGraw-Hill, New York, 1971.

NOTATION

The following symbols are used in this paper:

$\mathbf{C}$ = damping matrix;
$\mathbf{F}$ = force vector;
$\mathbf{G}$ = effective stiffness matrix;
$\mathbf{K}, \mathbf{K}_g$ = linear and geometric stiffness matrices, respectively;
$\mathbf{M}$ = mass matrix;
$\mathbf{P}$ = point matrix;
$\mathbf{Q}$ = generalized load vector;
$\bar{\mathbf{Q}}$ = generalized load vector acting on section i;
$\mathbf{T}$ = transfer matrix;
$\mathbf{u}, \dot{\mathbf{u}}, \ddot{\mathbf{u}}$ = displacement, velocity, and acceleration vectors, respectively;
$\mathbf{N}$ = force vector;
$\mathbf{N}_{\ell i}, \mathbf{N}_{r i}$ = left and right force vectors of strip i, respectively;
$\mathbf{Q}$ = generalized force vector;
Δt = size of time step;

$\mathbf{u}$ = displacement vector;

$\mathbf{u}_{\ell i}, \mathbf{u}_{ri}$ = left and right displacement vectors of strip i, respectively;

$\mathbf{z}$ = state vector;

$\mathbf{z}_0$ = unknown initial state vector;

$\mathbf{z}_{\ell i}, \mathbf{z}_{ri}$ = left and right state vectors of strip i, respectively; and

$\boldsymbol{\sigma}$ = stress vector.

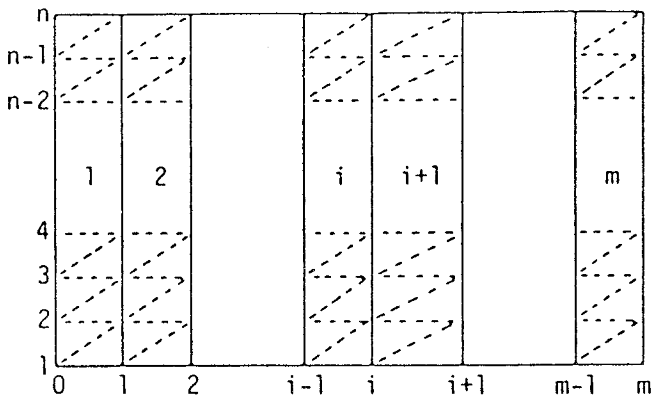

Fig.5-1 Subdivison of Plate into Strips and Finite Elements

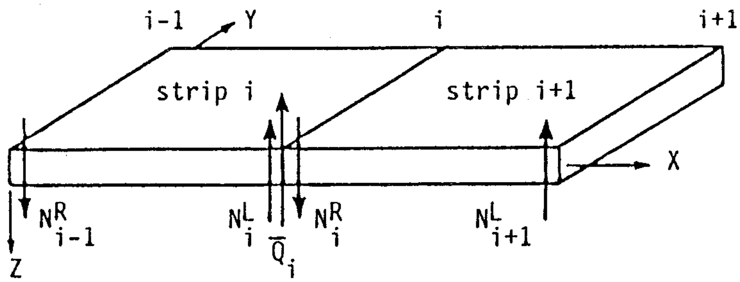

Fig.5-2 Equilibrium of Forces at Section i

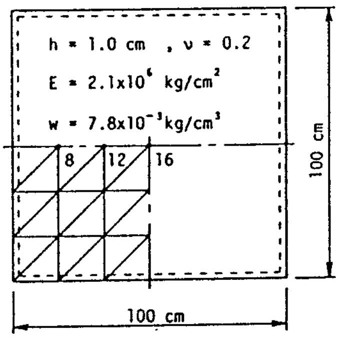

Fig.5-3 Simply Supported Square Plate

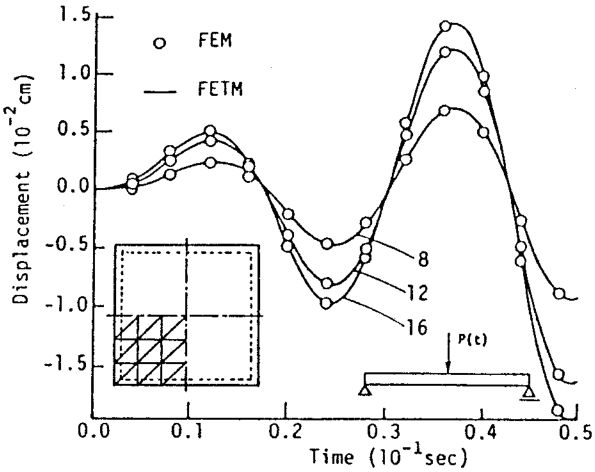

Fig.5-4(a) Displacement Response of Simply Supported Plate under Out-of-Plane Excitation (3x3 Elements)

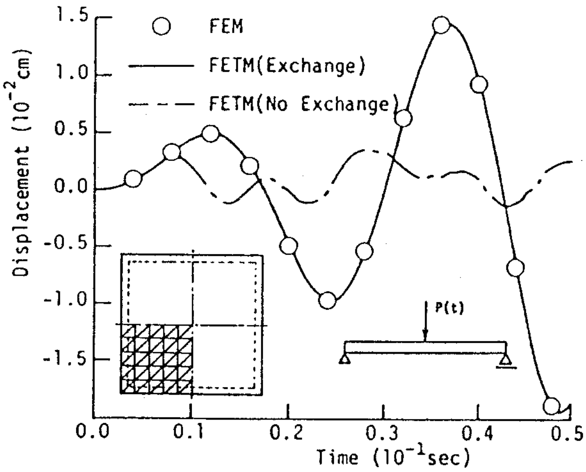

Fig.5-4(b) Displacement Response of Simply Supported Plate under Out-of-Plane Excitation (5x5 Elements)

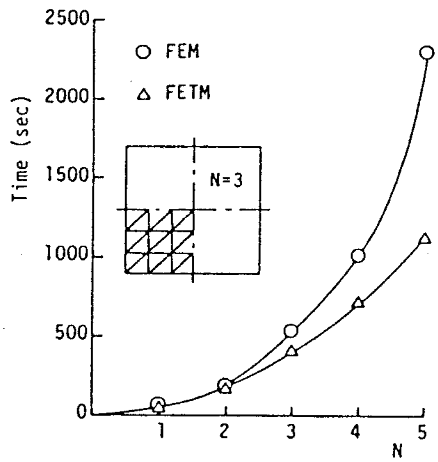

Fig.5-5 Comparison of Computation Time for Out-of-Plane Excitation

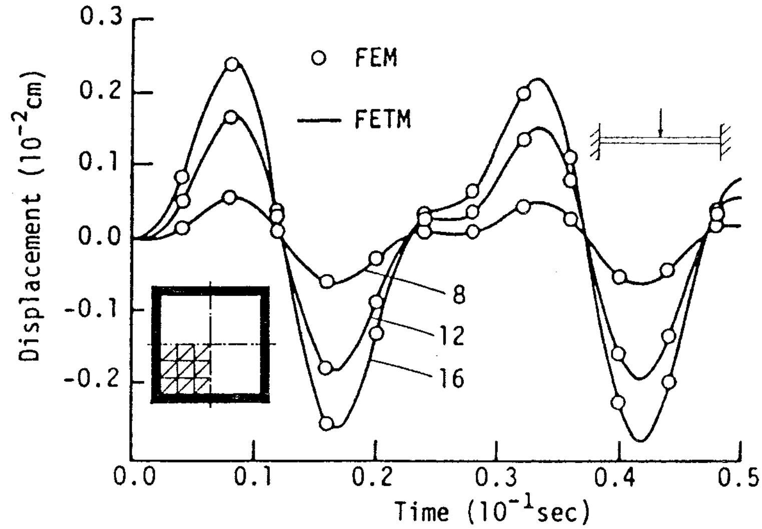

Fig.5-6(a) Displacement Response of All Edges Clamped Plate under Out-of-Plane Excitation (3x3 Elements)

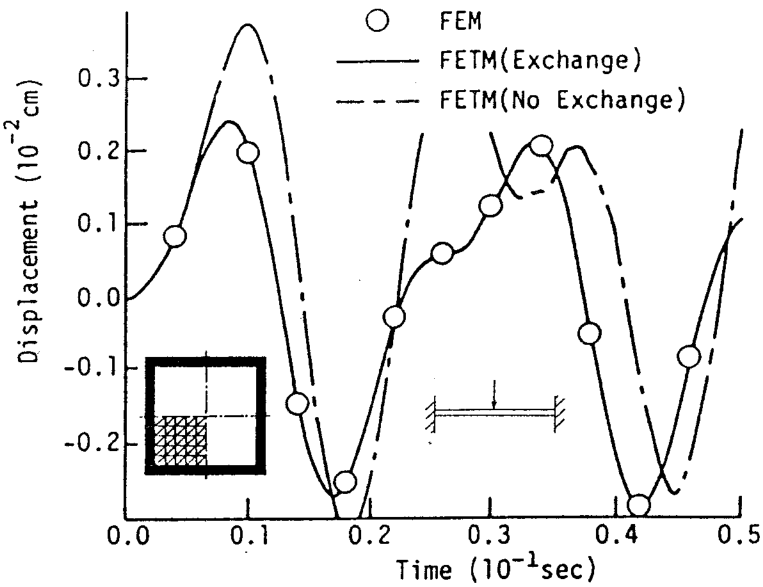

Fig.5-6(b) Displacement Response of All Edges Clamped Plate under Out-of-Plane Excitation (5x5 Elements)

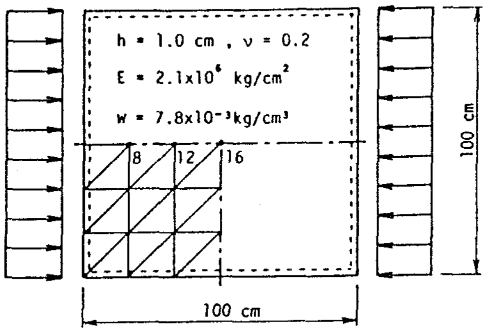

Fig.5-7 Simply Supported Plate under In-Plane Excitation

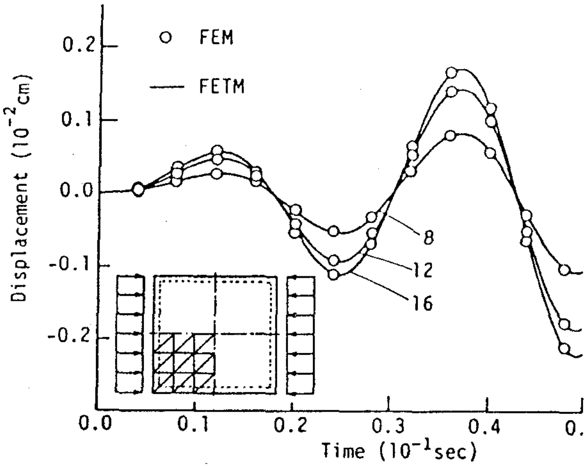

Fig.5-8(a) Displacement Response of Simply Supported Plate under In-Plane Excitation (3x3 Elements)

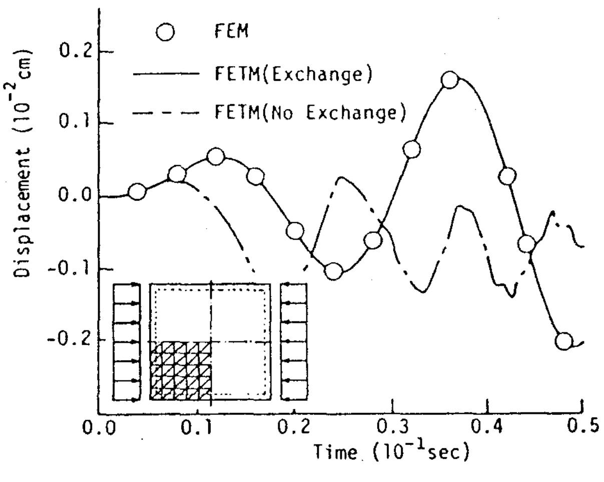

Fig.5-8(b) Displacement Response of Simply Supported Plate under In-Plane Excitation (5x5 Elements)

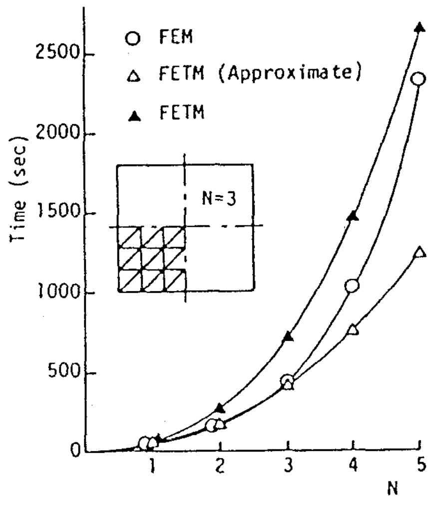

Fig.5-9 Comparison of Computation Time for In-Plane Excitation

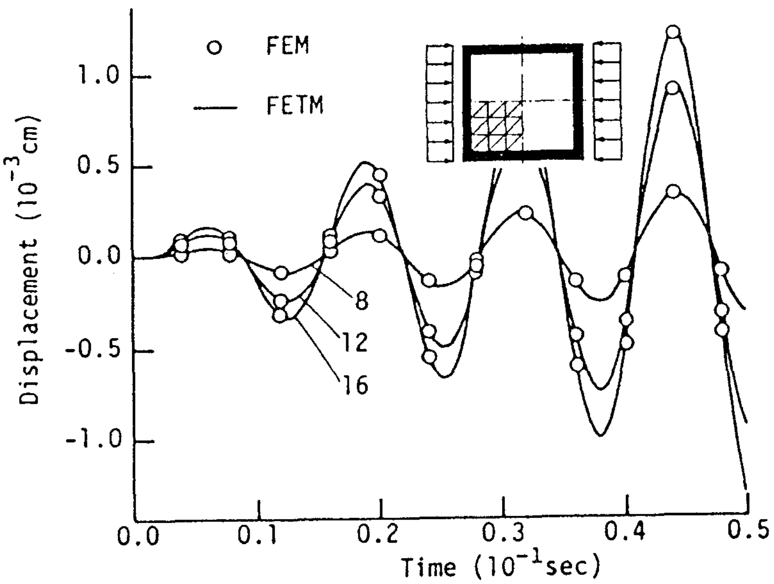

Fig.5-10(a) Displacement Response of All Edges Clamped Plate under In-Plane Excitation (3x3 Elements)

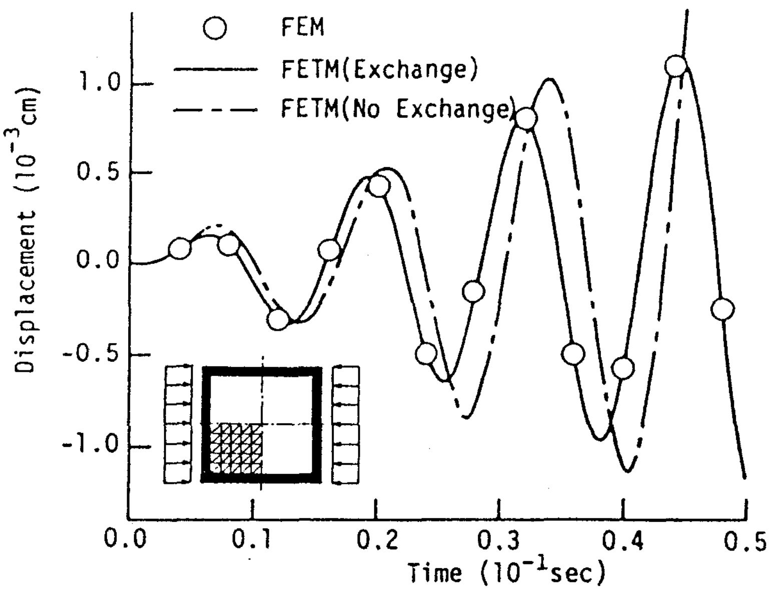

Fig.5-10(b) Displacement Response of All Edges Clamped Plate under In-Plane Excitation (5x5 Elements)

Chapter 6 NONLINEAR DYNAMIC ANALYSIS OF PLATES BY A COMBINED FINITE ELEMENT-TRANSFER MATRIX METHOD

6-1 INTRODUCTION

Nonlinear transient response of complex structures subjected to random excitations can be, generally, obtained by the direct integration method using finite element model, such as the Newmark β, Houbolt, Wilson Θ and central difference methods (2, 3, 4, 8, 13, 18). In these methods, it is, however, necessary to use a large number of nodes, resulting in a need of very large computers.

In this chapter the combined finite element - transfer matrix method (5, 6, 7, 10, 11, 14, 15, 20) described in previous chapter is extended to nonlinear dynamic problems of structures under various random excitations. The transfer matrix relating the state variables on the left and right boundaries of a strip is derived from nonlinear system of equations of motion for a strip. The Newmark β method is used for time integration, but other integration methods, such as the Houbolt, Wilson Θ, and central difference methods may be used. Equilibrium iteration based on the pseudo-force method is employed to improve the solution accuracy and to avoid the development of numerical instabilities. The Prandtl-Reuss′ law obeying the von Mises yield criterion is assumed, and a set of moving coordinate systems is used to take geometric nonlinearity into consideration in this chapter.

Some numerical examples of the plates subjected to out-of-plane and in-plane excitations are proposed and their results are compared with those obtained by other methods.

6-2 FINITE ELEMENT-TRANSFER MATRIX METHOD FOR NONLINEAR DYNAMIC ANALYSIS

The governing equation for a plate subjected to excitation at time $t_{s+1} = (s+1)\Delta t$, where s is the number of time steps Δt, generally given by

$$\mathbf{M}\,\ddot{\mathbf{u}}_{s+1} + \mathbf{C}\,\dot{\mathbf{u}}_{s+1} + \mathbf{A}_{s+1} = \mathbf{F}_{s+1} \qquad \cdots\cdots\cdots\cdots (6\text{-}1)$$

in which **M** and **C** are the mass and damping matrices; $\ddot{\mathbf{u}}_{s+1}$, $\dot{\mathbf{u}}_{s+1}$, and $\mathbf{F}_{s+1}$ are the acceleration, velocity and force vectors at time t_{s+1}, respectively; $\mathbf{A}_s$ is the equivalent nodal force opposing the displacement of the structure.

For linear elastic situations

$$\mathbf{A}_{s+1} = \mathbf{K}_\ell\,\mathbf{u}_{s+1} \qquad \cdots\cdots\cdots\cdots (6\text{-}2)$$

where $\mathbf{K}_\ell$ is the stiffness matrix; $\mathbf{u}_{s+1}$ the displacement vector, but for nonlinear situations $\mathbf{A}_{s+1}$ must be calculated from the stress distribution satisfying nonlinear conditions so that

$$\mathbf{A}_{s+1} = \int_V \mathbf{B}_{s+1}{}^T\,\boldsymbol{\sigma}_{s+1}\,dv \qquad \cdots\cdots\cdots\cdots (6\text{-}3)$$

where $\mathbf{B}_{s+1}$ is the appropriate matrix expressing the strains in terms of the nodal displacements at time t_{s+1}; $\boldsymbol{\sigma}_{s+1}$ the stress vector.

The equivalent force, $\mathbf{A}_{s+1}$, at time t_{s+1} can be estimated as

$$\mathbf{A}_{s+1} = \mathbf{A}_s + \mathbf{K}_s\,\Delta\mathbf{u} \qquad \cdots\cdots\cdots\cdots (6\text{-}4)$$

where $\mathbf{K}_s$ is the tangential stiffness matrix evaluated from conditions at time t_s, $\Delta \mathbf{u} = \mathbf{u}_{s+1} - \mathbf{u}_s$ is the incremental displacement. Assumption (6-4) implies a linearization of the incremental displacement between times t_s and t_{s+1}. Substituting Eq.(6-4) in Eq.(6-1) gives

$$\mathbf{M}\,\ddot{\mathbf{u}}_{s+1} + \mathbf{C}\,\dot{\mathbf{u}}_{s+1} + \mathbf{K}_s\,\Delta \mathbf{u} = \mathbf{F}_{s+1} - \mathbf{A}_s \qquad \cdots\cdots\cdots\cdots(6\text{-}5)$$

The solution of Eq.(6-5) yields, in general, approximate incremental displacement $\Delta \mathbf{u}$. To improve the solution accuracy and to avoid the development of numerical instabilities, it is generally necessary to employ iterations within each time step or selected time steps in order to maintain equilibrium.

As described previously, the Newmark β method is used, in this chapter, for time integration. In this method we assumed variations for the displacement, $\mathbf{u}$, and velocity, $\dot{\mathbf{u}}$ in the time interval Δt to be such that the values at beginning and end of the time step are related by equations of the form

$$\mathbf{u}_{s+1} = \mathbf{u}_s + \Delta t\,\dot{\mathbf{u}}_s + \left(\frac{1}{2} - \beta\right)\Delta t^2\,\ddot{\mathbf{u}}_s + \beta\,\Delta t^2\,\ddot{\mathbf{u}}_{s+1} \qquad \cdots\cdots(6\text{-}6)$$

$$\dot{\mathbf{u}}_{s+1} = \dot{\mathbf{u}}_s + (1-\gamma)\,\Delta t\,\ddot{\mathbf{u}}_s + \gamma\,\Delta t\,\ddot{\mathbf{u}}_{s+1} \qquad \cdots\cdots(6\text{-}7)$$

where β and γ are parameters that can be determined to obtain integration accuracy and stability. Solving Eq.(6-6) for $\ddot{\mathbf{u}}_{s+1}$ in terms of $\mathbf{u}_{s+1}$ and then substituting for $\dot{\mathbf{u}}_{s+1}$ in Eq.(6-7), we obtain equations for $\dot{\mathbf{u}}_{s+1}$ and $\ddot{\mathbf{u}}_{s+1}$, each in terms of the unknown displacement $\mathbf{u}_{s+1}$ only:

$$\dot{\mathbf{u}}_{s+1} = \frac{\gamma}{\beta\,\Delta t}\,\mathbf{u}_{s+1} + \bar{\mathbf{P}}_s \qquad \cdots\cdots\cdots\cdots(6\text{-}8)$$

$$\ddot{\mathbf{u}}_{s+1} = \frac{1}{\beta\,\Delta t^2}\,\mathbf{u}_{s+1} + \bar{\mathbf{R}}_s \qquad \cdots\cdots\cdots\cdots(6\text{-}9)$$

where

$$\bar{\mathbf{P}}_s = -\frac{\gamma}{\beta\ \Delta t}\mathbf{u}_s + (1-\frac{\gamma}{\beta})\dot{\mathbf{u}}_s + (1-\frac{\gamma}{2\beta})\ \Delta t\ \ddot{\mathbf{u}}_s \quad \cdots\cdots(6\text{-}10)$$

$$\bar{\mathbf{R}}_s = -\frac{1}{\beta\ \Delta t^2}\mathbf{u}_s - \frac{1}{\beta\ \Delta t}\dot{\mathbf{u}}_s - (\frac{1}{2\beta} - 1)\ddot{\mathbf{u}}_s \quad \cdots\cdots\cdots(6\text{-}11)$$

The functions $\bar{\mathbf{P}}_s$ and $\bar{\mathbf{R}}_s$ involve variables at previous time only, and hence can be considered as the historical part in the formulation. Substituting Eqs.(6-8) and (6-9) into the governing equations of motion (6-5) at time t_{s+1}, we have

$$\mathbf{G}\ \Delta\mathbf{u}_{s+1} = \Delta\mathbf{Q}_{s+1} \quad \cdots\cdots\cdots\cdots(6\text{-}12)$$

where

$$\mathbf{G} = \frac{1}{\beta\ \Delta t^2}\ \mathbf{M} + \frac{\gamma}{\beta\ \Delta t}\ \mathbf{C} + \mathbf{K}_s \quad \cdots\cdots\cdots\cdots(6\text{-}13)$$

$$\Delta\mathbf{Q}_{s+1} = \mathbf{F}_{s+1} + \mathbf{M}\ \{\frac{1}{\beta\ \Delta t}\ \dot{\mathbf{u}}_s + (\frac{1}{2\beta} - 1)\ \ddot{\mathbf{u}}_s\ \}$$

$$+ \mathbf{C}\ \{(\frac{\gamma}{\beta} - 1)\ \dot{\mathbf{u}}_s + (\frac{\gamma}{2\beta} - 1)\ \Delta t\ \ddot{\mathbf{u}}_s\ \} - \mathbf{A}_s \quad \cdots(6\text{-}14)$$

Eq.(6-12) is an equation with unknown variables $\Delta\mathbf{u}_{s+1}$ only, and hence the dynamic analysis of the plates at each time step (s = 1, 2, ···) can be treated as a static problem by considering $\Delta\mathbf{Q}_{s+1}$ to be a generalized external force acting on the plate.

To calculate the dynamic response of the given structure using the FETM method, it is required to formulate first the transfer matrix which transfers the incremental state variables (displacement and force) from left section of strip i to right section in Fig.6-1, at time t_{s+1}.

Proceeding as in previous chapter with linear vibration problems, we obtained:

$$\begin{Bmatrix} \Delta \mathbf{u}_r \\ \Delta \mathbf{N}_r \\ 1 \end{Bmatrix}_i = \begin{bmatrix} \mathbf{T}_{11} & \mathbf{T}_{12} & \mathbf{0} \\ \mathbf{T}_{21} & \mathbf{T}_{22} & \mathbf{0} \\ \mathbf{0} & \mathbf{0} & \mathbf{1} \end{bmatrix}_i \begin{Bmatrix} \Delta \mathbf{u}_\ell \\ \Delta \mathbf{N}_\ell \\ 1 \end{Bmatrix}_i \qquad \cdots\cdots\cdots\cdots (6\text{-}15)$$

or

$$\Delta \mathbf{z}_{r\,i} = \mathbf{T}_i \, \Delta \mathbf{z}_{\ell\, i} \qquad \cdots\cdots\cdots\cdots (6\text{-}16)$$

where

$$\mathbf{T}_{11} = -\mathbf{G}_{\ell r}^{-1} \mathbf{G}_{\ell \ell}, \qquad \mathbf{T}_{12} = \mathbf{G}_{\ell r}^{-1}$$

$$\mathbf{T}_{21} = \mathbf{G}_{r \ell} - \mathbf{G}_{r r} \mathbf{G}_{\ell r}^{-1} \mathbf{G}_{\ell \ell}, \quad \mathbf{T}_{22} = \mathbf{G}_{r r} \mathbf{G}_{\ell r}^{-1}$$

and $\mathbf{G}_{\ell\ell}$, $\mathbf{G}_{\ell r}$, $\mathbf{G}_{r\ell}$, and $\mathbf{G}_{rr}$ are the submatrices of matrix G in Eq.(6-13); $\Delta \mathbf{u}_{\ell i}$, $\Delta \mathbf{u}_{r i}$, $\Delta \mathbf{N}_{\ell i}$, and $\Delta \mathbf{N}_{r i}$ are the left and right displacement and force increment vectors of strip i at time t_{s+1}, respectively; $\Delta \mathbf{z}_{\ell i}$ and $\Delta \mathbf{z}_{r i}$ are the left and right incremental state vectors of strip i, respectively.

It is required next to derive the point matrix which relates the state vectors just to the left and right of section i, The deflections are continuous across the section, so that

$$\Delta \mathbf{u}_i^{R} = \Delta \mathbf{u}_i^{L} \qquad \cdots\cdots\cdots\cdots (6\text{-}17)$$

where $\Delta \mathbf{u}_i^{L}$ and $\Delta \mathbf{u}_i^{R}$ are the displacement increment vectors just to the left and right of section i, respectively.

Considering the equilibrium of forces in Fig.6-2, we obtain the following expression:

$$\Delta \mathbf{N}_i^{R} = \Delta \overline{\mathbf{Q}}_i + \Delta \mathbf{N}_i^{L} \qquad \cdots\cdots\cdots\cdots (6\text{-}18)$$

where $\Delta \mathbf{N}_i^{L}$ and $\Delta \mathbf{N}_i^{R}$ are the increment force vectors just to the left and right of section i, respectively, and $\Delta \overline{\mathbf{Q}}_i$ is the increment generalized load vector acting on section i, which is evaluated from the general loading function in Eq.(6-14). The above two relations (6-17) and (6-18) may be expressed in matrix notation as

$$\begin{Bmatrix} \Delta \mathbf{u} \\ \Delta \mathbf{N} \end{Bmatrix}_i^R = \begin{bmatrix} \mathrm{I} & \mathbf{0} \\ \mathbf{0} & \mathrm{I} \end{bmatrix}_i \begin{Bmatrix} \Delta \mathbf{u} \\ \Delta \mathbf{N} \end{Bmatrix}_i^L + \begin{Bmatrix} \mathbf{0} \\ \Delta \bar{\mathbf{Q}} \end{Bmatrix}_i \qquad \cdots\cdots\cdots\cdots (6\text{-}19)$$

The two matrix terms on the right-hand side of Eq.(6-19) may be brought together as a single term in the following way:

$$\begin{Bmatrix} \Delta \mathbf{u} \\ \Delta \mathbf{N} \\ 1 \end{Bmatrix}_i^R = \begin{bmatrix} \mathrm{I} & \mathbf{0} & \mathbf{0} \\ \mathbf{0} & \mathrm{I} & \Delta \bar{\mathbf{Q}} \\ \mathbf{0} & \mathbf{0} & 1 \end{bmatrix}_i \begin{Bmatrix} \Delta \mathbf{u} \\ \Delta \mathbf{N} \\ 1 \end{Bmatrix}_i^L \qquad \cdots\cdots\cdots\cdots (6\text{-}20)$$

or

$$\Delta \mathbf{z}_i^R = \mathbf{P}_i \, \Delta \mathbf{z}_i^L \qquad \cdots\cdots\cdots\cdots (6\text{-}21)$$

Once the transfer and point matrices have been formulated for each strip, the state vectors at the section are determined by the same procedures as those used in the standard transfer matrix method (19).

After continuous multiplications of the transfer matrix **T** and point matrix **P**, we obtain the relation between the state vector at the section i and the unknown state vector at left boundary, $\Delta \bar{\mathbf{z}}_0$:

$$\Delta \mathbf{z}_i = \mathbf{U}_i \, \Delta \bar{\mathbf{z}}_0 \qquad \cdots\cdots\cdots\cdots (6\text{-}22)$$

or

$$\begin{Bmatrix} \Delta \mathbf{u} \\ \Delta \mathbf{N} \\ 1 \end{Bmatrix}_i = \begin{bmatrix} \bar{\mathbf{U}} & \mathbf{f} \\ \mathbf{0} & 1 \end{bmatrix}_i \begin{Bmatrix} \Delta \bar{\mathbf{z}} \\ 1 \end{Bmatrix}_0 \qquad \cdots\cdots\cdots\cdots (6\text{-}23)$$

where $\mathbf{U}_i = \mathbf{P}_i \mathbf{T}_i \mathbf{P}_{i-1} \mathbf{T}_{i-1} \cdots \mathbf{P}_1 \mathbf{T}_1$, and $\mathbf{f}_i$ is the force vector of the generalized loads. When the last station m is reached, Eq.(6-23) becomes

$$\begin{Bmatrix} \Delta u \\ \Delta N \\ 1 \end{Bmatrix}_m = \begin{bmatrix} \bar{U} & f \\ 0 & 1 \end{bmatrix}_m \begin{Bmatrix} \Delta \bar{z} \\ 1 \end{Bmatrix}_0 \qquad \cdots\cdots\cdots\cdots (6\text{-}24)$$

The known state variables at the right-hand boundary are substituted into the above relationship to determine the unknown state variables in $\Delta \mathbf{z}_0$. After the initial state vector $\Delta \mathbf{z}_0$ is known, the state vectors at the sections can be obtained by recursively applying Eq.(6-22) until all the state vectors are known. Once, the displacements of the whole structure at time t_{s+1} are obtained, the velocities and accelerations at time t_{s+1} are evaluated from Eqs.(6-8) and (6-9), respectively. The entire procedure can then be repeated for time t_{s+2} and so on.

6-3 ALGORITHM FOR NONLINEAR ANALYSIS BY FETM METHOD

It is convenient for equilibrium iteration to express equilibrium equations (6-5) in an alternative form. With the superscripts i-1 and i being used to denote values at two successive equilibrium iterations, then the displacement change occurring between these two stage is

$$\delta \mathbf{u}_{s+1}^{\,i} = \Delta \mathbf{u}_{s+1}^{\,i} - \Delta \mathbf{u}_{s+1}^{\,i-1} \qquad \cdots\cdots\cdots\cdots (6\text{-}25)$$

Then consideration of Eq.(6-5) at iteration i at time t_{s+1} gives, on use of Eq.(6-25),

$$\mathbf{M}\, \ddot{\mathbf{u}}_{s+1}^{\,i} + \mathbf{C}\, \dot{\mathbf{u}}_{s+1}^{\,i} + \mathbf{K}_s\, \delta \mathbf{u}^i = \mathbf{F}_{s+1} - \mathbf{A}_{s+1}^{\,i-1} \qquad \cdots\cdots\cdots (6\text{-}26)$$

Two iteration methods; the pseudo-force method and the tangent stiffness method, may be employed here. In the pseudo-force method, the stiffness matrix, $\mathbf{K}_s$, is kept at a constant (initial) value, with dynamic equilibrium being maintained by successive iterations with a varying pseudo-force which is the right-hand-side term in Eq.(6-26). On the other hand, in the tangent stiffness method the stiffness matrix, $\mathbf{K}_s$, is varied throughout the computation, with the term $\mathbf{P}_{s+1}{}^{i-1}$ being replaced by an equilibrium correction term.

Since, in the FETM method, considerable computation time is required in the derivation of the transfer matrix, it is inappropriate to employed the tangent stiffness method for equilibrium iteration. The pseudo-force method is, therefore, adopted here. The essential steps in the numerical algorithm employed in this chapter are outlined below:

1. Calculate the effective stiffness matrix, **G**, and the transfer matrix, **T**, for each strip.
2. Calculate the effective incremental load vector, $\Delta\mathbf{Q}_{s+1}$.
3. Solve for the left boundary state vector increments:

$$\Delta\bar{\mathbf{z}}_0 = \bar{\mathbf{U}}^{-1}\mathbf{f}_{s+1} \qquad \cdots\cdots\cdots\cdots(6\text{-}27)$$

4. Calculate the incremental state vector at each strip by successive multiplications of the transfer and point matrices.
5. Compute the displacements, velocities and accelerations at time t_{s+1}.
6. If equilibrium iteration is not considered, go to step 12; otherwise, start the i-th iteration: $i+1 \rightarrow i$.
7. Evaluate the i-th approximate to the displacements, velocities and accelerations.
8. Evaluate the i-th residual loads:

$$\delta \mathbf{Q}_{s+1}{}^{i} = \mathbf{F}_{s+1}{}^{i-1} - \mathbf{M}\,\ddot{\mathbf{u}}_{s+1}{}^{i-1} - \mathbf{C}\,\dot{\mathbf{u}}_{s+1}{}^{i-1} - \mathbf{A}_{s+1} \quad \cdots (6\text{-}28)$$

9. Solve for the i-th corrected displacement increments:

$$\delta \bar{\mathbf{z}}_{\emptyset}{}^{i} = \bar{\mathbf{U}}^{-1}\,\mathbf{f}_{s+1}{}^{i} \quad \cdots\cdots\cdots\cdots (6\text{-}29)$$

10. Evaluate the corrected displacement increments

$$\Delta \mathbf{u}^{i} = \Delta \mathbf{u}^{i-1} + \delta \mathbf{u}^{i} \quad \cdots\cdots\cdots\cdots (6\text{-}30)$$

11. Check for convergence of the iteration process:
    If $\|\delta \mathbf{u}^{i}\|/\|\mathbf{u}_s + \Delta \mathbf{u}^{i}\| \leq$ tolerance, go to step 12.
    Otherwise, go to step 6 for the (i+1)th iteration.
12. Return to step 2 to process the next time step.

6-4 NUMERICAL EXAMPLES

1) Large Deformation Dynamic Analysis of Plates

In large deformation dynamic problem, the governing equation (6-5) is written as follows:

$$\mathbf{M}\,\ddot{\mathbf{u}}_{s+1} + \mathbf{C}\,\dot{\mathbf{u}}_{s+1} + (\mathbf{K}_{\ell} + \mathbf{K}_{gs})\Delta \mathbf{u} = \mathbf{F}_{s+1} - \mathbf{A}_{s} \quad \cdots\cdots\cdots (6\text{-}31)$$

where $\mathbf{K}_{gs}$ is the so-called geometric stiffness matrix evaluated from conditions at time t_s.

In the numerical calculation, the same triangular element as that used in Chapter 3 is used (Fig.6-3), and the effect of damping is neglected. The transformation of nodal displacements described in Chapter 3 is also employed for determining an equilibrium configuration of the plate at time t_{s+1}.

A plate bending problem is used to investigate the effect of equilibrium iterations in the large deformation problem. In this example, a simply supported square plate, shown in Fig.6-4(a), is loaded suddenly with a uniform out-of-plane load (Fig.6-4(b)).

Fig.6-4(c) shows comparisons between the dynamic responses of the deflections at the center of the plate obtained by the FETM method with and without equilibrium iteration. In the numerical calculation, a quarter of the plate is divided into 3 strips and each of which is divided into 6 triangular elements as shown in Fig.6-4(a), the size of the time step is taken to be equal to 4×10^{-4} sec, the maximum number of iterations is limited to 10 (ITERAM=10), and a convergence tolerance is taken to be equal to 0.000001. In Fig.6-4(c), the response curves with a time step of 1×10^{-4} sec and equilibrium iterations (ITERAM=10) are also shown. Considerable damping is observed in the response without equilibrium iteration. However, the result is remarkably improved by equilibrium iterations, and the response with $\Delta t=4 \times 10^{-4}$ sec is in good agreement with that with $\Delta t=1 \times 10^{-4}$ sec. Computation time for the time range shown in Fig.6-4(c) is 574 sec for $\Delta t=4 \times 10^{-4}$ sec (ITERAM=0), 1,462 sec for $\Delta t=4 \times 10^{-4}$ sec (ITERAM=10), and 4,250sec for $\Delta t=1 \times 10^{-4}$ sec (ITERAM=10).

Fig.6-7～9 show the comparisons of the results obtained by the FETM and finite element method. The simply supported plate and all edges clamped plate shown in Fig.6-5 are chosen for the numerical model, and these plates are assumed to be subjected to the three types of load as shown in Fig.6-6. In these example, a quarter of the plate is divided into 3 strips and each of which is divided into 6 triangular elements as shown in Fig.6-5, the size of the time step is taken to be equal to 4×10^{-4} sec, and a convergence tolerance is taken to be equal to 0.000001. The material properties of the plate are also given in Fig.6-5. In the finite element method, the same element and mesh pattern as those used in the FETM method are employed.

Fig.6-7(a) shows the comparisons of the dynamic responses at points A, B and C, those are indicated in Fig.6-5, of the simply supported plate loaded suddenly with a uniform out-of-plane load (p_0 = 0.4kg/cm^2) as shown in Fig.6-6(a). The results of both methods agree with each other within the error of 0.01%, thus can not be distincted in Fig.6-7(a). In Fig.6-7(a), the response at point A obtained by the linear analysis are also shown. By the effects of the geometrical nonlinearity, the amplitude and period of the deflection by the large deformation analysis are smaller than those by the linear analysis. Computation time for the range shown in Fig.6-7(a) is 1120.2sec for the FETM method, 1445.9sec for the finite element method.

Fig.6-7(b) shows the comparisons of the results of the all edges clamped plate loaded suddenly with a uniform out-of-plane load (p_0=0.6kg/cm^2) as shown in Fig.6-6(a). The similar results to the previous example are obtained. Computation time for the range shown in Fig.6-7(b) is 813.7sec for the FETM method, 940.8 sec for the finite element method.

Fig.6-8(a) shows the comparisons of the dynamic responses of the simply supported plate loaded suddenly at the center of plate with a concentrated out-of-plane load (P_0=400kg) shown in Fig.6-6(b). The results of both methods agree with each other within the error of 0.01%, thus can not be distincted in Fig.6-8(a) as in the case of a uniform load. In Fig.6-8(a) the results obtained by the linear analysis are also shown. Computation time for the range shown in Fig.6-8(a) is 1174.9sec for the FETM method, 1521.4sec for the finite element method.

Fig.6-8(b) shows the comparisons of the results of the all edges clamped plate loaded suddenly at the center with a concentrated out-of-plane load (P_0=600kg) as shown in Fig.6-6(b). The similar results to the previous example are obtained.

Computation time for the range shown in Fig.6-8(b) is 1031.3sec for the FETM method, 1199.8sec for the finite element method.

Fig.6-9(a) shows the comparisons of the dynamic responses at points A, B and C of the simply supported plate subjected to in-plane excitation ($p(t) = p_0 \sin\omega t$, $p_0 = 60 kg/cm^2$, $\omega = 39.8Hz$) as shown in Fig.6-6(c). The initial deflection of plate bending mode is assumed, and is defined as follows:

$$w_0 = \bar{w}_0 \sin\frac{\pi}{a}x \sin\frac{\pi}{a}y \qquad \cdots\cdots\cdots\cdots(6\text{-}32)$$

in which $\bar{w}_0$ = the maximum value of initial deflection and here $\bar{w}_0$ = 5h is assumed.

Close agreement exists in the results of both methods as in the case of out-of-plane load. In Fig.6-9(a), the results obtained by the linear analysis are also shown. In the linear analysis, the displacement grows rapidly, in the large deformation analysis, the displacement, however, grows gradually and the central portion of plate displaces to one side. Computation time for the range shown in Fig.6-9(a) is 970.8sec for the FETM method, 1260.8sec for the finite element method.

Fig.6-9(b) shows the comparisons of the dynamic responses at points A, B and C of the all edges clamped plate subjected to in-plane excitation ($p(t) = p_0 \sin\omega t$, $p_0 = 120 kg/cm^2$, $\omega = 81.5Hz$) as shown in Fig.6-6(c). The same initial deflection of plate bending mode as that assumed in the previous example is also assumed in this example.

The similar results to those for the simply supported plate are obtained. In Fig.6-9(b) the results obtained by the linear analysis are also shown. Computation time for the range shown in Fig.6-9(b) is 1045.9sec for the FETM method, 1277.6sec for the finite element method.

Fig.6-10(b) shows comparisons of computation time in the FETM method and the finite element method for 1×1 (1 strip with 2

3×3 (3 strips with 6 triangular elements), 4×4 (4 strips with 8 triangular elements) and 5×5 (5 strips with 10 triangular elements) mesh patterns, and these mesh patterns are illustrated in Fig.6-10(a). A simply supported square plate loaded suddenly with a uniform out-of-plane load (p_0 = 0.4kg/cm^2) is used in this example. The size of the time step is taken to be 4×10^{-4} sec and a convergence tolerance is taken to be 1×10^{-7}.

It is found from Fig.6-10(b) that although in computation time the FETM method has less of an advantage for a small number of element patterns, it has much more of an advantage for a number of element patterns. In Fig.6-10(b), computation time for the tangent stiffness iteration method, in which the transfer matrix must be derived for every time stage, is also shown to illustrate the efficiency of the pseudo-force iteration method.

2) Elasto-Plastic Dynamic Analysis of Plates

In elasto-plastic dynamic problem, the governing equation (6-5) is written as follows:

$$\mathbf{M}\,\ddot{\mathbf{u}}_{s+1} + \mathbf{C}\,\dot{\mathbf{u}}_{s+1} + \mathbf{K}_{ps}\,\Delta\mathbf{u} = \mathbf{F}_{s+1} - \mathbf{A}_s \qquad \cdots\cdots\cdots\cdots(6\text{-}33)$$

where $\mathbf{K}_{ps}$ is the stiffness matrix for inelastic situation evaluated from stresses at time t_s.

The Prandtl-Reuss′ law and the von Mises yield criterion (22,23) are assumed in the derivation of the inelastic stiffness matrix as in the static problem described in Chapter 3. In order to consider the extent of the yielded portions in the directions of the cross sections, the cross section of the plate is divided into some layers as shown in Fig.6-11. In the numerical calculation, the triangular element with three degrees of freedom per one node, shown in Fig.6-12, is employed here, and the effect of damping is neglected.

Figs.6-14∿16 show the comparisons of the results obtained by the FETM and finite element method. The same plates and mesh pattern as those used in the large deformation problem are also used here. These plates are assumed to be subjected to the three types of load as shown in Fig.6-13. The size of the time step is taken to be equal to 4×10^{-4} sec, and a convergence tolerance is taken to be equal to 0.0001. In the finite element method, the same element and mesh pattern as those used in the FETM method are employed.

Fig.6-14(a) shows the comparisons of the dynamic responses at points A and C, indicated in Fig.6-5, of the simply supported plate subjected to the uniformly distributed out-of-plane excitation ($p = p_0 \sin\omega t$; $p_0 = 0.4\text{kg/cm}^2$, $\omega = 39.8\text{Hz}$) as shown in Fig.6-13(a). The amplitudes of the responses of both methods, indicated by H in Fig.6-14(a), agree with each other within the error of 5.2%. In Fig.6-14(a), the results obtained by the linear analysis are also shown. The displacement of the linear analysis grows rapidly, that of the elasto-plastic analysis, however, grows gradually and reaches a steady state. Computation time for the range shown in Fig.6-14(a) is 788.7sec for the FETM method, 990.3sec for the finite element method.

Fig.6-14(b) shows the comparisons of the results of the all edges clamped plate subjected to the uniformly distributed out-of-plane excitation ($p = p_0 \sin\omega t$; $p_0 = 0.6\text{kg/cm}^2$, $\omega = 81.5\text{Hz}$) as shown in Fig.6-13(b). The amplitudes of the responses of both methods, indicated by H in Fig.6-14(b), agree with each other within the error of 0.56%. Computation time for the range shown in Fig.6-14(b) is 801.6sec for the FETM method, 971.9sec for the finite element method.

Fig.6-15(a) shows the comparisons of the dynamic responses of the simply supported plate subjected to the concentrated out-of-plane excitation ($P=P_0 \sin\omega t$; $P_0=400$kg, $\omega=39.8$Hz) shown in Fig.6-13(b). The amplitudes of the responses obtained by both methods, indicated by H in Fig.6-15(a), agree with each other within the error of 4.43%. In Fig.6-15(a), the results obtained by the linear analysis are also shown. Computation time for the range shown in Fig.6-15(a) is 787.9sec for the FETM method, 998.1sec for the finite element method.

Fig.6-15(b) shows the comparisons of the results of the all edges clamped plate subjected to the concentrated out-of-plane excitation ($P = P_0 \sin\omega t$; $P_0 = 600$kg, $\omega = 81.5$Hz) as shown in Fig.6-13(b). The amplitudes of the responses of both methods, indicated by H in Fig.6-15(b), agree with each other within the error of 0.60%. Computation time for the range shown in Fig.6-15(b) is 825.7sec for the FETM method, 974.9sec for the finite element method.

Fig.6-16(a) shows the comparisons of the dynamic responses at points A and C of the simply supported plate subjected to in-plane excitation ($p(t) = p_0 \sin\omega t$, $p_0 = 60$kg/cm^2, $\omega = 39.8$Hz) as shown in Fig.6-13(c). The initial deflection of plate bending mode is assumed, and is defined as follows:

$$w_0 = \bar{w}_0 \sin\frac{\pi}{a}x \sin\frac{\pi}{a}y \qquad \cdots\cdots\cdots\cdots (6\text{-}34)$$

in which $\bar{w}_0$ = the maximum value of initial deflection and here $\bar{w}_0$ = 5h is assumed.

The amplitudes of the responses of both methods, indicated by H in Fig.6-16(a), agree with each other within the error of 0.60%. In Fig.6-16(a), the results obtained by the linear analysis are also shown. Computation time for the range shown in

Fig.6-16(a) is 723.6sec for the FETM method, 868.9sec for the finite element method.

Fig.6-16(b) shows the comparisons of the dynamic responses at points A and C of the all edges clamped plate subjected to in-plane excitation ($p(t)=p_0 \sin\omega t$, $p_0=120kg/cm^2$ kg, $\omega= 81.5Hz$) as shown in Fig.6-13(c). The same initial deflection of plate bending mode as that assumed in the previous example is also assumed in this example.

The amplitudes of the responses of both methods, indicated by H in Fig.6-16(b), agree with each other within the error of 0.75%. In Fig.6-16(b), the results obtained by the linear analysis are also shown. Computation time for the range shown in Fig.6-16(b) is 734.0sec for the FETM method, 860.5sec for the finite element method.

Fig.6-17(b) shows comparisons of computation time of the FETM method and the finite element method for the elasto-plastic dynamic problem. The same mesh pattern as used in the large deformation problem are employed here and these mesh patterns are illustrated in Fig.6-17(a). A simply supported square plate subjected to the periodic uniform out-of-plane excitation ($p = p_0 \sin\omega t$; $p_0 = 0.4$ kg/cm^2, $\omega = 39.8Hz$) is used in this example. The size of the time step is taken to be 4×10^{-4} sec and a convergence tolerance is taken to be 0.001.

It is found from Fig.6-17(b) that the FETM method has much more of an advantage as a number of elements is increases. In Fig.6-17(b), computation time for the tangent stiffness iteration method, in which the stiffness and transfer matrices must be derived for every time stage, is also shown. The computation time for the pseudo-force iteration method is smaller than that for tangent stiffness method in every mesh pattern.

6-5 CONCLUSIONS

A linear transient analysis method based on a combined use of finite element and transfer matrix methods described in previous chapter is extended to nonlinear dynamic problems of plates under random out-of-plane and in-plane excitations. Equilibrium iterations are employed to improve the solution accuracy and to avoid the development of numerical instabilities. The Prandtl-Reuss′ law obeying the von Mises yield criterion is assumed, and a set of moving coordinate systems is used to take geometric nonlinearity into consideration.

A computer program based on this theory has been developed. In this program, procedures used in the finite element method based on load increment are employed except for the estimation of approximate displacements for each specified time step. From the numerical examples presented in this chapter, following conclusions are obtained:

(1) In inelastic and large deformation dynamic problems, good agreement exists between the transient responses of the plates under out-of-plane and in-plane excitations obtained by the FETM method and the conventional finite element method, which demonstrates the accuracy of the proposed method.

(2) Equilibrium iteration in each time step is effective to improve the solution accuracy and to avoid the development of numerical instabilities.

(3) Since, in the FETM method, considerable computation time is required in the derivation of the transfer matrix, the pseudo-force iteration method is more efficient compared to the tangent stiffness iteration method.

From the mentions described above, it is obtained that the FETM method can be applied successfully to the nonlinear dynamic analysis of plates subjected to out-of-plane and in-plane excitations by reducing the size of the matrix and computation time to relatively less than those obtained by the method based on the ordinary finite element procedure.

REFERENCES

1. Adeli, H., Gere, J.M. and Weaver Jr.W., "Algorithms for Nonlinear Structural Dynamics," J. ASCE, Vol.104, No.ST2, Feb., 1978, pp.263-280.
2. Bathe, K.J., Ramm, E. and Wilson, E.L., "Finite Element Formulations for Large Deformation Dynamic Analysis," International Journal for Numerical Methods in Engineering, Vol.9, 1975, pp.353-386.
3. Bathe, K.J. and Ozdemir, H., "Elastic-Plastic Large Deformation Static and Dynamic Analysis," Computers & Structures, Vol.6, 1976, pp.81-92.
4. Brebbia, C.A., Tottenham, H., Warburton, G.B., Wilson, J.M. and Wilson, R.R., "Vibrations of Engineering Structures," Springer-Verlag, Berlin, 1985.
5. Chiatti, G. and Sestieri, A., "Analysis of Static and Dynamic Structural Problems by a Combined Finite Element - Transfer Matrix Method," J. Sound & Vibration, Vol.67, No.1, 1979, pp.35-42.
6. Degen, E.E., Shephard, M.S. and Loewy, R.G., "Combined Finite Element - Transfer Matrix Method Based on a Mixed Formulation," Computers & Structures, Vol.20, No.1-3, 1985, pp.173-180.
7. Dokainish, M.A., "A New Approach for Plate Vibrations: Combination of Transfer Matrix and Finite - Element Technique," Trans. ASME Vol.94, No.2, 1972, pp.526-530.
8. Donéa, J., "Advanced Structural Dynamics," Applied Science Publishers, London, 1978.
9. Komatsu, S. and Kitada, T., "Refined Finite Element Analysis of Plane Elasto-Plastic Problems," Technology Reports of Osaka University, Vol.25, 1975, pp.415-437.
10. McDaniel, T.J. and Eversole, K.B., "A Combined Finite Element - Transfer Matrix Structural Analysis Method," J. Sound & Vibration, Great Britain, Vol.51, No.2, 1977, pp.157-169.
11. Mucino, H.V. and Pavelic, V., "An Exact Condensation Procedure for Chain-Like Structures Using a Finite Element-

Transfer Matrix Approach," Trans. ASME, J. Mech. Des., No.80-C2/DET-123, 1980, pp.1-9.

12. Murray, D.W. and Wilson, E.L., "Finite-Element Large Deflection Analysis of Plates," J. ASCE, Vol.95, No.EM1, Feb., 1969, pp.143-163.
13. Newmark, N.M., "A Method of Computation for Structural Dynamics," J. ASCE, Vol.85, No.EM3, 1959, pp.67-94.
14. Ohga, M., Shigematsu, T. and Hara, T., "Structural Analysis by a Combined Finite Element - Transfer Matrix Method," Computers & Structures, Vol.17, No.3, 1983, pp.321-326.
15. Ohga, M., Shigematsu, T. and Hara, T., "Structural Analysis by a Combined Finite Element - Transfer Matrix Method," J. ASCE, Vol.110, No.EM9, September, 1984, pp.1335-1349.
16. Ohga, M. and Shigematsu, T., "Transient Analysis of Plates by a Combined Finite Element - Transfer Matrix Method," Computers & Structures, Vol.26, No.4, 1987, pp.543-549.
17. Ohga, M. and Shigematsu, T., "Large Deformation Dynamic Analysis of Plates," J. ASCE, Vol.114, No.4, April, 1988, pp.624-637.
18. Park, K.C., "An Improved Stiffly Stable Method for Direct Integration of Nonlinear Structural Dynamic Equations," Journal of Applied Mechanics, American Society of Mechanical Engineers, Vol.42, 1975, pp.464-470.
19. Pestel, E.C. and Leckie, F.A., "Matrix Method in Elastomechanics," McGraw-Hill Book, New York, N.Y., 1963.
20. Sankar, S. and Hoa, S.V., "An Extended Transfer Matrix - Finite Element Method for Free Vibration of Plates," J. Sound & Vibration, Vol.70, No.2, 1980, pp.205-211.
21. Stricklin, J.A. and Haisler, W.E., "Formulations and Solution Procedures for Nonlinear Structural Analysis," Computers & Structures, Vol.7, 1977, pp.125-136.
22. Yamada, Y., "Matrix Methods of Strength of Materials," Baifukan, 1980 (in Japanese).
23. Yamada, Y., Yoshimura, N. and Sakurai, T., "Plastic Stress-Strain Matrix and its Application for the Solution of Elastic - Plastic Problems by the Finite Element Methods," Int. J. Mech. Sci., Vol.10, 1968, pp.343-354.

NOTATION

The following symbols are used in this paper:

$\mathbf{A}$ = equivalent force vector;
$\mathbf{B}$ = matrix expressing the strain in terms of the displacements;
$\mathbf{C}$ = damping matrix;
$\mathbf{F}$ = force matrix;
$\mathbf{G}$ = effective stiffness matrix;
$\mathbf{K}_\ell, \mathbf{K}_s$ = linear and tangent stiffness matrices, respectively;
$\mathbf{K}_g, \mathbf{K}_p$ = geometric and inelastic stiffness matrices, respectively;
$\mathbf{M}$ = mass matrix;
$\mathbf{P}$ = point matrix;
$\bar{\mathbf{Q}}$ = generalized load vector acting on section i;
$\mathbf{T}$ = transfer matrix;
$\mathbf{u}, \dot{\mathbf{u}}, \ddot{\mathbf{u}}$ = displacement, velocity, and acceleration vectors, respectively;
$\Delta\mathbf{N}$ = incremental force vector;
$\Delta\mathbf{N}_{\ell i}, \Delta\mathbf{N}_{r i}$ = left and right incremental force vectors of strip i;
$\Delta\mathbf{Q}$ = generalized incremental force vector;
Δt = size of time step;
$\Delta\mathbf{u}$ = incremental displacement vector;
$\Delta\mathbf{z}$ = incremental state vector;
$\Delta\mathbf{z}_0$ = unknown initial state vector;
$\Delta\mathbf{z}_{\ell i}, \Delta\mathbf{z}_{r i}$ = left and right incremental state vectors of strip i, respectively;
$\Delta\boldsymbol{\delta}$ = incremental displacement vector;
$\Delta\boldsymbol{\delta}_{\ell i}, \Delta\boldsymbol{\delta}_{r i}$ = left and right incremental displacement vectors of strip i, respectively; and
σ = stress vector.

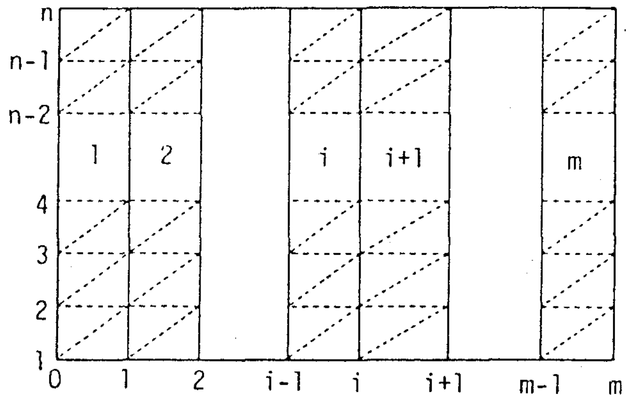

Fig.6-1 Subdivision of Plate into and Strips Finite Elements

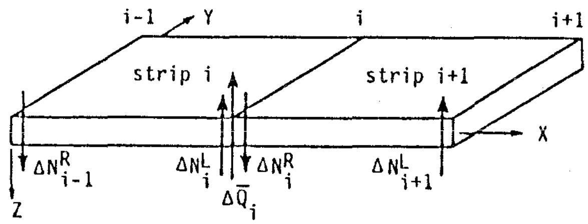

Fig.6-2 Equilibrium of Forces
at Section i

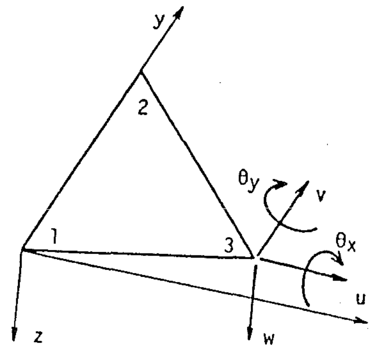

Fig.6-3 Triangular Element and
Degrees of Freedom

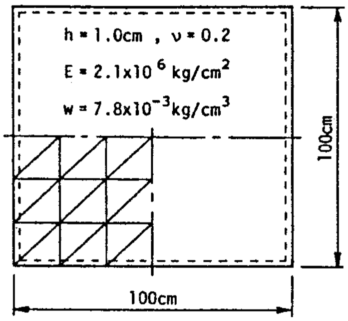

(a)

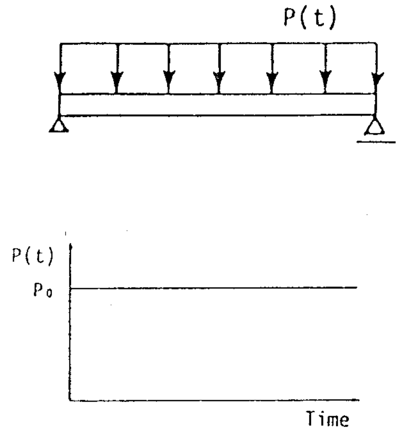

(b)

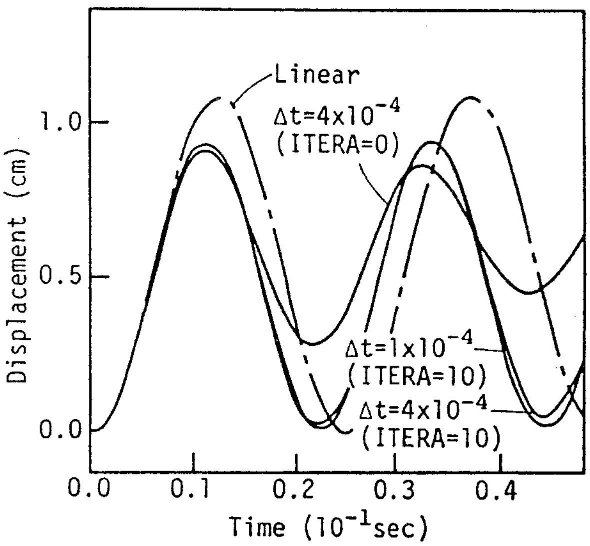

(c)

Fig.6-4 Comparison of the Responses with and without Equilibrium Iteration

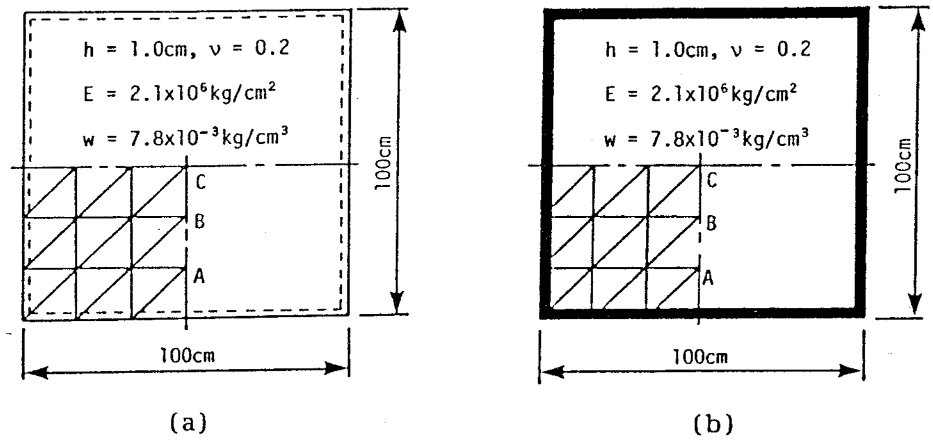

Fig.6-5 Plate Models in Large Deformation Dynamic Analysis

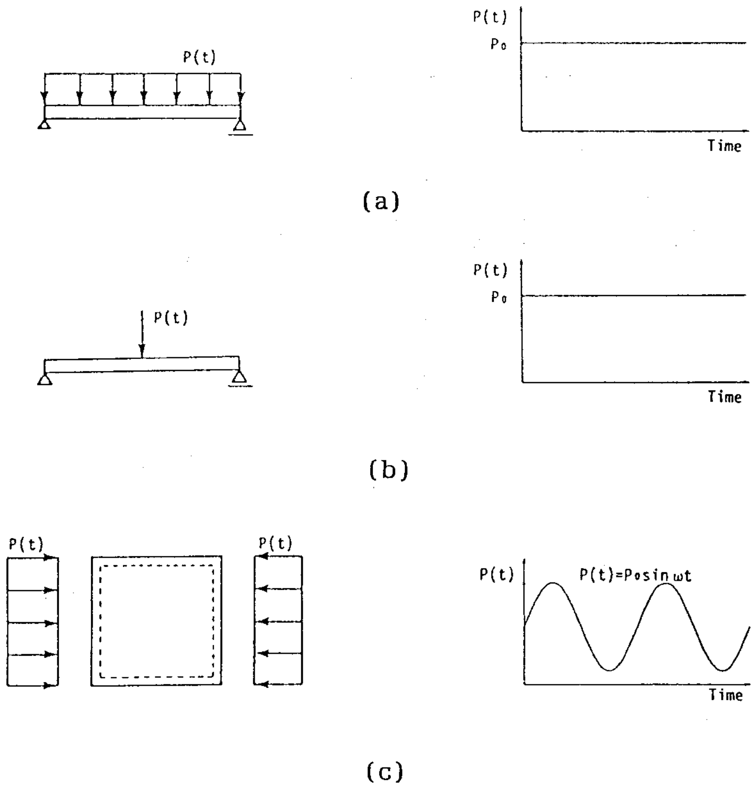

Fig.6-6 Load Models in Large Deformation Dynamic Analysis

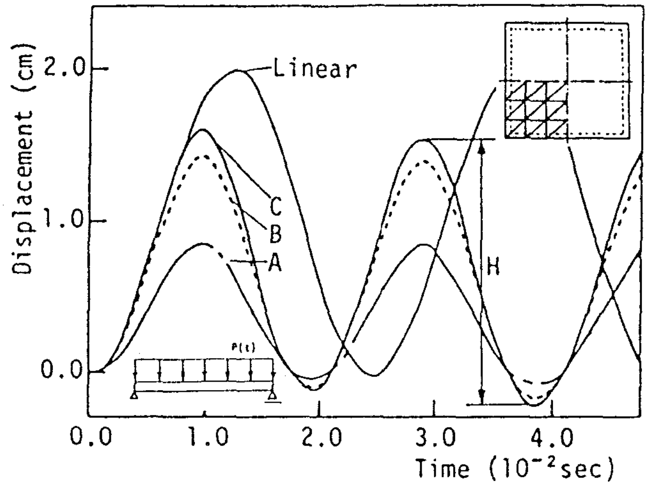

Fig.6-7(a) Comparisons of Responses of Simply Supported Plate Loaded Suddenly with Uniform Out-of-Plane Load

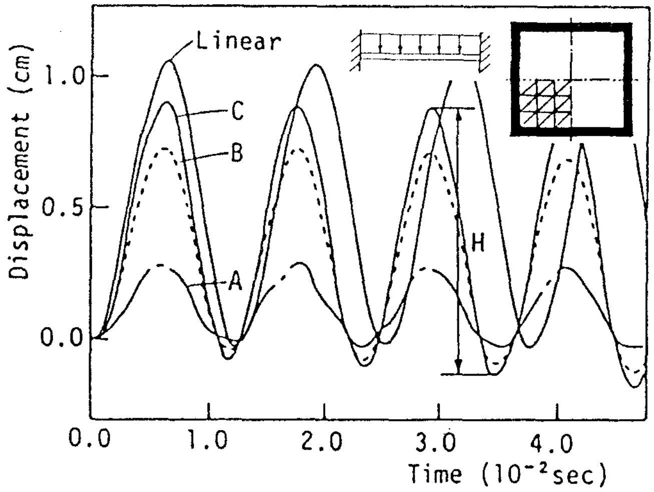

Fig.6-7(b) Comparisons of Responses of All Edges Clamped Plate Loaded Suddenly with Uniform Out-of-Plane Load

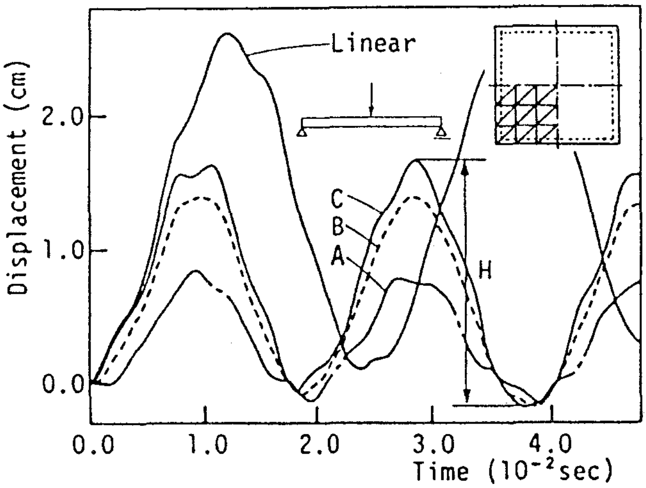

Fig.6-8(a) Comparisons of Responses of Simply Supported Plate Loaded Suddenly with Concentrated Out-of-Plane Load

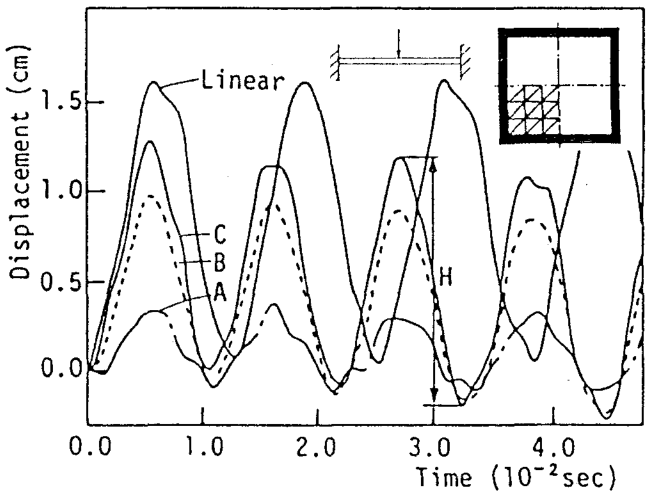

Fig.6-8(b) Comparisons of Responses of All Edges Clamped Plate Loaded Suddenly with Concentrated Out-of-Plane Load

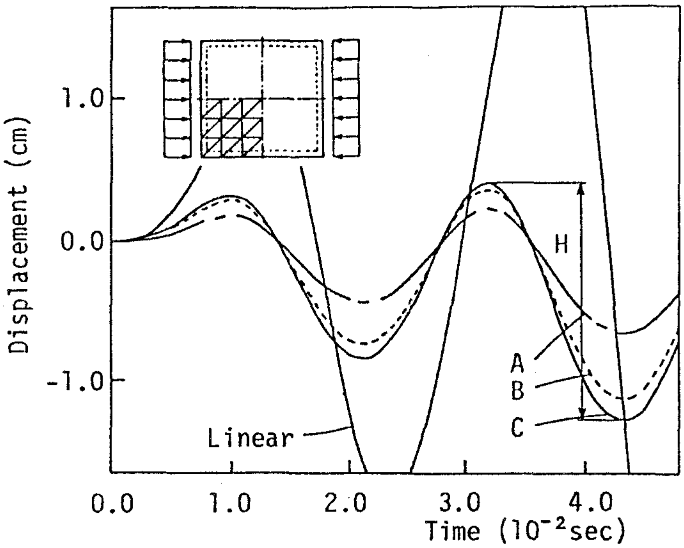

Fig.6-9(a) Comparisons of Responses of Simply Supported Plate Subjected to In-Plane Excitation

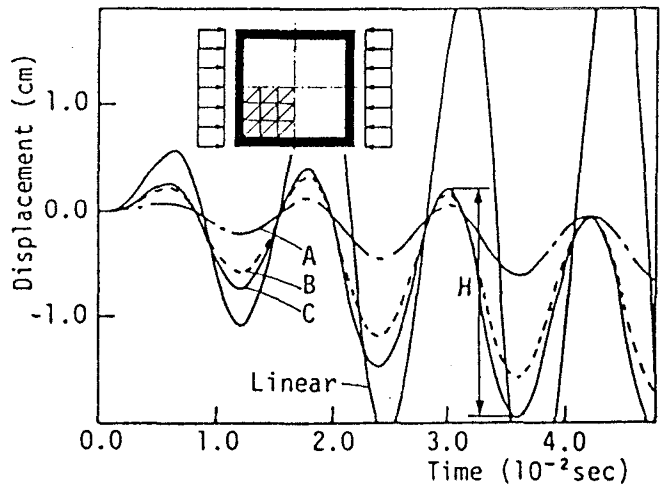

Fig.6-9(b) Comparisons of Responses of All Edges Clamped Plate Subjected to In-Plane Excitation

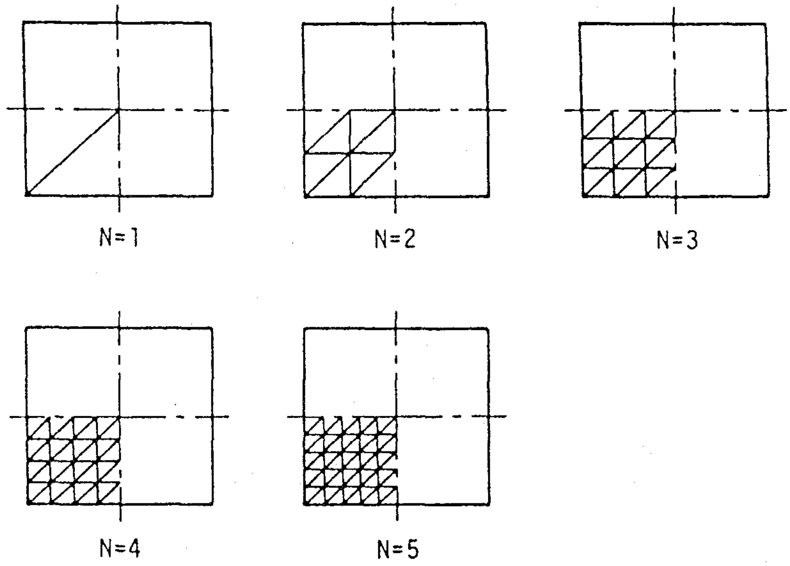

Fig.6-10(a) Mesh Patterns

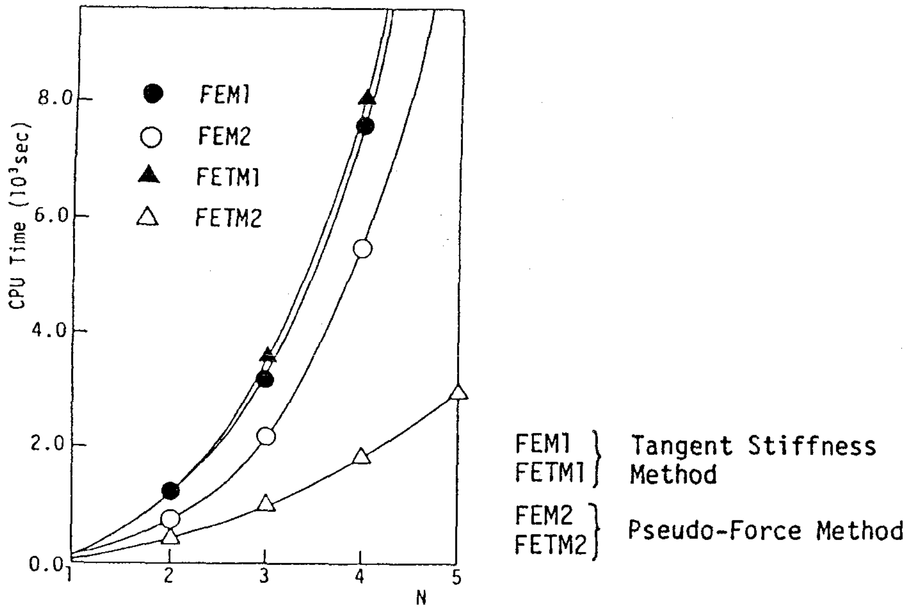

Fig.6-10(b) Comparisons of Computation Time in Large Deformation Analysis

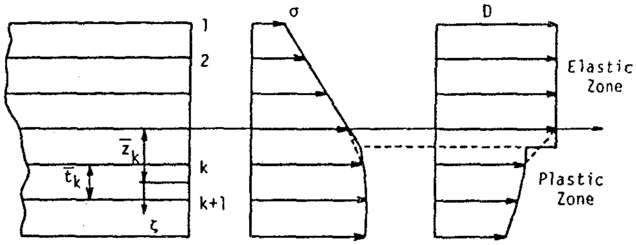

Fig.6-11 Subdivision of Cross Section into Layers

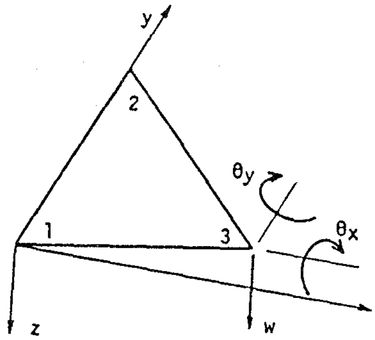

Fig.6-12 Triangular Element and Degrees of Freedom

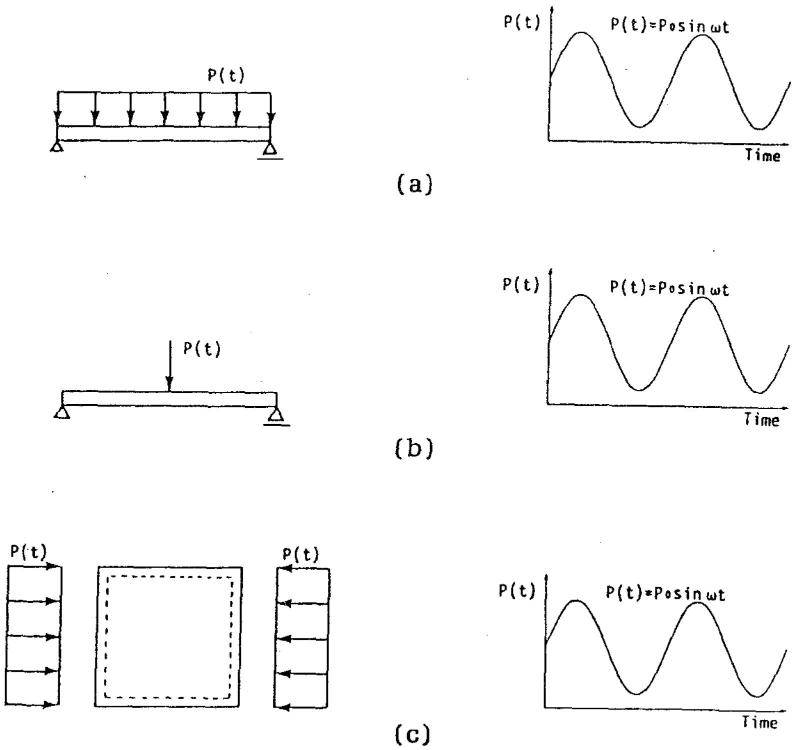

Fig.6-13 Load Models in Elasto-Plastic Dynamic Analysis

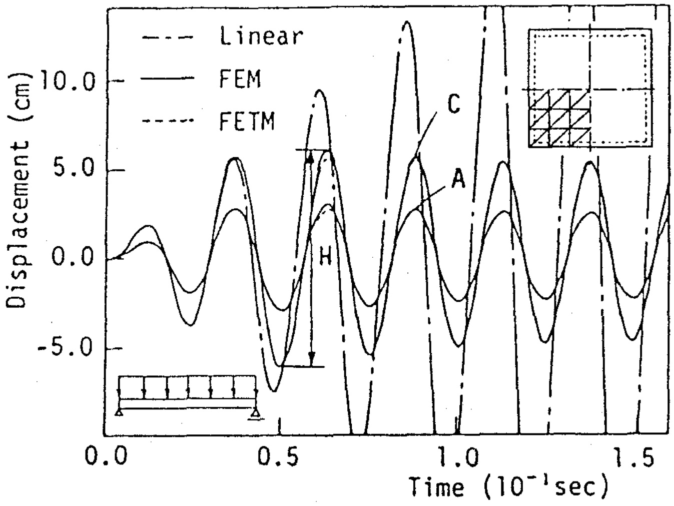

Fig.6-14(a) Comparisons of Responses of Simply Supported Plate Subjected to Uniformly Distributed Out-of-Plane Excitation

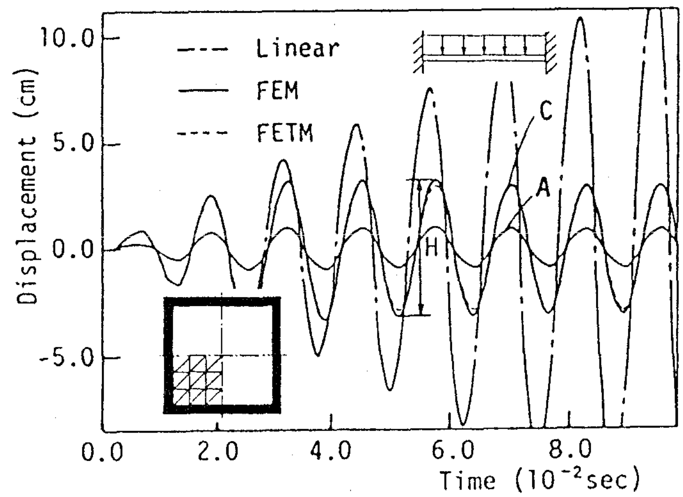

Fig.6-14(b) Comparisons of Responses of All Edges Clamped Plate Subjected to Uniformly Distributed Out-of-Plane Excitation

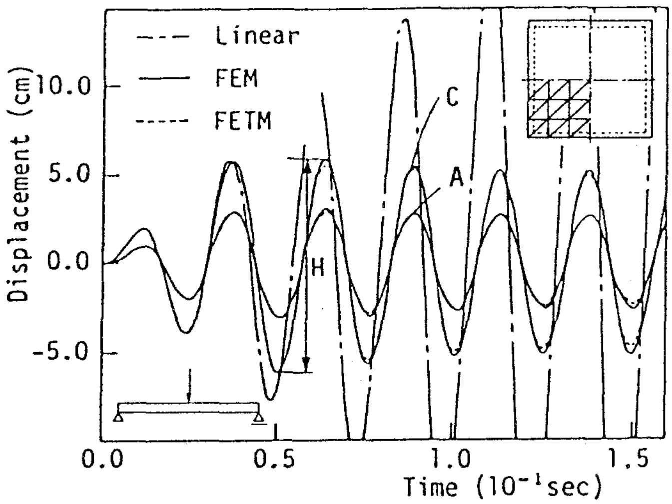

Fig.6-15(a) Comparisons of Responses of Simply Supported Plate Subjected to Concentrated Out-of-Plane Excitation

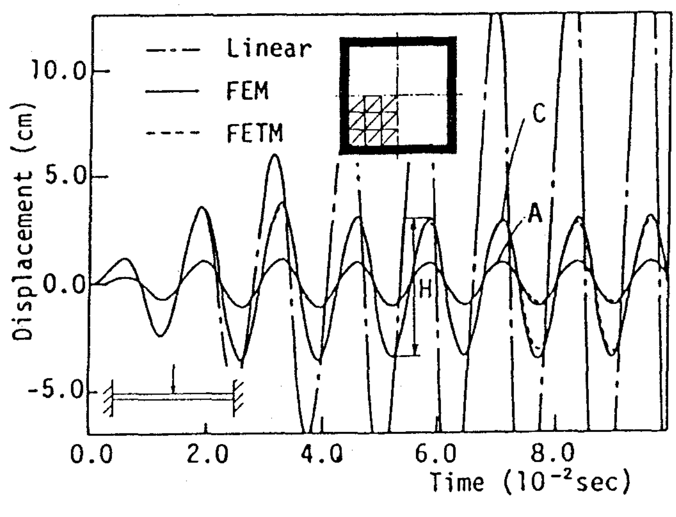

Fig.6-15(b) Comparisons of Responses of All Edges Clamped Plate Subjected to Concentrated Out-of-Plane Excitation

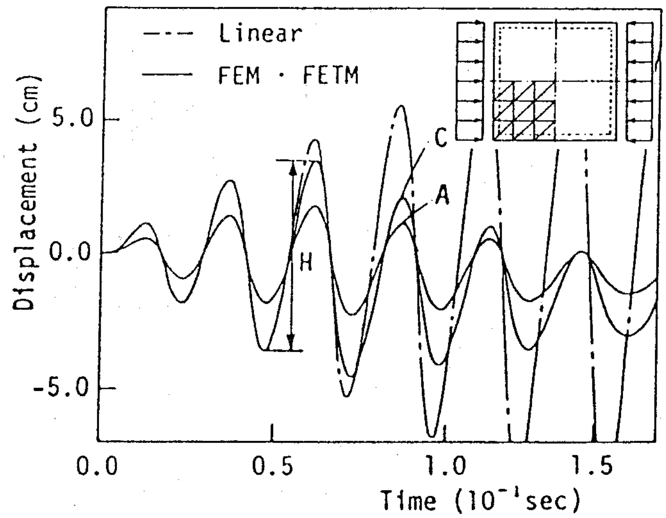

Fig.6-16(a) Comparisons of Responses of Simply Supported Plate Subjected to In-Plane Excitation

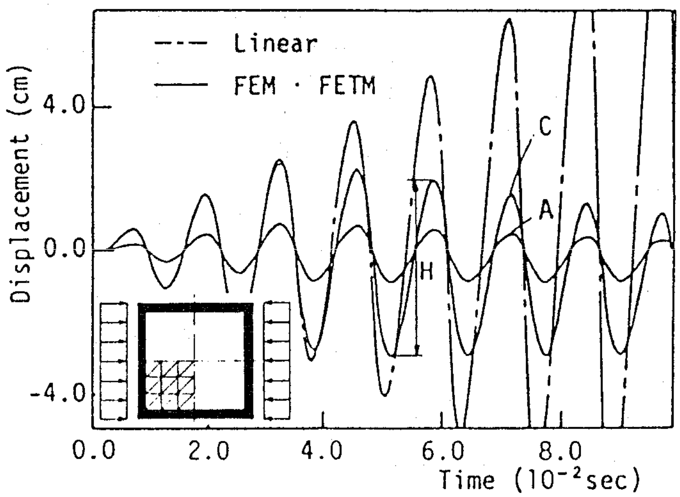

Fig.6-16(b) Comparisons of Responses of All Edges Clamped Plate Subjected to In-Plane Excitation

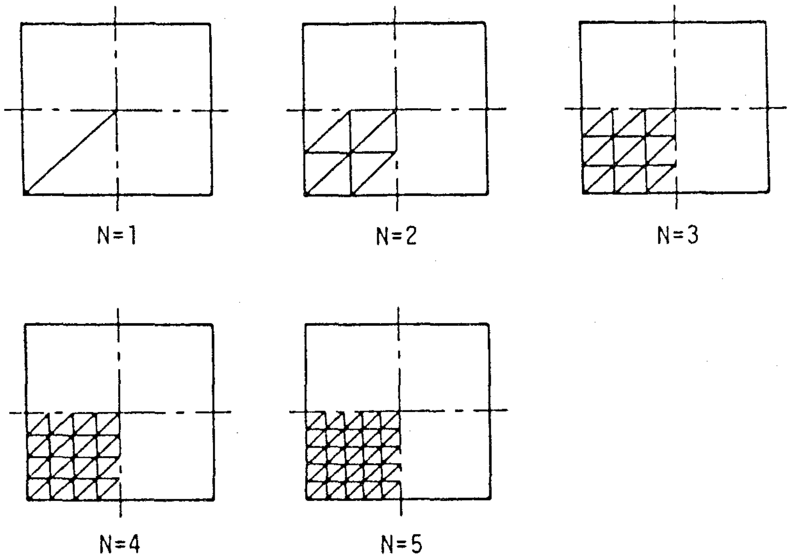

Fig.6-17(a) Mesh Patterns

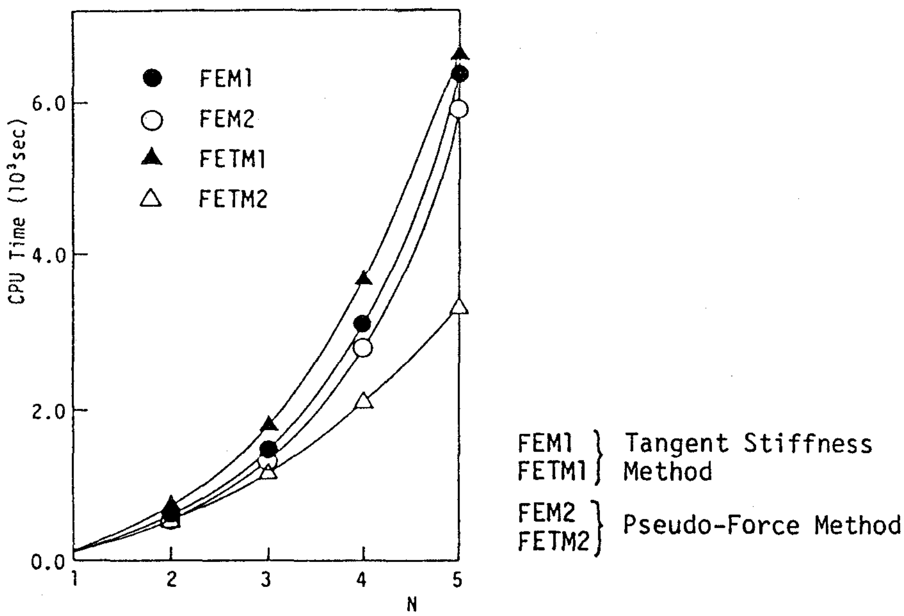

Fig.6-17(b) Comparisons of Computation Time in Elasto-Plastic Dynamic Analysis

Chapter 7 STRUCTURAL ANALYSIS BY A COMBINED BOUNDARY ELEMENT-TRANSFER MATRIX METHOD

7-1 INTRODUCTION

The boundary element method offers important advantages over domain-type methods such as the finite element method and the finite difference method, and has been applied to the solution of various engineering problems (4, 5, 6, 7, 16). One of the most interesting features of the boundary element method is that a much smaller resulting system of equations and a considerable reduction in the data required to solve the problem is obtainable. In addition, the numerical accuracy of the boundary element method can be greater than that of the finite element method. The main disadvantage of the boundary element method is, however, the difficulties that are encountered in non-homogeneous problems, i.e. finding fundamental solutions and defining the interfaces.

In order to overcome this disadvantage of the boundary element method, some techniques based on the subdividing of the body into regions have been proposed. Tomlin and Butterfield (18) extended the boundary element method to piecewise homogeneous anisotropic foundation engineering problems. This work was extended to three dimensions by Banerjee (2) and Lachat and Watson (9), whose main incentive for subdividing the body into distinct regions was to reduce the bandwidth of the resultant system of algebraic equations.

In this chapter, a new approach, based on the combination of the boundary element and transfer matrix (BETM) methods, is proposed for the problems where the subdividing of the body into regions is required. In this method, the system of equations of an individual region is determined in the same manner as in the boundary element method. However, the process of computation of the displacements and tractions at the boundaries is different and does not require the assembly of matrices for the entire structure. This method, therefore, permits the use of a large number of elements, without getting involved with large matrices. A much smaller computer is therefore sufficient.

7-2 BOUNDARY INTEGRAL EQUATION FOR IN-PLANE PROBLEMS

1) Two-Dimensional Elasticity

We introduce the rectangular cartesian coordinate system $O-x_1, x_2$ in which the axis x_1 and x_2 lie in middle plane of the plate as shown in Fig.7-1. The inner domain and the boundary are denoted by Ω and Γ, respectively.

If one considers an infinitesimal rectangular parallelepiped element surrounding a given point within the body, the equilibrium equation can be written as

$$\sigma_{ij,j} + f_i = 0 \qquad (i,j=1,2) \qquad \cdots\cdots\cdots\cdots (7\text{-}1)$$

where σ_{ij} are the components of the stress tensor and f_i are the components of the body force. Space derivatives are indicated by a comma, i.e., $\partial\sigma_{ij}/\partial x_j = \sigma_{ij,j}$. If the components of the stress tensor are assumed to be known at a certain point, the equivalent tractions acting on any plane through this point p_i can be computed by

$$p_i = \sigma_{ij} n_j \qquad \cdots\cdots\cdots\cdots (7\text{-}2)$$

where n_j represents the direction cosines of the normal to the plane. The strains at any point ε_{ij} can be represented as follows:

$$\varepsilon_{ij} = \frac{1}{2}(u_{i,j} + u_{j,i}) \qquad \cdots\cdots\cdots\cdots\cdot(7\text{-}3)$$

where u_i is the displacement component.

For the plane strain problem, the stresses and strains are related by the constitutive relations as follows :

$$\begin{Bmatrix} \sigma_{11} \\ \sigma_{22} \\ \sigma_{12} \end{Bmatrix} = \begin{bmatrix} \lambda+2G & \lambda & 0 \\ \lambda & \lambda+2G & 0 \\ 0 & 0 & G \end{bmatrix} \begin{Bmatrix} \varepsilon_{11} \\ \varepsilon_{22} \\ 2\varepsilon_{12} \end{Bmatrix} \qquad \cdots\cdots\cdots\cdots\cdot(7\text{-}4)$$

where

$$\lambda = \frac{E\nu}{(1+\nu)(1-2\nu)} \quad , \qquad G = \frac{E}{2(1+\nu)}$$

and E, G and ν are the modulus of elasticity, the shear modulus and the Poisson's ratio, respectively.

Let Γ_u denote the portion of the boundary on which displacements are prescribed and Γ_p the portion on which surface forces are prescribed, the boundary conditions are then represented as follows:

$$u_i = \bar{u}_i \ (\text{on } \Gamma_u), \quad p_i = \bar{p}_i \ (\text{on } \Gamma_p) \qquad \cdots\cdots\cdots\cdots\cdot(7\text{-}5)$$

where $\bar{u}_i$ and $\bar{p}_i$ are the prescribed displacement and surface forces. Note that the total boundary Γ of the body is equal to $\Gamma_u + \Gamma_p$.

2) Integral Equation for Two-Dimensional Elasticity

Taking into consideration the equilibrium equations (7-1) and the boundary conditions (7-5), the weighted residual statement can be written as

$$\int_{\Omega}(\sigma_{ij,j}+f_i)u_i^*d\Omega = \int_{\Gamma_p}(p_i-\bar{p}_i)u_i^*d\Gamma + \int_{\Gamma_u}(\bar{u}_i-u_i)p_i^*d\Gamma \quad \cdots\cdots(7\text{-}6)$$

where u_i^*, p_i^* are the displacement and surface force corresponding to the weighting field:

$$p_i^* = \sigma_{ij}^*\, n_j \quad \cdots\cdots\cdots\cdots(7\text{-}7)$$

The strain-displacement relationship (7-3) and the constitutive equations (7-4) are assumed to apply for the weighting field.

The first term in Eq.(7-6) can be integrated by parts, which gives

$$-\int_{\Omega}\sigma_{ji}\varepsilon_{ji}^*d\Omega + \int_{\Omega}f_i u_i^*d\Omega = -\int_{\Gamma_p}\bar{p}_i u_i^*d\Gamma - \int_{\Gamma_u}p_i u_i^*d\Gamma$$

$$+\int_{\Gamma_u}(\bar{u}_i-u_i)p_i^*d\Gamma \quad \cdots\cdots\cdots\cdots(7\text{-}8)$$

Integrating by parts again the first term in Eq.(7-8) and taking into consideration the reciprocity principle, one obtains

$$\int_{\Omega}\sigma_{ij,j}^*u_i d\Omega + \int_{\Omega}f_i u_i^*d\Omega$$

$$= -\int_{\Gamma_p}\bar{p}_i u_i^*d\Gamma - \int_{\Gamma_u}p_i u_i^*d\Gamma + \int_{\Gamma_u}\bar{u}_i p_i^*d\Gamma + \int_{\Gamma_p}u_i p_i^*d\Gamma \quad \cdots\cdots(7\text{-}9)$$

and using $\Gamma = \Gamma_u + \Gamma_p$ for the right-hand side integrals

$$\int_\Omega \sigma_{ij,j}{}^* u_i \, d\Omega + \int_\Omega f_i u_i{}^* d\Omega = -\int_\Gamma p_i u_i{}^* d\Gamma + \int_\Gamma u_i p_i{}^* d\Gamma \qquad \cdots\cdots (7\text{-}10)$$

The fundamental solution for the two-dimensional elasticity problem, i.e., the solution corresponding to the equation

$$\sigma_{ij,j}{}^*(\xi,\eta) + \delta_\ell(\xi,\eta) = 0 \qquad \cdots\cdots\cdots\cdots (7\text{-}11)$$

where $\delta_\ell(\xi,\eta)$ is the Dirac delta function and represents a unit load at ξ acting in the x_ℓ direction, η is the field point.

The Dirac delta function has the following properties:

$$\delta(\xi,\eta) = 0 \qquad \text{if } \xi \neq \eta$$

$$\delta(\xi,\eta) = \infty \qquad \text{if } \xi = \eta$$

$$\int g(\eta)\delta(\xi,\eta)d\Omega = g(\xi) \qquad \cdots\cdots\cdots\cdots (7\text{-}12)$$

Substituting Eq.(7-11) into Eq.(7-10) and taking into consideration Eq.(7-12), one can obtained

$$u_\ell(\xi) + \int_\Gamma u_k p_k{}^*(\xi,\eta)d\Gamma$$

$$= \int_\Gamma p_k u_k{}^*(\xi,\eta)d\Gamma + \int_\Omega f_k u_k{}^*(\xi,\eta)d\Omega \qquad \cdots\cdots\cdots\cdots (7\text{-}13)$$

where $u_\ell(\xi)$ represents the displacement at ξ in the x_ℓ direction, $u_k{}^*(\xi,\eta)$ and $p_k{}^*(\xi,\eta)$ are the displacement and traction at η respectively due to a unit forces acting at point ξ. If we consider unit forces acting at ξ in the two directions, Eq.(7-13) can then written

$$u_\ell(\xi) + \int_\Gamma u_k p_{\ell k}{}^*(\xi,\eta)d\Gamma$$

$$= \int_\Gamma p_k u_{\ell k}{}^*(\xi,\eta)d\Gamma + \int_\Omega f_k u_{\ell k}{}^*(\xi,\eta)d\Omega \qquad \cdots\cdots\cdots\cdots(7\text{-}14)$$

where $p_{\ell k}{}^*$ and $u_{\ell k}{}^*$ represent the tractions and displacements in the k direction due to unit forces acting in the direction ℓ. Eq.(7-14) relates the displacements at any point inside the domain and the displacements and surface forces on the boundary.

For plane strain problem the fundamental solutions are given by [4,6]

$$u_{\ell k}{}^*(\xi,\eta) = \frac{1}{8\pi G(1-\nu)}\{(3-4\nu)\ln\frac{1}{r}\delta_{\ell k} + \frac{r,_\ell\ r,_k}{r^2}\}$$

$$p_{\ell k}{}^*(\xi,\eta) = \frac{-1}{4\pi(1-\nu)r}[\frac{\partial r}{\partial n}\{(1-2\nu)\delta_{ij} + \frac{2r,_\ell\ r,_k}{r^2}\}$$

$$-(1-2\nu)(r,_\ell\ n,_k - r,_k\ n,_\ell)] \qquad \cdots\cdots\cdots\cdots(7\text{-}15)$$

where r is the distance between the points ξ and η as shown in Fig.7-2, $r,_i$ are the projections of the vector $\mathbf{r}$ on the axis x_i, n is the normal to the surface of the body. In order to obtain a boundary integral equation, we need to take the point ξ to the boundary. Considering the singularities existing in the left hand side integral, we obtained the following boundary integral equations:

$$c_{\ell k} u_k(\xi) + \int_\Gamma u_k p_{\ell k}{}^*(\xi,\eta)d\Gamma$$

$$= \int_\Gamma p_k u_{\ell k}^*(\xi,\eta)d\Gamma + \int_\Omega f_k u_{\ell k}^*(\xi,\eta)d\Omega \qquad \cdots\cdots(7\text{-}16)$$

For a smooth boundary the c_i coefficient is equal to $\delta_{\ell k}/2$.

3) Matrix Formulation of Boundary Integral Equation

Eq.(7-16) can be expressed in matrix form as follows:

$$\mathbf{c}\ \mathbf{u} + \int_\Gamma \mathbf{p}^*\mathbf{u}d\Gamma = \int_\Gamma \mathbf{u}^*\mathbf{p}d\Gamma + \int_\Omega \mathbf{f}\mathbf{u}^*d\Omega \qquad \cdots\cdots(7\text{-}17)$$

where

$$\mathbf{u} = \begin{Bmatrix} u_1 \\ u_2 \end{Bmatrix},\quad \mathbf{p} = \begin{Bmatrix} p_1 \\ p_2 \end{Bmatrix},\quad \mathbf{f} = \begin{Bmatrix} f_1 \\ f_2 \end{Bmatrix},$$

$$\mathbf{u}^* = \begin{bmatrix} u_{11}^* & u_{12}^* \\ u_{21}^* & u_{22}^* \end{bmatrix},\qquad \mathbf{p}^* = \begin{bmatrix} p_{11}^* & p_{12}^* \\ p_{21}^* & p_{22}^* \end{bmatrix} \qquad \cdots\cdots(7\text{-}18)$$

The boundary is now divided into elements. These can be constant, linear, quadratic, or higher order element.

Dividing the boundary into elements as shown in Fig.7-3, we can obtain the equation for the point i from Eq.(7-17) as follows:

$$\mathbf{c}_i\mathbf{u}_i + \sum_{j=1}^{m}\left(\int_{\Gamma_j}\mathbf{p}^*\Phi^T d\Gamma\right)\mathbf{u}_j = \sum_{j=1}^{m}\left(\int_{\Gamma_j}\mathbf{u}^*\Phi^T d\Gamma\right)\mathbf{p}_j + \sum_{j=1}^{n}\int_{\Omega_j}\mathbf{f}\mathbf{u}^*d\Omega \qquad \cdots\cdots(7\text{-}19)$$

or

$$\mathbf{c}_i\mathbf{u}_\ell + \sum_{j=1}^{m}\mathbf{h}_j\mathbf{u}_j = \sum_{j=1}^{m}\mathbf{g}_j\mathbf{p}_j + \mathbf{b}_i \qquad \cdots\cdots(7\text{-}20)$$

where the summation from j = 1 to m indicates summation over the m elements on the boundary, Γ_j is the boundary of the j element, and summation from j = 1 to n indicates summation over the internal cells, Ω_j is the surface of each of them. Φ is interpolation function.

Eq.(7-20) is a set of equations for node i which can be written as,

$$\mathbf{c}_i \mathbf{u}_i + (\bar{\mathbf{h}}_{i1} \quad \bar{\mathbf{h}}_{i2} \cdots \bar{\mathbf{h}}_{ij} \cdots \bar{\mathbf{h}}_{im}) \begin{Bmatrix} \mathbf{u}_1 \\ \mathbf{u}_2 \\ \vdots \\ \mathbf{u}_j \\ \vdots \\ \mathbf{u}_m \end{Bmatrix}$$

$$= (\mathbf{g}_{i1} \quad \mathbf{g}_{i2} \cdots \mathbf{g}_{ij} \cdots \mathbf{g}_{im}) \begin{Bmatrix} \mathbf{p}_1 \\ \mathbf{p}_2 \\ \vdots \\ \mathbf{p}_j \\ \vdots \\ \mathbf{p}_m \end{Bmatrix} + \mathbf{b}_i \qquad \cdots\cdots\cdots\cdots (7\text{-}21)$$

where $\mathbf{u}_j$ and $\mathbf{p}_j$ are the unknowns at nodes j, $\bar{\mathbf{h}}_{ij}$ and $\mathbf{g}_{ij}$ are the interaction coefficients relating node i with all the nodes on the boundary. We can write a matrix equation such as Eq.(7-21) for each of the nodes under consideration. Writing them together we have,

$$\begin{bmatrix} \mathbf{h}_{11} & \mathbf{h}_{12} \cdots & \mathbf{h}_{1j} \cdots & \mathbf{h}_{1m} \\ \mathbf{h}_{21} & \mathbf{h}_{22} \cdots & \mathbf{h}_{2j} \cdots & \mathbf{h}_{2m} \\ \vdots & \vdots & \vdots & \vdots \\ \mathbf{h}_{j1} & \mathbf{h}_{j2} \cdots & \mathbf{h}_{ij} \cdots & \mathbf{h}_{jm} \\ \vdots & \vdots & \vdots & \vdots \\ \mathbf{h}_{m1} & \mathbf{h}_{m2} \cdots & \mathbf{h}_{mj} \cdots & \mathbf{h}_{mm} \end{bmatrix} \begin{Bmatrix} \mathbf{u}_1 \\ \mathbf{u}_2 \\ \vdots \\ \mathbf{u}_j \\ \vdots \\ \mathbf{h}_m \end{Bmatrix}$$

$$
= \begin{bmatrix} \mathbf{g}_{11} & \mathbf{g}_{12}\cdots\mathbf{g}_{1j}\cdots\mathbf{g}_{1m} \\ \mathbf{g}_{21} & \mathbf{g}_{22}\cdots\mathbf{g}_{2j}\cdots\mathbf{g}_{2m} \\ \vdots & \vdots \\ \mathbf{g}_{j1} & \mathbf{g}_{j2}\cdots\mathbf{g}_{ij}\cdots\mathbf{g}_{jm} \\ \vdots & \vdots \\ \mathbf{g}_{m1} & \mathbf{g}_{m2}\cdots\mathbf{g}_{mj}\cdots\mathbf{g}_{mm} \end{bmatrix} \begin{Bmatrix} \mathbf{p}_1 \\ \mathbf{p}_2 \\ \vdots \\ \mathbf{p}_j \\ \vdots \\ \mathbf{p}_m \end{Bmatrix} + \begin{Bmatrix} \mathbf{b}_1 \\ \mathbf{b}_2 \\ \vdots \\ \mathbf{b}_j \\ \vdots \\ \mathbf{b}_m \end{Bmatrix} \qquad \cdots\cdots\cdots\cdots (7\text{-}22)
$$

or

$$
\mathbf{H}_p \mathbf{u}_p = \mathbf{G}_p \mathbf{q}_p + \mathbf{b}_p \qquad \cdots\cdots\cdots\cdots (7\text{-}23)
$$

where the submatrices $\mathbf{h}_{ij}$ on the diagonal are,

$$
\mathbf{h}_{ij} = \bar{\mathbf{h}}_{ij} + \mathbf{c}_i
$$

7-3 BOUNDARY INTEGRAL EQUATION FOR PLATE BENDING PROBLEMS

1) Governing Equation for Plate Bending Problems

We introduce the rectangular cartesian coordinate system O-xyz in which the axis x and y lie in the middle plane of the plate as shown in Fig.7-4. The inner domain and the boundary are denoted by Ω and Γ, respectively, and the thickness of the plate is denoted by h. the applied forces are per unit area inside the plate and per unit of length along Γ. The positive direction for moments and transverse shear forces is given in Fig.7-5.

From the Krichhoff-Love's Assumptions for plate bending problems, the moments and transverse shear forces can be written in terms of lateral deflection w as follows (17):

$$
M_{xx} = -D\left(\frac{\partial^2 w}{\partial x^2} + \nu\frac{\partial^2 w}{\partial y^2}\right), \qquad M_{yy} = -D\left(\frac{\partial^2 w}{\partial y^2} + \nu\frac{\partial^2 w}{\partial x^2}\right)
$$

$$
M_{xy} = M_{yx} = -D(1-\nu)\frac{\partial^2 w}{\partial x \partial y}, \qquad q_x = -D\frac{\partial}{\partial x}\left(\frac{\partial^2 w}{\partial x^2} + \nu\frac{\partial^2 w}{\partial y^2}\right)
$$

$$q_y = -D\frac{\partial}{\partial y}\left(\frac{\partial^2 w}{\partial x^2} + \nu\frac{\partial^2 w}{\partial y^2}\right) \qquad \cdots\cdots\cdots\cdots(7\text{-}24)$$

where $D = Eh^3/(1-\nu^2)$ is the bending rigidity of the plate, E and ν are the modulus of elasticity and the Poisson's ratio.

Using the notation described in Fig.7-6(a), the bending moment M_n and the twisting moment M_s on the boundary can be written as

$$\begin{aligned} M_n &= M_{xx}(n_x)^2 + M_{xy}(2n_x n_y) + M_{yy}(n_y)^2 \\ M_s &= -(M_{xx}-M_{yy})n_x n_y + M_{xy}(n_x{}^2-n_y{}^2) \end{aligned} \qquad \cdots\cdots\cdots\cdots(7\text{-}25)$$

where n_x and n_y are the cosines of the normal n with to the x and y axes, respectively.

Using the moments and transverse shear forces the equilibrium equations are given as follows:

$$\begin{aligned} &\frac{\partial Q_x}{\partial x} + \frac{\partial Q_y}{\partial y} + q = 0 \\ &\frac{\partial M_{xx}}{\partial x} + \frac{\partial M_{xy}}{\partial y} = Q_x \\ &\frac{\partial M_{yy}}{\partial y} + \frac{\partial M_{xy}}{\partial x} = Q_y \end{aligned} \qquad \cdots\cdots\cdots\cdots(7\text{-}26)$$

where q is the transverse load per unit area.

Substituting last two equations of Eq.(7-26) into first of Eq.(7-26), we can eliminate the shearing forces from Eq.(7-26) as follows:

$$\frac{\partial^2 M_{xx}}{\partial x^2} + 2\frac{\partial^2 M_{xy}}{\partial x\partial y} + \frac{\partial^2 M_{yy}}{\partial y^2} + q = 0 \qquad \cdots\cdots\cdots\cdots(7\text{-}27)$$

Let Γ_u denote the portion of the boundary on which displacements are prescribed and Γ_p the portion on which surface forces are prescribed, the boundary conditions are then represented as follows:

$$\text{(i)} \quad w = \bar{w}, \quad \beta_n = \bar{\beta}_n, \quad \beta_s = \bar{\beta}_s \qquad \text{on} \quad \Gamma_u$$

$$\text{(ii)} \quad Q = \bar{Q}, \quad M_n = \bar{M}_n, \quad M_s = \bar{M}_s \qquad \text{on} \quad \Gamma_p \qquad \cdots\cdots(7\text{-}28)$$

where upper bar indicates the prescribed quantities, β_n and β_s are the rotation components normal and tangential to the boundary, i.e., $\beta_n = -\partial w/\partial n$ and $\beta_s = -\partial w/\partial s$.

2) Integral Equation for Plate Bending Problems

Taking into consideration the equilibrium equation (7-27) and the boundary conditions (7-28), the weighted residual statement can be written as

$$\int_{\Omega} \left\{ \frac{\partial^2 M_{xx}}{\partial x^2} + 2\frac{\partial^2 M_{xy}}{\partial x \partial y} + \frac{\partial^2 M_{yy}}{\partial y^2} + q \right\} w^* d\Omega$$

$$= \int_{\Gamma_p} \{ (M_n - \bar{M}_n)\beta_n^* + (M_s - \bar{M}_s)\beta_s^* + (Q - \bar{Q}) w^* \} d\Gamma$$

$$- \int_{\Gamma_u} \{ (\beta_n - \bar{\beta}_n) M_n^* + (\beta_s - \bar{\beta}_s) M_s^* + (w - \bar{w}) Q^* \} d\Gamma \qquad \cdots\cdots\cdots\cdots(7\text{-}29)$$

where the superscript indicates the quantities corresponding to the weighting field.

Integrating this equation by parts twice, we obtain

$$-\int_{\Omega}\{M_{xx}\frac{\partial^2 w^*}{\partial x^2}+2M_{xy}\frac{\partial^2 w^*}{\partial x\partial y}+M_{yy}\frac{\partial^2 w^*}{\partial y^2}\}d\Omega - \int_{\Omega}qw^*d\Omega$$

$$= \int_{\Gamma_u}\{M_n\beta_n+M_s\beta_s+Qw\}d\Gamma + \int_{\Gamma_p}\{\overline{M}_n\beta_n{}^*+\overline{M}_s\beta_s{}^*+\overline{Q}w^*\}d\Gamma$$

$$+ \int_{\Gamma_u}\{(\beta_n-\overline{\beta}_n)M_n{}^*+(\beta_s-\overline{\beta}_s)M_s{}^*+(w-\overline{w})Q^*\}d\Gamma \qquad \cdots\cdots\cdots\cdots(7\text{-}30)$$

Using Eq.(7-24) and integrating by parts twice again, we obtain

$$\int_{\Omega}\{\frac{\partial^2 M_{xx}{}^*}{\partial x^2}+2\frac{\partial^2 M_{xy}{}^*}{\partial x\partial y}+\frac{\partial^2 M_{yy}{}^*}{\partial y^2}\}wd\Omega + \int_{\Omega}qw^*d\Omega$$

$$= -\int_{\Gamma_u}\{M_n\beta_n{}^*+M_s\beta_s{}^*+Qw^*\}d\Gamma - \int_{\Gamma_p}\{\overline{M}_n\beta_n{}^*+\overline{M}_s\beta_s{}^*+\overline{Q}w^*\}d\Gamma$$

$$+ \int_{\Gamma_u}\{M_n{}^*\overline{\beta}_n+M_s{}^*\overline{\beta}_s+Q^*\overline{w}\}d\Gamma + \int_{\Gamma_p}\{M_n{}^*\beta_n+M_s{}^*\beta_s+Q^*w\}d\Gamma \qquad \cdots\cdots(7\text{-}31)$$

and $\Gamma = \Gamma_u + \Gamma_p$ for the right side integrals

$$\int_{\Omega}\{\frac{\partial^2 M_{xx}{}^*}{\partial x^2}+2\frac{\partial^2 M_{xy}{}^*}{\partial x\partial y}+\frac{\partial^2 M_{yy}{}^*}{\partial y^2}\}wd\Omega + \int_{\Omega}qw^*d\Omega$$

$$= -\int_{\Gamma}\{M_n\beta_n{}^*+M_s\beta_s{}^*+Qw^*\}d\Gamma + \int_{\Gamma}\{M_n{}^*\beta_n+M_s{}^*\beta_s+Q^*w\}d\Gamma \qquad \cdots\cdots(7\text{-}32)$$

Introducing the effective vertical shear force

$$V = Q + \frac{\partial M_s}{\partial s} \qquad \cdots\cdots\cdots\cdots(7\text{-}33)$$

and considering Eq.(7-24), Eq.(7-32) can be written for smooth boundary as follows:

$$\int_{\Omega}\{D(\frac{\partial^4 w^*}{\partial x^4}+2\frac{\partial^4 w^*}{\partial x^2\partial y^2}+\frac{\partial^4 w}{\partial y^4})wd\Omega + \int_{\Omega} qw^* d\Omega$$

$$= -\int_{\Gamma}(M_n\beta_n{}^*+Vw^*)d\Gamma + \int_{\Gamma}(M_n{}^*\beta_n+V^*w)d\Gamma \qquad \cdots\cdots\cdots\cdots(7\text{-}34)$$

The fundamental solution for the plate bending problem, i.e., the solution corresponding to the equation

$$\frac{\partial^4 w^*}{\partial x^4} + 2\frac{\partial^4 w}{\partial x^2\partial y^2} + \frac{\partial^4 w}{\partial y^4} + \frac{\delta(\xi,\eta)}{D} = 0 \qquad \cdots\cdots\cdots\cdots(7\text{-}35)$$

where $\delta(\xi,\eta)$ is the Dirac delta function and represents a unit point load (Fig.7-6(b)).

The fundamental solution corresponding to Eq.(7-35) is given for the displacement as (6, 15)

$$w^*(\xi,\eta) = \frac{1}{8\pi D}r^2 \ln r \qquad \cdots\cdots\cdots\cdots(7\text{-}36)$$

where r is the distance between the points ξ and η as shown in Fig.7-6(b).

Differentiating Eq.(7-36) and using the notations described in Fig.7-6(b), one can obtain the rotations, moments, and shear forces corresponding to the fundamental solution as follows (6, 15):

$$\beta_n{}^* = \frac{1}{8\pi D}(1+2\ln r)r\cos\beta$$

$$M_n{}^* = -\frac{1-\nu}{4\pi}(1+\ln r) - \frac{1-\nu}{8\pi}\cos 2\beta$$

$$V^* = -\frac{\cos\beta}{4\pi r}\{2+(1-\nu)\cos 2\beta\} + \frac{1-\nu}{4\pi R}\cos 2\beta \qquad \cdots\cdots\cdots(7\text{-}37)$$

where R is the radius of curvature at a regular boundary point.

Substituting Eq.(7-36) into Eq.(7-32) and taking into consideration the properties of the Dirac delta function, one can obtained

$$w(\xi) + \int_\Gamma \{M_n{}^*\beta_n + V^* w\}d\Gamma = \int_\Gamma \{M_n \beta_n{}^* + Vw^*\}d\Gamma + \int_\Omega q w^* d\Omega \qquad \cdots\cdot(7\text{-}38)$$

Eq.(7-38) is the integral equation relating the deflection at the any point inside the domain $w(\xi)$ and the deflection w, effective shear force V, rotation β_n, and moment M_n on the boundary.

In order to obtain a boundary integral equation, we need to take the point ξ to the boundary. Considering the singularities of the fundamental solutions, we obtain the following boundary integral equation:

$$cw(\xi) + \int_\Gamma \{M_n{}^*\beta_n + V^* w\}d\Gamma = \int_\Gamma \{M_n \beta_n{}^* + Vw^*\}d\Gamma + \int_\Omega q w^* d\Omega \qquad \cdots\cdot(7\text{-}39)$$

We have two unknowns on the boundary, i.e., deflection or effective shear force, and rotation or moment. Hence we need another equation to solve the problem. This equation is given by differentiation of Eq.(7-39) with respect to the normal,

$$c\theta(\xi) + \int_\Gamma \left(\frac{\partial M^*}{\partial n}\beta_n + \frac{\partial V^*}{\partial n}w\right)d\Gamma$$

$$= \int_\Gamma \left(M_n \frac{\partial \beta_n{}^*}{\partial n} + V\frac{\partial w^*}{\partial n}\right)d\Gamma + \int_\Omega q\frac{\partial w^*}{\partial n}d\Omega \qquad \cdots\cdots\cdots(7\text{-}40)$$

Using the notations described in Fig.7-6(b), the fundamental solutions for Eq.(7-40) are given as follows (6, 15):

$$\frac{\partial w^*}{\partial n} = \frac{1}{2\pi D} r \ln r \cos\phi$$

$$\frac{\partial \beta_n^*}{\partial n} = \frac{1}{2\pi D} \{\cos\phi \cos\beta + \ln r \cos(\phi+\beta)\}$$

$$\frac{\partial M_n^*}{\partial n} = -\frac{1+\nu}{2\pi} \frac{\cos\phi}{r} + \frac{1-\nu}{2\pi} \frac{\sin\phi}{r} \sin 2\beta$$

$$\frac{\partial V^*}{\partial n} = \frac{1}{2\pi r^2} [\cos(\beta-\phi)\{2+(1-\nu)\cos 2\beta\}$$

$$+ 2(1-\nu)\sin\phi \cos\beta \sin 2\beta] - \frac{1-\nu}{\pi R r} \sin\phi \cos 2\beta \quad \cdots\cdots(7\text{-}41)$$

Eqs.(7-39) and (7-40) are the boundary integral equations for plate bending problem.

Proceeding in the similar manner as that in two-dimensional problem, we finally obtain a matrix equation as follows:

$$\mathbf{H}_b \mathbf{u}_b = \mathbf{G}_b \mathbf{q}_b + \mathbf{b}_b \quad \cdots\cdots\cdots\cdots(7\text{-}42)$$

7-4 BOUNDARY ELEMENT-TRANSFER MATRIX METHOD

1) Derivation of Transfer Matrix

As shown in Fig.7-7, a plate is considered as a combination of a number of separate subregions D_k $(k=1,2,\cdots m)$. For each of them the system of equations can be written as

$$\mathbf{H}_k \mathbf{u}_k = \mathbf{G}_k \mathbf{q}_k + \mathbf{b}_k \quad \cdots\cdots\cdots\cdots(7\text{-}43)$$

Eq.(7-43) is transformed by inverting $\mathbf{G}_k$, i.e.

$$\mathbf{q}_k = \mathbf{G}_k^{-1}\mathbf{H}_k\mathbf{u}_k - \mathbf{G}_k^{-1}\mathbf{b}_k \qquad \cdots\cdots\cdots\cdots(7\text{-}44)$$

or

$$\mathbf{q}_k = \mathbf{K}_k\mathbf{u}_k - \mathbf{f}_k \qquad \cdots\cdots\cdots\cdots(7\text{-}45)$$

Eq.(7-45) is similar in form to the finite element equation.

Matrix $\mathbf{K}_k$ is partitioned into nine submatrices. Eq.(7-45) then becomes:

$$\begin{Bmatrix}\mathbf{q}_\ell\\ \mathbf{q}_e\\ \mathbf{q}_r\end{Bmatrix}_k = \begin{bmatrix}\mathbf{K}_{\ell\ell} & \mathbf{K}_{\ell e} & \mathbf{K}_{\ell r}\\ \mathbf{K}_{e\ell} & \mathbf{K}_{ee} & \mathbf{K}_{er}\\ \mathbf{K}_{r\ell} & \mathbf{K}_{re} & \mathbf{K}_{rr}\end{bmatrix}_k \begin{Bmatrix}\mathbf{u}_\ell\\ \mathbf{u}_e\\ \mathbf{u}_r\end{Bmatrix}_k - \begin{Bmatrix}\mathbf{f}_\ell\\ \mathbf{f}_e\\ \mathbf{f}_r\end{Bmatrix}_k \qquad \cdots\cdots\cdots\cdots(7\text{-}46)$$

where the subscripts ℓ and r denote the left and right interfaces, respectively, and e denotes the external boundary.

Solving for the $\mathbf{u}_{e\,k}$ and substituting in the remaining equations, the following expressions are obtained:

$$\begin{Bmatrix}\mathbf{q}_\ell\\ \mathbf{q}_r\end{Bmatrix}_k = \begin{bmatrix}\mathbf{K}_{\ell\ell}-\mathbf{K}_{\ell e}\mathbf{K}_{ee}^{-1}\mathbf{K}_{e\ell} & \mathbf{K}_{\ell r}-\mathbf{K}_{\ell e}\mathbf{K}_{ee}^{-1}\mathbf{K}_{er}\\ \mathbf{K}_{r\ell}-\mathbf{K}_{re}\mathbf{K}_{ee}^{-1}\mathbf{K}_{e\ell} & \mathbf{K}_{rr}-\mathbf{K}_{re}\mathbf{K}_{ee}^{-1}\mathbf{K}_{er}\end{bmatrix}_k \begin{Bmatrix}\mathbf{u}_\ell\\ \mathbf{u}_r\end{Bmatrix}_k$$

$$+\begin{Bmatrix}\mathbf{K}_{\ell e}\mathbf{K}_{ee}^{-1}(\mathbf{q}_e+\mathbf{f}_e)-\mathbf{f}_\ell\\ \mathbf{K}_{re}\mathbf{K}_{ee}^{-1}(\mathbf{q}_e+\mathbf{f}_e)-\mathbf{f}_r\end{Bmatrix} \qquad \cdots\cdots\cdots\cdots(7\text{-}47)$$

$$\begin{Bmatrix}\mathbf{q}_\ell\\ \mathbf{q}_r\end{Bmatrix}_k = \begin{bmatrix}\mathbf{K}_{11} & \mathbf{K}_{12}\\ \mathbf{K}_{21} & \mathbf{K}_{22}\end{bmatrix}_k \begin{Bmatrix}\mathbf{u}_\ell\\ \mathbf{u}_r\end{Bmatrix}_k + \begin{Bmatrix}\mathbf{q}_1\\ \mathbf{q}_2\end{Bmatrix}_k \qquad \cdots\cdots\cdots\cdots(7\text{-}48)$$

By expanding and rearranging Eq.(7-48), it can be shown after a little algebraic manipulations that left and right interfaces can be related by the following expression:

$$\begin{Bmatrix}\mathbf{u}_r\\ \mathbf{q}_r\end{Bmatrix}_k = \begin{bmatrix}-\mathbf{K}_{12}^{-1}\mathbf{K}_{11} & \mathbf{K}_{12}^{-1}\\ \mathbf{K}_{21}-\mathbf{K}_{22}\mathbf{K}_{12}^{-1}\mathbf{K}_{11} & \mathbf{K}_{22}\mathbf{K}_{12}^{-1}\end{bmatrix}_k \begin{Bmatrix}\mathbf{u}_\ell\\ \mathbf{q}_\ell\end{Bmatrix}_k$$

$$+\begin{Bmatrix} -\mathbf{K}_{12}^{-1}\mathbf{q}_1 \\ \mathbf{q}_2-\mathbf{K}_{22}\mathbf{K}_{12}^{-1}\mathbf{q}_1 \end{Bmatrix}_k \qquad \cdots\cdots\cdots\cdots(7\text{-}49)$$

On simplifying the notation, we obtain

$$\begin{Bmatrix} \mathbf{u}_r \\ \mathbf{q}_r \end{Bmatrix}_k = \begin{bmatrix} \mathbf{T}_{11} & \mathbf{T}_{12} \\ \mathbf{T}_{21} & \mathbf{T}_{22} \end{bmatrix}_k \begin{Bmatrix} \mathbf{u}_\ell \\ \mathbf{q}_\ell \end{Bmatrix}_k + \begin{Bmatrix} \mathbf{T}_{F1} \\ \mathbf{T}_{F2} \end{Bmatrix}_k \qquad \cdots\cdots\cdots\cdots(7\text{-}50)$$

Adding one dummy equation to the system, the following equation can be obtained:

$$\begin{Bmatrix} \mathbf{u}_r \\ \mathbf{q}_r \\ 1 \end{Bmatrix}_k = \begin{bmatrix} \mathbf{T}_{11} & \mathbf{T}_{12} & \mathbf{T}_{F1} \\ \mathbf{T}_{21} & \mathbf{T}_{22} & \mathbf{T}_{F2} \\ \mathbf{0} & \mathbf{0} & 1 \end{bmatrix}_k \begin{Bmatrix} \mathbf{u}_\ell \\ \mathbf{q}_\ell \\ 1 \end{Bmatrix}_k \qquad \cdots\cdots\cdots\cdots(7\text{-}51)$$

or

$$\mathbf{z}_{r\,k}=\mathbf{T}_k\,\mathbf{z}_{\ell\,k} \qquad \cdots\cdots\cdots\cdots(7\text{-}52)$$

in which $\mathbf{z}_{r\,k}$, $\mathbf{z}_{\ell k}$ are so called state vectors which consist of the displacements and tractions at the interfaces of region $\mathbf{D}_k$. Eq.(7-52) can be recognized as the transfer matrix relating the state vectors of the left and right interfaces.

By applying the interface equilibrium and compatibility conditions, Eq.(7-52) can be rewritten as

$$\mathbf{z}_k = \mathbf{T}_k\,\mathbf{z}_{k-1} \qquad \cdots\cdots\cdots\cdots(7\text{-}53)$$

in which $\mathbf{z}_{k-1}$ and $\mathbf{z}_k$ are the right interface state vectors of region $\mathbf{D}_{k-1}$ and $\mathbf{D}_k$, respectively.

Once the transfer matrix has been formulated for each subregion, the displacements and tractions at the interfaces are determined by the same procedures as those used in the standard transfer matrix method (14).

Applying Eq.(7-53) to the continuous two regions $\mathbf{D}_k$, $\mathbf{D}_{k+1}$, and eliminating the state vector $\mathbf{z}_k$, we obtain the relation between the state vectors $\mathbf{z}_{k-1}$ and $\mathbf{z}_{k+1}$:

$$\mathbf{z}_{k+1} = \mathbf{T}_{k+1}\mathbf{T}_k\mathbf{z}_{k-1} \qquad \cdots\cdots\cdots\cdots (7\text{-}54)$$

Proceeding in the same manner over all the m regions, the following relation is obtained:

$$\mathbf{z}_m = \mathbf{U}_m\mathbf{z}_0 \qquad \cdots\cdots\cdots\cdots (7\text{-}55)$$

in which $\mathbf{U}_m = \mathbf{T}_m\mathbf{T}_{m-1}\cdots\mathbf{T}_1$.

It should be noted that by multiplying the transfer matrices $\mathbf{T}_k$, the order of matrix $\mathbf{U}$ does not increase but remains compatible with the matrices being multiplied. These are results in a reduced size matrix which embodies the entire system.

Once the system has been assembled as expressed by Eq.(7-55), the boundary conditions have to be satisfied by solving for the unknown terms in the initial state vector $\mathbf{z}_0$. After the initial state vectors are known the state vectors at the interface can be obtained by recursively applying Eq.(7-53) until all the state vectors at the interfaces are known. The stresses and displacements at any point within a region can be obtained in the same manner as that used in the subregions technique.

The derivation of the transfer matrix for a subregion, however, requires the inversions of matrix $\mathbf{G}_k$ in Eq.(7-44), sub-matrix $\mathbf{K}_{ee}$ in Eq.(7-47) and $\mathbf{K}_{12}$ in Eq.(7-49). These inversions are sources of some numerical errors. However, these inversions are done only once for each subregion and are not affected by the load vector. This is an advantage, especially if all the subregions have the same configuration.

It may be noted that in the subregions technique the matrix in Eq.7-73 is banded and it does not require full storage in the computer memory. It is the assembly of the various subregions that makes storage requirements increase, since the order of the global matrices increases too. On the other hand, in the proposed method the transfer matrix T_k is fully populated and requires full storage in the computer memory, but the global transfer matrix U does not increase in size, since it results from consecutive matrix multiplications as indicated by Eq.(7-55).

2) Exchange of the State Vectors

It is pointed out that, in the standard transfer matrix method, recursive multiplications of the transfer matrix are source of round off errors, and this is also true in the proposed method. In order to minimize these errors we introduce the technique described follows for the plates with many subregions. The equation relating the state vector at the section i and the initial unknown state vector may be written as follows:

$$\begin{Bmatrix} \mathbf{u} \\ \mathbf{q} \\ 1 \end{Bmatrix}_i = \begin{bmatrix} \mathrm{U}_u & \mathbf{f}_u \\ \mathrm{U}_q & \mathbf{f}_q \\ 0 & 1 \end{bmatrix}_i \begin{Bmatrix} \mathbf{z} \\ 1 \end{Bmatrix}_0 \qquad \cdots\cdots\cdots\cdots (7\text{-}56)$$

Solving for $\mathbf{z}_0$ in term of $\mathbf{u}_i$, the following expression can be obtained:

$$\mathbf{z}_0 = \mathrm{U}_u^{-1}\mathbf{u}_i - \mathrm{U}_u^{-1}\mathbf{f}_u \qquad \cdots\cdots\cdots\cdots (7\text{-}57)$$

Substituting in the remaining equation of Eq.(7-56), we obtain:

$$\mathbf{q}_i = \mathrm{U}_p \mathrm{U}_u^{-1}\mathbf{u}_i - \mathrm{U}_q \mathrm{U}_u^{-1}\mathbf{f}_u + \mathbf{f}_q \qquad \cdots\cdots\cdots\cdots (7\text{-}58)$$

Eq.(7-58) and the identity $\mathbf{u}_i = \mathbf{u}_i$ yield the alternative expression of Eq.(7-56):

$$\begin{Bmatrix} \mathbf{u} \\ \mathbf{q} \\ 1 \end{Bmatrix}_i = \begin{bmatrix} \mathbf{I} & \mathbf{0} \\ \mathbf{U}_q \mathbf{U}_u^{-1} & -\mathbf{U}_q \mathbf{U}_u^{-1} \mathbf{f}_u + \mathbf{f}_q \\ \mathbf{0} & 1 \end{bmatrix}_i \begin{Bmatrix} \mathbf{u} \\ 1 \end{Bmatrix}_0 \qquad \cdots\cdots\cdots\cdots (7\text{-}59)$$

or

$$\mathbf{z}_i = \mathbf{U}_i' \mathbf{z}_i' \qquad \cdots\cdots\cdots\cdots (7\text{-}60)$$

Hereafter matrix multiplications continue in the usual manner using, however, $\mathbf{z}_i'$ instead of $\mathbf{z}_0$.

3) Rotation Matrix for Axisymmetric Structure

For the axisymmetric structure, such as the thick cylinder shown in Fig.7-8, the transfer matrix must be derived for every strip. To improve the numerical efficiency of this method, we simplify the derivation procedure of the transfer matrix by using the rotation matrix of the coordinate system.

Considering that every strip has the same shape as shown in Fig.7-8, the transfer expression for strip k referred to the local coordinate system are described by using the transfer matrix for strip 1, $\mathbf{T}_1$, as follows:

$$\bar{\mathbf{z}}_{k\ell} = \mathbf{T}_1 \bar{\mathbf{z}}_{kr} \qquad \cdots\cdots\cdots\cdots (7\text{-}61)$$

where upper bar indicates the quantity referred to the local coordinate system. Introducing the rotation matrix, $\mathbf{R}_k$, relating the global coordinate system to the local one for strip k, Eq.(7-61) can be written referred to the global coordinate system as

$$\mathbf{z}_{k\,\ell} = \mathbf{R}_k{}^T \mathbf{T}_1 \mathbf{R}_k \mathbf{z}_{k\,r}$$
$$= \mathbf{T}_k \mathbf{z}_{k\,r} \qquad \cdots\cdots\cdots\cdots (7\text{-}62)$$

where $\mathbf{T}_k$ is the transfer matrix for strip k referred to the global coordinate system and it is assumed here that the global coordinate system coincides with the local one for strip 1. Thus the transfer matrices for every strip can be derived from the transfer matrix for strip 1 by only rotation of coordinate system.

4) Internal Condition

Consider a plate with internal support at section i, as shown in Fig.7-9. The equation relating the left state vector at the section i to the initial unknown state vector may be written as

$$\mathbf{z}_i = \mathbf{U}_i \; \mathbf{z}_0 \qquad \cdots\cdots\cdots\cdots (7\text{-}63)$$

or

$$\begin{Bmatrix} \mathbf{w} \\ \mathbf{z}^* \end{Bmatrix}_i = \begin{bmatrix} \mathbf{U}_A & \mathbf{U}_B \\ \mathbf{U}_C & \mathbf{U}_D \end{bmatrix}_i \begin{Bmatrix} \mathbf{z}_1 \\ \mathbf{z}_2 \end{Bmatrix}_0 \qquad \cdots\cdots\cdots\cdots (7\text{-}64)$$

where $\mathbf{w}_i$ are the displacements at the section i, $\mathbf{z}^*_i$ are the remaining components of the state vector $\mathbf{z}_i$, $\mathbf{z}_{1\,0}$ are the initial unknown state variables corresponding to $\mathbf{w}_i$, and $\mathbf{z}_{2\,0}$ are the remaining components of the initial state vector $\mathbf{z}_0$, From the intermediate support condition ($\mathbf{w}_i = \mathbf{0}$), we can eliminate the state variables $\mathbf{z}_{1\,0}$ from the initial unknown state vector as follows:

$$\begin{Bmatrix} \mathbf{w} \\ \mathbf{z}^* \end{Bmatrix}_i = \begin{bmatrix} \mathbf{0} \\ -\mathbf{U}_C \mathbf{U}_A{}^{-1} \mathbf{U}_B + \mathbf{U}_D \end{bmatrix}_i \mathbf{z}_{2\,0} \qquad \cdots\cdots\cdots\cdots (7\text{-}65)$$

Because of the reactions at the internal support, the shearing forces at this section are discontinuous. The equilibrium of the shearing forces at this section are, then, expressed as follows:

$$V_{iR} = V_{iL} + V_i^* \qquad \cdots\cdots\cdots\cdots (7\text{-}66)$$

where V_i^* are the reactions at the internal support. The equation relating the right state vector at the section i to the initial unknown state vector is, therefore, written as

$$\begin{Bmatrix} w \\ \beta \\ V \\ M \end{Bmatrix}_i = \begin{bmatrix} 0 \\ \hline -U_C \quad U_A^{-1} U_B + U_D \end{bmatrix}_i z_{20} + \begin{Bmatrix} 0 \\ 0 \\ V^* \\ 0 \end{Bmatrix}_i \qquad \cdots\cdots\cdots\cdots (7\text{-}67)$$

Adding one dummy equation to the system, the following equation can be obtained:

$$\begin{Bmatrix} w \\ \beta \\ V \\ M \end{Bmatrix}_i = \left[\begin{array}{c|c} 0 & 0 \\ \hline 0 & \\ I & -U_C U_A^{-1} U_B + U_D \\ 0 & \end{array}\right]_i \begin{Bmatrix} V_i^* \\ z_{20} \end{Bmatrix} \qquad \cdots\cdots\cdots\cdots (7\text{-}68)$$

or

$$z_i = U_i' z_0^* \qquad \cdots\cdots\cdots\cdots (7\text{-}69)$$

By the above technique, the transfer procedure can be performed throughout a section having internal support.

7-5 NUMERICAL EXAMPLES

1) Numerical Examples for In-Plane Problem

In order to investigate the accuracy as well as the capability of the proposed method for solution of two-dimensional problems some numerical examples are presented.

A cantilevered plate subjected at the free edge to a uniformly distributed in-plane load (Fig.7-10(a)), is analyzed for the first example. In the numerical calculation, the plate is divided into 1, 2, 4, 6, 8 and 10 regions, respectively, and each of which is subdivided into 6 (Pattern A) and 10 (Pattern B) constant elements for every discretizing pattern, as shown in Fig.7-10(b).

In Table 7-1, the displacement u at the free edge obtained by the BETM method is compared with those obtained by the boundary element method and subregions technique. In the numerical calculation for 10 regions of Pattern A and 6, 8 and 10 regions of Pattern B, the technique of exchanging state vectors described in this chapter is introduced to avoid the propagation of round-off errors. In the subregions technique the same discretizing patterns as those used in the BETM method are employed, and those for the boundary element method is also shown in Fig.7-10(b).

The results of the BETM method and subregions technique agree precisely, and these also agree well with those obtained by the boundary element method, which demonstrate the accuracy of the proposed method. Comparisons of computation times for the BETM method and other methods in this example are shown in Table 7-2. It becomes clear from Table 7-2 that although, in computation time, the BETM method has less advantage for the small number of regions model (1 and 2 regions of Pattern A; 1, 2, 4 and 6 regions of Pattern B), it has much advantage for the large number of regions model (4, 6, 8 and 10 regions of Pattern A; 8 and 10 regions of Pattern B).

Fig.7-11(a) shows a thick cylinder under internal pressure. The distributions of the displacement in radial direction obtained by the BETM methods with and without rotation matrix are shown in Figs.7-11(b) and 7-11(c). In the numerical calculation, a quarter of the cylinder is divided into 4 and 6 subregions, respectively, and each of which is divided into 10 boundary elements as shown in Figs.7-11(b) and 7-11(c). Close agreement exists in the results by both methods, thus can not be distincted in Figs.7-11(b) and 7-11(c). The results obtained by the boundary and finite element methods are also shown. Mesh patterns used in these methods are indicated in Figs.7-11(b) and 7-11(c), respectively. Although the result of the BETM method is a little smaller than those of other methods, good agreement exists between these sets of results.

Fig.7-12(c) shows the comparisons of the displacement in radial direction at point A, indicated in Fig.7-12(a), obtained by the BETM methods with and without rotation matrix for various mesh patterns (Fig.7-12(b)). In the numerical calculation, a quarter of the cylinder is divided into 4, 6, 8 and 10 subregions, respectively, and each of which is divided into 10 boundary constant elements for every discretizing pattern. Both results coincide completely with each other for every mesh pattern, and agree well with other results, which are also indicated in Fig.7-12(c). Fig.7-12(d) shows the comparisons of the computation time in this example. Computation time in the BETM method with rotation matrix is also 67% smaller compared to that in the BETM without rotation matrix for every mesh pattern.

Fig.7-13(a) shows a foundation supported on a medium in which the Young's modulus increases with depth, thus depicting a very real practical problem. A non-homogeneous medium, in the numerical calculation, is considered to be a combination of three homogeneous subregions as shown in Fig.7-13(a). The vertical and horizontal displacements of the ground along horizontal lines (y = 1.0 and 2.5m) are shown in Figs.7-13(b) and 7-13(c), and compared to the finite element method results. As shown in these figures, good agreement exists between these sets of results.

2) Numerical Examples for Plate Bending Problem

In order to investigate the accuracy as well as the capability of the proposed method for solution of plate bending problems some numerical examples are presented.

A simply supported plate under uniform out-of-plane load, shown in Fig.7-14(a), is analyzed for the first example. In the numerical calculation, the plate is divided into 1, 3 and 5 regions, respectively, each of which is subdivided into 12 constant elements for every discretizing pattern, as shown in Fig.7-14(b).

In Fig.7-14(c) and Table 7-3, the relation between the number of regions and the deflection at the midpoint of the plate obtained by the BETM method is compared with those obtained by the boundary element method and subregions technique. The discretizing pattern for the boundary element method is also shown in Fig.7-14(b). As shown in Table 7-3 complete agreement exists between the results of the BETM and subregion methods, and these results coincide well with other results for every discretizing pattern.

In Fig.7-14(d), the center line configurations obtained by the BETM method for 3 regions pattern are compared with those obtained by the finite element and boundary element methods. As shown in Fig.7-14(d), good agreement exists between the results obtained by the BETM method and other methods.

Figs.7-15(c), 7-15(d) and Table 7-4 show the results for a plate under concentrate load. The same plate and mesh patterns as those employed in the previous example are used here. Similar results to those of previous example are obtained.

A cantilevered plate subjected at the free edge to a line load, shown in Fig.7-16(a), is analyzed. The same discretizing patterns as in the previous example are employed here.

In Fig.7-16(c) and Table 7-5, the relation between the number of regions and the deflection at the midpoint of the free edge obtained by the BETM method is compared with those obtained by other methods.

In Fig.7-16(d), the centerline configurations obtained by the BETM method for 5 regions pattern are compared with those obtained by other methods. As shown in Fig.7-16(d), good agreement exists between the results obtained by the BETM method and other methods.

Figs.7-17(c), 7-17(d) and Table 7-6 show the results for a uniformly loaded cantilevered plate. The same plate and mesh patterns as those employed in the previous example are used here. Similar results to those of previous example are also obtained.

Fig.7-18(c) shows the centerline configurations of a cantilevered plate with variable thickness subjected at the free edge to a line load, shown in Fig.7-18(a). In the numerical calculation, the plate is divided into 8 strips with constant thickness (Fig.7-18(b)), and each of which is subdivided into 12 constant elements. In Fig.7-18(c), the results obtained by the finite element method (5 $\times$ 8 mesh pattern) are also shown. As shown in Fig.7-18(c), good agreement exists between the results obtained by the BETM method and the finite element method.

Fig.7-18(d) shows the comparison of the centerline configurations of a uniformly loaded cantilevered plate with variable thickness obtained by the BETM method and the finite element method. The same plate and mesh patterns as those employed in the previous example are used here. Similar results to those of the previous example are obtained.

Fig.7-19(b) shows the centerline configurations of a simply supported continuous plate with a internal support under uniform load, shown in Fig.7-19(a). In the numerical calculation, the plate is divided into 2 strips, and each of which is subdivided into 12 constant elements as shown in Fig.7-19(b). The technique for internal condition described in this chapter is introduced to overcome the section of internal support. In Fig.7-19(b), the results obtained by the finite element method are also shown. The mesh patterns employed in the finite element method are shown in Fig.7-19(b). As shown in Fig.7-19(b), good agreement exists between the results obtained by the BETM method and the finite element method.

Fig.7-20(b) shows the results for a uniformly loaded clamped continuous plate with a internal support(Fig.7-20(a)). The same mesh pattern as that employed in the previous example is used here. Similar results to those for a simply supported plate are obtained.

Fig.7-21(b) shows the centerline configurations of a simply supported continuous plate with 3 internal supports under uniform load, shown in Fig.7-21(a). In the numerical calculation, the plate is divided into 4 strips, and each of which is subdivided into 12 constant elements as shown in Fig.7-21(b). In Fig.7-21(b), the results obtained by the finite element method are also shown. The mesh patterns employed in the finite element method are indicated in Fig.7-21(b). As shown in Fig.7-21(b), good agreement exists between the results obtained by the BETM method and the finite element method.

Fig.7-22(b) shows the results for a partially loaded, simply supported continuous plate with 3 internal supports (Fig.22(a)). The same mesh pattern as that employed in the previous example is used here. Similar results to those of previous example are obtained.

7-6 CONCLUSIONS

A structural analysis method based on a combined use of boundary element - transfer matrix method is proposed for two-dimensional and plate bending problems. A transfer matrix is derived from the system of equations derived by the procedure based on the boundary element method. The technique of exchanging the state vectors is proposed to avoid the propagation of round-off errors occurred in recursive multiplications of the transfer matrix, and rotation matrix is employed for axisymmetric structures to reduce computational efforts. Furthermore, the technique for the structure with intermediate supports is proposed. From the numerical examples presented in this chapter, following conclusions are obtained:

(1) In the proposed method, the sizes of the matrices involved in the process of solution depend on the number of elements of only one subregion; the use of a large number of elements is therefore permitted without getting involved with large matrices. A much smaller computer is thus sufficient.

(2) In two-dimensional and plate bending problems, the results obtained by the BETM method agree well with those by the boundary element and finite element methods, which demonstrates the accuracy of the proposed method.

(3) The technique of exchanging the state vectors is very efficient to avoid the propagation of round-off errors occurred in many subregions pattern.

(4) By using the technique for intermediate simple support, the BETM method can be applied to continuous plate, and results

obtained by this method are agree well with those by the finite element method.

(5) To employ the rotation matrix for deriving the transfer matrix is efficient for axisymmetric structures in reducing computational efforts.

From the mentions described above, this method can be successfully applied to the long and non-homogeneous systems.

APPENDIX 7-1 SUBREGIONS TECHNIQUE

A piecewise homogeneous solid may be considered as a combination of a number of separate homogeneous regions $\mathbf{D}_k$ (k = 1,...., m), each having different elastic constant (Fig.7-7). For each region $\mathbf{D}_k$ with boundary surface $\mathbf{S}_k$ the resulting system of equations can be written as

$$\mathbf{H}_k \mathbf{u}_k = \mathbf{G}_k \mathbf{q}_k \qquad \cdots\cdots\cdots\cdots(7\text{-}70)$$

in which $\mathbf{u}_k$ and $\mathbf{q}_k$ are the displacements and tractions over the surface of the region $\mathbf{D}_k$; $\mathbf{H}_k$ and $\mathbf{G}_k$ are calculated using the elastic constants of region $\mathbf{D}_k$.

Eq.(7-70) may be rewritten as

$$(\mathbf{H}_\ell \ \ \mathbf{H}_e \ \ \mathbf{H}_r)_k \begin{Bmatrix} \mathbf{u}_\ell \\ \mathbf{u}_e \\ \mathbf{u}_r \end{Bmatrix}_k = (\mathbf{G}_\ell \ \ \mathbf{G}_e \ \ \mathbf{G}_r)_k \begin{Bmatrix} \mathbf{q}_\ell \\ \mathbf{q}_e \\ \mathbf{q}_r \end{Bmatrix}_k \qquad \cdots\cdots\cdots\cdots(7\text{-}71)$$

in which $\mathbf{u}_{\ell k}$ and $\mathbf{q}_{\ell k}$ are the displacements and tractions at the left interface of region $\mathbf{D}_k$, $\mathbf{u}_{rk}$ and $\mathbf{q}_{rk}$ are the displacements and tractions at the right interface, $\mathbf{u}_{ek}$ and $\mathbf{q}_{ek}$ are the displacements and tractions at the external boundary and $\mathbf{H}_{\ell k}$, $\mathbf{H}_{ek}$, $\mathbf{H}_{rk}$, $\mathbf{G}_{\ell k}$, $\mathbf{G}_{ek}$ and $\mathbf{G}_{rk}$ are the submatrices of $\mathbf{H}_k$ and $\mathbf{G}_k$.

Eq.(7-71) can be assembled in a final matrix for all individual surfaces S_1, S_2, ..., S_m. During the assembly process, which is very similar to that used in the finite element method, the unknown displacements and tractions at the common interfaces between the regions are eliminated by applying the interface equilibrium and compatibility conditions, e.g. for all interface elements between region $\mathbf{D}_k$ and $\mathbf{D}_{k+1}$ we have

$$\mathbf{u}_{ik} = \mathbf{u}_{rk} = \mathbf{u}_{\ell(k+1)}, \quad \mathbf{q}_{ik} = \mathbf{q}_{rk} = -\mathbf{q}_{\ell(k+1)} \qquad \cdots\cdots(7\text{-}72)$$

For a body divided into three regions, for instance, the global system of equations can be written as follows:

$$\begin{bmatrix} \mathbf{H}_{e1} & \mathbf{H}_{r1} & & & \\ & \mathbf{H}_{\ell 2} & \mathbf{H}_{e2} & \mathbf{H}_{r2} & \\ & & & \mathbf{H}_{r3} & \mathbf{H}_{e3} \end{bmatrix} \begin{Bmatrix} \mathbf{u}_{e1} \\ \mathbf{u}_{i1} \\ \mathbf{u}_{e2} \\ \mathbf{u}_{i2} \\ \mathbf{u}_{e3} \end{Bmatrix}$$

$$= \begin{bmatrix} \mathbf{G}_{e1} & \mathbf{G}_{r1} & & & \\ & -\mathbf{G}_{\ell 2} & \mathbf{G}_{e2} & \mathbf{G}_{r2} & \\ & & & -\mathbf{G}_{\ell 3} & \mathbf{G}_{e3} \end{bmatrix} \begin{Bmatrix} \mathbf{q}_{e1} \\ \mathbf{q}_{i1} \\ \mathbf{q}_{e2} \\ \mathbf{q}_{i2} \\ \mathbf{q}_{e3} \end{Bmatrix} \qquad \cdots\cdots\cdots\cdots(7\text{-}73)$$

By imposing the boundary conditions of the problem and remembering that both the displacements and tractions at the interface are considered as unknown, the system (7-73) can be reordered as

$$
\begin{bmatrix} H_{e1} & H_{r1} & -G_{r1} & & & & \\ & H_{\ell 2} & G_{\ell 2} & H_{e2} & H_{r2} & -G_{r2} & \\ & & & & H_{\ell 3} & G_{\ell 3} & H_{e3} \end{bmatrix} \begin{Bmatrix} u_{e1} \\ u_{i1} \\ q_{i1} \\ u_{e2} \\ u_{i2} \\ q_{i2} \\ u_{e3} \end{Bmatrix}
$$

$$
= \begin{bmatrix} G_{e1} & & \\ & G_{e2} & \\ & & G_{e3} \end{bmatrix} \begin{Bmatrix} q_{e1} \\ q_{e2} \\ q_{e3} \end{Bmatrix} \qquad \cdots\cdots\cdots\cdots (7\text{-}74)
$$

or

$$
\mathbf{H}\,\mathbf{u} = \mathbf{G}\,\mathbf{q} \qquad \cdots\cdots\cdots\cdots (7\text{-}75)
$$

According to the boundary conditions, the submatrices corresponding to the external boundary may interchange their positions. After Eq.(7-75) has been solved, the stresses and displacements at any point within a region can be obtained using the interior version of Eq.(7-71) for the appropriate domain. This subregions technique is also required for bodies with different dimensions in different directions.

REFERENCES

1. Altiero, N.J. and Sikarskie, D.L., "A Boundary Integral Method Applied to Plates of Arbitrary Plate Form," J. Computers & Structures, Vol.9, 1978, pp.163-168.
2. Banerjee, P.K., "Integral Equation Methods for Analysis of Piece-Wise Non-Homogeneous Three-Dimensional Elastic Solids of Arbitrary Shape," Int. J. Mech. Sci., Vol.18, 1976, pp.293-303.
3. Banerjee, P.K. and Butterfield, R., "Boundary Element Methods in Geomechanics," in Finite Elements in Geomechanics, Wiley, New York, 1977.

4. Brebbia, C.A. and Walker, S., "Boundary Element Techniques in Engineering," Butterworths, London, 1980.
5. Brebbia, C.A., "Boundary Elements-VI," Springer, Berlin, 1984.
6. Brebbia, C.A., Telles, J.C.F. and Wrobel, L.C., "Boundary Element Techniques-Theory and Applications," Springer, Berlin, 1984.
7. Brebbia, C.A. and Maier, G., "Boundary Elements VII," Springer, Berlin, 1985.
8. Jaswon, M.A. and Maiti, M., "An Integral Equation Formulation of Plate Bending Problems," J. Engng Math., Vol.2, 1968, PP.83-93.
9. Lachat, J.C. and Watson, J.O., "Progress in the Use of Boundary Integral Equations, Illustrated by Examples," Comput. Meth. Appl. Mech. Engng, Vol.10, 1977, pp.273-289.
10. Maiti, M. and Chakrabarty, S.K., "Integral Equation Solutions for Simply Supported Polygonal Plates," Int.J. Engn Sci., Vol.12, 1974, pp.793-806.
11. Mucino, H.V. and Pavelic, V., "An Exact Condensation Procedure for Chain-Like Structures Using a Finite Element - Transfer Matrix Approach," Trans. ASME, J. Mech. Des., No.80-C2/DET-123, 1980, pp.1-9.
12. Ohga, M., Shigematsu, T. and Hara, T., "Structural Analysis by a Combined Boundary Element Transfer Matrix Method," Computers & Structures, Vol.24, No.3, 1986, pp.385-389.
13. Ohga, M. and Shigematsu, T., "Bending Analysis of Plates with Variable Thickness by Boundary Element Transfer Matrix Method," Computers & Structures, Vol.28, No.5, 1988, pp.635-640.
14. Pestel, E.C. and Leckie, F.A., "Matrix Method in Elastomechanics," McGraw-Hill, New York, 1963.
15. Stern, M., "A General Boundary Integral Formulation for the Numerical Solution of Plate Bending Problems," Int. J. Solids & Struct., Vol.15, 1979, pp.769-782.
16. Tanaka, M. and Brebbia, C.A., "Boundary Elements VIII," Springer-Verlag, 1986.
17. Timoshenko, S.P. and Woinowsky-Krieger, S., "Theory of Plates and Shells," McGraw-Hill Kogakusha, Tokyo, 1959.
18. Tomlin, G.R. and Butterfield, R., "Elastic Analysis of Zoned Orthotropic Continua," J. ASCE, Vol.100, No.EM3, 1974, pp.511-529.

NOTATION

The following symbols are used in this paper:

$\mathbf{D}$ = flexural rigidity of plate;
E = modulus of elasticity;
f = components of body force;
G = shear elastic modulus;
M_{xx}, M_{yy}, M_{xy} = bending moments;
n = direction cosine;
p = surface force;
$\bar{p}$ = prescribed surface force;
p^* = surface force corresponding to weighting field;
q = transverse load;
Q_x, Q_y = transverse shear forces;
$\mathbf{R}$ = rotation matrix;
$\mathbf{T}$ = transfer matrix;
u = displacement;
$\bar{u}$ = prescribed displacement;
u^* = displacement corresponding to weighting field;
V = effective shear force;
V^* = reactions at internal support;
$\mathbf{z}$ = state vector;
$\mathbf{z}_0$ = unknown initial state vector;
β_n = rotation normal to boundary;
β_s = rotation tangential to boundary;
δ = Dirac delta function;
ε_{ij} = components of strain;
ε_{ij}^* = components of strain corresponding to weighting field;
ν = Poisson's ratio;
σ_{ij} = components of stress;
σ_{ij}^* = components of stress corresponding to weighting field; and
$\mathbf{\Phi}$ = interpolation function.

Table 7-1 Comparisons of Displacements for Cantilevered Plate Subjected to In-Plane Load

Pattern A

Scheme	Displacement (cm) 1 Strip	2 Strips	4 Strips	6 Strips	8 Strips	10 Strips
BEM	0.2245	0.3642	0.3966	0.4099	0.4138	0.4150
BEMS	0.2245	0.3090	0.3831	0.3832	0.3752	0.3690
BETM	0.2245	0.3090	0.3831	0.3832	0.3752	0.3690

Pattern B

Scheme	Displacement (cm) 1 Strip	2 Strips	4 Strips	6 Strips	8 Strips	10 Strips
BEM	0.2438	0.3353	0.4003	0.4155	0.4190	0.4201
BEMS	0.2438	0.2877	0.3531	0.4046	0.4204	0.4112
BETM	0.2438	0.2877	0.3531	0.4046	0.4204	0.4112

Table 7-2 Comparisons of Computation Times for Cantilevered Plate

Pattern A

Scheme	Computation Time (sec) 1 Strip	2 Strips	4 Strips	6 Strips	8 Strips	10 Strips
BEM	0.4	0.6	1.3	2.4	3.8	5.5
BEMS	0.4	0.9	2.5	5.7	11.3	19.9
BETM	0.9	1.0	1.2	1.5	1.7	2.0

Pattern B

Scheme	Computation Time (sec) 1 Strip	2 Strips	4 Strips	6 Strips	8 Strips	10 Strips
BEM	0.9	1.3	2.4	3.0	5.6	7.7
BEMS	0.9	2.4	8.3	12.2	25.6	47.2
BETM	2.9	3.2	3.8	4.4	5.2	5.8

Table 7-3 Comparisons of Displacements for Simply Supported Plate under Uniform Load

Scheme	Displacement (w^*) 1 Strip	3 Strips	5 Strips
BEM	0.003502	0.003983	0.004000
BEMS	0.003502	0.004001	0.003979
BETM	0.003502	0.004001	0.003979

$w^* = \dfrac{D}{qa^4} w; \quad w^*_{exact} = 0.004060$

Table 7-4 Comparisons of Displacements for Simply Supported Plate under Concentrated Load

Scheme	Displacement (w^*) 1 Strip	3 Strips	5 Strips
BEM	0.01019	0.01127	0.01134
BEMS	0.01019	0.01120	0.01110
BETM	0.01019	0.01120	0.01110

$w^* = \dfrac{D}{pa^2} w; \quad w^*_{exact} = 0.01160$

Table 7-5 Comparisons of Displacements for Cantilevered Plate Subjected to Line Load

Scheme	Displacement (w*) 1 Strip	3 Strips	5 Strips
BEM	0.001680	0.003206	0.003384
BETM	0.001680	0.002923	0.003436

$w^* = \frac{D}{pa^3} w$; w*(FEM, 6x6 Elements) = 0.003474

Table 7-6 Comparisons of Displacements for Cantilevered Plate under Uniform Load

Scheme	Displacement (w*) 1 Strip	3 Strips	5 Strips
BEM	0.058779	0.115954	0.121438
BETM	0.058779	0.107078	0.125253

$w^* = \frac{D}{qa^4}$ w*(FEM, 6x6 Eiements) = 0.129267

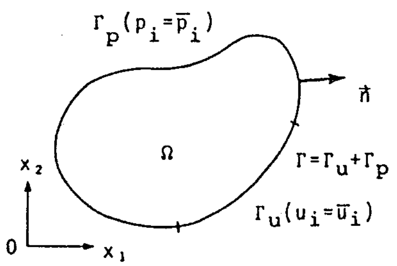

Fig.7-1 Coordinate System for In-Plane Problems

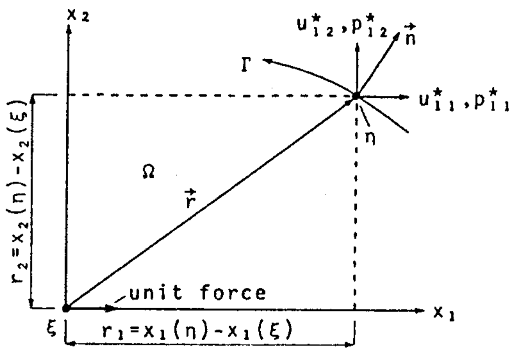

Fig.7-2 Fundamental Solution for In-Plane Problems

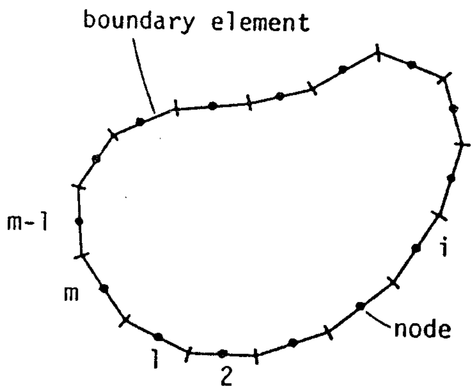

Fig.7-3 Boundary Discretization

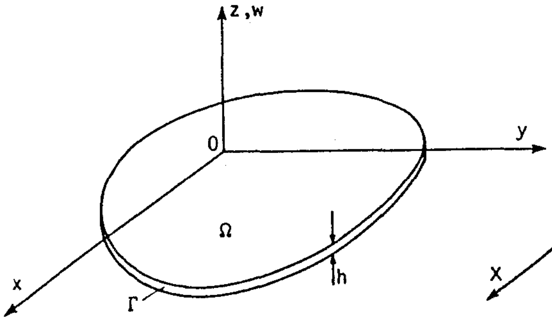

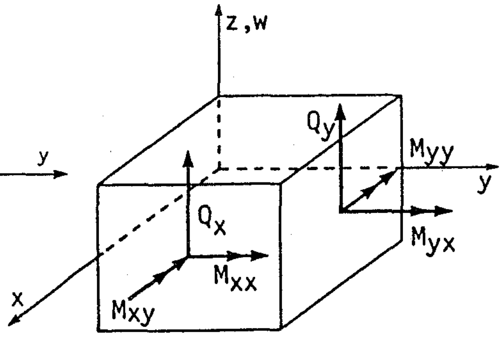

Fig.7-4 Coordinate System for Plate Bending Problems

Fig.7-5 Moments and Shear Forces

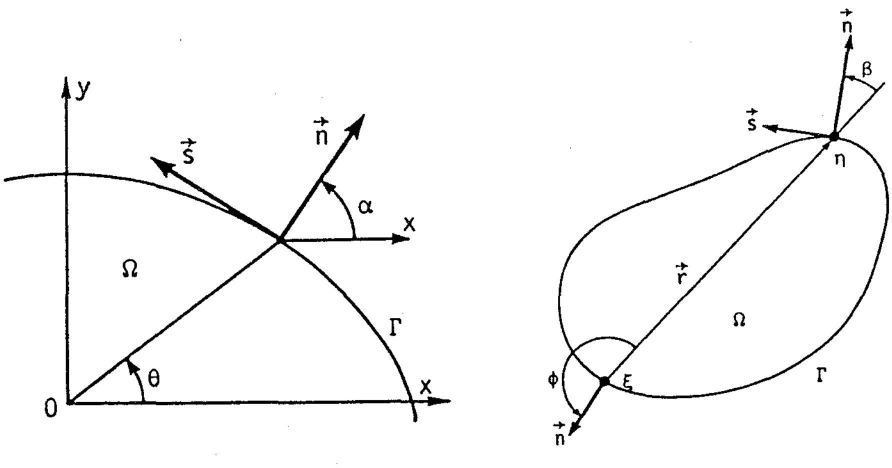

Fig.7-6 Notations for Plate Bending Problems

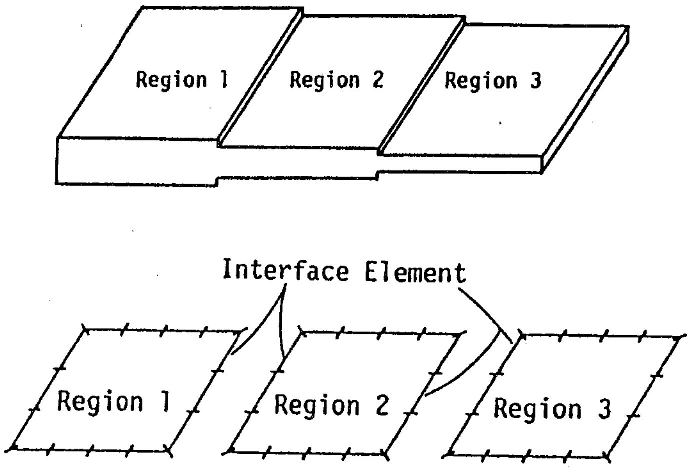

Fig.7-7 Plate Divided into Subregions

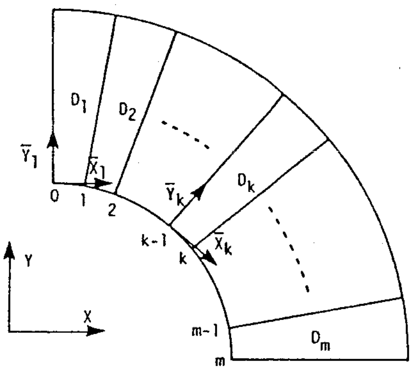

Fig.7-8 Think Cylinder Divided into Subregions

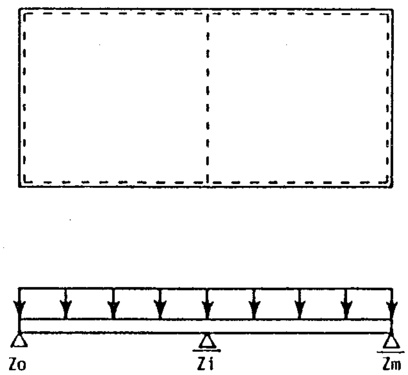

Fig.7-9 Plate with Internal Supports

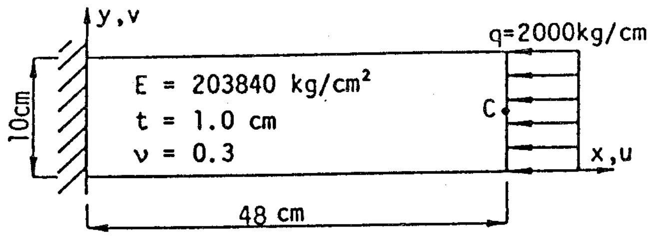

Fig.7-10(a) Cantilevered Plate Subjected to In-Plane Load

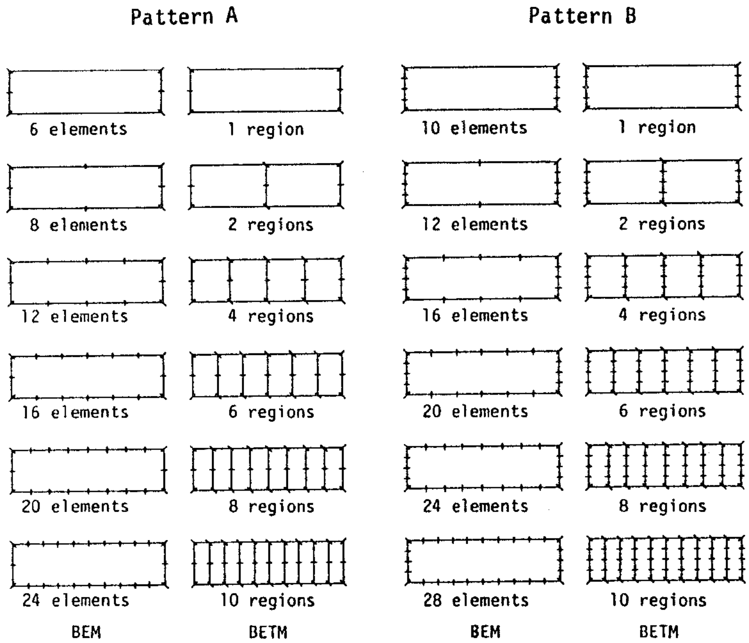

Fig.7-10(b) Discretizing Patterns

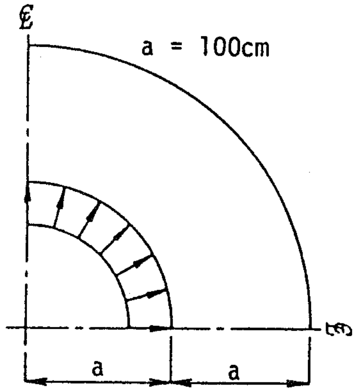

Fig.7-11(a) Thick Cylinder under Internal Pressure

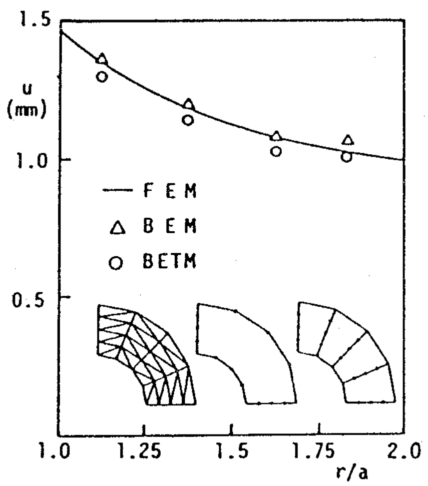

Fig.7-11(b) Displacement in Radial Direction (4 strips)

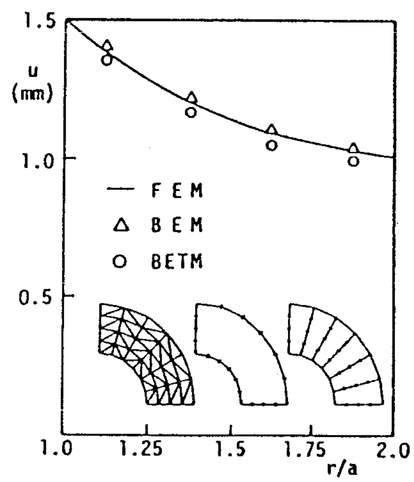

Fig.7-11(c) Displacement in Radial Direction (6 strips)

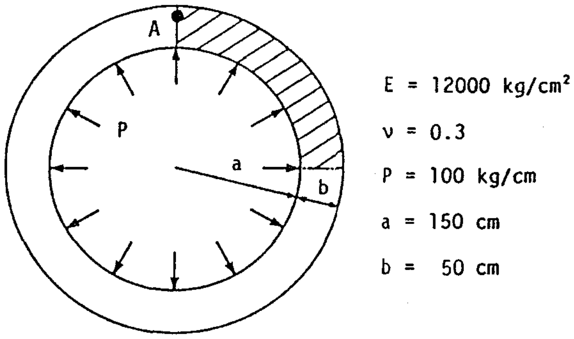

Fig.7-12(a) Thick Cylinder under Internal Pressure

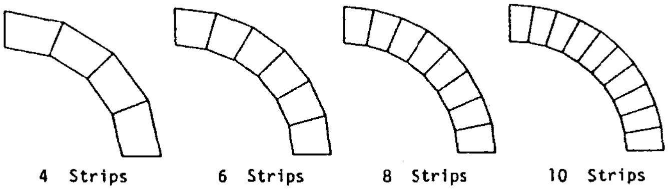

Fig.7-12(b) Discretizing Patterns

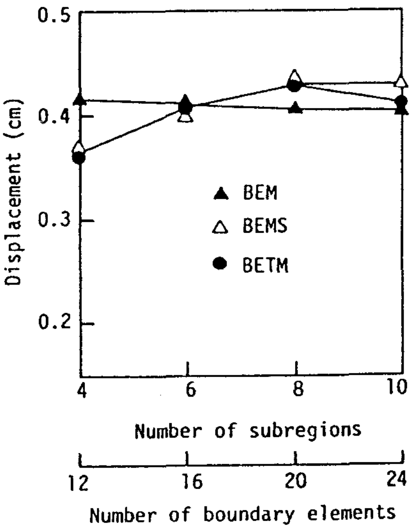

Fig.7-12(c) Comparison of Radial Displacement

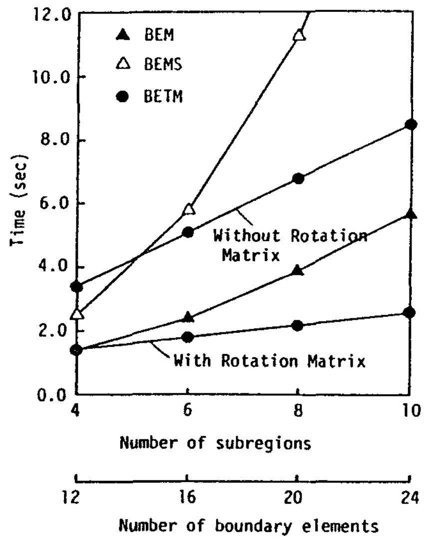

Fig,7-12(d) Comparison of Computation Time

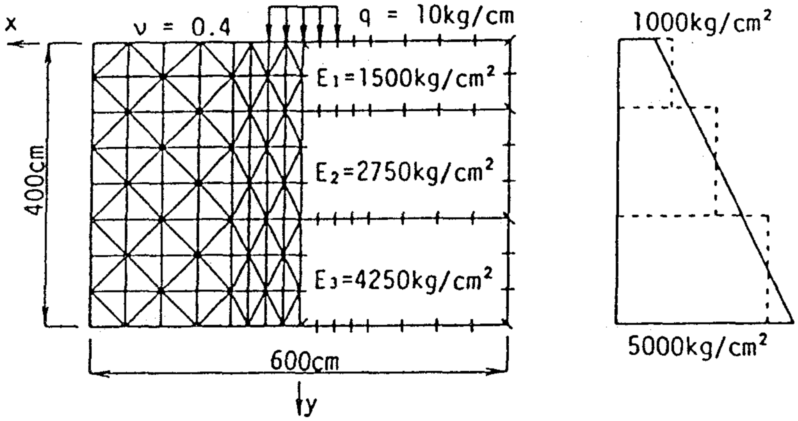

Fig.7-13(a) Foundation Supported on Medium

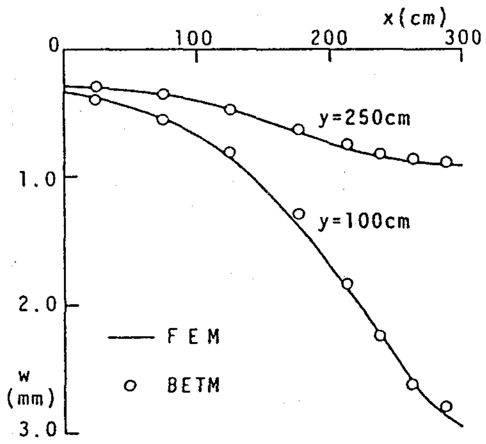

Fig.7-13(b) Vertical Displacements

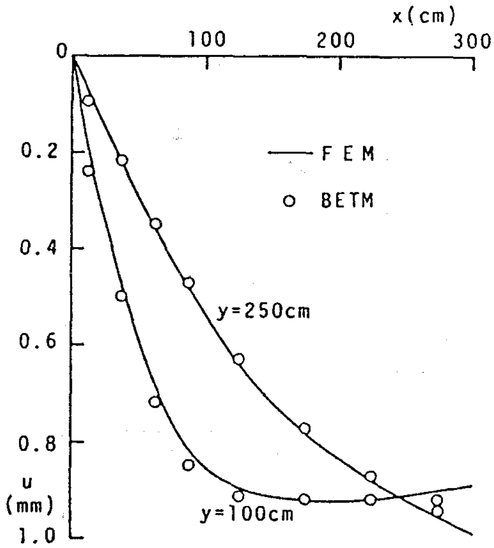

Fig.7-13(c) Horizontal Displacements

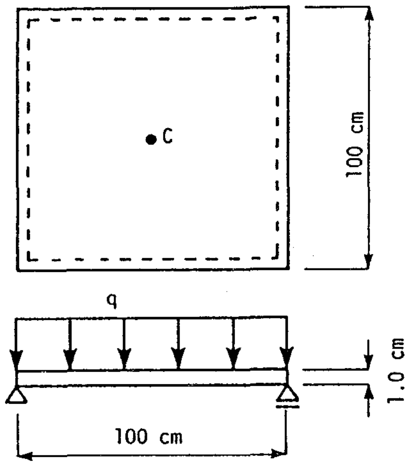

Fig.7-14(a) Simply Supported Plate under Uniform Out-of-Plane Load

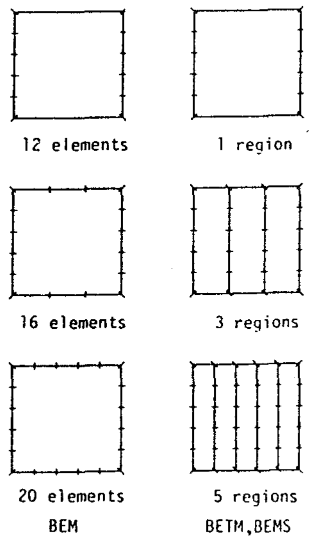

Fig.7-14(b) Discretizing Patterns

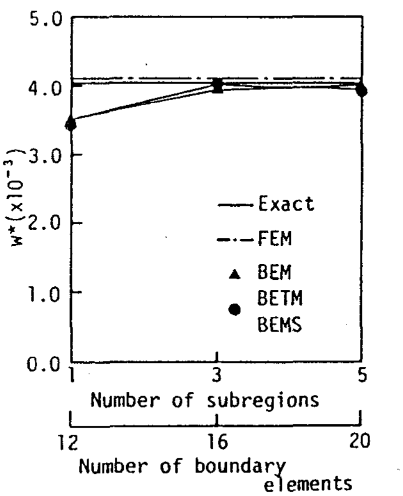

Fig.7-14(c) Relation between Number of Regions and Displacement ($w^* = D/qa^4 w$)

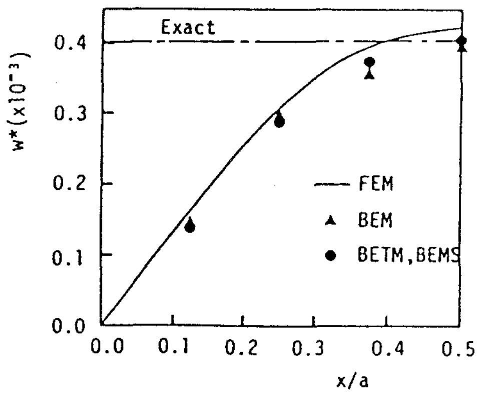

Fig.7-14(d) Centerline Configurations ($w^* = D/qa^4 w$)

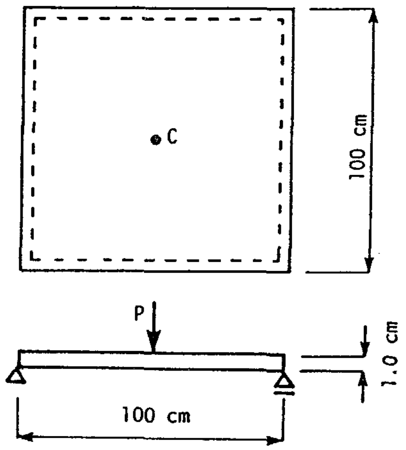

Fig.7-15(a) Simply Suppoted Plate under Concentrated Load

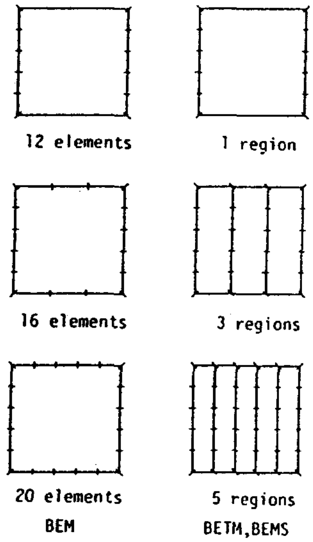

Fig.7-15(b) Discretizing Patterns

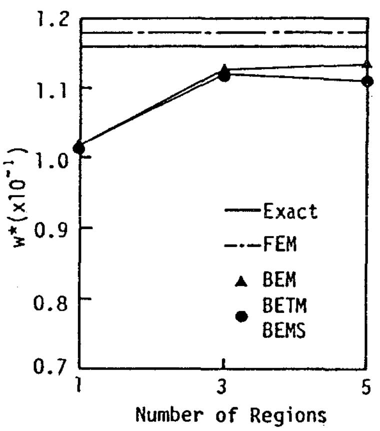

Fig.7-15(c) Relation between Number of Regions and Displacement ($w^* = D/qa^2w$)

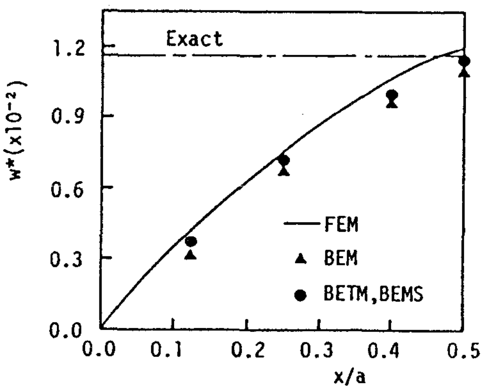

Fig.7-15(d) Centerline Configurations ($w^* = D/qa^2w$)

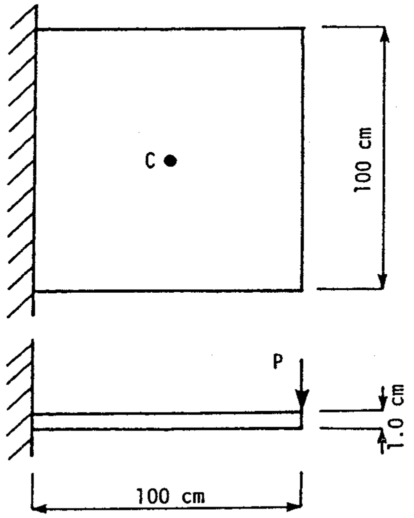

Fig.7-16(a) Cantilevered Plate Subjected to Line Load

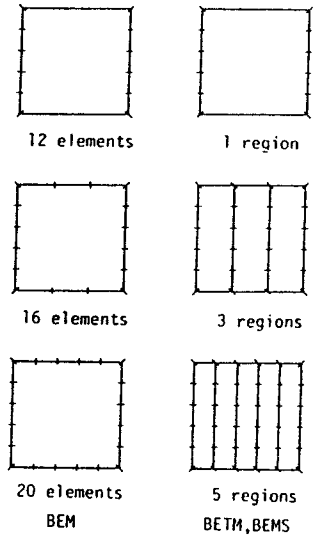

Fig.7-16(b) Discretizing Patterns

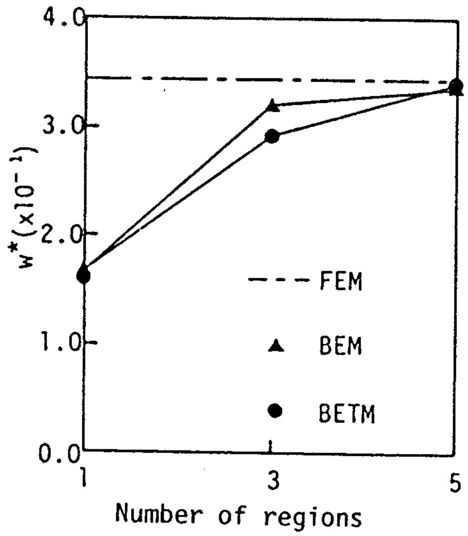

Fig.7-16(c) Relation between Number of Regions and Displacement ($w^* = D/qa^3w$)

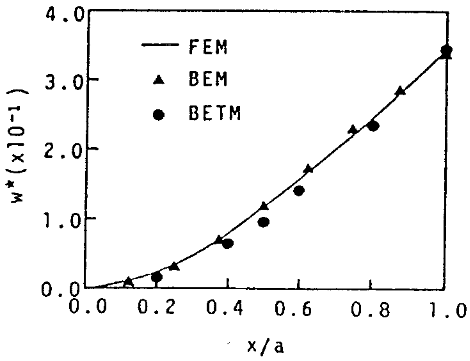

Fig.7-16(d) Centerline Configurations ($w^* = D/qa^3w$)

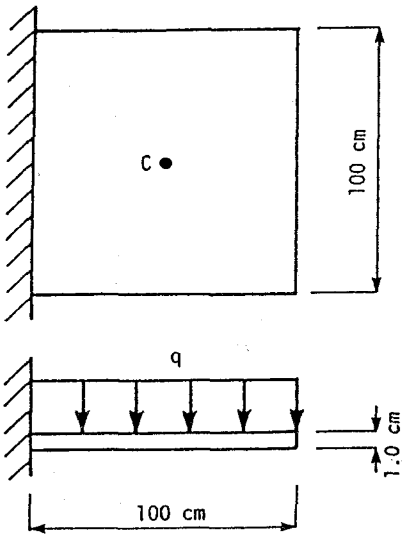

Fig.7-17(a) Cantilevered Plate under Uniform Load

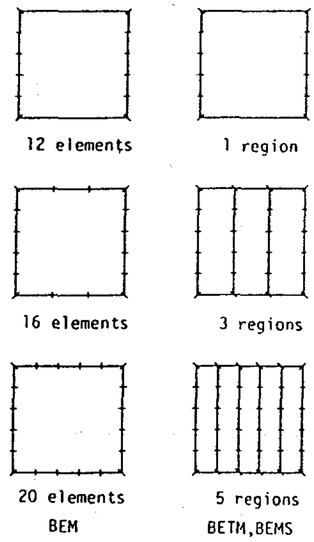

Fig.7-17(b) Discretizing Patterns

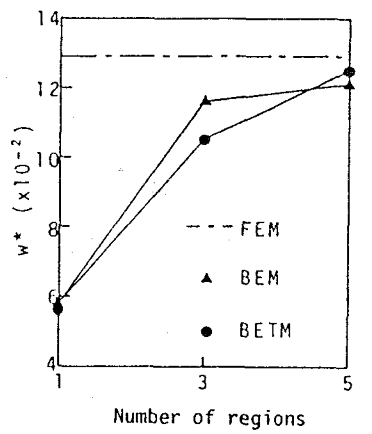

Fig.7-17(c) Relation between Number of Regions and Displacement ($w^* = D/qa^4 w$)

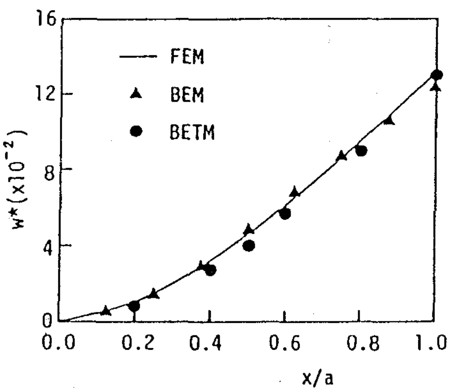

Fig.7-17(d) Centerline Configurations ($w^* = D/qa^4 w$)

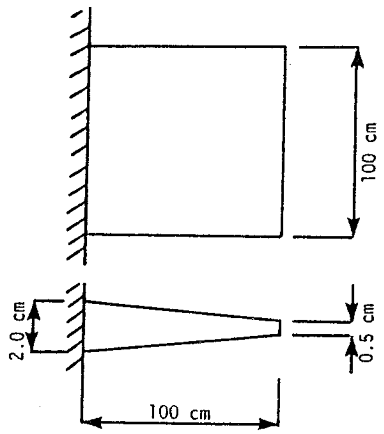

Fig.7-18(a) Cantilevered Plate with Variable Thickness

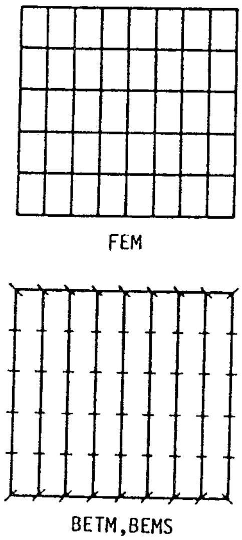

Fig.7-18(b) Discretizing Patterns

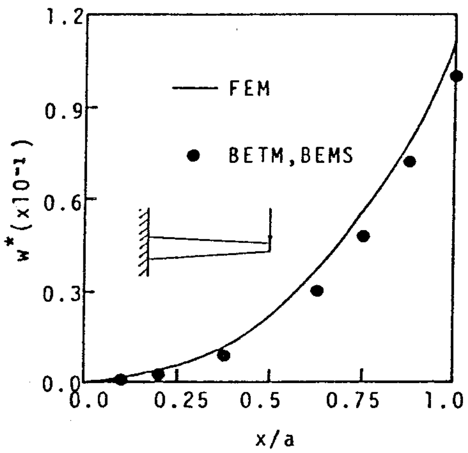

Fig.7-18(c) Centerline Configurations (Line Load, $w^* = D/qa^3 w$)

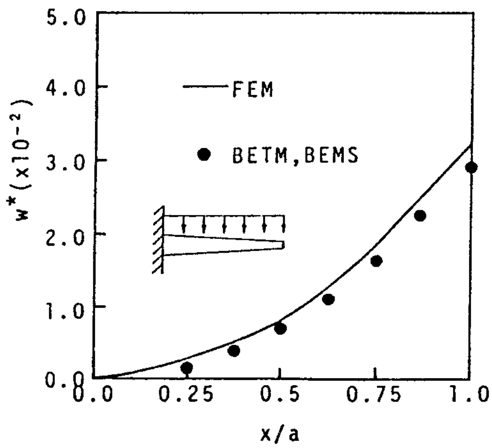

Fig.7-18(d) Centerline Configurations (Uniform Load, $w^* = D/qa^4 w$)

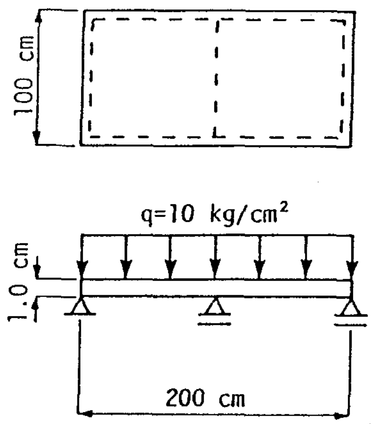

(a)

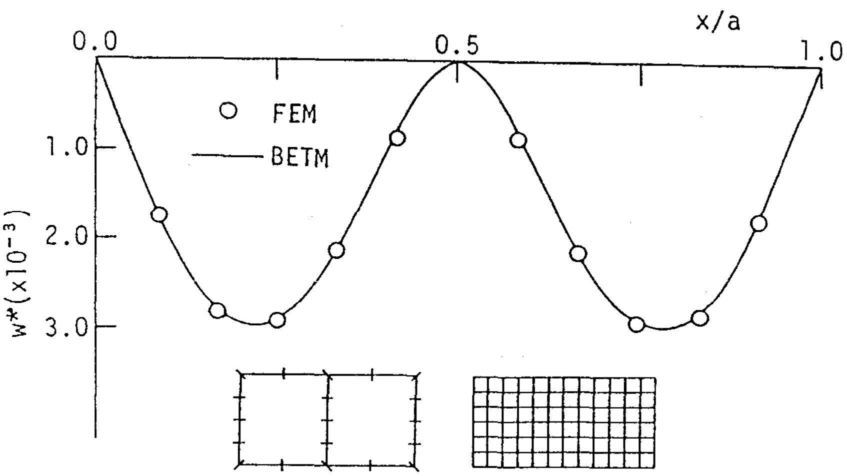

(b)

Fig.7-19 Centerline Configurations of Simply Supported Continuous Plate with a Internal Support (Uniform Load)

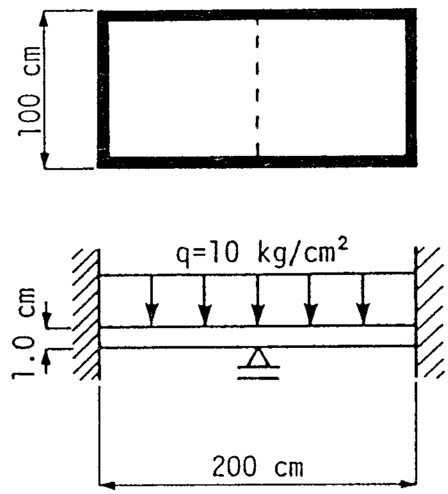

(a)

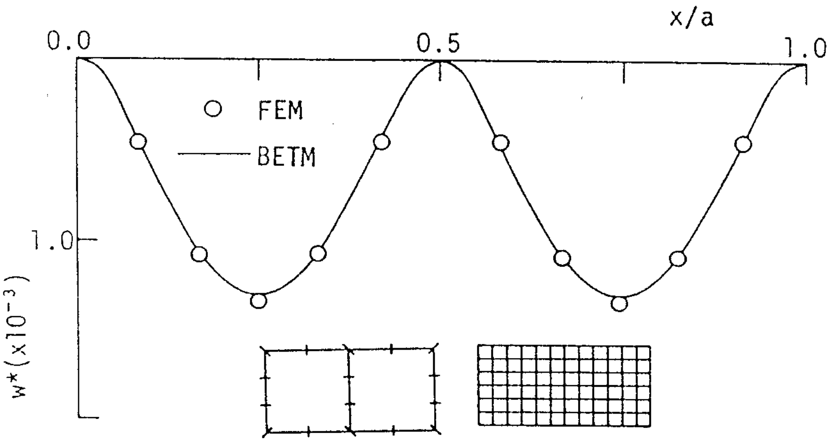

(b)

Fig.7-20 Centerline Configurations of Clamped Continuous Plate with a Internal Support (Uniform Load)

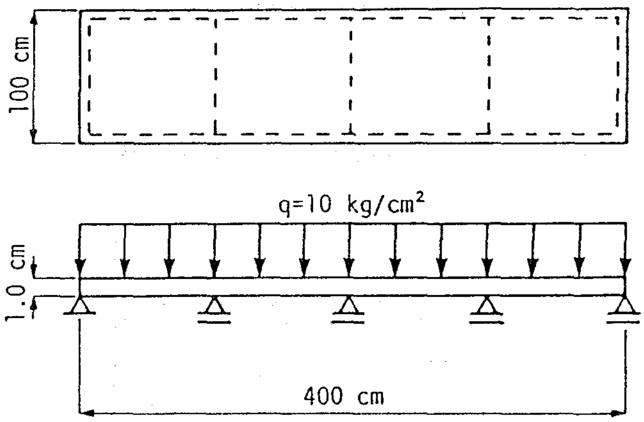

(a)

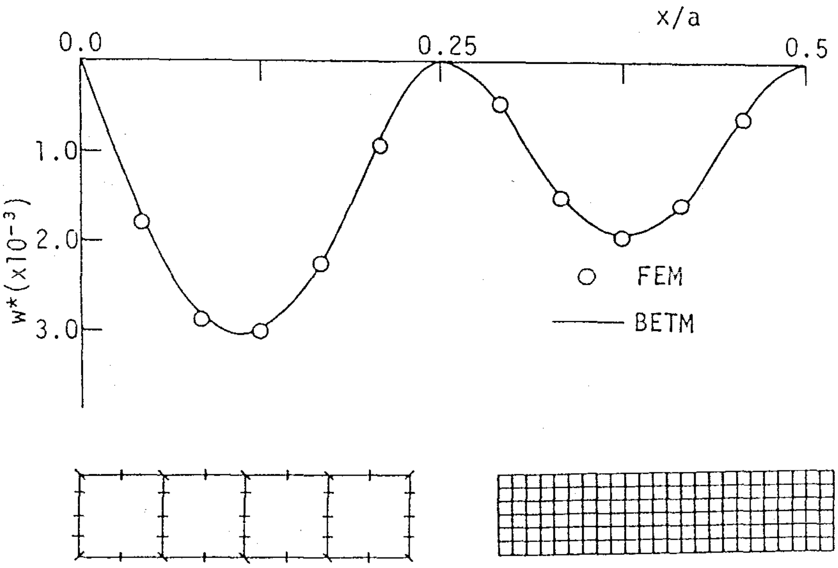

(b)

Fig.7-21 Centerline configurations of Simply Supported Continuous Plate with 3 Internal Supports (Uniform Load)

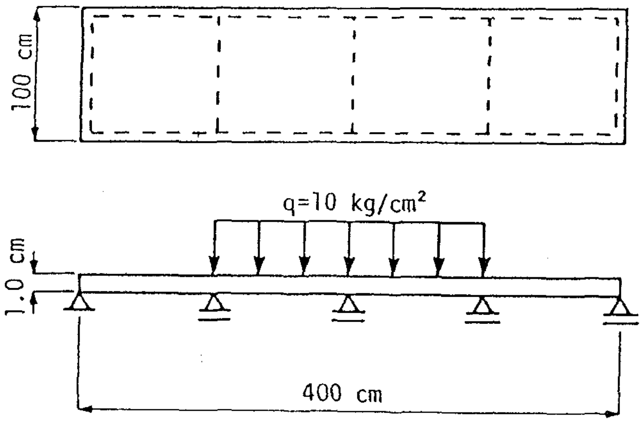

(a)

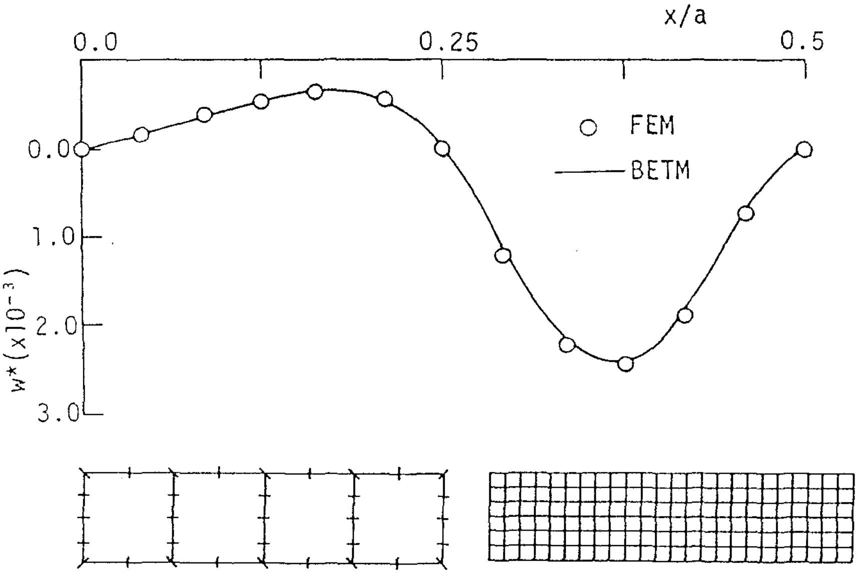

(b)

Fig.7-22 Centerline Configurations of Simply Supported Continuous Plate with 3 Internal Supports (Partial Load)

Chapter 8 CONCLUSIONS

In this paper, two structural analysis methods; 1) combined use of finite element and transfer matrix method, and 2) combined use of boundary element and transfer matrix method, are studied.

Main conclusions of each chapter have been drawn as follows.

Chapter 2

The procedures of the combined finite element - transfer matrix method are applied to the bending and buckling problems. Furthermore techniques for treating the complicated structures such as those with intermediate elastic and rigid columns, and with stiffeners are proposed.

(1) In bending and buckling problems good agreement exists between the FETM solutions and the exact solutions, which demonstrates the accuracy of this method.

(2) Since the size of the transfer matrix in the FETM method is equal to the number of degrees of only one strip, this method has the advantage of reducing the size of matrix to less than that obtained by the ordinary finite element method.

(3) Point matrices for elastic support and rib make possible the application of the FETM method to bending and buckling problems of the plates with intermediate elastic supports and stiffeners.

(4) By using the techniques for intermediate rigid column and simple support, the transformation procedure can be performed in a simple schematic manner.

Chapter 3

The combined finite element - transfer matrix method for the elastic-plastic problems with large displacement is studied. A computer program based on this theory has been developed.

(1) Good agreement exists between the results obtained by the FETM method and the conventional finite element method based on incremental procedures, which demonstrates the accuracy of this method in the elasto-plastic problems with large deformation.

(2) In the nonlinear problems, the FETM method has the advantage of reducing the size of matrix compared to the ordinary finite element method as in the linear problems.

Chapter 4

The combined finite element - transfer matrix method is extended to the linear and nonlinear problems of thin-walled members, and a computer program based on this theory has been developed.

(1) Good agreement exists between the results obtained by the FETM method and the standard finite element method not only in the linear problems but also in the nonlinear problems, which demonstrates the accuracy of the proposed method.

(2) From numerical examples presented in this chapter, it is shown that this method can be successfully applied to the long thin-walled members by reducing the size of the matrix and the computation time relative to less than that obtained by the finite element method.

(3) By adopting the transfer matrix for substructures derived in this chapter, complex thin-walled members, such as I-section and box-section plate girders with vertical stiffeners and web perforations, can be treated easily.

Chapter 5

A linear transient analysis method of the structures under random excitations by a combined finite element - transfer matrix method is proposed. An approximation is introduced in the equations of motion for the case of in-plane excitations in order to reduce computational efforts and the technique of exchanging the state vectors is proposed to avoid the propagation of round-off errors occurred in recursive multiplications of the transfer and point matrices.

(1) In the out-of-plane and in-plane excitations, good agreement exists between the results obtained by the FETM method and the conventional finite element dynamic analysis, which demonstrates the accuracy of linear transient analysis by the FETM method.

(2) In the case of in-plane excitations, the results by the FETM method based on the equations of motion with an approximation described in this chapter agree with those based on the equation without an approximation, and it becomes clear that this approximation of the equations is efficient to reducing computational efforts.

(3) The technique of exchanging the state vectors is very efficient for many strips pattern model to avoid the propagation of round-off errors.

Chapter 6

A linear transient analysis method based on a combined use of finite element and transfer matrix methods described in previous chapter is extended to nonlinear dynamic problems of plates under random out-of-plane and in-plane excitations. The Prandtl-Reuss′law obeying the von Mises yield criterion is assumed, and a set of moving coordinate systems is used to take geometric nonlinearity into consideration.

(1) In inelastic and large deformation dynamic problems, good agreement exists between the transient responses of the plates under out-of-plane and in-plane excitations obtained by the FETM method and the conventional finite element method, which

demonstrates the accuracy of the proposed method.

(2) Equilibrium iteration in each time step is effective to improve the solution accuracy and to avoid the development of numerical instabilities.

(3) Since in the FETM method, considerable computation time is required in the derivation of the transfer matrix, the pseudo-force iteration method is more efficient compared to the tangent stiffness iteration method.

Chapter 7

A structural analysis method based on a combined use of boundary element - transfer matrix method is proposed for two-dimensional and plate bending problems. The technique of exchanging the state vectors is proposed to avoid the propagation of round-off errors, and rotation matrix is employed for axisymmetric structures to reduce computational efforts. Furthermore, the technique for the structure with intermediate supports is proposed.

(1) In the proposed method, the sizes of the matrices involved in the process of solution depend on the number of elements of only one subregion; the use of a large number of elements is therefore permitted without getting involved with large matrices. A much smaller computer is thus sufficient.

(2) In two-dimensional and plate bending problems, the results obtained by the BETM method agree well with those by the boundary element and finite element methods, which demonstrates the accuracy of the proposed method.

(3) The technique of exchanging the state vectors is very efficient to avoid the propagation of round-off errors occurred in many subregions pattern.

(4) By using the technique for intermediate simple support, the BETM method can be applied to continuous plate, and results

obtained by this method are agree well with those by the finite element method.

(5) To employ the rotation matrix for deriving the transfer matrix is efficient for axisymmetric structures in reducing computational efforts.

From the mentions described above, this method can be successfully applied to the long and non-homogeneous systems.

The following subjects are required for future research and development.

FETM Method in Static Problem

(1) Investigation of efficiency and limitation of the FETM method in more practical problems.

(2) Study of effective nonlinear algorithm for the FETM method.

FETM Method in Dynamic Problem

In addition to the subjects prescribed in static problem, the following subjects are required.

(3) Application of the FETM method to inelastic dynamic problems with large deformation.

(4) Extension of this method to thin-walled members, such as box-section and I-section plate girders.

BETM Method

(5) Extension of the BETM method to nonlinear problems.

(6) Application of this method to thin-walled members, such as box-section and I-section plate girders.

(7) Investigation of efficiency and limitation of the BETM method with other boundary elements, such as linear and more higher order elements.

(8) Study of the relation between the discretizing pattern and the result not only in the BETM method but also in the boundary element method.

AUTHOR'S PUBLICATIONS

Publications

1. "Buckling Analysis of Shear-Elastic Plate with Stiffener", Proceeding of JSCE, No. 298, June 1980, pp.11-8, (with S. Misawa, T. Shigematsu and T. Hara, in Japanese).

2. "Untersuchung der Stabilität einseitig gedrückter, längsausgesteifter, orthotroper Rechteckplatten", Der Stahlbau, June 1982, pp.171-176 (with T. Shigematsu and T. Hara).

3. "Structural Analysis by a Combined Finite Element-Transfer Matrix Method", Computers & Structures, Vol. 17, No. 3, May, 1983, pp.321-326 (with T. Shigematsu and T. Hara).

4. "Zur numerischen und experimentellen Schwingungsuntersuchung von Bauwerken unter unregelmäßiger Belastung", Bauingigenieur, Vol. 59, 1984, pp.97-101 (with T. Shigematsu and T. Hara).

5. "Buckling Analysis of Thin Walled Opened and Cross Sectional Members with Shear Deformation", Trans. of AIJ, No.342, April, 1984, pp.39-44 (with T. Shigematsu and T. Hara, in Japanese).

6. "A Combined Finite Element - Transfer Matrix Method", Journal of Engineering Mechanics, ASCE, Vol. 110, No. 9, September, 1984, pp.1335-1349 (with T. Shigematsu and T. Hara).

7. "Numerische Berechnung bei nichtelastischen Schwingungssystemen mit Hilfe von Matrizenfunktionen", Bauingenieur, Vol. 60, 1985, pp.53-58 (with T. Shigematsu and T. Hara).

8. "Dynamische Stabilität des vorverformten Stabes unter pulsierender Axialbelastung", Bautechnik, Heft 2, 1986, pp.95-102 (with T. Shigematsu and T. Hara).

9. "Analysis of Thin-Walled Members by Finite Element - Transfer Matrix Method", Structural Eng./Earthquake Eng. Vol. 3, No. 1, April, 1986, pp.83s-90s (with T. Hara).

10. "Structural Analysis by a Combined Boundary Element - Transfer Matrix Method", Computers & structures, Vol. 24, No. 3, 1986, pp.385-389 (with T. Shigematsu and T. Hara).

11. "Transient Analysis of Plates by a Combined Finite Element - Transfer Matrix Method", Computers & Structures, Vol. 26, No. 4,1987, pp.543-549 (with T. Shigematsu).

12. "Dynamic Stability Analysis by a Matrix Function", Journal of Engineering Mechanics, ASCE, Vol. 113, No. 7, July, 1987, pp.1085-1100 (with T. Shigematsu and T. Hara).

13. Bending Analysis of Plates with Variable Thickness by Boundary Element-Transfer Matrix Method", Computers & Structures, Vol. 28, No. 5, 1988, pp.635-640 (with T. Shigematsu).

14. "Large Deformation Dynamic Analysis of Plates", Journal of Engineering Mechanics, ASCE, Vol. 114, No. 4, April, 1988, pp.624-637 (with T. Shigematsu).

Technical Papers in the Memoirs of the Faculty of Engineering, Ehime University

1. "On the Buckling Analysis of Shear-Elastic Plate with Stiffeners", , Vol. 9, No. 1, February, 1978, pp.91-101 (with S. Misawa, and T. Hara, in Japanese).

2. "On the Buckling Analysis of Sandwich Plate on Elastic Line Support", , Vol. 9, No. 2, February, 1979, pp.161-173 (with S. Misawa, T. Shigematsu and T. Hara, in Japanese).

3. "On the Buckling Analysis of Orthotropic Sandwich Plates", Vol. 9, No. 3, February, 1980, pp.69-77 (with S. Misawa, T. Shigematsu and T. Hara, in Japanese)

4. "Large Deflection Analysis of Multilayer Sandwich Plates", Engineering, Vol. 9, No. 4, February, 1981, pp.79-89 (with S. Misawa, T. Shigematsu and T. Hara, in Japanese).

5. "On the Buckling Analysis of Thin-Walled Cross Section Members", Vol. 9, No. 4, February, 1981, pp.101-112 (with S. Misawa, T. Shigematsu and T. Hara, in Japanese).

6. "On the Buckling Analysis of Thin-Walled Open and Closed Cross Section Members", Vol. 10, No. 1, February, 1982, pp.123-132 (with S. Misawa, T. Shigematsu and T. Hara, in Japanese).

7. "On the Buckling Analysis of Plates by FE-TM Method", Vol.10, No.1, February, 1982, pp.133-142 (with S. Misawa, T. Shigematsu and T. Hara, in Japanese).

8. "On the Bending Analysis of Plates by FE-TM Method", Vol.10, No.2, February, 1983, pp.151-159 (with T. Shigematsu and T. Hara, in Japanese).

9. "Buckling Analysis of Open Cylindrical Shells with Stiffener", Vol.10, No.3, February, 1984, pp.187-200 (with T. Shigematsu, T. Hara and T. Sugiyama, in Japanese).

10. "Buckling Analysis of Cylindrical Shells with Stiffener", by Transfer Matrix Method", Vol.10, No.4, February, 1985, pp.169-177 (with T. Shigematsu, T. Hara and T. Shugiyama, in Japanese).

11. "Structural Analysis by a Combined Boundary Element-Transfer Matrix Method", Vol.11, No.2, February, 1987, pp.141-149 (with S. Kataoka, in Japanese).

12. "Numerische Berechnungen der Dynamischen Stabilität bei axialbelastetem Stab mit Vorverformung", Vol.11, No.2, February, 1987, pp.151-159 (with T. Shigematsu and T. Hara).

13. "Large Deformation Dynamic Analysis of Thin Plates by FETM Method", Vol.11, No.3, February, 1988, pp.201-210 (with M. Murata, in Japanese).